The Neurobiological Mechanisms of Transcranial Direct Current Stimulation:

Insights from Human Neuroimaging and Psychophysics.

Claire J. Hanley

PhD Psychology

2015

Summary

The research aimed to investigate the neurobiological basis of transcranial direct current stimulation (tDCS); a neuromodulation technique capable of inducing prolonged changes in behavioural performance. The past 15 years have seen a dramatic increase in tDCS-oriented studies, yet the underpinnings of the method are not completely understood. Consequently, this series of experiments was designed to investigate the mechanisms that contribute to the effects of the method. Focusing on neuroimaging, modulations of excitatory and inhibitory neurochemicals were assessed using Magnetic Resonance Spectroscopy (MRS); incorporating distinct spectral editing sequences to define the precise role of inhibitory neurotransmission. Additionally, concurrent DC stimulation and Magnetoencephalography (MEG) was developed, which permitted the novel investigation of excitatory and inhibitory processes via the influence of tDCS on electrophysiological responses in the motor and visual systems. This simultaneous tDCS-MEG investigation is one of only a few existing studies and was the first such endeavour by a group based in the United Kingdom. Finally, a unique psychophysical approach was adopted whereby variations of a vibrotactile adaptation task were utilised to assess the effects of tDCS on amplitude discrimination ability. The paradigms used were specifically chosen due to their physiological similarity to tDCS, thereby enabling inferences on the underpinnings of the method on the basis of changes in somatosensory task performance. These studies provided varying degrees of support for the neurobiological mechanisms proposed in the existing literature, most likely reflecting the influence of distinctions in stimulation protocols and the presence of individual difference factors thought to modify responses to stimulation. Consequently, in addition to the established insights regarding the underpinnings of tDCS, valuable perspectives on the optimisation of stimulation-based methodology were achieved by conducting the outlined investigations.

Statements & Declaration

DECLARATION

This work has not been submitted in substance for any other degree or award at this or any other university or place of learning, nor is being submitted concurrently in candidature for any degree or other award.

Signed ……. (candidate) Date ……

STATEMENT 1

This thesis is being submitted in partial fulfillment of the requirements for the degree of PhD.

Signed ……. (candidate) Date ……

STATEMENT 2

This thesis is the result of my own independent work/investigation, except where otherwise stated.

Other sources are acknowledged by explicit references. The views expressed are my own.

Signed ……. (candidate) Date ……

STATEMENT 3

I hereby give consent for my thesis, if accepted, to be available online in the University's Open Access repository and for inter-library loan, and for the title and summary to be made available to outside organisations.

Signed ……. (candidate) Date ……

STATEMENT 4: PREVIOUSLY APPROVED BAR ON ACCESS

I hereby give consent for my thesis, if accepted, to be available online in the University's Open Access repository and for inter-library loans **after expiry of a bar on access previously approved by the Academic Standards & Quality Committee.**

Signed ……. (candidate) Date ……

Acknowledgments

"Passion has little to do with euphoria and everything to do with patience.
It is not about feeling good. It is about endurance.
Like patience, passion comes from the same Latin root: pati.
It does not mean to flow with exuberance. It means to suffer".

Mark Z. Danielewski – House of Leaves

The formation of this thesis represents a culmination of persistence and ambition as the path from my undergraduate to doctoral studies was certainly not the most direct of routes. Reflecting on my experiences as I reach this point in my academic journey, I have come to appreciate that nothing that is worth doing will ever be easy. True passion has little to do with euphoria and everything to do with patience.

To my supervisors, David McGonigle and Krish Singh, I would like to extend my thanks for your guidance and scientific expertise. Krish, your devotion to innovative research is outstanding – particularly as my project involved convincing you that it was a great idea to place a current source right underneath the MEG sensors. David, your enthusiasm for science is truly infectious and has been a great source of motivation. You encouraged me to push the boundaries of my capability, which has certainly contributed towards my progression as a researcher. I am extremely grateful to you both for the opportunity you have given me.

To any of my past and present colleagues who have inspired and encouraged me – thank you – particularly Mark Mikkelsen and John Evans for their enthusiasm with regard to the spectroscopy component of my research. As a great friend, I would also like to acknowledge Mark for being a source of support during the harder times.

To my family and partner Jamie – I cannot thank you enough for all the times you have listened to my concerns and above all, the fact you have always had faith in me. All of this would have been so much more difficult without your love and support.

Finally, I would like to acknowledge the influence of my late father, John Eric Hanley. Never one to accept knowledge as fact, his natural curiosity and desire to learn have become an integral part of my own mentality, which has no doubt guided me towards a scientific career. His advice to always believe in my ability has been a constant source of motivation. Consequently, this thesis is dedicated to my father who even in his absence has encouraged me to pursue my ambitions.

Publications

A number of experiments in this thesis have been submitted for publication in the form of journal articles or abstracts in conference proceedings.

Chapter 4

Rising Above the Noise: The Challenge of Combining tDCS & MEG.

Claire Hanley, Krish Singh & David McGonigle

19th Annual Conference on Biomagnetism (2014): Halifax, Canada (REF: P1-016)

tES-MEG: Simultaneous Combined Transcranial Electrical Stimulation and Magnetoencephalography.

David McGonigle, Krish Singh & Claire Hanley

1st International Brain Stimulation Conference (2015): Singapore, Asia.
Available online - doi: 10.1016/j.brs.2015.01.097

Chapter 5

Transcranial Modulation of Brain Oscillatory Responses:
A Concurrent tDCS-MEG Investigation.

Claire J. Hanley, Krish D. Singh & David J. McGonigle

Neuroimage
Available online - doi:10.1016/j.neuroimage.2015.12.021

Chapter 6

Stimulating Somatosensory Psychophysics:
A Double-Blind, Sham-Controlled Study of the Neurobiological Mechanisms of tDCS.

Claire J. Hanley, Mark Tommerdahl & David J. McGonigle

Frontiers in Cellular Neuroscience, 9:400
Available online - doi: 10.3389/fncel.2015.00400

List of Abbreviations

The following abbreviations and acronyms are frequently used throughout this thesis:

2AFC	Two alternative forced choice
2IFC	Two interval forced choice
AEQ	Adverse effects questionnaire
ASD	Autism spectrum disorder
CNS	Central nervous system
Cr	Creatine
CSP	Cortical silent period
DL	Difference limen
DSA	Dual-site adaptation
EPSP	Excitatory post-synaptic potential
ERD	Event related desynchronisation
ERS	Event related synchronisation
FID	Free induction decay
fMRI	Functional magnetic resonance imaging
GABA	Gamma-aminobutyric acid
GAD	Glutamic acid decarboxylase
Glx	Glutamate/glutamine composite
IPSC/IPSP	Inhibitory post-synaptic current/potential
LICI	Long interval intracortical inhibition
LTD	Long-term depression
LTP	Long-term potentiation
M1	Primary motor cortex
MEG	Magnetoencephalography
MEP	Motor evoked potential

MM	Macromolecules
MRI	Magnetic resonance imaging
MRS	Magnetic resonance spectroscopy
MSR	Magnetically shielded room
NAA	N-acetyl-aspartate
NMDA	N-methyl-D-aspartate
PMBR	Post movement beta rebound
PNS	Peripheral nervous system
S1	Primary somatosensory cortex
SAM	Synthetic aperture magnetometry
SEQ	Sequential amplitude discrimination task
SICI	Short interval intracortical inhibition
SIM	Simultaneous amplitude discrimination task
SNR	Signal-to-noise ratio
SSA	Single-site adaptation
tACS	Transcranial alternating current stimulation
tDCS	Transcranial direct current stimulation
tES	Transcranial electrical stimulation
TMS	Transcranial magnetic stimulation
tRNS	Transcranial random noise stimulation
V1	Primary visual cortex
VEF	Visual evoked field
VEP	Visual evoked potential

Table of Contents

Summary…… i
Statements & Declaration……..... ii
Acknowledgements……... iii
Publications……..... iv
List of Abbreviations……..…….... v
Table of Contents……..……. vii

1. General Introduction…… 1
1.1. Information Transfer in the Human Nervous System…… 2
1.1.1. From resting potential to action potential……. 2
1.1.2. Neurotransmission…… 3
1.1.3. Synaptic plasticity…… 5
1.2. Transcranial Direct Current Stimulation..... 6
1.2.1. A historical perspective of transcranial electric stimulation..... 6
1.2.2. Methodological advances in modern tDCS research..... 9
1.2.3. Physiological mechanisms governing the induction of tDCS effects..... 14
1.3. Functions of the Nervous System 18
1.3.1. The motor system..... 18
1.3.1.1. Structure & function of the motor system…… 18
1.3.2. The visual system..... 21
1.3.2.1. Structure & function of the visual system…….. 21
1.3.3. The somatosensory system..... 23
1.3.3.1. Structure & function of the somatosensory system..... 23
1.3.3.2. Dynamics of primary somatosensory cortex..... 26
1.4. Psychophysics..... 29
1.4.1. An introduction to the study of psychophysics..... 29
1.4.2. Measuring psychophysical task performance..... 30
1.5. Chapter Overview..... 33

2. Introduction to Neuroimaging Methods……..... 35
2.1. Magnetic Resonance Imaging (MRI)…… 35
2.1.1. The MRI system…… 36
2.1.2. Signal generation……... 37
2.1.3. Image generation……... 38
2.1.4. Magnetic Resonance Spectroscopy (MRS)……... 39
2.1.4.1. Overlap in the chemical shift spectrum……..... 41
2.1.4.2. Quantification & analysis…… 43
2.2. Magnetoencephalography (MEG)…… 46
2.2.1. The MEG system……... 46
2.2.2. Signal generation……... 48
2.2.3. Signal classification……... 49
2.2.4. Source localisation analysis……... 52

3. Experimental Chapter 1: Investigating the Neurochemical Underpinnings of Transcranial Direct Current Stimulation - A Magnetic Resonance Spectroscopy Study……..... 56
3.1. Abstract…….. 56
3.2. Introduction……..... 56

3.3. Methods…….. 61
3.3.1. Pilot testing…… 61
3.3.2. Subjects…….. 64
3.3.3. MRS acquisition……. 65
3.3.4. Transcranial direct current stimulation…….. 66
3.3.5. Experimental procedure……. 66
3.3.6. MRS data analysis & statistics……... 67
3.4. Results……. 68
3.4.1. Peripheral effects of tDCS……..... 68
3.4.2. MRS data quality……..... 69
3.4.3. tDCS-MRS…….. 72
3.5. Discussion……..... 75
3.5.1. Interpretation of findings……..... 75
3.5.2. Methodological issues & limitations…….. 79
3.5.3. Study design limitations & future considerations…….. 80
3.6. Conclusions……..... 83

4. Experimental Chapter 2: Rising Above the Noise – The Challenge of Combining Transcranial Direct Current Stimulation & Magnetoencephalography…….. 84
4.1. Abstract…… 84
4.2. Introduction……..... 84
4.3. Methods…….. 88
4.3.1. Subjects…….. 88
4.3.2. Experimental methods……... 88
4.3.2.1. Magnetoencephalography……..... 88
4.3.2.2. Transcranial direct current stimulation……..... 88
4.3.3. Experimental procedure……. 90
4.3.4. Data analysis…….. 91
4.4. Results……. 92
4.5. Discussion……... 98
4.6. Conclusions……. 100

5. Experimental Chapter 3: From Excitation and Inhibition to Electrophysiology - A Concurrent tDCS-MEG Investigation of the Effects of Brain Stimulation.…. 101
5.1. Abstract……..... 101
5.2. Introduction……... 101
5.3. Methods……..... 107
5.3.1. Subjects…….. 107
5.3.2. Visuomotor paradigm……... 107
5.3.3. MEG acquisition……..... 108
5.3.4. Transcranial direct current stimulation……..... 109
5.3.5. Experimental procedure……..... 110
5.3.6. MEG data analysis & statistics……..... 111
5.4. Results……..... 114
5.4.1. Peripheral effects of tDCS……..... 114
5.4.2. Cortical effects of tDCS……..... 115
5.4.2.1. Source localisation……... 115
5.4.2.2. Baseline activity……... 115
5.4.2.3. Task-induced responses……... 116
5.4.2.3.1. Motor beta band response……... 117

5.4.2.3.2. Visual gamma band response…….. 118
5.4.2.4. Group SAM/Randomisation……. 118
5.4.2.5. Transient & sustained visual gamma response……..... 118
5.4.2.6. Task-evoked responses……..... 120
5.4.2.6.1. Motor evoked response……... 120
5.4.2.6.2. Visual evoked response……... 122
5.5. Discussion…….. 123
5.5.1. Task-induced responses……. 123
5.5.2. Task-evoked responses…….. 124
5.5.3. Comparison of modulations in induced and evoked responses……. 125
5.5.4. Methodological considerations…….. 126
5.5.5. Effects of electrode montage & stimulation order……..... 129
5.6. Conclusions……..... 129

6. Experimental Chapter 4: Stimulating Somatosensory Psychophysics – A Double-Blind, Sham-Controlled Study of the Neurobiological Mechanisms of Transcranial Direct Current Stimulation.…… 131
6.1. Abstract……..... 131
6.2. Introduction……... 132
6.3. Methodology & Results……. 137
6.3.1. Experiment 1: Single-Site Adaptation & Amplitude Discrimination….. 137
6.3.1.1. Subjects…… 138
6.3.1.2. Vibrotactile task……... 138
6.3.1.3. Experimental procedure……... 139
6.3.1.4. Data analysis & statistics……. 139
6.3.1.5. Results…….. 141
6.3.2. Experiment 2: Repeatability of the Single-Site Adaptation Effect……... 142
6.3.2.1. Results……. 142
6.3.3. Experiment 3: tDCS & Amplitude Discrimination Performance……. 143
6.3.3.1. Subjects…… 143
6.3.3.2. Vibrotactile task……... 144
6.3.3.3. Transcranial direct current stimulation…… 145
6.3.3.4. Experimental procedure……... 146
6.3.3.5. Data analysis & statistics……. 147
6.3.3.6. Results…….. 148
6.3.3.6.1. Pre-tDCS data……..... 148
6.3.3.6.2. Post-tDCS data……..... 151
6.4. Discussion……. 156
6.4.1. Vibrotactile pilot studies……... 156
6.4.2. Vibrotactile-tDCS study……..... 158
6.4.2.1. Pre-tDCS findings……..... 158
6.4.2.2. Post-tDCS findings……..... 158
6.5. Conclusions……..... 164

7. Experimental Chapter 5: Modulation of Use-Dependent Plasticity in Primary Somatosensory Cortex – A Double-Blind, Sham-Controlled Transcranial Direct Current Stimulation Study……..... 165
7.1. Abstract……..... 165
7.2. Introduction……... 166
7.3. Methodology & Results……. 168

7.3.1. Experiment 1: Vibrotactile Pilot Study……..... 168
7.3.1.1. Subjects…… 168
7.3.1.2. Vibrotactile task……... 168
7.3.1.3. Experimental procedure……... 169
7.3.1.4. Data analysis & statistics……. 170
7.3.1.5. Results…….. 171
7.3.2. Experiment 2: Dual-site, Vibrotactile-tDCS Study……..... 173
7.3.2.1. Subjects……..... 173
7.3.2.2. Vibrotactile task……... 174
7.3.2.3. Transcranial direct current stimulation……..... 174
7.3.2.4. Experimental procedure……... 174
7.3.2.5. Data analysis & statistics……. 176
7.3.2.6. Results…….. 176
7.3.2.6.1. Pre-tDCS data……. 176
7.3.2.6.2. Post-tDCS data……..... 177
7.4. Discussion…….. 181
7.4.1. Vibrotactile pilot study……..... 182
7.4.2. Vibrotactile-tDCS study……..... 183
7.4.2.1. Pre-tDCS findings……..... 183
7.4.2.2. Post-tDCS findings……..... 185
7.5. Conclusions……..... 189

8. General Discussion……... 190
8.1. Neuroimaging Studies……..... 190
8.1.1. Magnetic Resonance Spectroscopy……... 190
8.1.2. Magnetoencephalography…….. 192
8.2. Behavioural Studies……... 193
8.2.1. Single-site adaptation……..... 194
8.2.2. Dual-site adaptation……... 195
8.3. General Limitations & Future Directions…….. 198
8.4. Closing Remarks……..... 204

9. References…… 205

10. Appendices……..... 246
Appendix 1: Edinburgh Handedness Inventory ……... 246
Appendix 2: tDCS Screening Form……... 247
Appendix 3: The 10-10 Electrode Placement System……... 248
Appendix 4: Adverse Effects Questionnaire…… 249
Appendix 5: G*Power Sample Size Output (tDCS-MRS)……... 255
Appendix 6: Consent Form (tDCS-MRS)…… 256
Appendix 7: Fit Error (tDCS-MRS)…….. 257
Appendix 8: NAA/Cr Correlations (tDCS-MRS)…… 258
Appendix 9: Creatine Statistics (tDCS-MRS)…….. 258
Appendix 10: Consent Form (tDCS-MEG)…….. 259
Appendix 11: Head Movement (tDCS-MEG)…….. 260
Appendix 12: Average Power Values (tDCS-MEG)……..... 260
Appendix 13: Group SAM Pairwise Comparisons (tDCS-MEG)……..... 261
Appendix 14: Peak Sustained & Transient Gamma Values (tDCS-MEG)……... 262

Appendix 15: Sustained Gamma Frequency Order Effect (tDCS-MEG)……. 263
Appendix 16: Transient Gamma Amplitude Order Effect (tDCS-MEG)……. 264
Appendix 17: Evoked Response Latency & Magnitude Values (tDCS-MEG)……..... 265
Appendix 18: G*Power Sample Size Output (SSA)……..... 267
Appendix 19: Counterbalancing (SSA)……..... 267
Appendix 20: Lack of Distinction between Anodal and Sham tDCS (SSA)..... 268
Appendix 21: Distinctions in Amplitude Discrimination Performance (SSA)……. 268
Appendix 22: tDCS Order Effect (SSA)…….... 269
Appendix 23: Counterbalancing (DSA)……..... 271

1. General Introduction

The rationale for the experimental work presented in this thesis was built upon the need for extended research into the generation of tDCS-induced after-effects, commonly observed using behavioural and cognitive paradigms. The origins of these effects, largely thought to reflect polarity-specific changes in cortical excitability, remain only partially understood despite investigations incorporating animal-based research and pharmacological interventions conducted in humans. It was, therefore, the aim of the research to extend the current evidence regarding the basic neurobiological mechanisms of the technique. In doing so, it was hoped that a better understanding of how tDCS effects are induced would be derived. This would then provide the means for future research to utilise such findings to refine the clinical applications of the method. To conduct such research in a non-invasive manner (suitable for human participants), the work documented here utilised the existing neurobiological evidence to probe specific aspects of human sensory function and related physiological systems. This was achieved by adopting a novel psychophysical perspective; using a behavioural paradigm with established physiological underpinnings similar to those shown to be altered by DC stimulation. Non-invasive neuroimaging methods were also utilised to gain insight into related aspects of electrophysiology (Magnetoencephalography, MEG) and neurochemistry (Magnetic Resonance Spectroscopy, MRS).

The following chapter introduces the basic elements of neurophysiology that are necessary to understand the concepts raised throughout the thesis. It also documents the origins of transcranial electrical stimulation, the advent of modern advances and the proposed physiological mechanisms underlying tDCS. It also serves to familiarise the reader with the aspects of human sensory function used to investigate the neurobiology of the method, focusing primarily on the overlapping mechanisms of tDCS and transient, task-based adaptation within the somatosensory system. Finally, as a means of inferring the association between sensory perception and physiological responses, the psychophysical procedures commonly used to define performance capacity are addressed. The imaging modalities MEG and MRS are discussed in the following methodology section. All experimental work is documented within separate, study-specific chapters.

1.1. Information Transfer in the Human Nervous System

1.1.1 From resting potential to action potential

The neuron is the basic functional unit of neural communication, enabling information transfer between the peripheral and central components of the nervous system (Figure 1.1). Signals from other neurons are received through the dendrites and are transferred to the cell body or soma. For the signal to be propagated further, the strength of the input must be sufficient to alter the resting membrane potential; governed by the movement of ions (atoms of positive or negative charge) across the cell membrane (in and out of intracellular space). Cations are ions of positive electrical charge that include sodium (Na^+), calcium (Ca^{2+}) and potassium (K^+), whereas anions such as chloride (Cl^-) are ions that possess a negative charge. Cell membranes vary in their permeability to these distinct classes and many are unique to a specific ion, constituting different types of voltage-gated or ion-dependent channels.

Figure 1.1. A typical nerve cell. Signals are transduced from the dendrites to the cell body. Those of sufficient strength to meet the voltage threshold will produce an action potential, which is generated at the axon hillock and propagated along the length of the axon to the pre-synaptic terminal. Image adapted from http://www.medtrng.com/anatomylesson/bhp13.htm.

At equilibrium, the chemical concentration and voltage gradients are balanced as sodium and potassium ions flow between intracellular and extracellular space (due to passive leakage and the related exchange-pump ratio), such that the influx of sodium is 1.5 times greater than the efflux of potassium. Membrane potential is only changed when these channels are allowed to open, altering the abundance of ions and the charge on either side of the cell membrane. At rest, intracellular space possesses a negative net charge (approximately -70 mV), which must be subject to a deviation of at least +15 mV in order to activate voltage-dependent sodium channels. This is the threshold for the generation of action potentials, which transmit the input from the axon hillock along the length of the axon thus permitting long-range information transfer.

Once the threshold is reached and sodium channels are opened, the electrochemical gradient triggers the necessary influx to push the charge towards 0 mV, referred to as depolarisation of the cell. This usually persists for several milliseconds, however, activation of voltage-dependent calcium channels can extend depolarisation or shorten

action potentials if calcium-activated potassium channels are engaged. Sodium channels begin to close as the inside of the cell reaches +30 mV and at this stage, potassium channels are opened. This results in a brief "refractory" period of hyperpolarisation (charge is forced above the resting potential of the neuron), where membrane potential peaks at -90 mV, before the resting potential is restored. In the instance of an input that induces an increasingly negative deviation in voltage, the likelihood of the action potential threshold being reached becomes less likely because membrane potential is pushed towards the potassium equilibrium and sodium channels remain closed.

1.1.2 Neurotransmission

At the synapse or junction between neurons, depolarisation of the pre-synaptic cell and the activation of voltage-dependent calcium channels triggers the release of neurotransmitters required to propagate the signal (Figure 1.2). These chemical substances are stored in pre-synaptic vesicles before being released into the synaptic cleft. They then bind to specialised receptors on the post-synaptic cell. Direct chemical transmission is achieved by activating ionotropic receptors; ion channels that are opened upon binding with the neurotransmitter to allow the membrane potential of the post-synaptic cell to be altered. Metabotropic receptors modify pre-synaptic neurotransmitter release and thus have an indirect influence on post-synaptic membrane potential, often via calcium-dependent potassium or chloride channels.

A synaptic potential that excites (depolarises) a post-synaptic cell is an excitatory post-synaptic potential (EPSP) and one that inhibits (hyperpolarises) is called an inhibitory post-synaptic potential (IPSP). The summation of these potentials will either allow or suppress further action potentials, thus determining the likelihood that continued transduction of the signal will take place. EPSPs are triggered by the release of the amino acid glutamate (Glu), which is derived from glutamine via the enzyme Glutaminase (found within pyramidal cells). It binds to either fast (α-amino-3-hydroxy-5-methyl-4-isoxazolepropionic acid; AMPA) or slow signalling (N-methyl-D-aspartate; NMDA) receptors. The latter plays a crucial role in synaptic plasticity, learning and memory, as discussed in the following section. IPSPs are generated by the release of γ-aminobutyric acid (GABA), which is synthesised from glutamate via the glutamic acid decarboxylase (GAD) enzyme (found within inhibitory interneurons, constituting 30% of cells in the human brain; McCormick, 1989). Distinct isoforms have been associated

with GABA production within the vesicles (GAD 65) and cytoplasm (GAD 67), the former having been linked to neurotransmission (Best, Stagg & Dennis, 2014).

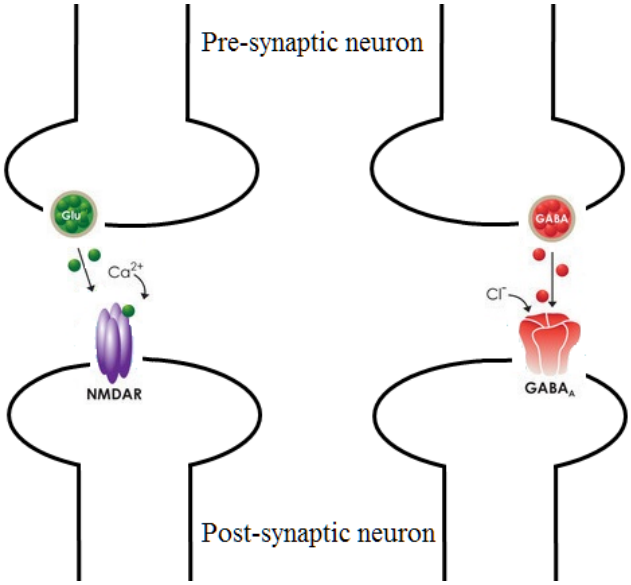

Figure 1.2. Excitatory and inhibitory neurotransmission. Examples of information transfer between neurons via chemical neurotransmission. Having reached the pre-synaptic terminal, the action potential triggers voltage-gated calcium channels to open and signal the release of neurotransmitters; in this instance the primary excitatory and inhibitory neurochemicals, glutamate (Glu) and γ-aminobutyric acid (GABA). These chemical substances cross the synaptic cleft and bind to specific receptor types on the post-synaptic neuron, which determine the action of the neurotransmitter. Activating glutamatergic receptors will excite the post-synaptic cell and increase the likelihood of signal propagation via summed EPSPs, while engagement of GABAergic receptors produces inhibition that will likely suppress the generation of further action potentials.

As the primary inhibitory neurotransmitter in the human brain, the main role of GABA is to activate ionotropic chloride-gated, $GABA_A$ receptors to rapidly modulate excitation via feed-forward inhibitory connections to pyramidal cells (for an overview of basic cell types, see Figure 1.3). Extrasynaptic $GABA_A$ receptors also exist which are said to control 'GABAergic tone' via an increase in chloride permeability, brought about by a spill over of the neurotransmitter from the synaptic cleft (Stagg, 2014). GABA can also act on metabotropic potassium channels to regulate excitatory activity by reducing the rate of glutamate neurotransmission or by altering the action of $GABA_A$ receptors (via feedback-inhibition of pre-synaptic $GABA_B$ receptors).

This image has been removed by the author for copyright reasons.

Figure 1.3. Basic cells of the cerebral cortex. On the left of the image are cells that respond to glutamate e.g. A) pyramidal cell. On the right of the image are cells that respond to GABA e.g. B) double bouquet cell, C,E) basket cells, D) chandelier cells (image adapted from http://webvision.med.utah.edu/imageswv/BasicCells). Connections between multiple pyramidal cells (dark gray triangle) propagate excitation (line with small dark gray arrow), whereas activation of GABAergic interneurons (light gray circle) will lead to inhibition (line with small light gray circle). Connections also exist between excitatory and inhibitory cell types, where interneurons are able to modulate the excitation exerted by pyramidal cells (image adapted from Buzsáki, 2006).

1.1.3 Synaptic plasticity

Connections between neurons can become stronger or weaker, often depending on the extent of their use; a concept known as synaptic plasticity. This can occur over multiple time scales, making information transfer capacity extremely dynamic. Representing a prolonged alteration in the rate of post-synaptic potentials, enduring from several hours to days (Lømo, 1966; Bliss & Lømo, 1973; Madison, Malenka & Nicoll, 1991), long-term potentiation (LTP) is characterised as the use-dependent strengthening of synapses and is driven by increased receptor density and sensitivity. Long-term depression (LTD) reflects the opposite changes. Several factors are crucial for the induction of LTP, which primarily concerns NMDA receptors. For example, it is not sufficient for glutamate to simply bind to these ligand-gated, voltage-dependent channels (Wigstrom, Gustafsson, Huang & Abraham, 1986; Gustafsson, Wigstrom, Abraham & Huang, 1987). Depolarisation of the post-synaptic membrane must occur simultaneously with synaptic activation, such that the magnesium (Mg^{2+}) block at NMDA channels is removed to allow calcium into the post-synaptic cell (Malenka, Kauer, Zucker & Nicoll, 1988; Lynch, Larson, Kelso, Barrionuevo & Schottler, 1983). NMDA channels are often referred to as "coincidence detectors", seeking the arrival of these synchronised events. The influx of calcium and resulting change in intracellular concentration plays a major role in the onset of LTP e.g. via boosted synaptic transmission due to an enhancement of pre-synaptic, protein kinase C enzymes, shown to reverse the action of NMDA blockade induced by antagonistic substances (Kleschevnikov & Routtenberg, 2001).

Much of the initial work into the underlying mechanisms of LTP/LTD was conducted in the hippocampus. More recently, research has taken place to establish the occurrence of these phenomena in the neocortex (Hess & Donoghue, 1994/1996). Here, GABAergic interneurons have also been shown to influence LTP induction within structures of the cerebral cortex (McDonnell, Orekhov & Ziemann, 2007). Trepel and Racine (2000) determined that administration of the benzodiazepine and $GABA_A$ agonist Diazepam

resulted in a failure to induce LTP, following trains of electrical stimulation via implanted microelectrodes. Therefore, increased inhibition due to enhanced $GABA_A$ receptor efficiency appears to be able to block changes in synaptic strength, which indicates that a balance between glutamatergic excitation and GABAergic inhibition is required for LTP to take place. The induction of prolonged changes in synaptic strength and the related influence of these neurotransmitter systems are of central importance to the action of tDCS, as will be discussed in the following section.

1.2. Transcranial Direct Current Stimulation

1.2.1 A historical perspective of transcranial electrical stimulation

Transcranial electrical stimulation (tES) refers to a range of neuromodulation techniques, which involve the application of a weak electric current to the brain in order to produce changes in cortical excitability (for extensive reviews, see Wassermann & Grafman, 2005; Nitsche, Cohen, Wassermann, Priori, Lang & Antal, 2008; Paulus, 2011). Its origin dates back to 43-48 AD where Scribonius Largus used electric fish to provide relief from headache. Galen was also said to have treated headache related discomfort in this manner, while the 11th century physician Ibn-Sidah suggested the procedure may be beneficial for those suffering with epilepsy (Kellaway, 1946). Galvani and Volta pioneered the use of current stimulation in a psychiatric setting as a treatment for melancholic patients, demonstrated by Aldini in 1804 (Parent, 2004: Figure 1.4). Potential applications to aid in the recovery of stroke were also put forward prior to the advent of modern methods (Hellwag & Jacobi, 1802). Despite much promise from these early investigations, the application of current for the alleviation of physical and psychological symptoms promptly ceased with the emergence of electroconvulsive therapy (ECT; Cerletti, 1950).

This image has been removed by the author for copyright reasons.

Figure 1.4. tES methodology across history. A) The use of galvanic current delivered to the scalp to treat melancholia as conducted by Italian physicist Giovanni Aldini in 1804 (image taken from Parent, 2004). B) Modern tES delivered using rubber electrodes and saline soaked sponges via a battery operated device (image taken from the neuroConn website).

It was not until the late 1950's/early 1960's that tES began to re-emerge, when several animal studies investigated the effects of direct current application to the surface of the brain. This was the foundation for what is now referred to as transcranial direct current stimulation (tDCS), which is the main focus of this thesis. In an *in vitro* study, Terzuolo and Bullock (1956) demonstrated the capacity of DC stimulation to modulate the spontaneous firing of cells in slice preparations from crayfish and lobster. Subsequent *in vivo* studies, in which current was applied directly to the cortex of anesthetised rats and cats, demonstrated the effect of distinct polarities and the influence of stimulation duration on spontaneous and evoked activity.

Creutzfeldt, Fromm and Kapp (1962) determined that three quarters of cells studied in visual and motor cortex responded to a current of 200 μA but that the polarity of the applied current led to marked differences in the exhibited response pattern (Figure 1.5). This study was one of the first demonstrations of the characteristic response of neurons to DC stimulation, illustrating that surface-positive (anodal) currents led to depolarisation and surface-negative (cathodal) currents resulted in hyperpolarisation, primarily at the site of the axon hillock. The apical dendrites appeared to be largely unresponsive to stimulation. Accordingly, spontaneous activity increased following the administration of a positive current with an opposite decrease shown for negative current. There was, however, an inversion of this response to polarising currents for cells at depths greater than 3 mm within the motor cortex, where the direction of the potential gradient is likely reversed. This demonstrates the importance of considering cell orientation when observing such effects of cortical stimulation.

Bindman, Lippold and Redfearn (1964) confirmed the polarity-specific findings of Creutzfeldt et al. (1962) and also established the effect of stimulation duration on cortical responses. Application of a positive current for durations exceeding 5 minutes led to an increase in the size of somatosensory evoked potentials. The opposite was found following similar durations of negative current, which reduced evoked potentials for 30 minutes post-cessation. Changes in spontaneous firing were also noted in the expected direction. At longer durations, these after-effects persisted for up to 5 hours and often only reached their peak around 15-30 minutes after the current had been terminated (Figure 1.6). The response change observed during stimulation also had not fully developed until several minutes of stimulation had elapsed, illustrating the sustained evolution of the observed modifications.

Figure 1.5. Changes in spontaneous firing following DC stimulation. Delivery of cathodal, surface-negative (a) and anodal, surface-positive (c) stimulation in comparison to resting baseline activity (b) (image taken from Creutzfeldt et al., 1962).

Purpura and McMurtry (1965) stimulated the ventrolateral nucleus of the thalamus for durations of 5-40 s and recorded the associated intra- and extracellular response from motor cortex. Stimulation was delivered with densities of either 30-80 or 100-400 $\mu A/mm^2$. The former category failed to produce any change in membrane potential, while the latter was not excessively strong such that it induced signs of seizure activity. In a similar manner to Bindman et al. (1964), the study demonstrated extended activity (increased amplitude and duration of EPSPs, as well as increased frequency of spike discharges) beyond the cessation of positive current. However, the duration of the after-effects here were much shorter due to the reduced stimulation durations. This finding demonstrates how the length of stimulation is an essential consideration in the formation of prolonged changes and is largely independent of current intensity. Importantly, the authors also describe the responsiveness of both pyramidal and non-pyramidal cell types, with the latter being more susceptible to lower intensities. This demonstrates the relative contribution of pyramidal cells and interneurons to the observed modifications in cortical response (Stagg & Nitsche, 2011).

Beyond simple modifications of visual and motor responses, a series of experiments focusing on memory retrieval in rats demonstrated that anodal stimulation aided memory consolidation, while a reduction in the ability of the animals to retain recently acquired information was evident following cathodal stimulation of the medial cortex (Albert, 1966a/1966b). These experiments act to further enhance the available knowledge of the capabilities of tDCS by showing how the influence of the technique is applicable beyond low-level sensation to more complex cognitive demands.

Figure 1.6. Effect of prolonged DC stimulation. Persistent effects, up to 2 hours post-termination, following negative stimulation (b-c), compared to a period of baseline activity (a-b) (image taken from Bindman et al., 1964).

The brief re-emergence of DC stimulation failed to have an impact beyond the previously outlined animal research for many years. It was not until relatively recently that interest in the method was reignited, following the first human studies into the influence of tDCS on visual and motor processing (Korsakov & Matveeva, 1982; Elbert, Lutzenberger, Rockstroh & Birbaumber, 1981). At this time, the induction of intracranial currents following stimulation in the region of 1.5 mA was demonstrated in human subjects due to undergo epilepsy surgery, thus corroborating the findings of the preceding animal literature (Dymond, Coger & Serafetinides, 1975). In this instance, the procedure was invasive. However, the use of tDCS in human subjects is commonly performed by applying the current via rubber electrodes placed on the scalp. The onset of these human studies instigated the need for investigations into the pathways the current was likely to take given various electrode configurations as well as renewed explorations into the underlying physiological mechanisms. It was this drive for continued investigation into the influence of tDCS on the human brain and the desire to understand the related neurobiological processes that ultimately contributed to its recent resurgence in use (as stated by Utz, Dimova, Oppenländer & Kerkhoff, 2010).

1.2.2 Methodological advances in modern tDCS research

The most recent incarnation of tDCS was prompted by the research of Priori, Berardelli, Rona, Accornero and Manfredi (1998). This research, like the majority of tDCS investigations conducted to date, concerned the influence of weak DC stimulation on the motor system. The authors were the first to use Transcranial Magnetic Stimulation (TMS) to assess changes in cortical excitability associated with the application of weak current (<0.5 mA). tDCS was administered via two electrode pads; the active electrode positioned on the scalp superior to primary motor cortex (M1) and the reference placed on the chin. The motor threshold of fifteen participants was measured before and after brief periods (7 s) of cathodal and anodal tDCS. Using single TMS pulses, thresholds were established as the lowest intensity required to elicit a motor evoked potential (MEP) response in 50% of successive trials. In this study, the terms cathodal and anodal refer to the direction of current flow, where the electrode configuration remains the same but the polarity is reversed such that there is a designated active and reference electrode. These terms are also commonly used to correspond to the precise location of the electrodes themselves, where the current always flows from the active to the reference electrode but the configuration is altered to achieve the desired influence of applying a positive or negative current to the target region. Cortical excitability was

found to be unchanged after cathodal stimulation but motor threshold was reduced by 8% in amplitude following anodal stimulation, suggesting that a sufficient amount of current was able to pass through the skull and polarise the underlying cortex. Priori et al. went on to attribute this MEP suppression to the hyperpolarisation of superficial excitatory interneurons. These early findings showed the potential of tDCS to rapidly and reversibly alter neuronal activity, however, it was not until the work of Nitsche and Paulus (2000) that the importance of current intensity and duration was established.

Administering weak intensity current (0.2-1 mA) across a variety of durations (4 s, 1-5 minutes), Nitsche and Paulus (2000) further investigated changes in cortical excitability as measured by MEPs following anodal and cathodal stimulation. Delivering tDCS via a montage that has become archetypal for primary motor cortex stimulation (5x7 cm^2 electrodes - left hemisphere M1/right hemisphere frontopolar region), anodal tDCS was found to increase MEPs by 40% while cathodal stimulation produced a 30% reduction. Compared to Priori et al. (1998), Nitsche and Paulus established the opposite pattern of results for anodal stimulation. This has been attributed to the difference in duration and current strength but also the time between the delivery of the separate polarities, which were administered within the same session in the preceding study. Cathodal preceded anodal tDCS during Priori et al's research and the residual effects of hyperpolarisation may have contributed to the anodal results. In contrast, Nitsche and Paulus (2000) confined exposure to each polarity to a separate day thus avoiding confounding carry-over effects. This approach has since become common practice and repeated exposure to tDCS is often delayed by 24 hours to a week, such that cortical excitability is able to return to baseline levels. The study also provided insight into common peripheral side-effects of tDCS, establishing that an intensity of 0.4 mA produced an itching sensation underneath the electrodes in the majority of participants. This is an important consideration for the implementation of functionally inactive, sham tDCS, if subjects are to be blinded to the nature of the stimulation they receive. For this reason, sham tDCS often incorporates a brief (<~30 s) period of current flow to mimic these peripheral sensations before the current is terminated.

What was particularly fascinating about the results of Nitsche and Paulus (2000) was that they provided the first demonstration of tDCS-induced after-effects elicited via the scalp in human subjects (Figure 1.7). The observed MEP changes persisted for several minutes before returning to stable, baseline values. These after-effects only occurred as a product of sufficient intensity (3 minutes, 1 mA) and duration (5 minutes, 0.6 mA).

This indicates that while adjustments in resting membrane potential are sufficient to account for changes following a brief exposure to tDCS (4 s, minimum current density 0.017 mA/cm²), a separate mechanism must be responsible for any effects outlasting this brief period. Having established similar prolonged effects to those documented in rats (Bindman et al., 1964), the authors proposed that changes in short-term potentiation, as a result of the initial modification in spontaneous firing, were likely to underlie the emergence of after-effects. A follow-up study (Nitsche & Paulus, 2001) was able to draw further attention to the potential of tDCS to induce transient neuroplastic change. Using a current intensity of 1 mA, after-effects lasting for 30-90 minutes were observed for both polarities following stimulation durations of 9-13 minutes. Unlike MEP changes following short duration stimulation, MEPs following 13 minutes of tDCS initially appeared to be stable as opposed to rapidly returning to baseline. This enhanced the evidence that tDCS was capable of modulating mechanisms responsible for regulating neuroplasticity, which surpass its potential to briefly alter the resting membrane potential of neurons. A measure of neuronal damage (serumneuron-specific enolase) was also sought during the study, which highlighted the safe use of current densities in the region of 0.029 mA/cm².

These initial landmark studies ensured that tDCS began to be viewed as a viable neurostimulation technique. The research dramatically improved the comprehension of how variations in polarity, intensity and duration could be used to explore the effects of altered cortical excitability in humans. By enhancing the understanding of its capabilities, guidelines on accepted tDCS exposure levels have been established to ensure the method is used within safe limits and produces minimal side effects, such as irritation and skin burns (Nitsche, Liebetanz, Lang, Antal, Tergau & Paulus, 2003a; Iyer, Mattu, Grafman, Lomarev, Sato & Wassermann, 2005; Poreisz, Boros, Antal & Paulus, 2007; Loo, Martin, Alonzo, Gandevia, Mitchell & Sachdev, 2011; Brunoni, Amadera, Berbel, Volz, Rizzerio & Fregni, 2011a). Accordingly, much emphasis has been placed on establishing the suitability of volunteers and comprehensive screening forms are administered as part of the recruitment process to ensure subjects are free from associated contraindications, such as a history of neurological or psychiatric disorders that may influence cortical excitability. Although Purpura and McMurtry (1965) failed to note seizure activity in cats when the maximum current used was delivered directly to the cortex, making the likelihood of seizure induction in healthy humans highly unlikely, the use of screening criteria has without doubt contributed to the prevention of a single seizure episode following tDCS.

Figure 1.7. Prolonged after-effects in human subjects. Polarity-specific, cortical excitability change and persistent after-effects, indexed by changes in MEP amplitudes, following 5 minutes of stimulation at a current intensity of 1 mA (image taken from Nitsche & Paulus, 2000).

Despite the promising nature of the technique and its proposed ability to modulate synaptic efficacy, tDCS is regarded as limited in terms of the precision of current delivered due to the size of the electrodes used. Nonetheless, advances in knowledge relating to current density have seen attempts to improve the focality of the method. Keeping current density stable but reducing the size of the active electrode to 10% of the standard size, Nitsche, Doemkes, Karakoese, Antal, Liebetanz, Lang... and Paulus (2007) noted similar changes in cortical excitability while refining the stimulation area under the electrode. This is where the maximum field strength is situated as determined by Miranda, Lomarev and Hallet (2006) (although the precise distribution of current is likely to be subject to individual differences in anatomical features; Opitz, Paulus, Will, Antunes & Thielscher, 2015). The results of Nitsche et al. (2007) demonstrated the importance of current density as opposed to electrode size per se in producing effective stimulation. The study also demonstrated that the reference electrode could be made functionally redundant by increasing its size (such that current density was below 0.017 mA/cm^2), while not affecting the influence of the active electrode. Although largely speculative at this early stage, these methodological advances (coupled with the developing insight into the proposed mechanisms underlying the short-term and more prolonged after-effects) also fuelled interest in the technique. Consequently, Priori et al. (1998) and Nitsche and Paulus (2000, 2001) paved the way for continued exploration of tDCS in the motor domain.

Investigations have since taken place in many other domains, including visual perception, memory and learning (Antal, Paulus & Nitsche, 2011; Zaehle, Sandmann, Thorne, Jäncke & Herrmann, 2011; Clark, Coffman, Mayer, Weisend, Lane, Calhoun... & Wassermann, 2012; Lally, Nord, Walsh & Roiser, 2013). tDCS research has also extended to somatosensory processing. To date, combined tDCS and basic, behavioural tactile perception studies have focused on Quantitative Sensory Testing (QST; Bachmann, Muschinsky, Nitsche, Rolke, Magerl, Treede... & Happe, 2010; Grundmann, Rolke, Nitsche, Pavlakovic, Happe, Treede... & Bachmann, 2011; Jürgens, Schulte, Klein & May, 2012), frequency discrimination (Rogalewski, Breitenstein,

Nitsche, Paulus & Knecht, 2004) and aspects of spatial discrimination (Ragert, Vandermeeren, Camus & Cohen, 2008; Yau, Celnik, Hsiao & Desmond, 2014; Fujimoto, Yamaguchi, Otaka, Kondo & Tanaka, 2014). However, this field has been dramatically underrepresented compared to that of motor and vision studies.

Researchers have also acknowledged the potential of applying tDCS to multiple neurological and psychiatric disorders. tDCS has been shown to facilitate stroke rehabilitation (Fusco, De Angelis, Morone, Maglione, Paolucci, Bragoni & Venturiero, 2013; Stagg & Johansen-Berg, 2013; O'Shea, Boudrias, Stagg, Bachtiar, Kischka, Blicher & Johansen-Berg, 2014), alleviate sensory deficits in multiple sclerosis (Mori, Nicoletti, Kusayanagi, Foti, Restivo, Marciani & Centonze, 2013), reduce cognitive symptoms in schizophrenia (Agarwal, Shivakumar, Bose, Subramaniam, Nawani, Chhabra... & Venkatasubramanian, 2013), decrease the perception of experimentally induced pain and that associated with Fibromyalgia (Antal, Brepohl, Poreisz, Boros, Csifcsak & Paulus, 2008; Villamar, Wivatvongvana, Patumanond, Bikson, Truong, Datta & Fregni, 2013) and improve mood in major depression (Ferrucci, Bortolomasi, Vergari, Tadini, Salvoro, Giacopuzzi... & Priori, 2009) (for reviews on the clinical application of tDCS, see Brunoni, Nitsche, Bolognini, Bikson, Wagner, Merabet... & Fregni, 2012; Mondino, Bennabi, Poulet, Galvao, Brunelin & Haffen, 2014).

In relation to other neurostimulation methods (e.g. TMS), tDCS is inexpensive, portable and offers additional benefits with regard to the efficiency of blinding both subjects and researchers to the nature of the stimulation delivered, thus making it ideal for clinical trials (Priori, Hallett & Rothwell, 2009). Alternative tES methods may also prove to be useful in a clinical setting. Transcranial alternating current stimulation (tACS) delivers electrical stimulation that oscillates at a desired frequency, while the frequency of current delivered will vary within a broader specified range during transcranial random noise stimulation (tRNS) (Paulus, 2011; Antal & Paulus, 2013). These methods have the capacity to induce more pronounced and less predictable patterns of neuronal activity than DC stimulation, to synchronise or perturb cortical oscillatory rhythms that have been implicated in a range of disorders (Helfrich, Schneider, Rach, Trautmann-Lengsfeld, Engel & Herrmann, 2014; Van Doren, Langguth & Schecklmann, 2014; Uhlhaas & Singer, 2006). However, the clinical benefits of tDCS (and tES in general) would be greatly advanced if the neurobiological underpinnings of the method were better appreciated. It is this desire to better apply the technique that has encouraged research into the influence of tDCS at a physiological level.

1.2.3 Physiological mechanisms governing the induction of tDCS effects

Early animal research established that the size of evoked potentials and changes in spontaneous firing rate following stimulation were a product of current polarity (Creutzfeldt et al., 1962; Bindman et al., 1964). An increase in evoked potential amplitude and firing rate was attributed to depolarisation of cells subject to anodal stimulation. Likewise, suppressed cell responsivity via hyperpolarisation was said to account for the actions of cathodal stimulation. These results were supported during the initial human studies in which increased and decreased motor thresholds were interpreted in the context of polarity-specific changes in spontaneous firing (Nitsche & Paulus, 2000/2001). However, recent research has outlined how this approach is likely to be over-simplified, with specific features of a given cell exhibiting stimulation induced changes in excitability depending on their susceptibility to become polarised as opposed to a general state of de/hyperpolarisation applying to the entire cell (Figure 1.8: Rahman, Reato, Arlotti, Gasca, Datta, Parra & Bikson, 2013; de Berker, Bikson & Bestmann, 2013).

Figure 1.8. Effects of polarisation on pyramidal cells. According to the orientation (radial/tangential) and location of the cell (deep/superficial cortical layer), unique polarisation profiles are likely to be induced via tDCS. For example, following anodal stimulation, a deep (layer V) pyramidal cell in a radial orientation will exhibit depolarisation of the soma but hyperpolarisation at the dendrites (image taken from Rahman et al., 2013).

Aside from shaping our knowledge of the physiological underpinnings of anodal and cathodal polarities, the animal literature and subsequent human research indicate that there are separate mechanisms which govern the effects of brief stimulation compared to those derived following more prolonged exposure. Accordingly, a distinction has been made between effects that take place during stimulation and those that arise and are persistent after stimulation cessation (Stagg & Nitsche, 2011). The work of Bindman et al. (1964) and Purpura and McMurtry (1965) determined that applying constant current to the cortex for longer than a few seconds led to effects that persisted beyond cessation. This distinction was evident at short durations (e.g. 5-40 s, Purpura & McMurtry, 1965) and was also prominent at extended durations (e.g. 9-13 minutes, Nitsche & Paulus, 2001).

At brief durations, changes in cortical excitability were attributed to rapidly recovering fluctuations in resting membrane potential, governed by voltage-gated ion channels. Support for this notion has subsequently been established via research involving human subjects, which maintains that the influence of tDCS during stimulation is purely dependent on changes in membrane excitability (Nitsche, Liebetanz, Schlitterlau, Henschke, Fricke, Frommann... & Tergau, 2004a). Pharmacological evidence suggests that blocking the action of sodium (Carbamezipine, CBZ) and calcium channels (Flunarizine, FLU) results in diminished anodal tDCS effects (Nitsche, Fricke, Henschke, Schlitterlau, Liebetanz & Lang, 2003b). However, similar results were not found for cathodal tDCS, perhaps because the impact of cathodal stimulation is to induce hyperpolarisation, which mimics the already induced effect of pharmacologically blocking sodium and calcium channels. Therefore, short stimulation durations of several seconds typically lead to changes in membrane excitability, characterised by changes in the flow of sodium and calcium ions. The after-effects resulting from longer durations, were speculated to mimic short/long-term potentiation and depression type mechanisms, depending on the duration of current administered. This implicates alterations in synaptic plasticity, not found at shorter durations, suggesting a role for tDCS in the modulation of associated neurotransmitter functions and receptor activation.

Pharmacological interventions have been used to determine the respective roles of glutamate and GABA in the induction of tDCS modulations. Liebetanz, Nitsche, Tergau & Paulus (2002) demonstrated a suppression of the after-effects of both anodal and cathodal tDCS following administration of the NMDA antagonist Dextromethorphane (DMO), illustrating the involvement of these specific glutamatergic receptors. Identical results have also been found for cathodal stimulation during a subsequent study (Nitsche et al., 2003b: Figure 1.9). Further evidence for the role of NMDA in anodal after-effects has been produced using D-cycloserine (CYC), a partial NMDA agonist (Nitsche, Jaussi, Liebetanz, Lang, Tergau & Paulus (2004b), which prolonged the duration of the resulting after-effect. The involvement of NMDA receptors is thought to be dependent upon an initial depolarisation, brought about by the change in sodium and calcium levels, which appears to be the case for the after-effects of anodal tDCS. Such synchronised depolarisation and binding of glutamate to the post-synaptic cell would fulfil the coincidence detection criteria for NMDA receptors to propagate a rise in intracellular calcium and subsequently elicit LTP. However, there is less certainty regarding the precise nature of the NMDA response to cathodal stimulation.

Furthermore, the $GABA_A$ agonist Lorazepam (LOR) has been shown to modulate the typical increase in excitability following, but not during, anodal tDCS (Nitsche et al., 2004a). However, the same cannot be said for cathodal stimulation as no impact of LOR was found on the related after-effects. Therefore, anodal tDCS effects are likely to be driven by glutamatergic and GABAergic mechanisms as they have been suggested to engage both excitatory pyramidal cells and inhibitory interneurons (Nitsche, Seeber, Frommann, Klein, Rochford, Nitsche... & Tergau, 2005; Radman, Ramos, Brumberg & Bikson, 2009; Medeiros, de Souza, Vidor, de Souza, Deitos, Volz... & Torres, 2012). Cathodal after-effects seem to depend largely on changes in NMDA receptor response. As GABA is synthesised from glutamate via the GAD enzyme, concentrations of glutamate and GABA are expected to be correlated (Krause, Márquez-Ruiz & Cohen Kadosh, 2013). Consequently, any changes in GABA linked to cathodal tDCS may simply relate to the more crucial alteration of glutamate levels.

Figure 1.9. Influence of NMDA receptor block on tDCS after-effects. The administration of Dextromethorphane (DMO) resulted in the abolishment of stimulation effects derived under placebo (PLC) (image taken from Nitsche et al, 2003b).

Use of Magnetic Resonance Spectroscopy (MRS) to non-invasively quantify levels of neurotransmitters in a given voxel, has also allowed for an enhanced understanding of the neurochemical basis of tDCS effects. Following 10 minutes of stimulation at 1 mA, Stagg, Best, Stephenson, O'Shea, Wylezinska, Kincses... and Johansen-Berg (2009) demonstrated a significant reduction in glutamate concentration, with a correlated GABA decrease, associated with cathodal tDCS. This further suggests that diminished excitation underlies the effect of stimulation with a negative current, while the correlated GABA reduction is predicted to be driven primarily by the related increase in glutamate. Within the same study, levels of GABA were shown to be reduced following anodal tDCS, supporting the role of changes in intracortical inhibition in the induction of LTP-like, tDCS after-effects related to positive current application (Figure 1.10). The likely mechanism for this outcome originates from the prolonged membrane depolarisation induced by anodal tDCS. This increase in cortical excitability is proposed to eventually lead to a change in neurotransmission, with the production of GABA being halted by resulting modifications in the action of the GAD enzyme. The abundance of glutamate not used to produce GABA is available to bind to post-synaptic

NMDA receptors, which enhances activity at the synapse and leads to increased EPSPs to complement the depolarisation, all of which contributes to the induction of LTP.

Figure 1.10. Role of neurotransmission in tDCS after-effects. Change in concentrations of glutamate (gray bar) and GABA (white bar) in a sensorimotor voxel (as a ratio to NAA) following 10 minutes of stimulation with an intensity of 1mA. Note the significant reduction in GABA for anodal stimulation and the significant reduction in glutamate for cathodal stimulation, which also correlated with the reduction in GABA (images taken from Stagg et al., 2009).

The use of paired-pulse TMS protocols, shown to probe specific receptor types (Liepert, Schwenkreis, Tegenthoff & Malin, 1997), has allowed for the further fractionation of the role of GABA (Nitsche et al., 2005). A reduction in cortical silent period (CSP) duration following anodal tDCS has been found, illustrating the involvement of $GABA_B$ receptors in the generation of anodal after-effects (Tremblay, Beaulé, Lepage & Théoret, 2013). A reduction in short-interval intracortical inhibition (SICI), a measure of $GABA_A$ receptor response, has also been demonstrated following anodal tDCS (Antal, Terney, Kühnl & Paulus, 2010a). Therefore, both fast and slow acting inhibitory mechanisms are likely to be modulated by prolonged durations of tDCS.

To a lesser extent, the influence of dopamine and serotonin on tDCS after-effects has also been investigated (Nitsche, Lampe, Antal, Liebetanz, Lang, Tergau & Paulus, 2006; Kuo, Paulus & Nitsche, 2008; Nitsche, Kuo, Karrasch, Wächter, Liebetanz & Paulus, 2009; Brunoni, Kemp, Shiozawa, Cordeiro, Valiengo, Goulart... & Benseñor, 2013; Monte-Silva, Kuo, Hessenthaler, Fresnoza, Liebetanz, Paulus & Nitsche, 2013; Fresnoza, Stiksrud, Klinker, Liebetanz, Paulus, Kuo & Nitsche, 2014a). Specifically, such research emphasises the role of these monoamines in the modulation of excitatory and inhibitory processes, already outlined as crucial factors in the generation of these prolonged effects. Fresnoza, Paulus, Nitsche & Kuo (2014b) determined a non-linear relationship between tDCS (anodal and cathodal) and the status of the dopaminergic system (under low, medium and high doses of D1-like receptor enhancement (L-DOPA) and D2 receptor block (Sulpiride)). This relationship manifested as an abolishment of the anodal excitability enhancement (observed under placebo) for low and high doses while a medium dose failed to modify the after-effect. Following cathodal stimulation, the observed decrease in cortical excitability was reversed to become a facilitation effect under low and high doses, however, a medium dose eliminated the typical after-effect.

The authors explain these results as a product of the impact of D1 and D2 receptors on NMDA and GABAergic receptors. Interestingly, the tDCS results mimicked those of a parallel experiment concerning excitatory and inhibitory Paired Associative Stimulation (PAS), shown to engage glutamatergic synapses and induce changes in neuroplasticity (Stefan, Kunesch, Cohen, Benecke & Classen, 2000). Therefore, these results further support the importance of excitatory and inhibitory mechanism while emphasising the mediating role of additional neurotransmitter systems in the generation of tDCS after-effects.

The outlined research has provided a foundation of compelling evidence, which has cumulatively formed our understanding of tDCS physiology. However, these studies are in a minority compared to the abundance of behaviour-oriented research. Furthermore, findings derived from similar studies often do not align – for example, MEP amplitude modulation varies greatly for identical protocols – to the extent that there is a lack of consist evidence in support of the cognitive and neurobiological effects of tDCS in the existing literature (Horvath, Carter & Forte, 2014; Horvath, Forte & Carter, 2015a/2015b). To fully comprehend the effects of tDCS, their origin must first be better clarified through continued investigations such as those conducted for the purpose of this thesis. Research of this nature should assist in the ultimate aim of tDCS research; the optimisation of its use in conjunction with the most physiologically-relevant, neurological and psychiatric disorders (in the clinical domain) and behavioural/cognitive paradigms (in a research setting).

1.3. Functions of the Nervous System

1.3.1 The motor system

1.3.1.1 Structure & function of the motor system

The motor system is responsible for the selection, planning and execution of movements. Unlike the majority of systems (that carry sensory inputs towards the central nervous system via afferent fibers), motor responses are expressed via efferent connections that descend from the cerebral cortex to the muscles. This specific review of the motor system will focus on the control of voluntary actions made in order to fulfil certain movement-oriented goals (as utilised by the task featured in Chapter 5). For a

detailed overview, see the relevant chapters in the following texts (Rosenzweig, Breedlove & Watson, 2005; Purves, Cabeza, Huettel, LaBar, Platt & Woldorff, 2013).

At the level of M1 in the precentral gyrus (Rizzolatti & Luppino, 2001), commands to generate actions are initiated that predominantly correspond to the precise movement to be executed as opposed to the muscle group targeted (Evarts, 1968; Kakei, Hoffman & Strick, 1999; Vargas-Irwin, Shakhnarovich, Yadollahpour, Mislow, Black & Donoghue, 2010). These commands are encoded by upper motor neurons, which have been shown to be selective for specific directions of movements (Georgopoulos, Kalaska, Caminiti & Massey, 1982; Merchant, Naselaris & Georgopoulos, 2008). This property of M1 cells indicates a high degree of processing specificity, which is a common feature of primary cortical regions within the systems documented throughout this sub-chapter. Use-dependent, adaptive changes in plasticity following motor-based learning tasks have also been observed in M1 (another recurring theme among many sensory systems: Nudo, Milliken, Jenkins & Merzenich, 1996; Matsuzaka, Picard & Strick, 2007). This refinement of receptive fields appears to be based on local changes in intracortical inhibition and excitation and can manifest as temporary or long-lasting changes that have applications from learning new skills to stroke rehabilitation (Karni, Meyer, Rey-Hipolito, Jezzard, Adams, Turner & Ungerleider, 1998; Liepert, Miltner, Bauder, Sommer, Dettmers, Taub & Weiller, 1998; Hund-Georgiadis & von Cramon, 1999; Floyer-Lea, Wylezinska, Kincses & Matthews, 2006; Bachtiar & Stagg, 2014).

Despite the importance of M1, the commands that define the control of movements are not simply generated by single M1 neurons. Instead they are the product of inputs from neuronal populations across the entire motor network, comprising of several local and distant regions, all of which are integrated in the brainstem (Kalaska, Scott, Cisek & Sergio, 1997) (Figure 1.11). The supplementary motor area (SMA) adjacent to the precentral gyrus has been shown to sub-serve the generation of complex, internally-generated voluntary movement sequences, while prefrontal cortex has been demonstrated to be integral to the planning and formation of externally cued movements (Mushiake, Inase & Tanji, 1991; Halsband, Matsuzaka & Tanji, 1994; Hoshi & Tanji, 2004). Interestingly, evidence of “readiness potential” responses prior to actual movement activity have been documented in the SMA and premotor regions before they are evident in M1, indicating a role for these supplementary regions in the preparation and temporary inhibition of cued responses prior to their execution (Kornhuber & Deecke, 1964; Eagleman, 2004; Shibasaki & Hallett, 2006).

Additional regions such as the basal ganglia and cerebellum have been proposed to have an active role in the modulation of movement control (by influencing the response of upper motor neurons in M1 and the brainstem), with the former being shown to mediate the speed and direction of movements and the latter having been implicated in the coordination of skilled movement (Takakusaki, Saitoh, Harada & Kashiwayanagi, 2004; Manto, Bower, Conforto, Delgado-García, da Guarda, Gerwig... & Timmann, 2012). Consequently, these regions exert top-down control over local circuitry via M1 and the brainstem, specifying what each muscle group should do and how it should be doing it.

Figure 1.11. Location of the motor system. Lateral (left) and medial (right) representations of the site of M1, SMA and premotor cortex about the precentral gyrus (image taken from Purves et al., 2013).

Having passed through the brainstem, the efferent input travels down the axons of motor neurons from precentral gyrus to the spinal cord, predominantly via the lateral corticospinal or pyramidal tract (Figure 1.12). Prior to entering the spinal cord, these fibers cross the midline or decussate at the level of the medulla, meaning that commands from the left hemisphere control muscles in the right side of the body. Regions of cortex and spinal cord are topographically organised thus producing correspondence between the brain and body, such that the representation of the body within these central nervous system structures is mapped to the configuration of the innervated muscles (Leyton & Sherrington, 1917; Dum & Strick, 2002; Levine, Lewallen & Pfaff, 2013).

Figure 1.12. Corticospinal tract. The primary efferent pathway connecting central and peripheral nervous system structures that initiate and execute goal-oriented actions (image taken from Purves et al., 2013).

Both large and small motor neurons in the spinal cord generate contractions by targeting action potentials towards the desired muscle group. Large motor neurons produce phasic action potentials and project to fast-twitch muscles to enable transient, dynamic movement, whereas small motor neurons innervating slow-twich fibers fire in a more tonic fashion to cause sustained, rhythmic movement (Ellisman, Rash, Staehelin &

Porter, 1976). These action potentials are propagated from the spinal cord via multiple branches of the axons of lower motor neurons to the neuromuscular junction, where the motor neurons synapse with the muscles. This triggers the release of acetylcholine, which signals the muscle fibers to also produce action potentials that allow an influx of sodium and calcium ions. In turn, this generates the necessary change in actin and myosin (proteins integral to muscle movement e.g. contraction and force exerted) to produce the desired action (Pollard & Cooper, 2009).

1.3.2 The visual system

1.3.2.1 Structure & function of the visual system

In order to form a visual perceptual representation of environmental stimuli, firstly, the lens of the eye must focus light onto the retina (for a detailed overview of the visual system, see Snowden, Thompson & Troscianko, 2012). Here, sub-types of photoreceptor convert light energy into bioelectrical impulses (the process of transduction; Hudspeth & Logothetis, 2000). Of the two main receptor classes, Cones are responsible for vision under conditions of daylight with high densities in the fovea, at the centre of the visual field. Rods are highly sensitive to movement, are primarily located in the periphery and respond best in low light conditions. These receptors connect to bipolar cells which synapse with retinal ganglion cells. The magnocellular sub-type has been demonstrated to be specialised for motion detection, whereas the parvocellular cells respond to colour. Both types of retinal ganglion cells project separately to the lateral geniculate nucleus (LGN) of the thalamus in each hemisphere via the optic nerve across the optic chiasm, where a partial decussation (or fiber cross-over) takes place to form separate optic tracts (Figure 1.13).

At the level of the LGN, layers of magnocellular and parvocellular cells remain segregated as does sensory information from each eye. Koniocellular cells are also present in the LGN, which are specialised for blue-yellow colour vision whereas parvocellular cells are responsive to green-red distinctions. The LGN was initially characterised as a somewhat passive relay centre for visual information prior to reaching the cortex, however, research has shown this region to respond to modulations in attention thus highlighting its active role in visual perception (Kastner, Schneider & Wunderlich, 2006). Light signals corresponding to the position on the retina are

translated to the LGN such that neighbouring regions of the visual field are also represented as adjacent in the LGN (Chen, Zhu, Thulborn & Ugurbil, 1999). This is known as retinotopic mapping, which allows us to form an effortlessly coherent and streamlined perception of a visual scene. From the LGN, the optic radiations synapse with primary visual cortex, also commonly referred to as striate cortex or V1, with each hemisphere separated by the calcarine sulcus of the occipital lobe. The topographic representation found in the LGN is maintained in V1, meaning that regions of the visual field are also represented as adjacent in the cortex (Engel, Glover & Wandell, 1997; Tootell, Hadjikhani, Vanduffel, Liu, Mendola, Sereno & Dale, 1998).

Figure 1.13. Visual system. Cross-sectional representation of the connections between peripheral and central nervous system structures within the visual system (image taken from Snowden et al., 2012).

It should, however, be noted that the visual field image is represented as rotated both vertically and horizontally within primary visual cortex (e.g. the lower left visual field will be projected to the upper right portion of V1; Wandell, Dumoulin & Brewer, 2007). While receptive fields in the retina and LGN are represented as concentric circles with specific regions of excitation and inhibition (Hartline, 1938; Kuffler, 1953; Leenie, 2003), V1 is organised in columns of neurons specialised to respond to specific stimulus attributes, such as orientations (e.g. the grating pattern presented during the task administered in Chapter 5). This was first noted in the visual cortex of cats by Hubel and Wiesel (1963) who suggested that such processing specificity was an indication of stimulus tuning. Therefore, the authors concluded that the content processed by V1 must be increasingly refined and filtered throughout the visual system, with increased stimulus complexity needed to evoke a response. Similar findings have also been found in non-human primates (Hubel & Wiesel, 1974).

Accordingly, areas beyond V1 (known as extrastriate regions, Figure 1.14) perform increasingly specialised functions. In isolation, V1 and V2 are widely regarded to only process simple object structure, V3 is concerned with shape perception and spatial localisation, whereas V4 and V5/MT neurons process aspects of colour and motion perception, respectively (Zeki, 1973; Rodman & Albright, 1987; Zeki, Watson, Lueck, Friston, Kennard & Frackowiak, 1991; McKeefry & Zeki, 1997; Snowden, Thompson & Troscianko, 2012). However, multiple feed-forward as well as horizontal and feed-

back connections exist between regions of visual cortex, such that further refined and comprehensive responses are enabled (Hupe, James, Payne, Lomber, Girard & Bullier, 1998; Kourtzi, Tolias, Altmann, Augath & Logothetis, 2003; Callaway, 2004). Additionally, neurons in V1 have been shown to demonstrate response dynamics (as have those within the retinal ganglion cells and LGN), where receptive field size is modulated as a product of stimulus context (Gilbert, 1996; Kohn, 2007). As previously outlined, the capacity for receptive field plasticity is, however, by no means unique to the visual system.

Figure 1.14. Extrastriate regions of the visual system. From V1, receptive fields of neurons respond to more complex visual stimuli, which is subject to hierarchical processing within multiple extrastriate regions that demonstrate specialised responses for certain stimulus features (image taken from Snowden et al., 2012).

1.3.3 The somatosensory system

1.3.3.1 Structure & function of the somatosensory system

The human somatosensory system is responsible for the transfer and processing of sensory signals arising from stimulation of the surface of the body. These signals encompass information relating to specific receptor types for pain (nociceptors), chemical levels (chemoreceptors), temperature (thermoreceptors) and touch (mechanoreceptors) (McGonigle, 2004; Mountcastle, 2005). From the peripheral afferent fibers innervating the surface of the skin ascending to the spinal cord and thalamus of the central nervous system, these signals ultimately arrive at the cerebral cortex and undergo initial processing in primary somatosensory cortex (S1; Pleger & Villringer, 2013).

Organised in functionally specific columns of receptors (Mountcastle, 1957), S1 contains a one-to-one representation of the entire surface of the body, existing such that adjacent areas of skin correspond to neighbouring regions of cortex (Kurth, Villringer, Mackert, Schwiemann, Braun, Curio... & Wolf, 1998; McGonigle, Aston, Josephs & Frackowiak, 1998; Sanchez-Panchuelo, Francis, Bowtell & Schluppeck, 2010). Therefore, information is transferred such that the position of a cortical neuron is related to its peripheral receptive field, thus creating a somatotopic map. The space occupied by each part of the body within this cortical representation (often illustrated using the

sensory homunculus; Penfield & Rasmussen, 1950) is illustrative of the wealth of sensory information received (Figure 1.15).

Consequently, a disproportionate amount of cortex is allocated to the hands, particularly the thumb and index finger (D1 and D2), due to the fine detail represented by the receptive fields of each digit (Sutherling, Levesque & Baumgartner, 1992; Francis, Kelly, Bowtell, Dunseath, Folger & McGlone, 2000; Koch, Habermehl, Mehnert, Schmitz, Holtze, Villringer... & Obrig, 2010; Sanchez-Panchuelo et al., 2010). Due to their contribution to tactile perception, the consideration of the somatosensory system documented here will focus on the processing of touch (mechanical distortion) as a result of stimulation delivered to the glabrous skin of the hand (documented in conjunction with the tasks administered in Chapters 6 & 7).

Figure 1.15. Somatosensory homunculus (representation of the hand). In accordance with earlier findings, the representation derived from MEG data illustrates the locations of equivalent current dipoles (ECD) related to the respective regions of the body (the size of which was taken as an indication of spatial extent). Note the size and relative importance of the hand compared to the chest region, demonstrating the wealth of sensory input from the digits (image taken from Nakamura et al., 1998).

At the periphery, mechanoreceptors transduce the initial mechanical distortion into a representation that can be interpreted by the nervous system, in terms of a change in electrical potential. There are four receptor sub-types characterised on the basis of their response to this alteration, which results in a state of depolarisation following an increase in sodium and potassium flow (Johansson & Valbo, 1979; Bolanowski, Gescheider, Verrillo & Checkosky, 1988). Ruffini corpuscles (SA2) and Merkel disks (SA1) are referred to as slow adapting (SA) receptors, which maintain the change in electrical potential throughout the duration of the stimulus. Therefore, SA types are recruited to respond to tonic stimuli, such as prolonged pressure, which do not vary over time. Conversely, Meissner (RA) and Pacinian (PC) corpuscles are classified as rapid adapting (RA) receptors and respond to phasic stimuli, such as vibration, eliciting brief bursts of activity prior to falling silent following the onset of a more dynamic stimulus. Each receptor sub-type is therefore specialised to respond to particular stimulus characteristics. Ruffini corpuscles have been identified to respond to stretch and Merkel disks to pressure, which are predominantly static stimuli, whereas Meissner corpuscles are dedicated to the detection of low frequency vibration (‘flutter’, 20-50 Hz), and

Pacinian corpuscles, which reside in deeper, subcutaneous tissue, detect vibratory stimuli of higher frequency (100-300 Hz) (for a review of mechanoreceptor function, see Johnson, 2001; Gescheider, Bolanowski & Verrillo, 2004).

These somatosensory receptor sub-types form the initial stage of the dorsal column otherwise known as the medial lemniscal pathway (Figure 1.16), linking the discriminative touch systems of the peripheral and central nervous systems (Nolte & Sundsten, 2002; Mountcastle, 2005; Hains, 2007; Kamali, Kramer, Butler & Hasan, 2009).

Figure 1.16. Processing of tactile information. A) The Dorsal Column pathway. This ascending system transports signals relating to discriminative touch from the peripheral to central nervous system. B) The location of Primary (S1) and Secondary (S2) Somatosensory cortices. From S1, basic tactile information enters a processing hierarchy, where representations become more complex upon reaching S2 (images taken from Purves et al., 2013).

At the level of the CNS, afferent fibers ascend the spinal cord to the brain stem via the dorsal column. Stimuli detected in fibers below mid-thoracic level, such as those at the hands, project to the gracile fasciculus, which synapses with gracile nucleus second order neurons upon entering the medulla. Beyond this point, projections decussate to form the medial lemniscus after which the body's surface is represented contralaterally. Projections then ascend to the ventral posterior lateral (VPL) nucleus of the thalamus to synapse with third order neurons. At the level of the thalamus, sub-regions of the VPL project to the post-central gyrus of the anterior parietal cortex (Brodmann's areas 3b, 3a, 1 and 2; Brodmann, 1909), in concordance with Geyer, Schleicher & Zilles, 1999). Results of functional magnetic resonance imaging (fMRI) studies show similar clusters of activity corresponding to these sub-regions (Moore, Stern, Corkin, Fischl, Gray, Rosen & Dale, 2000; Nelson & Chen, 2008; Overduin & Servos, 2008; Sanchez-Panchuelo, Besle, Beckett, Bowtell, Schluppeck & Francis, 2012). From area 3b towards posterior parietal cortex (BA 5, 7) a processing hierarchy is evident from a change in receptive field size, from small to large, with a decline in the simplicity and specificity of neural responses (Sinclair & Burton, 1993; Ploner, Schmitz, Freund & Schnitzler, 2000; Ruben, Schwiemann, Deuchert, Meyer, Krause, Curio... & Villringer, 2001). As such, area 3b contains the largest number of neurons possessing high-level detail of the surface of the body (Iwamura, 1998). For this reason it is considered to represent true primary somatosensory cortex.

1.3.3.2 Dynamics of primary somatosensory cortex

In order for a sensory system to efficiently engage in information processing, it is necessary for the underlying physiological mechanisms to be optimised to respond to incoming stimuli. As in the motor and visual systems, somatosensory neurons are capable of transiently altering their response properties based on stimulus history (Tommerdahl, Favorov & Whitsel, 2010). Following repeat or continued exposure, S1 pyramidal cells undergo a reduction in firing rate in response to vibrotactile stimuli with similar properties (Kelly & Folger, 1999; Chen, Friedman & Row, 2003). This process has been referred to as vibrotactile adaptation. However, as opposed to representing an afferent habituation effect, as previously proposed (Verrillo, Fraioli & Smith, 1969), there appears to be a more complex, facilitatory mechanism at its core. This has been outlined in an extensive review of somatosensory dynamics, in which vibrotactile adaptation was described as a process geared towards enhanced efficiency of tactile stimulus processing rather than simple response dampening (Kohn & Whitsel, 2002). The beneficial nature of vibrotactile adaptation has previously been illustrated during investigations of both frequency and amplitude discrimination tasks. Subjects demonstrated an enhanced behavioural capacity to perform each task when they had been exposed to stimuli prior to being tested (Goble & Hollins, 1993; Goble & Hollins, 1994; Delemos & Hollins, 1996). These pioneering studies represent a practical demonstration of somatosensory dynamics, illustrating how stimulus history can sharpen subsequent responses.

There has been much debate as to the stage at which vibrotactile adaptation arises. While research indicates that adaptation is able to occur at the level of the peripheral nervous system (Bensmaia, Leung, Hsiao & Johnson, 2005; Leung, Bensmaia, Hsiao & Johnson, 2005), compelling physiological evidence suggests that the response modifications required for the type of rapid adaptation in question predominantly occur at the level of the cortex. There have been reports that the reduction in spiking rate of RA peripheral neurons is dramatically attenuated, compared to that of their cortical counterparts, following exposure to flutter stimuli (O'Mara, Rowe & Tarvin, 1988; Whitsel, Kelly, Delemos & Quibrera, 2000). This demonstrates that peripheral fibers do not adapt as readily and firing rates remain stable even during long periods of stimulation. Peripheral afferent adaptation also appears to require longer periods of stimulation than are sufficient to produce a behavioural effect, which can be detected

following exposure times in the order of milliseconds (Whitsel, Kelly, Quibrera, Tommerdahl, Li, Favorov... & Metz, 2003).Therefore, given the time scale on which adaptation typically operates, CNS processes are likely to govern any change in short-term plasticity.

To further define the role of CNS processes in stimulus-driven plasticity, past research has examined the influence of specific neurotransmitters. Fluctuations in the prevalence of the major inhibitory and excitatory CNS neurotransmitters, GABA and glutamate, as well as the action of related post-synaptic receptors ($GABA_A$, NMDA), have been suggested to underlie vibrotactile adaptation (Lee & Whitsel, 1992). Accordingly, the role of the excitation/inhibition balance has been emphasised during animal-based investigations, largely conducted in rats and non-human primates, which have documented the time-course of responses of pyramidal neurons in primary somatosensory cortex (Lee, Whitsel & Tommerdahl, 1992). Using optical intrinsic signal imaging (OIS), it was demonstrated that cutaneous flutter stimulation initially resulted in widespread activation of single neurons but rapidly developed into a refinement of receptive fields (Whitsel et al., 2003). This refinement manifested as a reduction in response magnitude and a filtering of afferent signal input to more relevant sub-regions of the activated macrocolumns (those minicolumns best able to localise and process the stimulus). During this time, firing became increasingly synchronised at the population level. With continued exposure, the spatial pattern of activation within S1 also changed. The redundant surrounding regions were subject to increased lateral inhibition (Figure 1.17a) and a consequent suppression of spiking activity, thereby entering a state of hyperpolarisation.

Figure 1.17. Lateral inhibition. A) The process of lateral inhibition facilitates the localisation of sensory input by increasing excitation (magnitude of the response) at the site of the stimulus while inhibiting the response of neighbouring columns of neurons. B) A task-specific example of lateral inhibition following adaptation to stimuli of increasing intensity. These 3D surface maps show enhanced absorbance at the precise site of the stimulus (red) and a decrease in the proximal region (blue) due to an elevation in inhibition (image taken from Simons et al., 2005).

These emergent changes in S1 response have subsequently been shown to be intensified with increased duration and amplitude of tactile stimulation (Simons, Tannan, Chiu, Favorov, Whitsel & Tommerdahl, 2005; Chiu, Tommerdahl, Whitsel & Favorov, 2005; Simons, Chiu, Favorov, Whitsel & Tommerdahl, 2007; Figure 1.17b). Accordingly,

increased absorbance (reflecting neurovascular response as a marker of neuronal activity) at the site of the stimulus has been observed alongside inhibition of the surrounding region. Local competitive interactions between minicolumns, therefore, appear to be essential in shaping the response to repetitive stimuli, thus supporting the role of GABAergic, lateral inhibition in vibrotactile adaptation (Tommerdahl, Favorov & Whitsel, 2002).

The proposed role of GABAergic inhibition has also been demonstrated via studies concerning the influence of adaptation on vibrotactile task performance, within clinical populations. Such research has primarily concerned Autism Spectrum Disorder (ASD), in which dysfunctional GABA-mediated minicolumnar connectivity is thought to be responsible for the sensory symptoms exhibited (Casanova, Buxhoeveden, Switala & Roy, 2002; Casanova, Buxhoeveden & Gomez, 2003; Uhlhaas & Singer, 2006, Uhlhaas & Singer, 2012). There is often a marked distinction in task performance between those with ASD and healthy controls, following adaptation. This has been found during tasks such as spatial localisation, temporal order judgement and amplitude discrimination (Tommerdahl, Tannan, Cascio, Baranek & Whitsel, 2007; Tommerdahl, Tannan, Holden & Baranek, 2008; Tannan, Holden, Zhang, Baranek & Tommerdahl, 2008). Typically, performance in healthy controls will either be enhanced or degraded, depending on the precise task parameters. However, Autistic individuals do not appear to be as susceptible to the effects of adaptation, often performing similarly during baseline and adaptation trials. This illustrates how altered CNS sensitivity, characterised here in part as a GABAergic deficiency, is able to dramatically change normal stimulus processing capabilities with regard to the impact of adaptation. Pharmacologically-induced alterations in CNS sensitivity have also highlighted the involvement of glutamate-mediated, NMDA receptors in the adaptation process. Healthy subjects administered with the NMDA receptor antagonist (Dextromethorphan, DXM) were also shown to exhibit an attenuation of the typical adaptation effect when comparing post-drug scores to those obtained prior to DXM consumption (Folger, Tannan, Zhang, Holden & Tommerdahl, 2008). Interestingly, DXM only influenced performance of the adaptation task as placebo and active drug groups obtained similar scores on a non-adaptation version of the task, thus highlighting the role of alterations in CNS processing on adaptation-specific as opposed to global task mechanisms. Therefore, these results further extend the available evidence suggesting that the influence of adaptation on performance levels is likely a product of the status of GABAergic and

glutamatergic function. Crucially, as vibrotactile adaption appears to be mediated by similar physiological processes thought to underlie the after-effects of DC stimulation, it represented a useful tool with which to validate our understanding of tDCS mechanisms.

1.4. Psychophysics

1.4.1 An introduction to the study of psychophysics

The field of Psychophysics emerged from the desire of those investigating psychological phenomena to link observed sensory responses to their underlying neural mechanisms. Exploration of the relationship between stimuli and sensations dates back to the work of Ernst Weber, who observed that the strength of a stimulus is proportional to a relative increase in the resulting sensation; referred to as Weber's Law (Weber, 1834). Therefore, the perceived distinction between two stimuli (referred to as the just noticeable difference; JND) is proportional to stimulus intensity, although this was not shown to hold for values at the lower end of the stimulus range. Gustav Fechner, regarded as the founder of Psychophysics, built on the work of Weber in order to measure the capacity of sensory systems to perceive stimuli of varying intensity. In his seminal work, Elements of Psychophysics, Fechner (1860) explicitly states the reciprocal correspondence between physiological and psychological domains, inferring that a psychophysical approach could be used to test physiological hypotheses. This characterises Psychophysics as both descriptive, in its capacity to determine sensory thresholds, and also analytical as it is able to test physiological theories of how these perceptual thresholds are realised (Gescheider, 2013). The work of Bolanowski, Gescheider, Verillo and Checkosky (1988) in quantifying mechanoreceptor channels, as well as the vibrotactile discrimination research of Goble and Hollins (1993) and Delemos and Hollins (1996) are prime examples. Approaching key research questions from the perspective of scientific measurement has greatly enhanced the ability of those in the field of Psychology to explore the neural underpinnings of all sensory domains. Consequently, the field of Psychophysics has guided investigation into the mechanisms underlying perception within individual systems and undoubtedly aided in the comprehension of sensory dynamics, such as those previously illustrated.

1.4.2 Measuring psychophysical task performance

Initial psychophysical testing made use of paradigms designed to establish the detection capacity of subjects, defined as absolute threshold, corresponding to the lowest stimulus able to elicit a sensation. For this purpose, simple paradigms designed to determine whether the subject had detected a target stimulus were implemented. These are referred to as one alternative forced choice (1AFC) or one interval forced choice (1IFC) designs, corresponding to yes/no responses (Kingdom & Prins, 2009). However, these paradigms are highly susceptible to response bias, where certain responses are favoured, and no data for false positive rates is gathered.

When determining the JND between two stimuli, a typical measurement used is the difference limen (DL). At the level of perception, this corresponds to the smallest degree of difference between two stimuli needed such that they are perceived as different. From a neural perspective, the DL relates to the threshold level where there is a discernable difference in the neural response to each stimulus (Gescheider, 2013). This is commonly measured using 2AFC and 2IFC paradigms. Through implementing these task designs, participants' are asked to determine at which of two locations or in which of two intervals the designated target appears. These paradigms offer the advantage of characterising responses as both hits and misses, taking false positives and false negatives into consideration. However, it is still a possibility that bias will be oriented towards preferred locations or intervals (as discussed in Klein, 2001).

The execution of each paradigm can be implemented via several unique approaches (for a comprehensive review, see Leek, 2001). The Method of Constant Stimuli (MOCS) has been one of the most popular means of stimulus presentation due to its robust ability to generate consistent threshold estimates. As part of the MOCS approach, a range of test stimuli are defined prior to the administration of the task (as documented by Treutwein, 1995). Several iterations of the same stimulus value are presented to participants in a randomised order. A psychometric function is used to illustrate an individual's response rate, often as the proportion of correct responses for each chosen intensity value (Wichmann & Hill, 2001). The stimulus property being varied is typically plotted on the X axis alongside the rate of responses on the Y axis. When the data are plotted they create a sigmoidal curve, with easier discriminations (larger gap between stimuli) being performed with a high success rate and those which are more difficult being performed with success rates closer to chance levels (Figure 1.18). Performance at 0.75 correct is often chosen as the criteria for threshold estimation as this point represents the number

of correct responses between chance and ceiling levels (Klein, 2001). Aside from estimating threshold, psychometric functions can be used to determine variability in responses by considering the steepness of the slope, which indicates measurement noise and the transition between levels of intensity being presented.

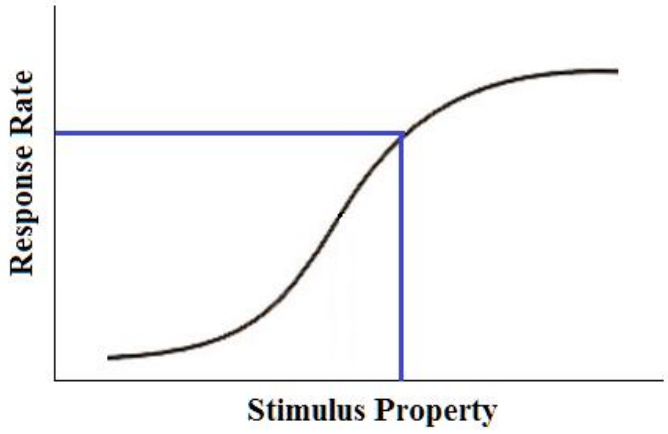

Figure 1.18. Psychometric curve. Responses are plotted as a product of their accuracy in relation to a stimulus property of interest e.g. intensity. A participant's performance capacity or threshold is established by assessing at which level of the stimulus the participant obtains a desired level of accuracy e.g. 75% correct.

While this approach is considered a rigorous and precise measure, the fixed stimulus values do not allow researchers to probe the finer detail of discrimination ability. Presenting multiple repetitions of various stimulus values also tends to lead to prolonged experimental runs, making MOCS vulnerable to fatigue effects. For this reason it is generally considered to be an inefficient means of threshold estimation. Other methods have since been favoured to streamline the threshold estimation process.

As an alternative to MOCS, a staircase approach can be adopted. Here, response tracking based on correct and incorrect responses is used to determine the presented stimulus values (Treutwein, 1995). The intensity of the test stimulus is gradually decreased, towards the value of the standard. Using a set step-size, typically beginning in a 1up/1down fashion, participants are able to decrease or increase the gap between the two stimuli with a correct or incorrect response, respectively. This enables a rapid descent towards the final threshold. Stricter criteria may be adopted or implemented part way through an experimental run, in order to further refine the threshold estimate (e.g. Levitt, 1970, 2 up/1 down; two correct answers are needed to reduce the gap between standard and test stimuli, equating to the point of 70.71% correct). These trials tend to cause a rapid fluctuation in the accuracy of responses, which is evident as an oscillation in performance when the responses are plotted (Kingdom & Prins, 2009). As such, an

abundance of interspersed correct and incorrect responses is often observed around the participant's threshold until it is reached (Figure 1.19).

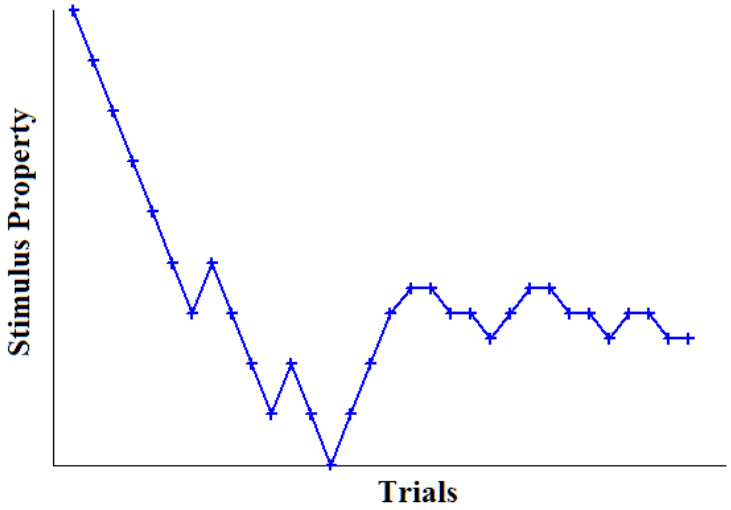

Figure 1.19. Staircase procedure. Responses are plotted as a product of the stimulus property of interest e.g. intensity, across trials. Correct responses allow for progression towards achieving ceiling levels of performance while incorrect responses present participants with simpler trials. A participant's performance capacity or threshold is commonly established by averaging performance over a period of final trials or a set number of reversals.

Test stimuli are delivered above threshold (suprathreshold) at the onset, often starting at values high enough to be well outside the expected range of performance. Experimental trials can be terminated after a designated number of reversals have been achieved or a set number of trials have been completed. Thresholds are often calculated as an average across several of the final trials. The staircase procedure enables thresholds to be measured with far fewer trials, while still providing accurate and reliable outcomes, vastly reducing the time needed for data acquisition. For this reason it is one of the most commonly adopted procedures.

The aforementioned staircase approach is classified as an adaptive method, meaning that stimulus levels are not fixed and the nature of responses to previous trials determines subsequent stimulus values (Falmagne, 1986). In this way, participant performance determines the order of stimulus presentation because every trial the participant performs tailors the stimulus set to their unique capability, which ultimately further refines their threshold. In more complex algorithms, threshold estimates are continually tracked and typically updated by averaging across performance levels on each trial or at stages where the stimulus changes direction (reversals). Parameter Estimation by Sequential Testing (PEST) is one of the most highly regarded methods to implement this adaptive approach (initially developed by Taylor & Creelman, 1967).

The technique differs from the standard up/down method of adjusting stimulus values because it does not adhere to a single step-size (Figure 1.20).

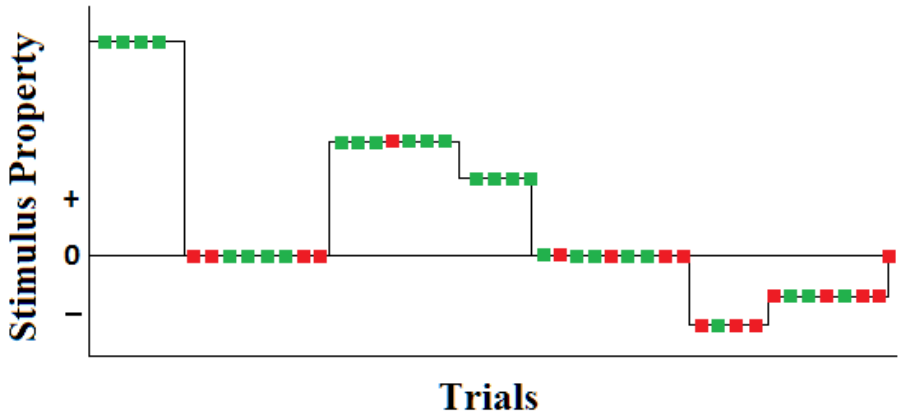

Figure 1.20. PEST procedure. A series of trials are delivered which commonly incorporate suprathreshold, threshold and subthreshold stimuli. Each set will vary in step-size and the nature of each individual response (correct/positive responses, green; incorrect/negative responses, red) does not trigger an immediate change in the stimulus, such that thresholds are established on termination of the trials. Instead it contributes to an average of performance capacity tracked over the entire experimental run.

PEST has been developed to utilise information from the entire experimental run as opposed to averaging over a number of final trials or reversals, making threshold estimates more representative of each participant's ability. However, using PEST, there is a step-size reduction across trials as performance is geared towards a specific criterion e.g. 70.71%, which can lead to prolonged experimental runs if it is not easily achieved (Leek, 2001).

1.5. Chapter Overview

As outlined at the start of the chapter, the literature review presented here formed the basis of the subsequent experimental work. A recurring theme emerged that, despite the existence of compelling behavioural effects, the neurobiological processes underpinning tDCS are not completely understood. This inevitably limits the conclusions that can be derived from such studies and the application of the method in a clinical setting. Therefore, the body of work put forward in this thesis was designed to offer novel, complementary perspectives on the excitatory and inhibitory processes thought to underlie tDCS.

Details relating to the neuroimaging modalities used to implement this research are documented in chapter 2. Conducting a Magnetic Resonance Spectroscopy (MRS) investigation was an intuitive step in order to study aspects of neurotransmission. In

chapter 3, changes in the concentration of glutamate (Glx) and GABA were quantified following anodal and sham tDCS. The research also explicitly focused on the precise role of inhibitory neurotransmission by incorporating distinct spectral editing sequences to produce standard and optimised estimates of GABA in the selected voxel within motor cortex. Magnetoencephalography (MEG) was utilised as it provides insight into the response of neurons via oscillatory dynamics across frequency bands. Gamma and beta responses were established to be of specific interest as they are reported to be generated through the interplay of glutamatergic pyramidal cells and GABAergic interneurons. This suggests that further inferences could be drawn on excitatory and inhibitory processes via tDCS-induced modulations of these rhythms. Chapter 4 details the challenges faced in implementing concurrent tDCS-MEG and the minimisation of associated electromagnetic noise, while chapter 5 documents how a visuomotor task was used to obtain the necessary gamma and beta band data in spatially separate brain regions. Evoked responses were also obtained and assessed for tDCS-induced alterations both during and after anodal and sham stimulation, thereby enabling the investigation of 'online' and 'offline' effects.

As the effects of tDCS are often observed in relation to task performance, it was important to also consider the method in relation to behaviour. It was proposed that similar conclusions to those possible with the neuroimaging studies could be reached at a behavioural level, providing the selected paradigm was understood in relation to its underlying neurobiology. In chapters 6 and 7, variations of a vibrotactile adaptation paradigm with similar physiological mechanisms to tDCS were executed in conjunction with stimulation delivered via unihemispheric and bihemispheric somatosensory electrode montages. Alterations in performance following anodal, cathodal and sham stimulation were interpreted in relation to these neurobiological similarities, thus providing a unique complementary perspective on our understanding of the method. Finally, by reviewing the existing literature and conducting the aforementioned studies, a number of general concerns emerged - beyond those related to tDCS mechanisms. These issues are discussed in chapter 8.

2. Introduction to Neuroimaging Methods

The following neuroimaging techniques were used to investigate specific aspects of tDCS neurophysiology.

2.1. Magnetic Resonance Imaging (MRI)

Early experiments in Nuclear Magnetic Resonance (NMR) theory (Bloch, Hansen & Packard, 1946; Purcell, Torrey & Pound, 1946) determined that a signal could be detected from nuclei in a magnetic field when radiofrequency (RF) energy was applied. Hahn (1950) later discovered that a "spin-echo" of this signal could be generated by delivering further pulses of RF energy. However, the application of these principles to produce images using the technique we now know as Magnetic Resonance Imaging (MRI), did not begin to develop until the 1970's. Damadian (1971) invented the first superconducting magnet and soon after Sir Peter Mansfield demonstrated the excitation of spatially distinct image slices (Mansfield, 1977). This led Mansfield and Paul Lauterbur to win the Nobel prize for Physiology or Medicine in 2003.

It was initially proclaimed that the principles of NMR wouldn't "revolutionise industry or help the housewife" (reported in the Boston Herald; McRobbie, Moore, Graves & Prince, 2006) but MRI has since become an incredibly valuable tool, particularly within the biomedical community. This is due to the ability of MRI to non-invasively quantify differences in tissues throughout the body, based on their inherent properties. This is in contrast to its predecessors, Computerised Tomography (CT) and Positron Emission Tomography (PET). It is, therefore, ideally placed to study disease states resulting in alterations of tissue volume and composition (Filler & Saha, 2009). MRI has also been an extremely influential technique in the field of neuroscience. With the advent of modern, higher-field systems and refined programming of sequences, images can be generated with a spatial resolution of millimetres (McRobbie et al., 2006). For this reason, our understanding of the human brain has undoubtedly been advanced by studies employing MRI to investigate how elements of cognition relate to aspects of neural structure and function (using volumetric measures, diffusion tensor imaging and functional MRI: Raz, Lindenberger, Rodrigue, Kennedy, Head, Williamson... & Acker, 2005; Upadhyay, Ducros, Knaus, Lindgren, Silver, Tager-Flusberg & Kim, 2007). Interest in establishing the role of neurotransmission in relation to perception and behaviour has also increased in recent years, made possible with the development of

MR spectroscopy (Sumner, Edden, Bompas, Evans & Singh, 2010; Puts, Edden, Evans, McGlone & McGonigle, 2011; Boy, Evans, Edden, Lawrence, Singh, Husain & Sumner, 2011).

2.1.1 The MRI system

The main component of an MRI scanner is the static magnetic field (B_0), which in a 3 Tesla (3T) device is approximately 60,000 times the strength of the Earth's magnetic field. It is produced by passing a current through niobium-titanium coils embedded in copper. When cooled to approximately 4° K, these coils lose electrical resistance, such that the current is perpetually present. This superconducting state is ensured by surrounding the magnet coils with liquid helium. Shimming coils are integrated into the magnet to maximise field homogeneity. Figure 2.1 shows the scanner configuration.

Figure 2.1. MRI system. An illustration of the coil configuration of an MRI scanner (image taken from http://humanconnectome.org/about/pressroom/project-news/connectome-skyra-update-new-gradients-installed-human-subject-testing-approved/).

Additionally, radiofrequency (RF) coils are integrated into the bore of the magnet. These coils consist of transmitter and receiver components. Transmitter coils generate the RF pulses required to produce the MR signal (detailed below). This creates a field at a right angle to the static field, known as B_1. These pulses are delivered with a specified bandwidth, amplitude and phase. The signals produced by the application of these RF pulses are detected by the receiver coils, which maximise detection of the signal and minimise noise interference. To diminish the influence of external RF sources, the MRI scanner is placed in a shielded room, consisting of steel or copper and aluminium plates. Portals, known as wave guides, are integrated into the design to ensure necessary cables can run between the control room and the magnet room.

Separate sets of gradient coils are mounted to the bore of the magnet and exist in three planes, corresponding to; left/right (X), top/bottom (Y) and bore-aligned (Z) orientations. Therefore, X and Y gradients are perpendicular to B_0, representing transverse gradients, whereas the Z gradient is longitudinal and parallel to the static field. Gradient amplifiers are used to generate the electric currents needed by the coils

to produce alterations in the magnetic field in each plane, in accordance with a specific RF pulse sequence. The use of shielding coils to cancel out the external gradient field prevents rapid switching of the gradient coils from inducing eddy currents and causing signal loss. These resulting alterations in the strength of the magnetic field caused by the gradient switching enable spatial encoding. This illustrates how regions of space, pertaining to cerebrospinal fluid (CSF), grey and white matter tissue types, contribute to the obtained signal. The volumetric images resulting from this process are made up of sections, or slices, that illustrate frequency and phase-based information. This is achieved by applying a frequency encoding gradient during data acquisition to alter the frequency of the MR signal at different locations. Prior to this, a phase encoding gradient is initiated to alter the phase angle of the MR signal in different regions. Each slice forms the total brain volume, which is used to resolve a 3D image of how the MR signal changes over time and space (as illustrated in Figure 2.2).

2.1.2 Signal generation

The field of MRI was derived from the principles of Nuclear Magnetic Resonance (NMR) (Bloch et al., 1946; Purcell et al., 1946). The fundamental element of NMR and thus MRI, is the nucleus, typically of hydrogen molecules found in water that comprise of a single positively charged proton. Protons exhibit spin, otherwise referred to as precession, about their axes. Under normal circumstances, these spins are non-uniform and do not pertain to a single orientation. In the presence of a magnetic field, for example B_0, the precession of individual spins becomes aligned. In this longitudinal plane, the majority of spins are oriented in a spin-up/parallel manner (aligned with the field) while the rest precess in a spin-down/anti-parallel fashion (against the field).

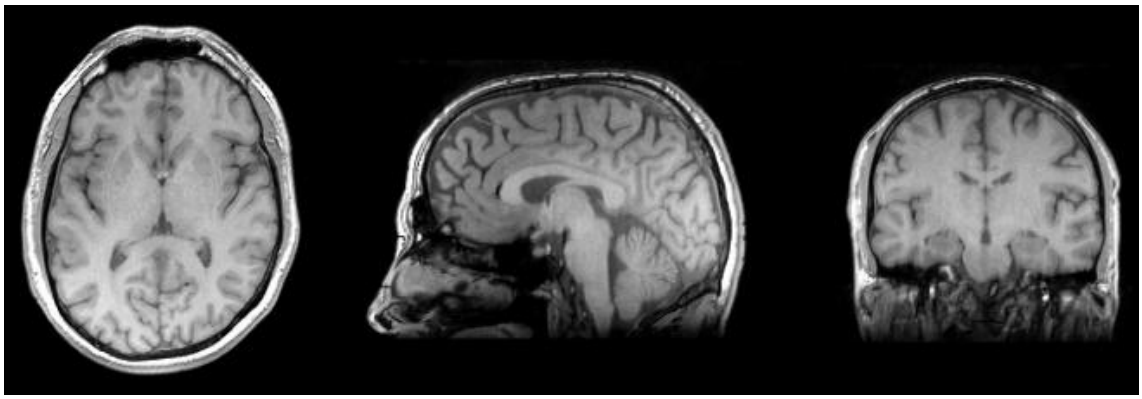

Figure 2.2. Structural MRI. An example of the type of high resolution, 3D structural brain image that can be generated at field strengths of 3T. L-R: axial, sagittal and coronal planes.

Alignment against the direction of the field requires additional energy, such that anti-parallel spins are termed high energy with the opposite, low energy, for parallel spins. Crucially, B_0 aligns the magnetic field produced by the spins (magnetic moment) due to the turning force generated by the constant, off-axis rotation of each spin (angular momentum). In this parallel or anti-parallel state (equilibrium), spins are oriented but remain out of phase. This means they possess low levels of net magnetisation (sum of the force exerted by each spin); the basis of the MR signal (Figure 2.3). This is because of the magnitude of the main field to which net magnetisation in the longitudinal plane (Z) is compared. For this reason, it is more efficient to measure net magnetisation in the transverse plane (X-Y), perpendicular to B_0.

In order to assess transverse magnetisation, the low energy spins need to be perturbed to a high energy stage and flipped to the transverse plane. Therefore, transmitter coils induce field B_1 by switching RF pulses on and off. The frequency of the pulses needed to excite the spins is known as the Larmor or resonant frequency, which is their rate of precession (proportional to the magnetic field). This defines the electromagnetic energy applied by the RF pulse, which is absorbed by the targeted tissues to create more high energy spins. The angle of the pulse is responsible for switching the plane of net magnetisation, which is delivered at 90° to flip from the longitudinal to transverse axis. The energy applied is released as an RF wave as the spins return to equilibrium. This is identical in resonant frequency to the initial excitation pulse. For this reason, the RF receiver coils that measure the resulting voltage are tuned to the Larmor frequency.

Figure 2.3. Proton precession in the magnetic field. In the presence of the static field, the majority of spins are in the parallel as opposed to anti-parallel state and are therefore, aligned with B_0. The application of RF pulses alters this balance. The energy delivered by the pulses is absorbed by the nuclei and spins change from a low to high energy, anti-parallel state. This energy is emitted when the pulses are switched off and the nuclei return to equilibrium, which forms the basis of the MR signal (image taken from http://www.expertsmind.com/topic/proton-nuclear-magnetic-resonance-spectroscopy/larmor-frequency-and-energy-transitions-913941.aspx).

2.1.3 Image generation

The signal emitted from the loss of applied thermal energy, as equilibrium is restored (longitudinal magnetisation decay), is the foundation for so-called T_1 contrast images. A measureable signal is also apparent as a product of phase coherence decay. The RF

pulses delivered are not only used to perturb the energy state of the spins but also to align them with respect to their phase within the spin cycle. The spins lose phase coherence due to the movement of each individual proton within the tissue (spin-spin interaction). This decay of phase coherence (transverse magnetisation decay) forms the basis of T_2 contrast images. The interaction between protons produces changes in the magnetic field exerted upon them causing their phase angle to alter. This is characterised by free induction decay (FID) but is typically quantified using spin-echo techniques. The initial 90° pulse is followed by a 180° pulse, which refocuses the decay process and reverses the phase angle of the spins, such that they revert back into phase at the same rate as the interval between pulses. Therefore, the relaxation or change in net magnetisation in different planes can be measured across time (Bloembergen, Purcell & Pound, 1948). These values are inherently different for certain tissue types and vary in speed; with T_2 decay occurring in milliseconds compared to the more prolonged recovery of seconds for the T_1 signal. The weighting of the images, whether they are defined by the recovery of spin alignment or decay of phase coherence in different tissue types, will have a bearing on the specified parameters. For example, the time between excitation pulses (repetition time; TR) and the interval between the pulse and the time at which data is acquired (echo time; TE). T_1 contrast images require a moderate TR and a short TE, such that equilibrium is not yet achieved prior to repeated excitation and to minimise the influence of T_2 contrast. T_2 images require a moderate TE and a sufficiently long TR to ensure the opposite.

2.1.4 Magnetic Resonance Spectroscopy (MRS)

Aside from assessing tissue volume and composition, MRI technology provides the capacity to quantify neurochemicals *in vivo*. This is achieved using Magnetic Resonance Spectroscopy (MRS), which is performed by exploiting the difference in the resonant frequency, or chemical shift, of each substance. Protons are shielded from the static field, to varying degrees, due to the proximity to surrounding electrons, which changes their resonance. The RF pulses used to excite hydrogen nuclei, therefore, allow the peak of each metabolite to be measured according to the number of protons at corresponding points of the chemical shift spectrum. This is expressed in parts per million (ppm), which is a measure that does not vary with field strength. The first *in vivo* ^{1}H MRS study was performed by Behar, den Hollander, Stromski, Ogino, Shulman, Petroff and Pritchard (1983) and shortly after Bottomley, Edelstein, Foster and Adams (1985)

produced the first neurochemical spectra. The representation of metabolite peaks is acquired by using the gradient coils to selectively direct the RF pulses to a pre-specified voxel, usually 3 cm^3 in size to ensure good SNR because the detected substances are in the millimolar range (mM). The FID from this voxel is recorded and used to produce the chemical shift spectrum as opposed to a 3D structural image.

Stimulated Echo Acquisition Mode (STEAM; Frahm, Merboldt, Hänicke & Haase, 1985) or Point Resolved Spectroscopy (PRESS; Bottomley, 1987) sequences are typically used to perform single voxel spectroscopy. STEAM involves the delivery of 3 slice-selective 90° pulses, one from each gradient axis. PRESS incorporates an initial 90° pulse, which is followed by two 180° pulses. This produces a double spin-echo as the first pulse generates the initial echo, which is then refocused by the final frequency-selective pulse. For this reason, PRESS produces a signal-to-noise ratio twice that of STEAM. The magnitude of the peaks resolved is dependent on the parameters of the RF pulses, which should feature a sufficiently long TR (~1500-2000 ms) and short TE (~30-80 ms). This is due to each metabolite having unique T_1 recovery and T_2 decay times, the influence of which needs to be removed in order to produce accurate spectra.

The detection of chemical shift differences is problematic in the presence of water at high concentrations within the tissue of interest, which is estimated to be 70% for grey matter and 83% for white matter (McIlwain, 1985). Due to its abundance, the magnitude of the water signal at 4.7 ppm needs to be suppressed to resolve peaks of smaller metabolites in the spectrum (Dreher & Leibfritz, 2005). This is achieved by selectively defocusing the water resonance while refocusing the other metabolites, for example, with the chemical shift selective method for water suppression (CHESS; Haase, Frahm, Hanicke & Matthaei, 1985) or Mescher-Garwood frequency selective refocusing technique (MEGA; Mescher, Tannus, Johnson & Garwood, 1996). Estimates of linewidth demonstrate the homogeneity of the selected voxel on the basis of the water resonance and as such are an indication of data quality.

Homogeneity of the static field is crucial to the sensitivity of the method and obtaining viable spectra. To ensure sensitivity is not compromised on a participant-by-participant basis, first-order shimming should be conducted by passing a constant current through the gradient coils (Juchem, Nixon, Diduch, Rothman, Starewicz & de Graaf, 2010). Acquiring multiple averages or repetitions of the experiment, as well as conducting MRS at higher field strengths, also improves SNR and thus the detection of spectral peaks (Ugurbil, Adriany, Andersen, Chen, Garwood, Gruetter... & Zhu, 2003).

Additionally, the position of the voxel of interest is crucial to data quality as lipid contamination can occur if it is placed too close to the skull. Contamination from CSF may also occur if the voxel is placed over the ventricles. Providing data quality is sufficient, MRS sequences provide robust measurements of N-acetyl aspartate (NAA) at 2 ppm, the Glutamate/Glutamine composite (Glx) at 2.1-2.5 ppm, Creatine (Cr) at 3 ppm, Choline (Cho) at 3.2 ppm and Myo-inositol (mI) at 3.6 ppm. Other metabolites do not fall into the millimolar range detectable by MRS (Mekle, Mlynárik, Gambarota, Hergt, Krueger & Gruetter, 2009). However, some neurochemicals are available in sufficient concentrations but need to be resolved using spectral editing techniques.

2.1.4.1 Overlap in the chemical shift spectrum

The presence of overlapping peaks in the chemical shift spectrum means it is difficult to quantify certain metabolites. This largely occurs because resonances may be split into multiple small peaks (multiplets), which decrease their overall magnitude, due to their interaction with other hydrogen nuclei. As addressed previously (in the context of T_2 decay), nuclei may directly influence one another due to their spatial proximity but they may also indirectly impact upon each other on the basis of their chemical relationship. The latter is referred to as J-coupling and is caused when a substance comprises of more than one resonating nucleus, in the opposite anti- or parallel state (de Graaf, 2013). To remove this spectral overlap and resolve such peaks, spectral editing techniques can be employed. Rothman, Arias-Mendoza, Shulman and Shulman (1984) pioneered these so-called J-difference editing sequences, which feature an "on" and an "off" experiment. During the "off" experiment, standard spectra are acquired while the "on" experiment incorporates editing pulses to selectively refocus one of the multiple spins, thus perturbing J-evolution. The results of each experiment can be subtracted from each other to produce a difference spectrum, which features only the peaks which are affected by the editing pulses. Although such methods are sensitive to any inconsistencies between experiments, such as participant movement, magnet drift and gradient heating, they provide an incredibly useful means of resolving peaks that would otherwise be undetectable.

Such an editing technique is required to quantify concentrations of the inhibitory neurotransmitter γ-aminobutyric acid (GABA), which is only present at concentrations of 1 mM in the human brain (Figure 2.4a). J-difference editing for GABA quantification was first proposed by Rothman, Petroff, Behar and Mattson (1993) and has since been

shown to produce robust spectra from multiple brain regions (Mikkelsen, Singh, Sumner & Evans, 2015).

GABA comprises of three multiplets, corresponding to its methylene (CH_2) groups that overlap with NAA, Cr, and Glx peaks (Puts & Edden, 2012; Figure 2.4b). The most widely used sequence to disentangle these peaks is a combination of MEGA for water suppression and PRESS to form the chemical shift spectrum (MEGA-PRESS), developed by Mescher, Merkle, Kirsch, Garwood and Gruetter (1998). To specifically target GABA, frequency-selective editing pulses can be applied to one of the coupled resonances. Accordingly, the GABA peak at 1.9 ppm is coupled to that at 3 ppm but not to any of the other metabolites at that frequency. The "off" experiment inversion pulses are delivered at a frequency that will not excite any of the targeted spins e.g. 7.5 ppm. By delivering editing pulses at 1.9 ppm in the "on" experiment, only the resonances in that range and those it is coupled to will be affected and subsequently feature in the edited difference spectrum (Mullins, McGonigle, O'Gorman, Puts, Vidyasagar, Evans & Edden, 2014) (Figure 2.4c).

Figure 2.4. Resolving GABA with MEGA-PRESS. A) The acquisition of standard chemical-shift spectra does not allow for the quantification of GABA (the position of which is indicated by the coloured markers). B) GABA does not present as a single peak due to J-coupling, which means the GABA spin-system is distributed across the spectrum (denoted by the colour-coded methylene groups). C) By placing editing pulses at selected points of the spectrum, in separate acquisitions (ON/OFF experiments), the chemical relationship between GABA peaks can be used to form an edited, J-difference spectrum. Images A & B were taken from Puts & Edden (2012). Image C was taken from Mullins et al. (2014).

MEGA-PRESS experiments are typically performed with short TEs, to minimise the influence of T_1 and T_2 relaxation times, but this introduces the issue of macromolecule (MM) contamination. MMs are characterised as the resonances of amino acids such as lysine and arginine (Near, 2014). They are present in the difference spectrum because the resonance at 1.7 ppm is close enough to the inversion pulse delivered at 1.9 ppm to be partially excited. Additionally, the 1.7 ppm MM peak is coupled to another resonance, which overlaps and is therefore co-edited with the GABA peak at 3 ppm (Edden, Puts & Barker, 2012a). This means that MMs substantially interfere with the accurate quantification of GABA, contributing to as much as 50% of the 3 ppm signal at 3T (de Graaf, 2013). To reduce the influence of the MM signal, with respect to altering

the TE, would require TEs >80 ms and would lead to a greater impact of relaxation, particularly T_2 decay (for an insight on how short TEs influence spectra, see Seeger, Mader, Nägele, Grodd, Lutz & Klose, 2001). Edden, Intrapiromkul, Zhu, Cheng and Barker (2012b) determined that GABA can be reliably measured with a variety of TEs but in a separate study demonstrated that a TE of 80 ms was optimal for MM suppression (Edden et al., 2012a). This was due to increased SNR relating to the precision of editing pulses, which can be lengthened to 20 ms. Therefore, the suppression of the MM signal is often performed within these parameters by adopting a symmetrical editing approach (Henry, Dautry, Hantraye & Bloch, 2001). This technique involves placing editing pulses symmetrically about the 1.7 ppm MM resonance (at 1.9 ppm and 1.5 ppm). This excites the MM resonance during both "on" and "off" experiments, meaning it does not feature in the difference spectrum. However, the 1.9 ppm pulse excites the coupled 3 ppm GABA resonance such that it can be successfully resolved without the MM contribution. Although the concentration estimate still contains a small (~5-10%) contribution from homocarnosine, what remains is a more optimised estimate of GABA for the selected voxel than that resolved for measures of "GABA+MM".

2.1.4.2 *Quantification & analysis*

In order to quantify metabolites, such as GABA, it is common to reference the neurochemical of interest to an internal reference substance to produce a ratio. This acts as a relative as opposed to absolute measure of concentration. NAA, Creatine and Water are typically used as references due to their abundance and consistency across measures (Kreis, Ernst & Ross, 1993). However, it is important to note that some usually stable metabolites have been shown to be altered in certain disease states e.g. NAA, as a metric of neuronal integrity, is changed in multiple sclerosis (Bjartmar, Kidd, Mörk, Rudick & Trapp, 2000). These concentration ratios can be derived from peak fitting; modelling the best estimate of the peak and fitting that function to the derived data (Near, 2014). Here, the residual or fit error represents a measure of data quality as the difference between the curve fitted to the data and the data itself. Cramer-Rao lower bounds (CRLB) also provide insight into quantification errors and indicate the lowest standard deviation of model parameter estimates (Cavassila, Deval, Huegen, Van Ormondt & Graveron-Demilly, 2001). Accordingly, CRLB should be < 20% of the total concentration value. Lorentzian or Gaussian functions are commonly used to model

spectral peaks and the software packages used to implement these models can be constrained to prevent implausible fits, such as establishing negative peaks.

Widely used analysis programs include jMRUI (Naressi, Couturier, Castang, De Beer & Graveron-Demilly, 2001), LCModel (Provencher, 1993), TARQUIN (Wilson, Reynolds, Kauppinen, Arvanitis & Peet, 2011) as well as Gannet (Edden, Puts, Harris, Barker & Evans, 2014), which was used to analyse spectroscopy data related to the project because of its application to GABA quantification. Gannet produces user-friendly pdf format documents displaying the fitting outcome alongside estimates of linewidth and fit error (Figure 2.5). It can also be used to perform segmentation of the related structural data to provide information on relative tissue volumes, to guide further refined estimates of GABA concentration.

Gannet is implemented via MATLAB and its main functions are GannetLoad and GannetFit. GannetLoad involves the conversion of FID data in the time-domain to the frequency-domain using a fast Fourier transform (FFT) to split the data into its constituent frequency components. Zero-filling is implemented to smooth the spectra. Frequency and phase correction are applied to minimise differences from the receiver and transmit coils in order to remove subtraction artefacts. This is assessed using the Choline peak, which does not directly overlap the GABA signal. Pairs of outliers (constituting "on/off" experiments) more than 3 standard deviations from the mean are removed by the software. This occurs prior to time averaging the data to generate the GABA-edited as well as the "off" spectra, where standard peaks from Creatine, NAA and Glx remain present. GannetFit is used to quantify the edited 3 ppm GABA peak (producing GABA:Cr and GABA:H_20 ratios). This is achieved using a non-linear least squares fitting method to estimate the area under each peak. The GABA peak is fitted as a single Gaussian function, between 2.79-3.55 ppm, whereas Creatine is defined as a Lorentzian peak, between 2.72-3.12 ppm. Water is fitted as a Gaussian-Lorentzian curve at a chemical shift of 3.8-5.6 ppm.

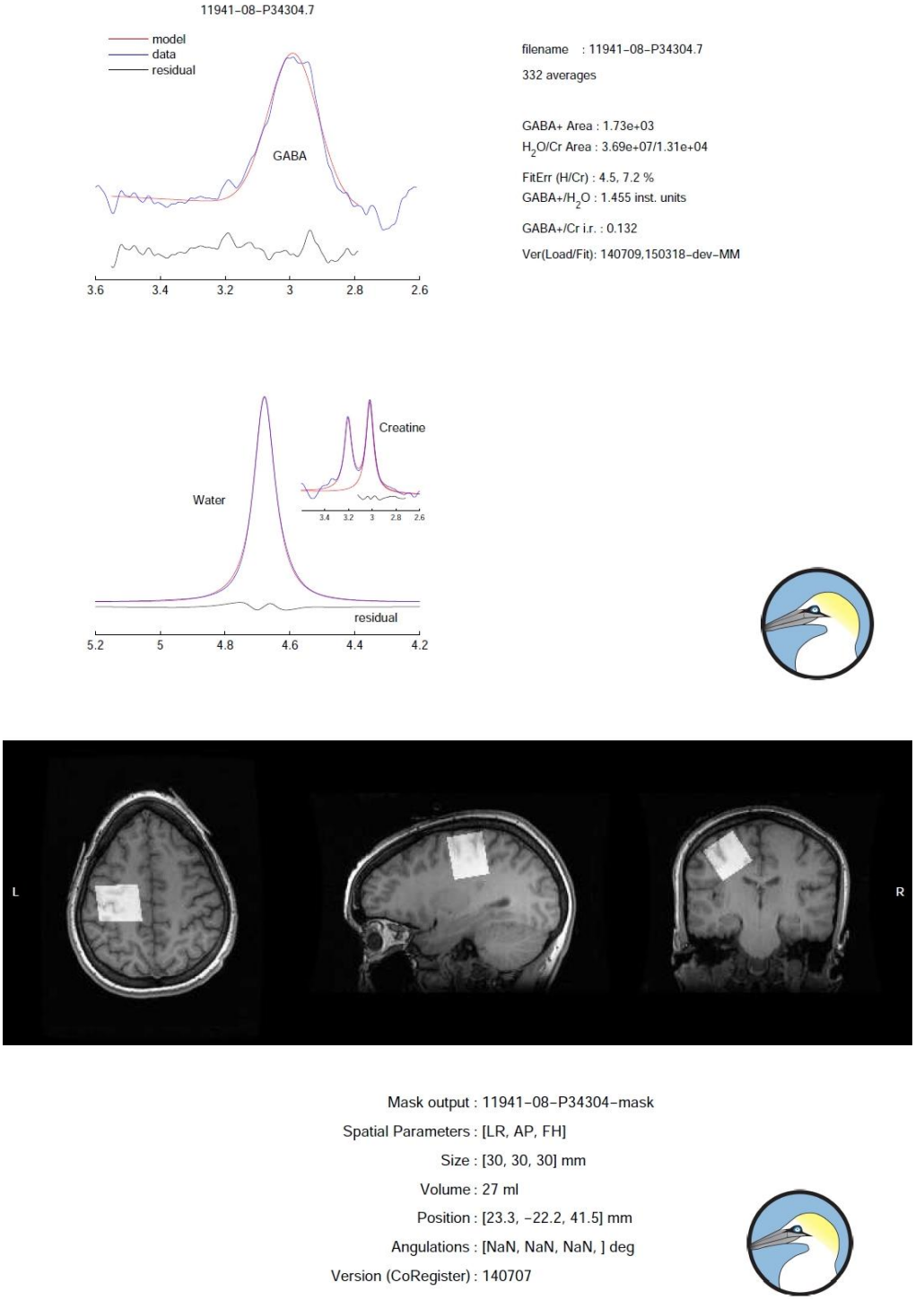

Figure 2.5. Gannet output. Ratios reflecting the concentration of GABA at 3 ppm are derived by peak fitting of the edited signal, the Creatine signal from the "off" spectra and the unsuppressed water signal, relating to the voxel of interest.

2.2. Magnetoencephalography (MEG)

Magnetoencephalography (MEG) is a non-invasive technique that passively measures magnetic fields arising from the brain. These fields are generated by changes in the electrical activity of cells, which makes MEG a direct measure of neuronal function in contrast with other methods such as BOLD contrast fMRI. The method also possesses an exquisite temporal resolution; detecting real-time fluctuations in cortical activity within the order of milliseconds (Baillet, Mosher & Leahy, 2001). The first MEG recordings from the brain were made in the early 1970's by David Cohen, which gave rise to the field of Biomagnetism (Cohen, 1972). Since this time, substantial advances have been made with regard to the hardware used to acquire neuromagnetic data. For example, whole-head systems are now commonplace as opposed to the single-channel devices that were initially manufactured (Ahonen, Hämäläinen, Kajola, Knuutila, Laine, Lounasmaa... & Tesche, 1993; Hari & Salmelin, 2012). Therefore, the scope and complexity of the research questions that can be successfully tackled has subsequently evolved. This has also been facilitated by the development of analysis software, which has produced refined algorithms to localise sources of activity.

2.2.1 The MEG system

MEG recordings require sensitive electronics to detect the magnetic fields produced by the human brain. For accurate estimates of neuromagnetic activity, sensors that are sufficiently sensitive to detect weak signals, in the range of femtoteslas (fT), must be utilised. Additionally, as more prominent fields are inevitably detected, the prevention of interference and the removal of residual noise from the obtained signal become inherently necessary (Supek & Aine, 2014).

At the core of the MEG system are the superconducting quantum interference devices (SQUIDs) that act as extremely sensitive, magnetic field sensors (1 fT/√Hz). Co-developed by James Zimmerman and David Cohen, these superconducting loops with integrated Josephson junctions are typically made of niobium, which can withstand extreme cooling and heating to room temperature. Each SQUID chip is approximately 10 mm^2 in size and must be immersed in liquid helium, at approximately 4° K, to maintain its sensitivity. The SQUIDs are situated in a helmet-shaped cryogenic vessel or dewar, either in the liquid helium reservoir itself or the adjacent vacuum space (Figure 2.6). The shape of the dewar allows for the ideal spatial configuration of the sensors

(approximately 300 in modern systems), which are situated around the surface of the head for maximal detection of possible sources (Hämäläinen, Hari, Ilmoniemi, Knuutila & Lounasmaa, 1993).

As MEG signals are typically < 100 fT, it is essential that larger, environmental noise sources can be minimised and removed from the data collected. The most efficient means of reducing the impact of external noise is to locate the MEG system within a magnetically shielded room (MSR) (Nowak, 1998). These structures are made from multiple layers of nickel-alloy and aluminium or copper plates, which provide ferromagnetic and eddy-current shielding against high-frequency noise sources (such as radio frequency waves) (Erne, 1983). Additionally, to increase the sensitivity of the sensors and maximise the signal, pick-up coils that exceed the size of the SQUID loops form part of the hardware. These structures suppress low-frequency components of noise, resulting from nearby environmental sources such as the movement of cars or use of appliances. Alongside input coils, integrated into the SQUID loops, these superconductive flux transformers detect magnetic flux and transfer it to the SQUIDs.

Figure 2.6. MEG System. A subject seated underneath the dewar in a magnetically shielded room. The dewar is filled with liquid helium, which maintains the superconductive status of the SQUIDs (image taken from Baillet et al., 2001).

The pick-up coils used are typically magnetometers or gradiometers, of which there are axial and planar configurations (Figure 2.7). Magnetometers comprise of single coils, whereas gradiometers feature an additional coil of the opposite orientation; parallel to the source (axial) or perpendicular to the source (planar). The configuration of the coils determines their sensitivity profile to the source of activity, known as the lead field. Gradiometers measure the magnetic field across the coils and are better able to detect small, dynamic changes in fields generated by the brain. This is because they are able to distinguish them from the static nature of gross, distant sources, on the basis of the spatial gradients produced. Therefore, gradiometers are preferable where environmental noise is of greatest concern. Aside from the in-built noise cancellation properties of the hardware, additional software-based noise reduction techniques may need to be implemented. For this reason, gradiometer pick-up coils commonly also correspond to additional reference channels, which detect magnetic fields further away from the head.

This allows for the creation of higher-order synthetic gradiometers, which further filter out distant sources of noise and thus improve the signal-to-noise ratio.

Figure 2.7. Pick-up coil configurations. Magnetometers comprise of single coils and gradiometers feature additional coils of opposite orientation. Axial configurations detect sources just outside of the sensor, whereas planar configurations detect sources right underneath the SQUID loop (image adapted from Singh, K. (2009). Magnetoencephalography. In Senior, C., Russell, T. and Gazzaniga, M. (eds), Methods in Mind (1st Ed), pp. 291–326).

2.2.2 Signal generation

Active neuronal populations produce cellular currents and this electrophysiological activity generates accompanying magnetic fields, which can be measured outside of the scalp. These fields arise at the site of the apical dendrites of post-synaptic neurons and are the proposed source of MEG recordings. More specifically, the fields measured by MEG primarily relate to the superficial (layer III) and deep (layer V) excitatory, pyramidal cells (Rönnqvist, McAllister, Woodhall, Stanford & Hall, 2013). The longitudinal direction of the dendrites of pyramidal cells enables them to produce a measureable voltage (open-field), unlike the non-uniform configuration of interneuron dendrites, whose activity sums to zero outside the scalp (closed-field) (Sarvas, 1987; Lopes da Silva, 2011). Source orientation is, therefore, a key consideration for signal detection in MEG. Accordingly, while tangential sources (parallel to the scalp e.g. within sulci) are readily detected, radial sources (oriented towards or away from the scalp e.g. at the crests of gyri) do not produce a measurable field (Nunez & Silberstein, 2000). This makes radial sources largely invisible to MEG. However, truly undetectable sources are thought to be in the minority due to the spatial extent of activity required to produce a measureable signal (Hillebrand & Barnes, 2002).

Single neurons generate field strengths of ~500 pA (picoamps), which is too weak for the pick-up coils to detect as only signal strengths in the range of tens of femtotesla can be measured by MEG. This is compounded by the distance between the coils and the cortex of each subject. There is an approximate distance of 17.5 mm between the dewar and the coils (CTF-MEG systems; Muthukumaraswamy, 2014), on top of which, the distance between the dewar and cortical surface has been estimated to be between 16-26 mm (for primary motor cortex; Stokes, Chambers, Gould, Henderson, Janko, Allen & Mattingley, 2005). This produces an approximate total distance of just under 40 mm

between the SQUID array and the cortex. Deep sources are at an obvious disadvantage in this respect as the magnetic field decays with increasing distance from the source, which is already further away from the coils than more superficial, cortical regions. Considering the apparent limitations, it is estimated that an area containing approximately 10,000-50,000 neurons is required to be active to generate a discernable field (Murakami & Okada, 2006; Nauhaus Busse, Carandini & Ringach, 2009). Furthermore, it is not only the sheer amount of active neurons that contributes to the MEG signal but also their synchrony (Denker, Roux, Lindén, Diesmann, Riehle & Grün, 2011). For this reason, it is widely accepted that the sum of simultaneous activity of large neuronal populations (represented as equivalent current dipoles) is detected by MEG as opposed to the activity of isolated action potentials, which would be too small, rapid and asynchronous to observe (Lopes da Silva, 2011).

While glutamatergic pyramidal cells generate the post-synaptic currents that sum to form the local field potentials (LFPs) measured by MEG, it is the regulation of excitatory action via GABAergic, inhibitory post-synaptic currents (IPSCs) that allow the necessary response synchronisation to emerge (Cobb, Buhl, Halasy, Paulsen & Somogyi, 1995). These inhibitory currents are largely thought to be exerted by fast-spiking interneurons (particularly basket cells), which have direct connections to multiple pyramidal cells as well as other inhibitory cells (Bartos, Vida & Jonas, 2007; Cardin, Carlen, Meletis, Knoblich, Zhang, Deisseroth… & Moore, 2009). The influence of these IPSCs on the excitatory cells produces a uniform change in firing rate, when inhibition is lifted from the cell population in question. Therefore, the balance of excitation and inhibition is proposed to be of extreme importance to the resulting activity observed at the MEG sensors (Buzsáki, 2006; Ray & Maunsell, 2010).

2.2.3 Signal classification

Aspects of neuronal activity measured by MEG can be classified on the basis of several categories. Firstly, there is a distinction between evoked and induced responses. Evoked fields are the magnetic equivalent of event related potentials (ERPs) in Electroencephalography (EEG) and many MEG studies have sought to isolate stimulus-specific, evoked responses to their respective primary cortical generators e.g. somatosensory (Salmelin & Hari, 1994), auditory (Pantev, Bertrand, Eulitz, Verkindt, Hampson, Schuierer & Elbert, 1995), visual (Fylan, Holliday, Singh, Anderson & Harding, 1997). These fields are phase-locked to the onset of a particular stimulus and

as such are highly transient in nature (Tallon-Baudry & Bertrand, 1999). For this reason, it is possible to merge the trial data from a recording in order to obtain an average of the signal in the time-domain (addressed in terms of response magnitude and latency). In contrast, induced responses are non phase-locked to stimulus onset and temporarily jittered because they do not consistently align with the stimulus onset stage of the trial (Figure 2.8a). It is, therefore, not possible to simply average a set of trials to obtain average responses as they are not stable in time. This difference is likely related to the neurobiological distinction between evoked and induced responses. Evoked fields have been classified as resulting from fluctuations in membrane potential leading to altered PSPs whereas induced responses are said to arise from modifications in synaptic function, which evolve as opposed to occurring routinely on cue (Pfurtscheller & Lopes da Silva, 1999).

Figure 2.8. Evoked and Induced Responses. A) The impact of signal averaging on induced responses (image adapted from Tallon-Baudry & Bertrand, 1999). B) Event-related induced responses in the beta band, localised to left motor cortex, and accompanying readiness field prior to movement (image adapted from Cheyne, 2013). C) Stimulus-induced gamma band response in right medial visual cortex (image adapted from Koelewijn et al., 2011).

Rather than being classified by the latency at which they occur post-stimulus, induced responses are characterised in terms of the rhythmic frequency at which they oscillate (since the first investigation by Hans Berger, 1929). For this reason, they are commonly assessed in the time-frequency domain. This is achieved by using spectral analysis techniques to determine changes in power (amplitude^2) or amplitude ($\sqrt{}$power) at a given frequency interval, for each single trial, prior to obtaining the average response. These oscillations can be classified as either task-induced (as previous outlined) or spontaneous. Spontaneous or on-going oscillations can be observed at rest, in the absence of task activity, and represent background levels of activity (Brookes, Woolrich, Luckhoo, Price, Hale, Stephenson... & Morris, 2011). Importantly, the results of Brookes et al. (2011) were corroborated by resting state network activity derived using fMRI. This highlights the ability of MEG to accurately localise neural activity, despite its proposed limitations in terms of spatial specificity (which may be largely unfounded, providing accurate co-registration and minimal subject movement are ensured; Troebinger, López, Lutti, Bestmann & Barnes, 2014).

Oscillatory responses are typically divided into the following frequency bands; theta (< 4 Hz), delta (4-7 Hz), alpha (8-14 Hz), beta (15-30 Hz) and gamma (> 30 Hz). As an example of the dynamic rhythmic activity measured by MEG, changes in oscillatory power have been observed in relation to motor movement within the beta band (for reviews, see Cheyne, 2013; Kilavik, Zaepffel, Brovelli, MacKay & Riehle, 2013). Deecke, Weinberg and Brickett (1982), Tiihonen, Kajola and Hari (1989) and more recently van Elk, van Schie, van den Heuvel and Bekkering (2010) observed the preparatory, Bereitschaftsfield or readiness field, 1-2 s prior to simple finger movements. This has been characterised as a decrease in neuronal synchrony from baseline levels in anticipation of movement (Wheaton, Carpenter, Mizelle & Forrester, 2008), otherwise referred to as an event related desynchronisation (ERD) (Pfurtscheller & Lopes da Silva, 1999). Conversely, an increase in neuronal synchrony or event related synchronisation (ERS) has been observed approximately 300 ms after movement onset, which is sustained for approximately 500 ms (Jurkiewicz, Gaetz, Bostan & Cheyne, 2006). This post-movement beta rebound (PMBR) in oscillatory power is said to represent the recovery of the motor system, which is transiently inhibited prior to allowing subsequent responses (Chen, Yaseen, Cohen & Hallett, 1998; Chen & Hallett, 1999) (Figure 2.8b). The ERD and ERS appear to have distinct cortical generators, with the ERD localised to post-central gyrus compared to the more anterior location of the ERS, within pre-central gyrus (Jurkiewicz et al., 2006).

During the execution of movement, power in the beta band has been shown to be relatively low compared to that demonstrated in the periods of ERD and ERS (van Wijk, Daffertshofer, Roach & Praamstra, 2009). In contrast to the beta band response, the gamma band (60-90 Hz) demonstrates bursts of synchronisation during movement for up to 300 ms (Schoffelen, Oostenveld & Fries, 2005; Cheyne, Bells, Ferrari, Gaetz & Bostan, 2008; Muthukumaraswamy, 2010). This is thought to facilitate the initiation of movement following the preparatory phase. Importantly, these MEG findings are in accordance with data from electrocorticography (ECoG) investigations conducted in epilepsy patients (Pfurtscheller, Graimann, Huggins, Levine & Schuh, 2003). Furthermore, a recent innovative study by Joundi, Jenkinson, Brittain, Aziz and Brown (2012) used 20 and 70 Hz tACS to alter motor processing and illustrate the dissociation of activity in the beta and gamma bands. The use of the stimulation intervention also enabled the authors to highlight the causal influence of these oscillatory changes (20 Hz tACS enhanced inhibition of movement on no-go trials, while 70 Hz stimulation improved response rates on go trials).

Synchronisation of induced gamma band oscillations in visual cortex has also been observed during MEG experiments, in response to contrast stimuli (Hoogenboom, Schoffelen, Oostenveld, Parkes & Fries, 2006; Swettenham, Muthukumaraswamy & Singh, 2009). Typically, a transient, evoked spike of activity is noted prior to the more sustained, induced response, which can last for around 1 s (Figure 2.8c). Muthukumaraswamy, Singh, Swettenham and Jones (2010) proposed separate cortical origins within V1 for each of these components due to a dissociation between the amplitude of evoked and induced responses within individuals. Such a result further highlights the distinction between the neuronal responses that contribute to evoked and induced activity (Pfurtscheller & Lopes da Silva, 1999). As in motor cortex, the outcome of the MEG investigations is corroborated by findings from invasive means, for example, LFP recordings from anesthetised cats (Eckhorn, Bauer, Jordan, Brosch, Kruse, Munk & Reitboeck, 1988; Gray & Singer, 1989). The gamma literature suggests that changes in gamma band synchronisation and coherence across regions are crucial for successful neuronal communication, particularly regarding feed-forward signalling and integration or "binding" of stimuli (Tiesinga, Fellous, Salinas, Jose & Sejnowski, 2004; Fries, 2005; Fries, 2009). Oscillatory activity, therefore, appears to play an extremely important role in the formation of responses across stimulus domains.

2.2.4 Source localisation analysis

The neuronal responses recorded by MEG exist as measures of magnetic flux in sensor space and many single sensors in the SQUID array are likely to detect the same source. Therefore, to determine the origin of a particular signal in the brain, the data must be reconstructed in source space by implementing source localisation algorithms. Such approaches provide possible solutions to the inverse problem; the formation of an estimate of the likely location of a current source given what has been recorded by the sensors (Mosher, Leahy & Lewis, 1999; Baillet et al., 2001). As multiple combinations of sensors may account for an observed source, the inverse problem is subject to non-uniqueness and definitive localisation is impossible. Therefore, to realistically constrain the estimate of how the sources are generated, the sensitivity profile of the sensors can be computed to solve the forward problem; a prediction of sensor level data given a particular source strength and location. Given that the sensor level data is already known, this allows the solution to the forward problem to guide source localisation.

Initial source reconstruction methods involved modelling the activity of a number of current dipoles to account for the observed data, given the assumption that only a few would be active during a brief period of time (~100 ms). Such algorithms attempt to reduce the difference between predicted and observed fields and rely on the enhancement of signal-to-noise ratio afforded by averaging across trials. However, when multiple sources of activity are present, dipole fitting methods can become unreliable (Supek & Aine, 1993; Salmelin & Hämäläinen, 1995). They are also prone to error when using a sub-set of sensors as opposed to the entire array (Vrba, Cheung, Cheyne, Robinson & Starr, 1999). Using a beamformer-based approach, such source reconstruction errors can be avoided (for a review, see Hillebrand & Barnes, 2005). They also possess the advantage of being well-suited to assessing changes in induced responses, rather than purely phase-locked, evoked wave forms, due to their use of single-trial data.

Beamformers act as spatial filters, searching through source space to focus on target activity and suppress activity from other locations. Synthetic Aperture Magnetometry (SAM) is a beamformer method that is particularly effective at also suppressing external, non-physiological sources of noise (Robinson & Vrba, 1999; Vrba & Robinson, 2001). For example, accurate source localisation estimates of primary somatosensory cortex activity have been derived using SAM, in the presence of artefacts generated by a thermal pain stimulator device (Adjamian, Worthen, Hillebrand, Furlong, Chizh, Hobson... & Barnes, 2009). However, the success of noise cancellation is dependent on the extent of the artefacts (Hillebrand, Fazio, De Munck & Van Dijk, 2013) and whether the sources of interference can be both temporally and spatially distinguished from the activity of interest (Taulu & Simola, 2006). For this reason, it is advantageous if noise sources are correlated across the sensors.

To implement the SAM algorithm, the surface of the brain is partitioned into a grid of voxels, representing equivalent current dipoles that signify potential source locations of mass neuronal activity (Figure 2.9). The number of sources is not specified a-priori as is required using a least-squares method. Instead, the algorithm searches through each of these voxels to produce a set of weights. These weights represent the time course for each source location and, therefore, indicate the weighted contribution of each sensor to the identified source. In order to form the beamformer weights, covariance and lead field matrices must be specified. A covariance matrix is formed for each frequency band of interest. The covariance matrix is derived from the data and estimates the relationship

between the sources, to determine the sensor-level variance that can be explained by the source. This step is crucial as SAM assumes that the time course of the source, at each of the sensors, is independent and uncorrelated. For this reason, it may not recover activity from bilateral or temporally synchronous sources.

Figure 2.9. Synthetic Aperture Magnetometry (SAM). Overview of the steps implemented to generate estimates of source power. The single trial data is used to form the covariance matrix and the forward solution is computed at each voxel, in order to generate the beamformer weights for each region. These weights indicate the contribution of each of the sensors to the observed source. Power estimates are then derived from the data by assessing differences between the active and baseline sections of the trials (image taken from Cheyne, 2013).

The lead field matrix is generated as the forward model, often using the multiple local spheres model, as opposed to complex boundary element models or simplistic single-sphere models (Huang, Mosher & Leahy, 1999). To estimate brain shape, the multiple-spheres model uses individual structural MRI images to create a separate sphere in the brain for each MEG sensor, such that each sensor has its own forward model. This appears to be the most accurate and computationally efficient way of characterising source space in relation to the sensors, likely due to the lack of distortion of magnetic fields as they exit the scalp (Leahy, Mosher, Spencer, Huang & Lewine, 1998).

For each voxel, the source estimate is the product of the actual sensor-level data (from the covariance matrix) multiplied by the predicted sensor activity (from the lead field matrix). This estimate is in relation to the centre of the brain. The weights are normalised in this way to minimise the bias in sensor level noise, which would otherwise remain constant irrespective of variations in source depth (Hillebrand & Barnes, 2005). By computing a subtraction between the active task period of the trials and the baseline period, t-statistic images can be generated to visualise source power. It should, however, be noted that these SAM images are not homogenously smooth and the areas of highest power are those with the highest spatial resolution (Barnes & Hillebrand, 2003). This means that regions of lower power will be subject to blurring and the extent of activity cannot be reliably interpreted. Additionally, as a scalar beamformer, SAM performs a search for the single source orientation that projects the most power as opposed to establishing spatial filters for each primary vector. In comparison, vector beamformers compute multidimensional weights (e.g. Linearly Constrained Minimum Variance, LCMV - Van Veen, Van Drongelen, Yuchtman &

Suzuki, 1997; Dynamic Imaging of Coherent Sources, DICS - Gross, Kujala, Hämäläinen, Timmermann, Schnitzler & Salmelin, 2001). However, the scalar, optimised orientation approach appears to be at least comparable to the vector method (Sekihara, Nagarajan, Poeppel & Marantz, 2004).

From the individual SAM images, regions of peak source power can be established. Subsequently, 'virtual sensors' can be formed at these sites, which further refine source localisation estimates by regenerating the time course for the weights at that precise region. Adopting smaller, band-specific, frequency windows further enhances the localisation of the source, whereas broad windows favour frequency bands lower in the spectrum where there is more power (Demanuele, James & Sonuga-Barke, 2007). The virtual sensor data can be used to visualise evoked fields as the generated phase-locked component (evagram) averages the data in the time-domain. However, the advantage of using the beamformer method is most apparent in relation to induced responses. The analysis of data on the basis of single-trials enables SAM to accurately define these responses, which are unsuitable for signal averaging. Plotting the non phase-locked component (agram), time-frequency spectrograms can be generated to visualise induced responses; with the time course (trial timing, typically in seconds) and frequency (Hz) on the X and Y axes. Amplitude is denoted by the colour of the response, in correspondence to the accompanying heat map (as in Figures 2.8b & 2.8c).

To draw inferences at group level, peak magnitude and latency or frequency and amplitude values can be derived from the virtual sensor data. Estimates of average power across a frequency band of interest can also be obtained for the induced responses. These values can subsequently be analysed using statistical packages. Additionally, group SAM images can be generated and projected onto a normalised brain template to be able to perform non-parametric permutation tests (Singh, Barnes & Hillebrand, 2003). This method presumes that assignment to conditions is arbitrary (that they possess 'exchangeability'), such that alternatives to the original statistical outcome can be found by altering the condition labels and forming alternate combinations of the data (Nichols & Holmes, 2002). A series of random-replacement permutations, where these combinations are assessed, are performed to find the distribution of statistics under the null hypothesis. This determines whether the established p value falls within the accepted range or whether it is likely to have been a spurious finding.

3. Experimental Chapter 1

Investigating the Neurochemical Underpinnings of Transcranial Direct Current Stimulation - A Magnetic Resonance Spectroscopy Study

3.1. Abstract

The effects of tDCS are thought to be driven by aspects of neurobiological function that reflect the status of excitatory and inhibitory mechanisms, such as the concentration of key neurotransmitters. To test this proposal, the study aimed to replicate previous findings obtained using magnetic resonance spectroscopy (MRS), which suggest that anodal tDCS is able to modulate concentrations of glutamate/glutamine (Glx) and γ-aminobutyric acid (GABA). In order to investigate the generation of stimulation-induced changes in neurotransmission, anodal and sham tDCS (1 mA, 600 s) was administered to sensorimotor cortex between pre- and post-tDCS MRS acquisitions. Furthermore, differences in the sequence parameters used to obtain the GABA data were investigated by deriving neurochemical concentrations from macromolecule (MM) suppressed and non-suppressed acquisitions. No significant modulations were apparent in levels of Glx or GABA, with and without macromolecules. Baseline GABA concentration was shown to predict response to tDCS but this relationship was present for both active and sham modalities. The results highlight the potential contribution of individual difference factors in the generation of tDCS-induced alterations in plasticity.

3.2. Introduction

Throughout the literature, the neurobiological underpinnings of tDCS after-effects have been likened to long-term potentiation and depression (LTP/LTD) (for an overview; see Medeiros et al., 2012). Characterised as use dependent change in synaptic strength (Lømo, 1966; Bliss & Lømo, 1973), LTP/LTD was initially linked to the action of post-synaptic N-methyl-D-aspartate (NMDA) receptors, which respond selectively to glutamate (Glu). More recently, a role for interneurons responsive to γ-aminobutyric acid (GABA) has also been established (Trepel & Racine, 2000; McDonnell, Orekhov & Ziemann, 2007). As the primary inhibitory neurotransmitter in the human brain, the role of GABA is to modulate excitation. Accordingly, enhanced inhibition will block LTP induction and both $GABA_A$ and $GABA_B$ receptors have been proposed to play an integral role in the formation and maintenance of synaptic connections (Gaiarsa, Caillard & Ben-Ari, 2002; Gaiarsa, Kuczewski & Porcher, 2011). To rapidly regulate levels of excitation, GABA activates ionotropic chloride-gated, $GABA_A$ receptors at the

synapse to induce hyperpolarisation and elicit inhibitory post-synaptic potentials (IPSPs). Extrasynaptic $GABA_A$ receptors also exist which are said to control 'GABAergic tone' (Stagg, 2014), which describes the tonic level of inhibitory activity. Through the stimulation of potassium channels, metabotropic $GABA_B$ receptors regulate excitatory activity by reducing the rate of glutamatergic neurotransmission or by altering the action of $GABA_A$ receptors via feedback-inhibition of pre-synaptic $GABA_B$ receptors. Considering the dynamics of excitatory regulation via GABAergic mechanisms, there is a clear basis on which to suggest that a combination of both glutamatergic and GABAergic mechanisms are responsible for the induction of LTP/LTD.

This interplay is attributed to the biochemical relationship of these neurotransmitters; whereby GABA is synthesised from glutamate via the enzyme glutamic acid decarboxylase (GAD), of which there are two main isoforms associated with GABA production within the vesicles (GAD 65) and cytoplasm (GAD 67) (Kaufman, Houser & Tobin, 1991; Stagg, Bachtiar & Johansen-Berg, 2011a; Best, Stagg & Dennis, 2014). Therefore, substances that differentially alter inhibition and excitation will often have opposite effects on GABAergic and glutamatergic function. Zhang, Wang, Gao, Ge, Zhang, Wu and Xu (2009) illustrated this concept by demonstrating an increase in GABA and decrease in glutamate, in response to the anaesthetic agent Propofol. However, this is not always the case and these neurochemicals have also been shown to be independent. For example, Gabapentin (an analgesic agent that stimulates GAD and was initially designed to prevent seizures) has been shown to increase GABA in visual cortex with no resulting alteration in glutamate (Cai, Nanga, Lamprou, Schinstine, Elliott, Hariharan... & Epperson, 2012). These outcomes may be related to whether excitatory or inhibitory drive is most crucial to the resulting response. Propofol primarily engages glucose metabolism and excitation mechanisms (Westphalen & Hemmings, 2006), whereas Gabapentin modulates inhibition having been synthesised to mimic the action of GABA. Evidently, changes in the status of excitatory and inhibitory mechanisms can have very distinct effects on neurotransmission.

Such modulations in excitatory and inhibitory processes have been repeatedly observed following direct current stimulation. Since the early animal studies (Creutzfeldt et al., 1962; Bindman et al., 1964; Purpura & McMurtry, 1965), DC stimulation has been conceptualised in relation to its ability to alter cortical excitability. Exploring the effects of stimulation in humans, Nitsche and Paulus (2000, 2001) elaborated on the ability of

tDCS to induce prolonged excitability changes that exceeded the scope of transient fluctuations in resting membrane potential. Using TMS to elicit MEPs as a physiological metric of excitability, the authors documented elevated thresholds following anodal stimulation and reduced thresholds following cathodal stimulation. Postulating a role for stimulation-induced changes in specific ionic and neurotransmitter systems, pharmacological interventions were subsequently used to determine the respective roles of glutamate and GABA. Liebetanz et al. (2002) demonstrated a suppression of the after-effects of both anodal and cathodal tDCS following administration of the NMDA antagonist Dextromethorphan (DMO), illustrating the involvement of these specific glutamatergic receptors. Identical results were found during a subsequent study (Nitsche et al., 2003b). Further evidence for the role of NMDA has been produced using D-cycloserine (CYC) an NMDA agonist (Nitsche et al., 2004b), which prolonged the duration of the resulting anodal after-effect. In relation to inhibitory mechanisms, the $GABA_A$ receptor agonist Lorazepam (LOR) has been shown to modulate the typical increase in excitability following anodal tDCS (Nitsche et al., 2004a).

The use of paired-pulse TMS protocols, shown to probe specific aspects of cortical function (Liepert et al., 1997), has also allowed for insight into the proposed neurobiological mechanisms of tDCS. Firstly, measures of intracortical facilitation and inhibition have been shown to be modulated following anodal stimulation, at durations exceeding 7 minutes (Nitsche et al., 2005). The resulting increase in facilitation and decrease in inhibition was not found during a brief exposure to tDCS (4 s), confirming the distinction between the physiological mechanisms engaged at short and long stimulation durations. Additionally, a reduction in cortical silent period (CSP) duration following anodal tDCS has been found, illustrating the involvement of $GABA_B$ receptors in the generation of anodal after-effects (Tremblay et al., 2013). A reduction in short-interval intracortical inhibition (SICI), a measure of $GABA_A$ receptor response, has also been demonstrated following anodal tDCS (Antal, Terney, Kühnl & Paulus, 2010a). Therefore, both fast and slow acting inhibitory mechanisms are likely to be modulated by prolonged durations of tDCS.

Sparking the recent surge of interest in multi-modal tDCS investigations, a number of proton Magnetic Resonance Spectroscopy (^{1}H-MRS) studies have been conducted to explicitly assess the neurochemical basis of tDCS effects. MRS represents a non-invasive method of neurotransmitter quantification for a given voxel of interest.

Measured in parts per million (ppm), the chemical shift spectrum features a GABA peak at 3 ppm and a glutamate/glutamine (Glx) peak at 3.75 ppm. Concentrations of these neurochemicals (derived using MEGA-PRESS at a range of voxel locations) are relatively small (GABA: 0.8-1.8mM, Glx: 8-10mM) but have been shown to be highly reproducible, in relation to both within-session and between-session variability (Bogner, Gruber, Doelken, Stadlbauer, Ganslandt, Boettcher... & Hammen, 2010; O'Gorman, Michels, Edden, Murdoch & Martin, 2011; Wijtenburg, Rowland, Edden & Barker, 2013; Near, Ho, Sandberg, Kumaragamage & Blicher, 2014; Mikkelsen, Singh, Sumner & Evans, 2015). As a valuable tool in clinical imaging, MRS investigations of these neurochemicals have involved the classification of associations between concentrations in sensorimotor cortex and multiple sclerosis (Bhattacharyya, Phillips, Stone, Bermel & Lowe, 2013), anterior cingulate cortex (ACC) and autism spectrum disorder (Bejjani, O'Neill, Kim, Frew, Yee, Ly... & Levitt, 2012; Brix, Ersland, Hugdahl, Gruner, Posserud, Hammar... & Beyer, 2015), medial frontal cortex and schizophrenia (Rowland, Krause, Wijtenburg, McMahon, Chiappelli, Nugent... & Hong, 2015), as well as ACC and occipital cortex in relation to the processing of acute pain (Cleve, Gussew & Reichenbach, 2015). In a behavioural setting, GABA concentration has also been shown to be associated with vibrotactile frequency discrimination capacity (Puts, Edden, Evans, McGlone & McGonigle, 2011) as well as both short (Floyer-Lea, Wylezinska, Kincses & Matthews, 2006) and long-term (Sampaio-Baptista, Filippini, Stagg, Near, Scholz & Johansen-Berg, 2015) motor learning performance, which has practical implications for stroke rehabilitation.

Combining stimulation of primary motor cortex with MRS, Stagg et al. (2009) established a reduction in GABA following anodal tDCS (10 minutes, 1 mA). A significant reduction in the concentration of the glutamate-glutamine composite, alongside a correlated GABA decrease, was also demonstrated following cathodal tDCS. Subsequent research established a significant increase in Glx under the active electrode after anodal tDCS, delivered to parietal cortex (30 minutes, 2 mA; Clark, Coffman, Trumbo & Gasparovic, 2011). This was later found to be associated with enhanced parietal and fronto-parietal network connectivity (predictable on the basis of individual Glx concentrations; Hunter, Coffman, Gasparovic, Calhoun, Trumbo & Clark, 2015). The decrease in GABA brought about by anodal tDCS has also been suggested to increase functional connectivity within the resting state motor network (Stagg, Bachtiar, Amadi, Gudberg, Ilie, Sampaio-Baptista... & Johansen-Berg, 2014). Furthermore, a relationship has been established between the extent of anodal tDCS-

induced decreases in GABA and motor learning capacity (Stagg, Bachtiar & Johansen-berg, 2011b). This pattern of results has recently been replicated at 7 T and extended to a motor memory, force adaptation task (Kim, Stephenson, Morris & Jackson, 2014). Importantly, these findings are in agreement with the previously outlined stimulation-induced outcomes established using TMS protocols to index changes in cortical excitability. Taken together, changes in excitatory and inhibitory neurotransmission can be directly observed as a result of tDCS, which in turn appear to be associated with alterations in measures of neural communication and information transfer capacity as well as behavioural performance. These changes in neurotransmission are likely a result of altered synaptic plasticity and receptor function, which governs the synthesis and subsequent availability of such metabolites.

Despite the promising nature of findings derived from these MRS studies, it is important to note that the signals pertaining to the neurotransmitters of interest are not entirely pure. Glutamate is quantified as Glx because the signal cannot be separated from that of glutamine at 3 T. Likewise, the minute GABA signal at 3 ppm requires spectral editing techniques to be resolved at 3 T because it normally overlaps with creatine, which is more abundant (Mullins et al., 2014). The edited spectrum includes only the resonances coupled to the GABA peak but the signal of interest is co-edited with, and contaminated by, that of macromolecules (MM) (Edden et al., 2012a). However, symmetric suppression or metabolite nulling can be implemented to largely remove this contamination and produce optimised measures of GABA (Henry et al., 2001; Terpstra, Ugurbil & Gruetter, 2002).

Measures of GABA with and without macromolecule suppression have been shown to exhibit a trend towards a positive correlation in sensorimotor cortex but not occipital cortex (Harris, Puts, Barker & Edden, 2014), potentially indicating the influence of regional variations in both GABA and MM (Durst, Michael, Tustison, Patrie, Raghavan, Wintermark & Velan, 2015). Typically, the MM contribution is 50% of the total GABA signal (de Graff, 2014) and a recent publication has emphasised the importance of accounting for this, particularly with respect to inconsistencies in voxel positioning that could lead to differences in grey matter content and thus variable MM contamination (Bhattacharyya, 2014). However, MM correction and/or suppression techniques are not commonly employed at present. Concentration estimates of the inhibitory neurotransmitter are, therefore, often referred to as “GABA+”. This is an important consideration for studies seeking to modify regionally specific GABA

concentrations as it cannot be definitively inferred that GABA itself is being modulated, where MM contamination is present. To date, tDCS studies of GABA-MRS have not taken this contamination into account by acquiring MM suppressed spectra. This raises obvious issues for the certainty with which it can be said that GABA is driving the effects of tDCS. In turn, this inevitably impacts upon how these neuroimaging findings can be translated to assist in the formation of targeted stimulation-based interventions, for neurological and psychiatric disorders.

The current study aimed to explicitly address this issue by acquiring data from both MM-suppressed and non-suppressed GABA-MRS sequences, before and after anodal and sham stimulation. To facilitate insight into the role of excitatory neurotransmission and to allow for comparison to the existing literature (Stagg et al., 2009; Clark et al., 2011), Glx data was also obtained. In line with previous findings, it was predicted that non-suppressed GABA would be significantly reduced and Glx would be increased after anodal stimulation, compared to sham. Given that the 'true' local GABA concentration (in the absence of additional signal components) has been proposed to underlie the observed effects of tDCS, a reduction in GABA was also expected to be present, perhaps even to a greater extent, for the MM-suppressed acquisitions. Finally, the magnitude of change in GABA following tDCS has been shown to correlate with performance on specific tasks with learning-based outcome measures (Stagg et al., 2011b; Kim et al., 2014), which highlights the importance of individual differences in the physiological response to stimulation. This poses the question of whether pre-existing variations in GABA might also be able to influence subsequently assessed metrics of change e.g. post-tDCS GABA levels. Such an explicit association between baseline GABA concentration and percentage change in GABA levels following tDCS has not previously been demonstrated. It was anticipated that such a relationship would be evident for both the MM-suppressed and non-suppressed GABA measures.

3.3. Methods

3.3.1. Pilot testing

Prior to participant recruitment, initial testing took place to determine the safety and feasibility of conducting combined tDCS-MRS research at CUBRIC. Firstly, a phantom was used to assess the likelihood of adverse temperature changes underneath the electrodes due to RF heating (in the absence of stimulation). The phantom consisted of a small square container (~15 cm^2) filled with agar; a gelatinous substance traditionally

used for MRI quality assurance (QA) purposes (Hellerbach, Schuster, Jansen & Sommer, 2013). A Medrad Veris monitor with fibre optic probes was used to measure the temperature under an electrode pad and at a remote reference location. The phantom was placed in the bore of the magnet and baseline temperatures were noted for 20 minutes, prior to 30 minutes of scanning with sequences of the highest possible specific absorption rates (SAR SPGR; 2.8-3.1 watts/kg). As evident in Figure 3.1a, the temperature increase underneath the electrode was largely proportional to that at the reference location as the SAR output was elevated. The maximum temperature difference between the probes was 1.1°C at the highest SAR output (Figure 3.1b). Therefore, it was determined that no adverse RF heating from the presence of the electrodes was to be anticipated and the procedure was safe for participants to undergo.

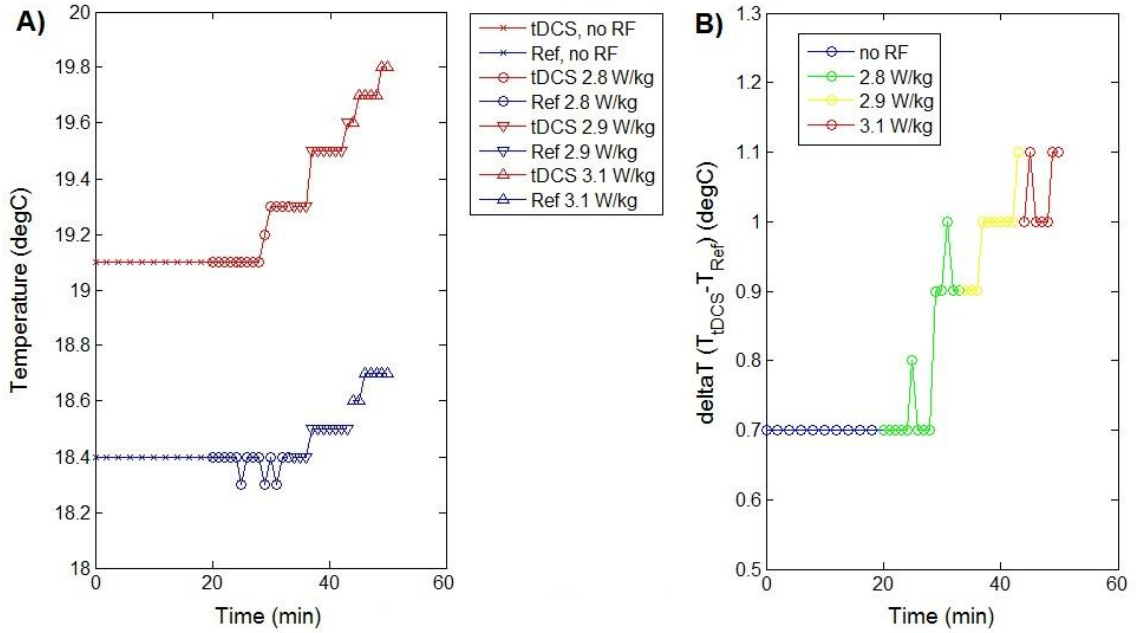

Figure 3.1. Assessment of temperature change in an agar phantom. A) Temperature readings from the probe underneath the electrode pad (tDCS) and at the reference location (Ref) as SAR output increased. B) Values reflecting temperature differences between the electrode pad and reference probe as SAR output increased.

Subsequently, a manganese chloride (MnCl2) phantom was utilised to determine the effect of the presence of the tDCS electrodes on the static signal-to-noise ratio (SNR) and signal-to-fluctuation noise ratio (SFNR), which represents an index of temporal stability. An echo planar imaging (EPI), QA sequence was used to acquire the data (30 x 4 mm slices with a 2 mm gap; 300 volumes; TE=35 ms; TR=2000 ms). SNR was calculated as the mean signal across a 21 x 21 mm voxel region in two slices at the centre of the phantom, divided by the standard deviation of an acquired noise image

(determined by subtracting the second from the first images in the timeseries). SFNR was calculated as the standard deviation in voxel signal over time, divided by the mean signal from that voxel over the timecourse (as detailed in Friedman & Glover, 2006) and is reported as the mean SFNR value from the voxel at the centre of the phantom.

Baseline measures were 133.6 for SNR and 263.5 for SFNR (Figure 3.2a). These values were within one standard deviation of the average of the previous 10 QA scans (SNR=132.9 ± 2.7; SFNR=266.8 ± 4.9). With the tDCS system in place, the following values were obtained: SNR=115.2; SFNR=250.1 (Figure 3.2b), which would be sufficient to detect changes in brain activity during a typical fMRI research study (Parrish, Gitelman, LaBar & Mesulam, 2000). These readings corresponded to a decrease in both SNR (-13.8%) and SFNR (-5.1%), considered to be an acceptable drop in data quality such that the experiment could continue (as specified by the MRI lab manager, Dr. John Evans).

Although not directly relevant to the design of the current study (as outlined below), a noteworthy observation was that a far more dramatic decrease was observed during anodal stimulation: SNR=52 (-39%), SFNR=126 (-48%). This may largely be due to the onset of the stimulation as demonstrated by the marked fluctuation in signal during the first ~30 volumes (Figure 3.2c). Note also the inhomogeneity of the signal in the SFNR map and brightening in the region corresponding to the reference electrode pad, highlighting an interaction between the electrodes and the RF field. This suggests that when running stimulation concurrently with data acquisition there is likely to be extensive signal variability in the regions of most interest. Yet surprisingly, field maps from concurrent tDCS-fMRI experiments have only been reported to show 'minimal perturbation of signal' around the electrodes (Holland, Leff, Josephs, Galea, Desikan, Price... & Crinion, 2011).

Quality assurance was also determined using a PRESS sequence: TE=35 ms, TR=1500 ms, 128 averages using a 3 cm^3 voxel prescribed at the centre of the phantom (designed to correspond to the centre of the RF coil; L/R=0, S/I=0, A/P=30 cm). These scans incorporated the use of a GE "Braino" phantom (GE Medical Systems, Milwaukee, WI, USA), which mimics the metabolites found in the human brain: 12.5 mM of N-acetyl-L-aspartic acid, 12.5 mM of L-glutamic acid, 10 mM of creatine hydrate, 7.5 mM of myo-inositol, 5 mM of DL-lactic acid, 3 mM of choline chloride, sodium azide (0.1%), 50 mM of potassium phosphate monobasic, 56 mM of sodium hydroxide and 1 mL/L of Gd-DPTA Magnevist.

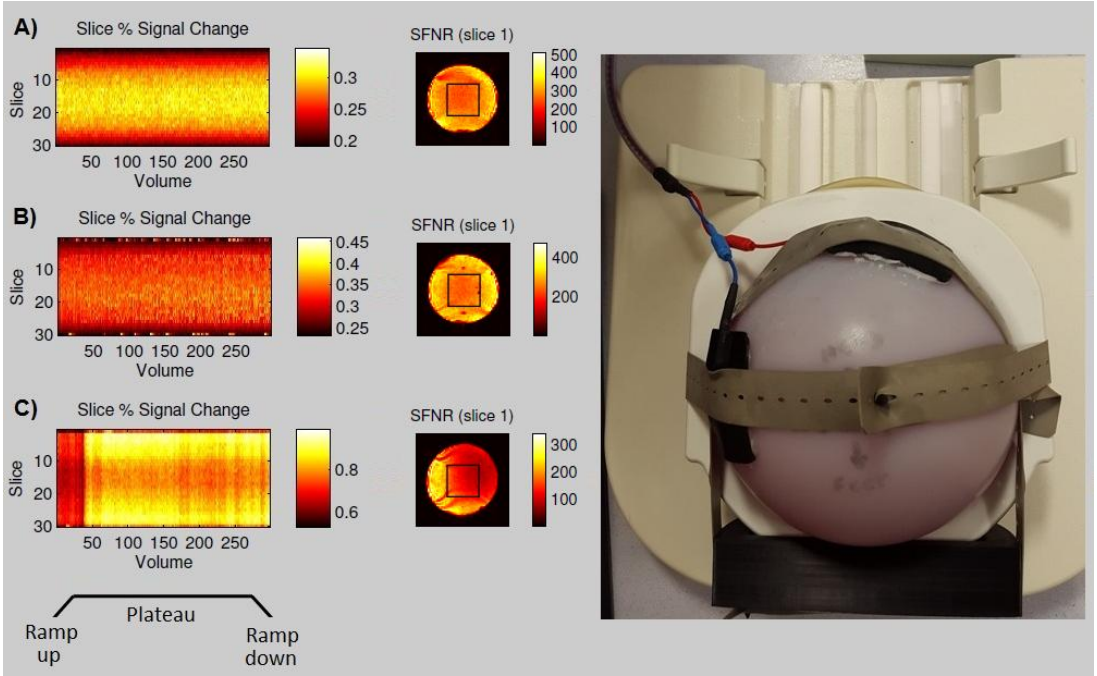

Figure 3.2. Assessment of SNR and SFNR in a manganese chloride phantom. Data obtained during A) a baseline EPI QA scan, B) an EPI QA scan where the tDCS electrodes were attached to the phantom, C) an EPI QA scan where anodal tDCS stimulation was administered. Slice % Signal Change: Each pixel represents the mean percentage signal for volume (V), slice (S) and volume (V-1), slice (S) (e.g. for a value of 1% for volume 50, slice 20 would represent a mean signal change of 1% across all voxels within that slice from between volume 49 and 50). Note the uniform signal change throughout the acquisition period when the electrodes were present compared to when stimulation was delivered, where a distinction in slice % signal change is evident for the current ramp (corresponding to the first ~30 volumes) and plateau phases. SFNR: Noise variability in the first of the two assessed slices. Similar to the signal change plots, note the instability of noise during stimulation. Substantial inhomogeneity is present across the phantom, most noticeably in the region underneath each electrode pad.

During the baseline scan, the SNR for creatine was 569.2. When the electrodes were attached to the phantom, a slight decrease in the initial value was evident: Cr SNR=553.8 (-2.7%). This was less pronounced than that found for the EPI sequence. This may be because MRS represents a more static measure than EPI, which is generally more sensitive to noise and temporal variation as it is primarily used in event-related fMRI experiments to detect rapid fluctuations in haemodynamics. Nonetheless, both the obtained measures suggested that sufficient SNR would result from the prospective experimental protocol.

3.3.2. Subjects

To determine the ideal sample size, power calculations were performed on effect size data relating to the GABA concentrations derived by Stagg et al. (2009). Power calculations were performed using G*Power Version 3.1 (University of Dusseldorf, Germany; Faul, Erdfelder, Lang & Buchner, 2007). Based on the data, a sample size of

N=8 was recommended (assuming two-tailed significance, Appendix 5). However, due to differences in aspects of study design (scan acquisition time, number of conditions), a sample of 16 subjects was recruited. All subjects were aged 22-33 *(M=26.44; SD=3.20)* and were determined to be right-hand dominant (Edinburgh Handedness Inventory, Oldfield, 1971; Appendix 1). Upon expressing an interest in taking part in the study, subjects were screened to determine their eligibility (Appendix 2). Those with any contraindications were excluded from the study. All procedures were carried out with the approval of the local ethics committee.

3.3.3. MRS acquisition

A 3 T General Electric Signa HDx scanner with an eight-channel head coil was used to acquire the single voxel, ^{1}H-MRS data. The voxel measured 3 cm^3 and was positioned within left sensorimotor cortex, based on the location of the hand knob region (Yousry, Schmid, Alkadhi, Schmidt, Peraud, Buettner & Winkler, 1997; as adopted by Evans, McGonigle & Edden, 2010 and Puts, Edden, Evans, McGlone & McGonigle, 2011). Sagittal and coronal fast spin echo, T2-weighted localisers were acquired to plan the alignment of the voxel (rotated to be parallel to the cortical surface). 3D Fast Spoiled Gradient echo (FSPGR) MRI scans were acquired in an axial orientation with 1 mm^3 isotropic voxel resolution to allow precise voxel positioning and to facilitate tissue segmentation. A screenshot was taken of the sensorimotor voxel position during session one, which was used to assist voxel placement in session two.

Spectra were obtained using MEGA-PRESS sequences, in order to provide simultaneous water suppression and editing of the GABA signal at 3 ppm (Mescher et al., 1998). Accordingly, an initial 90° pulse was applied before two subsequent 180° refocusing pulses, with Gaussian editing pulses placed between the 90° and first 180° pulse and between the two 180° pulses. During ON/OFF experiments, editing pulses were either positioned at 1.9 and 7.5 ppm or at 1.9 and 1.5, to be symmetrical about the 1.7 ppm MM resonance. As previously outlined, while the former separates the GABA peak from more abundant, overlapping metabolites such as creatine, the latter also removes the contribution of J-coupled macromolecules in order to resolve an optimised GABA peak. All scans featured 20 ms editing pulses, an 80 ms TE, an 1800 ms TR and consisted of 332 averages (~ 10 minutes), with a spectral width of 5 kHz (4096 points). Measures of Glx were obtained from the difference spectra of the non MM-suppressed sequence.

3.3.4. Transcranial direct current stimulation

A DC-Stimulator MR device (neuroConn, Germany) was used to deliver direct current stimulation. Subjects took part in two separate sessions and were randomly assigned to one of four session orders, defined by stimulation (Anodal (A) & Sham (S)) and sequence type (GABA with MM contamination (GABA'+MM) & GABA without MM contamination (GABA'); as referred to by Mikkelsen et al., 2015). Each session took place at least 24 hours apart. The experiment was double-blind (made possible using the "study" mode option, in which stimulation parameters were pre-defined and executed using codes for active and sham stimulation). Stimulation duration was set to 600 s for each session, with an additional 10 s current onset/offset period. MR-compatible rubber electrodes, measuring 5x7 cm (35 cm^2), were attached to the scalp using Ten20 conductive paste. Anodal stimulation was delivered with a current of 1 mA (current density = 0.029 mA/cm^2). For sham stimulation, the neuroConn device initially ramped up the current to mimic the peripheral effects of active tDCS before ramping down. During the stimulation period, the device continued to discharge current spikes every 550 ms (110 μA over 15 ms) to enable continuous impedance readings. The average current over time was not more than 2 μA. In conjunction with the 10-10 system (Appendix 3; Chatrian, Lettich & Nelson, 1985), the electrodes were positioned at C3 (left hemisphere, active) and Fp2 (right hemisphere, reference), designed to stimulate sensorimotor cortex (Figure 3.3a). The tDCS device was located within the control room and was connected to the electrodes via neuroConn RF filter boxes and cables passed through the waveguide, as depicted in Figure 3.3b.

This image has been removed by the author for copyright reasons.

Figure 3.3. Administration of tDCS within the MRI scanner. A) The electrode pads were positioned at sites C3 (active) and Fp2 (reference). B) Direct current stimulation was administered via a series of RF filter boxes and cables, such that the device could be positioned outside of the magnet room (image adapted from Tremblay et al., 2014).

3.3.5. Experimental procedure

Subjects began each session by completing the necessary consent and screening forms (see Appendix 6 for the study-specific consent form). They were then prepared for tDCS as outlined previously, before being taken into the magnet room and positioned in the scanner. Before the onset of the first scan, a brief period of stimulation (~10-20 s)

was delivered to determine whether impedance levels were sufficient to begin stimulation. Such durations of active stimulation have been shown to produce highly transient changes in cortical excitability, which should have returned to baseline before the first recording (Bindman et al., 1964; Purpura & McMurtry, 1965; Nitsche et al., 2003b).

Both GABA'+MM and GABA' sequences were used to acquire data, before and after stimulation. This produced four GABA-MRS scans per session. Stimulation took place while participants were inside the scanner but did not coincide with MRS acquisition. Participants were in the MR scanner for 90 minutes in total. For the duration of the scan session, participants were asked to rest and attend to a nature documentary to standardise the procedure across subjects. At the end of each session, participants were asked to complete an Adverse Effects Questionnaire (AEQ; Appendix 4) to provide details of any side-effects experienced. Each experimental session lasted approximately 120 minutes.

3.3.6. MRS data analysis & statistics

The spectra were processed using an in-house version of Gannet 2.0 (Edden et al., 2014); a toolbox for the analysis of MRS data implemented via MATLAB (MathWorks; Cambridge, UK). Its main functions are GannetLoad and GannetFit. GannetLoad involves the conversion of free induction decay (FID) data in the time-domain to the frequency-domain, using a fast Fourier transform (FFT). Zero-filling is used to smooth the spectra, while frequency and phase correction are applied to remove subtraction artefacts. Pairs of outliers (constituting "ON/OFF" experiments) more than 3 standard deviations from the mean are removed by the software. This occurs prior to time averaging of the data to generate the GABA-edited and "OFF" spectra, where standard peaks for creatine, NAA and Glx remain present. GannetFit was used to quantify the edited 3 ppm GABA signal by applying a non-linear least squares fitting method to estimate the area under each peak. Concentrations were defined as GABA:NAA or Glx:NAA ratios, in institutional units (iu). To ensure that change in the metabolite of interest had occurred, concentrations referenced to creatine were also derived. The GABA peak at 3 ppm was fitted as a single Gaussian function between 2.79-3.55 ppm. The Glx peak at 3.75 ppm was fitted as a double Gaussian between 3.45-4.10 ppm. NAA at 2 ppm and Cr at 3 ppm were defined as Lorentzian curves between 1.75-2.25 ppm and 2.72-3.12 ppm, respectively (Cr was obtained from the OFF spectra). The sensorimotor voxel was co-registered to the corresponding anatomical image to produce

a voxel mask for each participant. These masks were used to allow segmentation of the voxel into the respective volumes for each different tissue component. Accordingly, partial volume maps were calculated for cerebrospinal fluid (CSF), grey matter (GM) and white matter (WM), using the FMRIB Software Library's (FSL) segmentation and brain extraction tools; FAST (Zhang, Brady & Smith, 2001) and BET (Smith, 2002).

The GABA and Glx spectra were subsequently assessed for evidence of contamination e.g. subtraction and/or motion based artefacts, based on visual inspection of the post-alignment spectra (after frequency correction of the data) and the structure of the resolved peaks. Three researchers were involved in the quality assurance procedure. A single GABA dataset (N=15) and four Glx datasets (N=12) were excluded, due to the presence of spurious water echo and lipid contamination artefacts. Inter-rater reliability was 0.67 as assessed using Fleiss' kappa statistic (Fleiss, 1971; Landis & Koch, 1977), indicating substantial inter-rater agreement (Viera & Garrett, 2005).

SPSS for Windows software (Version 20; IBM, New York) was used to assess the significance of alterations in the derived concentration ratios, using Repeated Measures ANOVAs. Of key importance was the distinction between ratios obtained during anodal and sham stimulation for; GABA'+MM, GABA' and Glx. These analyses incorporated the factors; Time (Pre, Post) and tDCS (Anodal, Sham). Only the spectra obtained from the GABA'+MM scans were used to quantify Glx. The mean fit errors for the GABA'+MM and GABA' sequences were compared to determine whether there were any significant differences in noise between each measure of GABA. tDCS order (Anodal/Sham, Sham/Anodal) was incorporated into the analyses as a between-subject variable. Lastly, an assessment of whether baseline, pre-tDCS concentration levels were able to predict percentage change in post-tDCS ratios was performed, using a series of bivariate Pearson's correlations. P values less than 0.05 were considered significant.

3.4. Results

3.4.1. Peripheral effects of tDCS

Impedance values were 11.6 ± .069 kΩ for anodal stimulation and 11.7 ± .063 kΩ for sham stimulation. Participants reported mild to moderate tingling and itching sensations underneath the electrode pads during tDCS (for average responses, see Figure 3.4). There was no significant difference between the sensations experienced during the

active or sham conditions (F(1,15)=.254, p=.621), suggesting that participants were unaware of the nature of the stimulation they received on a given session.

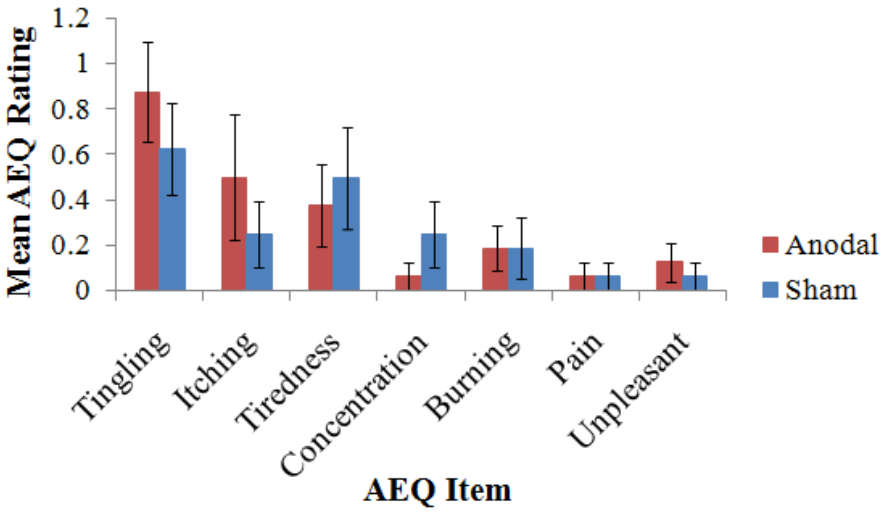

Figure 3.4. AEQ Responses. Average responses to the questionnaire items experienced during stimulation. The scale of responses ranged from 0 (not experienced) to 1-5, indicating heightened severity of the sensation experienced. Error bars represent ± 1 standard error (S.E.M).

3.4.2. MRS data quality

Average line width was 7.74 ± 0.73 Hz and Cr FWHM was 10.44 ± 0.99 Hz, indicating good shim quality and peak resolution based on past acquisitions at CUBRIC (average Cr FWHM: ~10 Hz). Following segmentation, voxel tissue fraction was as follows: CSF (0.06 ± 0.02), GM (0.30 ± 0.03), WM (0.64 ± 0.04). No significant differences were found between the two sessions for CSF (t(15)=-.110, p=.914), GM (t(15)=.659, p=.520) or WM (t(15)=-.446, p=.662). These values also did not differ in relation to the stimulation administered (F(1,15)=1.155, p=.299).

To assess precision in voxel placement, the FSPGRs from each session were registered to each other and the resulting transformation matrix was used to align the two voxel masks, using FMRIB's Linear Image Registration Tool (FLIRT; Jenkinson & Smith, 2001). The repeatability of within-subject voxel placement was 89.73 ± 3.78%, highlighting a high degree of precision in the prescription of the voxel across sessions (Figure 3.5).

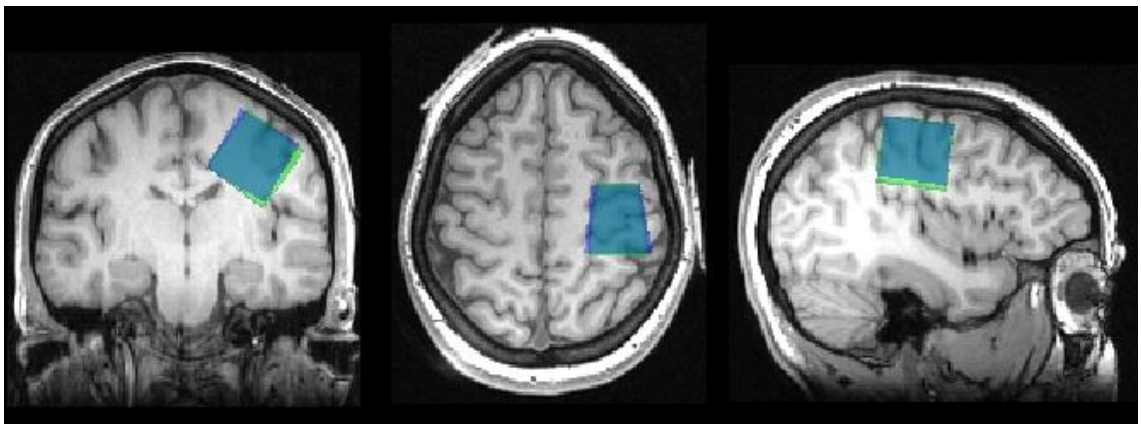

Figure 3.5. Voxel placement repeatability. The structural image from a single subject with the position of the voxels prescribed to left sensorimotor cortex during each session. Images are inverted such that the right side of the image relates to the left hemisphere of the brain and vice versa.

Following symmetric editing, the fraction of the total signal retained was 0.40 ± 0.10 for the NAA ratio and 0.30 ± 0.09 for the Cr ratio, slightly lower than previously documented (Mikkelsen et al., 2015). Regional variation and differences in reference metabolites may account for this. Representative spectra derived from each sequence are shown in Figure 3.6.

With regard to average fit error, GABA'+MM:NAA was 5.46 ± 1.34% compared to GABA':NAA which was 11.25 ± 3.01%. Fit error for Glx:NAA was 5.34 ± 1.55%. Statistical analysis of GABA measurement fit error produced a main effect for Sequence ($F(1,14)=122.572$, $p=.000$). The variables Time ($F(1,14)=4.163$, $p=.061$) and tDCS ($F(1,14)=1.179$, $p=.296$) were non-significant. No interactions were significant. These results indicate that the peaks derived from the GABA' measurements were more difficult to fit, with a trend towards higher post-tDCS fit errors (Appendix 7).

In relation to the creatine ratios, GABA+'MM:Cr was 8.37 ± 1.34% compared to GABA':Cr which was 11.75 ± 2.86%. Fit error for Glx:Cr was 8.51 ± 1.53%. The main effect of Time was significant ($F(1,14)=5.231$, $p=.038$), as was the main effect of Sequence ($F(1,14)=65.655$, $p=.000$). The main effect of tDCS was non-significant ($F(1,14)=.024$, $p=.880$), as were the interactions, similar to the NAA ratios.

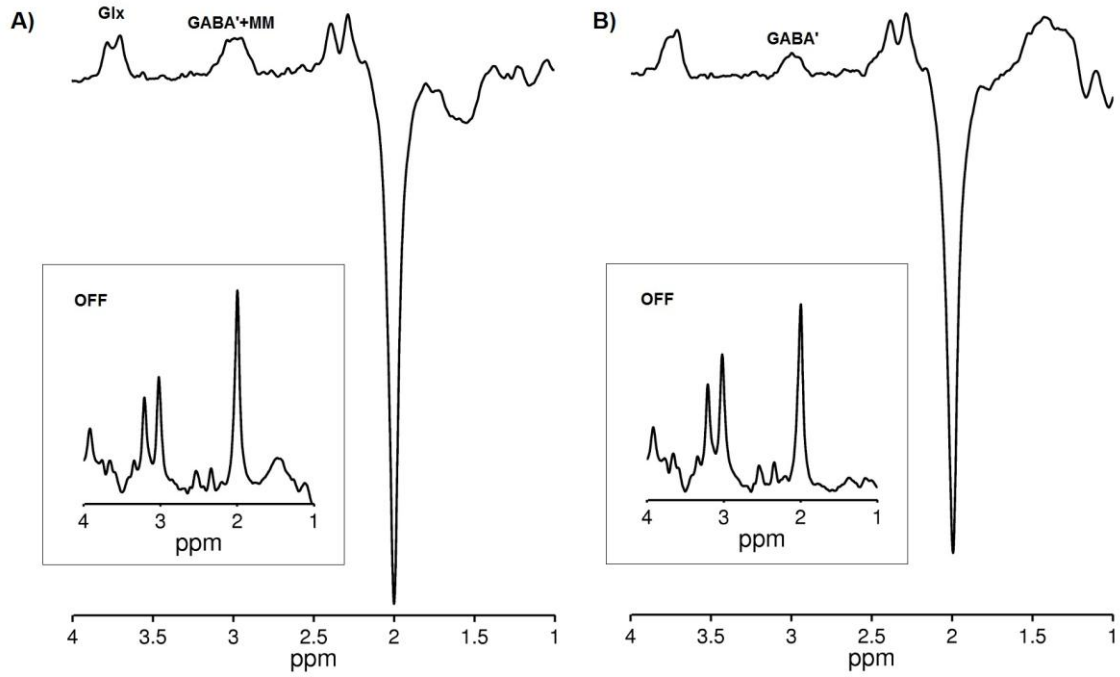

Figure 3.6. Chemical shift spectra. Representative difference spectra from a single subject, prior to tDCS, resulting from A) the standard GABA-edited acquisition and B) the symmetric editing sequence. Note the substantial difference in the GABA peak at 3 ppm between sequences. The insets shows the respective OFF spectra, where GABA is not evident due to the overlapping creatine peak. Spectra were scaled to NAA as it was the chosen reference metabolite.

Motion-induced drift was assessed using standard deviation values derived for the frequency of the water peak. These values were entered into a 2 x 2 Repeated Measures ANOVA to assess differences in Time (Pre, Post) and tDCS (Anodal, Sham), for each sequence type (standard acquisition and symmetric editing). With regard to the standard acquisition, the main effect of Time was found to be significant ($F(1,14)=37.025$, $p=.000$), demonstrating an increase in standard deviation at the post-tDCS time point. The main effect of tDCS ($F(1,14)=1.392$, $p=.258$) and the interaction ($F(1,14)=.947$, $p=.347$) were non-significant. This pattern was also evident for the symmetric editing sequence: Time ($F(1,14)=10.291$, $p=.006$), tDCS ($F(1,14)=.048$, $p=.829$), Time*tDCS ($F(1,14)=1.582$, $p=.229$). While drift changed significantly over the course of each session, it is unlikely that fluctuations in the region of 0.46 to 0.78 Hz, as noted here, would introduce subtraction artefacts or have a discernable impact on the SNR and editing efficiency of each sequence (Bhattacharyya, Lowe & Phillips, 2007; Evans, Puts, Robson, Boy, McGonigle, Sumner... & Edden, 2013).

3.4.3. tDCS-MRS

Pre and post differences in peak amplitude and spectral width, resulting from the anodal tDCS condition, are shown in (Figure 3.7). Mean values and standard deviations reflecting pre/post concentration change are given in (Table 3.1). These values show the expected direction of change for Glx (increase) and GABA (decrease), following anodal stimulation.

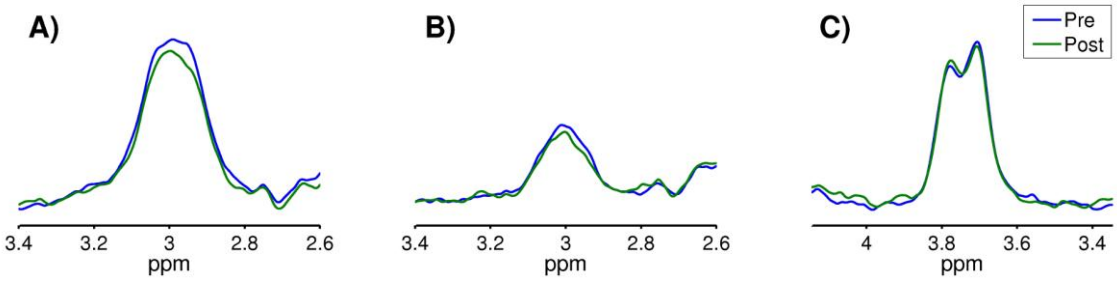

Figure 3.7. Post-tDCS modulation of GABA and Glx. Peaks representing A) GABA'+MM, B) GABA' and C) Glx demonstrate the distinction between spectra acquired prior to and after anodal tDCS.

NAA and Cr concentration ratios (e.g. GABA':NAA, GABA':Cr) for each of the metabolites were positively correlated before and after the delivery of tDCS; providing evidence for the stability of the reference metabolites (all $p<.01$ after 10,000 bootstrapped iterations; see Appendix 8). Therefore, the analysis outlined here is focused on ratios to the primary reference, NAA. Results of the analysis featuring creatine ratios can be found in Appendix 9.

The 2x2 ANOVAs used to investigate the differences between concentration ratios, produced the following results for each sub-analysis. For the GABA'+MM:NAA ratio, the main effects of Time ($F(1,14)=.016$, $p=.902$) and tDCS ($F(1,14)=.373$, $p=.551$) were non-significant, as was the interaction ($F(1,14)=1.289$, $p=.275$). For the GABA':NAA ratio, there was a significant main effect of Time ($F(1,14)=5.641$, $p=.032$), indicating a decline in concentration at the post-tDCS time point. There was also a trend towards a main effect of tDCS ($F(1,14)=3.231$, $p=.094$), indicating a reduction in concentration for the anodal condition. The Time*tDCS interaction was non-significant ($F(1,14)=1.299$, $p=.273$). For the Glx:NAA ratio, the main effects of Time ($F(1,11)=.000$, $p=1.000$) and tDCS ($F(1,11)=.042$, $p=.841$) were non-significant, as was the interaction ($F(1,11)=2.703$, $p=.128$). The between-subject factor tDCS order was non-significant for all the conducted analyses.

Table 3.1. Neurochemical concentrations. Mean ± standard deviation values for concentrations reflecting ratios to A) NAA and B) Creatine. Values were obtained before and after, anodal and sham tDCS. Concentration ratios are given in institutional units (iu).

A)

GABA'+MM:NAA

Pre Anodal	Post Anodal	Pre Sham	Post Sham
.067 ± .007	.065 ± .005	.064 ± .009	.066 ± .008

GABA':NAA

Pre Anodal	Post Anodal	Pre Sham	Post Sham
.026 ± .007	.021 ± .005	.026 ± .006	.026 ± .008

Glx:NAA

Pre Anodal	Post Anodal	Pre Sham	Post Sham
.046 ± .004	.049 ± .005	.049 ± .004	.047 ± .006

B)

GABA'+MM:Cr

Pre Anodal	Post Anodal	Pre Sham	Post Sham
.130 ± .013	.122 ± .010	.123 ± .018	.128 ± .017

GABA':Cr

Pre Anodal	Post Anodal	Pre Sham	Post Sham
.038 ± .011	.029 ± .006	.037 ± .010	.035 ± .011

Glx:Cr

Pre Anodal	Post Anodal	Pre Sham	Post Sham
.088 ± .007	.093 ± .013	.097 ± .018	.105 ± .050

Additionally, analysis was performed to determine the relationship between baseline GABA concentration and percentage change in response to tDCS (Figure 3.8). With regard to the anodal condition, a significant, negative correlation was found for GABA'+ MM ($r(15)=-.646$, $p=.009$, CI=-.855 -.362) and GABA' ($r(15)=-.760$, $p=.001$, CI=-.922 -.493), suggesting those with higher baseline GABA experienced a larger percentage decrease. Unfortunately, the respective sham correlations were also significant: GABA'+ MM ($r(15)=-.750$, $p=.001$, CI=-.924 -.380), GABA' ($r(15)=-.594$, $p=.020$, CI=-.802 -.022). The confidence intervals for the sham GABA' correlation (10,000 permutations) were incredibly broad, indicating a lack of reliability. However, the sham GABA'+MM correlation was consistent. No statistical differences between correlation coefficients could be established, using the Hotellings-Williams test.

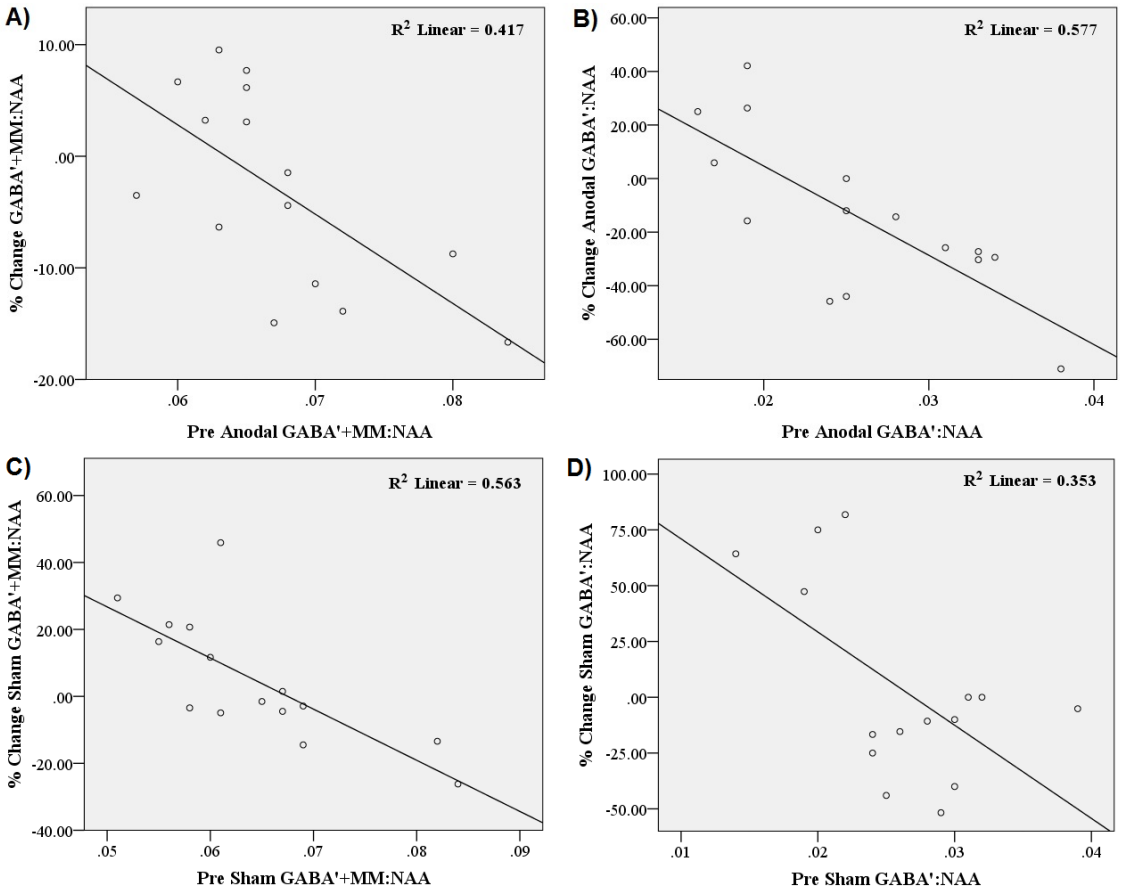

Figure 3.8. Relationship between baseline GABA and response to tDCS. Scatterplots show the significant, negative correlation between baseline concentration and the percentage change response to tDCS. The top row illustrates correlations for the anodal condition, A) GABA'+MM and B) GABA'. The bottom row illustrates correlations for the sham condition, C) GABA'+MM and D) GABA'. Higher baseline concentrations predict larger, post-tDCS percentage decreases in all instances.

In summary, good quality data was acquired as evidenced by the repeatability of voxel placement, linewidth values and standard deviations for motion-induced frequency drift. Fit error differed between acquisition types, although this was to be expected because of the change in shape of the GABA peak due to the decrease in signal inherent to the symmetric editing sequence. With regard to the influence of tDCS, the mean concentration ratios suggested that differences between pre- and post-anodal stimulation had arisen for each of the sub-analyses, in the expected direction. However, these observations failed to reach the criteria for statistical significance. Additionally, response to tDCS (with respect to percentage concentration change in GABA), was shown to be predicted by baseline levels, derived from both GABA measures. However, this was the case for both the active and sham conditions.

3.5. Discussion

The study was designed to assess the role of the primary excitatory and inhibitory neurotransmitters in the effects of tDCS. Accordingly, GABA-optimised ^{1}H-MRS sequences, with and without macromolecule suppression, were used to derive concentrations of the respective neurochemicals. Statistical evidence in support of the expected decrease in GABA and increase in Glx, following 10 minutes of anodal DC stimulation, was not apparent. However, a global effect of baseline GABA concentration on tDCS response was established, albeit irrespective of stimulation type.

3.5.1. Interpretation of findings

The available literature converges on the notion that the effects of anodal tDCS are driven by a prolonged increase in cortical excitability and resulting changes in neuroplasticity, therefore, implicating the function of glutamatergic pyramidal cells and GABAergic interneurons (Bindman et al., 1964; Liebetanz et al., 2002; Nitsche et al., 2003b; Stagg & Nitsche, 2011; Medeiros et al., 2012; Monte-Silva et al., 2013). While there are a limited number of publications addressing the impact of anodal tDCS on neurotransmission as assessed using magnetic resonance spectroscopy, it is anticipated that levels of glutamate (Glx) and GABA should significantly increase and decrease, respectively (Stagg et al., 2009; Clark et al., 2011). It is, therefore, surprising that such results did not occur during the present study.

A recent addition to the literature, representing the first concurrent tDCS-MRS study, confirmed the expected GABA decrease in M1 following 20 minutes of stimulation at 1 mA (Bachtiar, Near, Johansen-Berg & Stagg, 2015). However, a subsequent simultaneous tDCS-MRS investigation observed no significant alterations in GABA and only a transient increase in Glx (Hone-Blanchet, Edden & Fecteau, in press). This result may simply be due to the chosen electrode montage and/or regional differences in neurotransmitter concentrations (Durst et al., 2015) but such methodological discrepancies inevitably prevent comparisons between studies and thus increase the complexity of evaluating the current findings.

Given the existing variation in experimental tDCS protocols, an advantage of the present study is that the parameters closely replicated those of Stagg et al. (2009). Key factors such as the reference metabolite, voxel location, electrode montage, stimulation intensity and duration were all highly similar, if not identical. However, it should be noted that the data were analysed using different software packages (jMRUI as opposed

to Gannet) and, therefore, spectral peaks were fitted in a slightly different manner. Stagg et al. (2009) used two Gaussian functions to fit GABA and Glx, and also used a Gaussian to fit NAA, whereas this study adopted a single Gaussian approach for GABA and fitted the NAA peak with a Lorentzian curve. Gannet is specifically optimised to quantify GABA concentration from edited spectra (Edden et al., 2014), so it represented an ideal choice in this instance. However, while the difference between analysis methods and peak fitting parameters has been reported to be small (Mullins et al., 2014), distinctions do exist that could modify the outcome - particularly where results are on the boundary of significance. O'Gorman, Michels, Edden, Murdoch and Martin (2011) demonstrated that the within-subject reproducibility of GABA levels derived from MEGA-PRESS data was enhanced by using LCModel in comparison to JMRUI or in-house Matlab scripts. This lends support to the notion that the selection of analysis software can have a significant influence on the overall findings but also inevitably raises questions regarding the standardisation of metabolite quantification.

Additionally, Stagg and colleagues utilised a smaller, 2 cm^3 voxel which may have been advantageous. Lower SNR is inherent to smaller voxels but use of a 3 cm^3 voxel in the present study may not have had the desired effect of simply increasing signal without adding additional noise. Specifically, the prescription of a relatively large voxel would be more likely to overlap with the ventricles and generate a greater contribution from tissue types that contain less GABA than is found in grey matter. This could have translated to a minimisation of the likelihood that the study was able to detect tDCS-induced changes in GABA levels, where there was a potential lack of availability of the metabolite to begin with. The fact that metabolite concentrations were not corrected for respective tissue fractions may have also compounded this issue. Given the within-subjects focus of the study and ~90% repeatability of voxel prescription, this is unlikely to have caused substantial variations in voxel structure to be sufficient to alter quantification (at least between sessions with active and sham tDCS). However, there is still the possibility that the detection and quantification of GABA in general could have been enhanced by utilising a smaller voxel.

Despite the non-significance of the results, the changes that did emerge were in the anticipated directions. With regard to excitatory neurotransmission, the study found a slight increase in the level of Glx (4.95 ± 8.96%). This non-significant change is in accordance with Stagg et al. (2009), however, a subsequent study reported an 11% rise in Glx (referenced to the unsuppressed water signal), when comparing pre- and post-

stimulation levels (Clark et al., 2011). This particular study did not incorporate a sham control condition, which hinders the validity of the findings. The study also utilised 2 mA stimulation for a duration of 30 minutes. While increases in intensity and duration may not have a linear influence on the resulting effect (Batsikadze, Moliadze, Paulus, Kuo & Nitsche, 2013), these parameters far exceed those of the current study. Glx was also acquired from a parietal voxel, as opposed to sensorimotor cortex, using a standard PRESS sequence as opposed to MEGA-PRESS. Indeed, the PRESS sequence would be more likely to detect changes in Glx as the echo time (40 ms) was optimised to resolve glutamate, which may also account for this discrepancy in findings.

Focusing on inhibitory neurotransmission, the mean percentage change in GABA' concentration was -10.01 ± 38.40% (similar to that established using a metabolite nulling approach; Stagg et al., 2009). However, the sample used here exhibited substantial variations in their response to stimulation, leading to far higher standard deviation values than those found in the aforementioned study. A similar spectroscopy study has also documented a high degree of inter-individual variability (Kim et al., 2014), which has recently been acknowledged as a general concern surrounding stimulation research (Horvath, Carter & Forte, 2014; Wiethoff, Hamada & Rothwell, 2014). Putting the results of the present study into context, only 10 of the 15 participants responded in the expected direction, with the remaining five exhibiting no change or an increase in post-stimulation, GABA' concentration. Therefore, it is likely that these individual differences represent a major contributing factor in the lack of significant evidence found in this instance. For this reason, conducting analyses on an individual basis, and/or ensuring sufficient samples are recruited such that participants can be classified as responders or non-responders, may be advantageous.

It is also likely that inter-individual variability was responsible for driving the observed correlations between baseline GABA levels and percentage change in response to tDCS. The relationship between tDCS-induced change in GABA concentration and performance on motor learning tasks has previously been demonstrated (Stagg et al., 2011b; Kim et al., 2014) as has that of response to tDCS and BOLD fMRI signal change (Stagg et al., 2011b). However, a significant association between an individual's pre- and post-stimulation GABA levels has not previously been reported. It is, however, puzzling that this was not only applicable to active tDCS but also extended to the results of the sham condition. The upper limit of the confidence intervals for the GABA' sham condition approached zero, providing evidence for a spurious correlation, however, the

bounds of the GABA'+MM sham association show the correlation coefficient to be extremely robust. This indicates that, irrespective of stimulation modality, those with higher GABA levels at baseline experienced larger decreases in concentration after tDCS.

This could have been due to a natural decline in GABA across the course of each session, which may be particularly applicable for GABA' where a significant main effect of Time was found. Using a pre-existing dataset acquired to assess measurement repeatability, this was not evident for either GABA'+MM (-2.1%) or GABA' (-0.1%) in a sample of 15 participants (Mark Mikkelsen, personal correspondence). This dataset was acquired from occipital as opposed to sensorimotor cortex but featured a longer acquisition time of 15 minutes (512 averages), which would be expected to produce exaggerated reductions in GABA if they occurred systematically over time. Alternatively, the sham condition may have resulted in an active stimulation effect, although the influence of the initial ramp up of the current on sodium and calcium channel flux would be proposed to dissipate by the time the post-stimulation acquisitions took place (Purpura & McMurtry, 1965; Nitsche et al, 2003b). The phenomenon of 'regression to the mean' may offer an additional explanation, whereby an extreme value on one factor is likely to correspond to a more average value on the other factor. Despite random sampling, the population of the present study may not have exhibited representative data. Therefore, what should have been regarded as measurement noise became an indication of an actual effect.

Finally, in keeping with the theme of 'regression to the mean', the data could also reflect transient changes in the physiological state of participants. It is possible that those taking part in the study may have been anxious about being in the MRI scanner or having transcranial stimulation. This would mean fearfulness in these individuals would be higher at the start of the sessions. GABAergic neurotransmission is expected to correlate negatively with anxiety because it acts to regulate the arousal response (Goddard, 2016), meaning GABA levels would be predicted to increase during the sessions as participants become more relaxed, potentially leading to feelings of drowsiness. Accordingly, medication designed to promote sleep in those with insomnia acts on $GABA_A$ receptors to enhance their ability to suppress arousal (Luppi, Peyron & Fort, 2016). This may have occurred in subjects who initially exhibited low GABA but whose GABA levels increased towards the end. Therefore, initial feelings of anxiety could have abolished the expected tDCS effect in these individuals, meaning it only

emerged in those who were more relaxed at the start. Conversely, that GABA decreased in both active and sham modalities may suggest that the physiological state of the typically responding individuals was also driving the correlations; whereby their initial degree of relaxation led them to demonstrate high GABA at the start of the sessions which later decreased (thus mimicking the expected response to tDCS). This group may have experienced an increased stress response towards the end of the sessions due to the discomfort of being in a supine position for approximately 90 minutes. Therefore, distinctions in anxiety and relaxation could have produced the pattern of results evident in the correlation data (although the likelihood of similar experiences occurring across sessions, following exposure to the testing environment, is unclear). In future, it may be advantageous to ascertain general levels of anxiety in prospective participants at the screening phase and to determine context-specific anxiety prior to and after testing sessions to investigate the possible role of fearfulness.

3.5.2. Methodological issues & limitations

While combined tDCS-spectroscopy studies have highlighted the role of neurotransmitters in the generation of resulting after-effects, such research often fails to produce the 'gold standard' Time*tDCS interaction. Such a result specifically implicates change at the post-anodal tDCS time point compared to pre- and sham stimulation, baseline measures. Pharmacological studies, incorporating agents known to enhance or block receptor function, frequently demonstrate such findings (Liebetanz et al., 2002; Nitsche et al., 2003b; Nitsche et al., 2004a; Nitsche et al., 2004b; Kuo et al., 2008; Monte-Silva et al., 2013; Fresnoza et al., 2014b). This indicates that the effects of tDCS can be modulated by agents that act at a synaptic level but such change may not be entirely visible to spectroscopy measures of neurotransmission.

While stimulation-induced alterations in cortical excitability have been shown to correlate with levels of glutamate, no such relationship has been documented with regard to GABA (using traditional SICI/LICI protocols to engage $GABA_A$ and $GABA_B$ receptors; Stagg, Bestmann, Constantinescu, Moreno, Allman, Mekle... & Rothwell, 2011c). Accordingly, there is much debate as to the nature of the signal measured by GABA-MRS, which appears to be able to detect extrasynaptic GABA and as such, is likely to reflect the general status or 'tone' of the system as opposed to any specific (e.g. synaptic) contribution (Stagg et al., 2011a). This has recently been confirmed by administration of Tiagabine, a selective GAT-1 reuptake blocker, which produced no change in GABA levels in the assessed occipital and limbic voxels of interest (Myers,

Evans, Kalk, Edden, & Lingford-Hughes, 2014). Therefore, the adjustment in synaptic signalling, that should have taken place due to the increase in extracellular concentration permitted by the reuptake blocker, did not change the GABA concentration measured by MRS. If this is also the case for tDCS, synaptic changes may not readily translate to the type of inferences that can be made with spectroscopy. However, while techniques such as Positron Emission Tomography or Carbon-13 nuclear magnetic resonance imaging offer a more targeted perspective on neurobiology, it is important to note that despite its lack of specificity, MRS is currently the only means of non-invasively addressing neurochemical change *in vivo*. Furthermore, advances in methodology, incorporating higher magnetic field strengths, may present a way to help circumvent this issue by enhancing frequency selectivity and the resolution of peaks that cannot normally be separated or are otherwise obscured in the spectrum (Puts & Edden, 2012).

Issues of methodological specificity also extend to the choice of acquisition parameters, particularly the placement of editing pulses. The study represented the first attempt to quantify tDCS-induced change in GABA concentrations using multiple sequences, with and without macromolecule contamination. While symmetric suppression methods produce more optimised GABA concentrations, they are subject to lower SNR and more prone to the effects of frequency drift (as is the acquisition of metabolite-nulled spectra, which are susceptible to motion artefacts between acquisitions; Harris et al, 2014). Conversely, although further advances in suppression techniques are needed to optimise efficiency, great caution must be adopted when interpreting the results of 'GABA+' acquisitions. This means it is often challenging to determine which method is the most advantageous. Although the results of the GABA' analysis produced the most compelling descriptive findings, the changes that occurred during both the GABA'+MM and GABA' acquisitions failed to reach significance. Subsequently, the study is unable to infer that GABA as opposed to GABA+ is implicated in the generation of anodal tDCS after-effects.

3.5.3. Study design limitations & future considerations

A number of design limitations may have prevented the observation of tDCS effects on the selected neurochemicals. Firstly, change in the reference metabolite(s) was not explicitly assessed in the present study and could have potentially masked the effect of tDCS on GABA and Glx. While this is unlikely because the majority of the literature has found no effect of anodal stimulation on levels of NAA or creatine (Rango,

Cogiamanian, Marceglia, Barberis, Arighi, Biondetti & Priori, 2008; Stagg et al., 2009), it is important to note that Clark et al. (2011) established an increase in N-acetylaspartate and N-acetylaspartylglutamate (tNAA) following anodal stimulation. However, this finding was most likely due to aspects of the stimulation protocol (e.g. longer than usual duration, higher current strength/density) and the authors acknowledge that these parameters may have more closely mimicked the effects of electroconvulsive therapy (ECT), which has been shown to alter NAA in several regions (Merkl, Schubert, Quante, Luborzewski, Brakemeier, Grimm… & Bajbouj, 2011). Duration dependent effects may have also led to the discovery of an increase in NAA levels within dorsolateral pre-frontal cortex (Hone-Blanchet et al., in press). This result was found during 20 minutes of anodal stimulation but was absent immediately after stimulation had ceased, indicating that any fluctuations in NAA are likely a result of transient excitatory changes as opposed to persistent alterations in metabolism and neuronal function.

With regard to the administered stimulation, it is likely that the different polarities produce distinct effects at a neurochemical level. Stagg et al. (2009) observed a significant decrease in GABA and Glx following cathodal stimulation, whereas only a reduction in GABA was exhibited for anodal stimulation. As the current study utilised a single, positive polarity, alongside the sham modality, such complementary effects could not be ascertained. The study also did not assess "online" changes that may have emerged during the stimulation period. To assess the temporal evolution of the effects of tDCS, acquisition of chemical shift spectra during tDCS (although technically more challenging) could be incorporated in future. Given that the prolonged changes in neurotransmission are proposed to occur at longer intervals (Nitsche et al., 2003b; Nitsche et al., 2005), stimulation duration would be increased to ~20 minutes in such studies (similar to Bachtiar et al., 2015 and Hone-Blanchet et al., in press).

A number of individual difference factors may have also masked the extent of any stimulation-induced after-effects. Firstly, there is evidence to suggest that GABA levels are dependent on gender and menstrual cycle phase (Epperson, Haga, Mason, Sellers, Gueorguieva, Zhang... & Krystal, 2002; Harada, Kubo, Nose, Nishitani & Matsuda, 2011; O'Gorman et al., 2011). The observed fluctuation in the GABA concentration of females compared to males has also been demonstrated to determine responses to tDCS (Chaieb, Antal & Paulus, 2008). The present study recruited participants of each gender and did not establish menstrual cycle phase in females, which could have meant that

natural variations in GABA prevented the observation of those that arose as a result of stimulation. To address this limitation, single-sex studies could be performed – incorporating an entirely male sample – or female participation could be based on a specific cycle phase. Alternatively, a recent study suggested that oral contraceptives regulate GABA levels measured via magnetic resonance spectroscopy (de Bondt, de Belder, Vanhevel, Jacquemyn & Parizel, 2015), such that inclusion on these grounds may provide the means to conduct more adequately controlled, mixed gender studies.

In addition to the basic role of gender, Epperson, O'Malley, Czarkowski, Gueorguieva, Jatlow, Sanacora... and Mason (2005) established an interaction between gender and nicotine intake, whereby female smokers did not experience the same cyclic fluctuations in cortical GABA as non-smokers. In the follicular phase, where concentrations were proposed to be most similar between genders, GABA concentration was also significantly decreased in female compared to male smokers. This suggests that females are likely to be particularly prone to the effects of nicotine, which have been shown to modulate the synthesis of the inhibitory neurotransmitter via $GABA_A$ type receptors (Porcu, Sogliano, Cinus, Purdy, Biggio & Concas, 2003; Smith, Gong, Hsu, Markowitz, Ffrench-Mullen & Li, 1998). The present study did not ascertain the prevalence of smokers in the recruited sample and, therefore, the influence of nicotine on plasticity induction may have represented a confounding variable.

The effects of nicotine on stimulation-induced neuroplasticity have also been demonstrated in groups of non-smokers (having administered nicotine via transdermal patches and nasal sprays; Thirugnanasambandam, Grundey, Adam, Drees, Skwirba, Lang… & Nitsche, 2011; Grundey, Thirugnanasambandam, Kaminsky, Drees, Skwirba, Lang… & Nitsche, 2012a). Such acute exposure to nicotine has been shown to abolish the after-effects of anodal tDCS. Accordingly, Batsikadze, Paulus, Grundey, Kuo & Nitsche (2014) established that a medium dose of Varenicline, a nicotinic acetylcholine receptor agonist thought to mimic the effects of smoking, was sufficient to abolish the effects of anodal stimulation. The activation of these receptors was proposed to alter plasticity induction via an increase in intracellular calcium. While the influx of calcium ions is integral for glutamatergic LTP, excessive levels trigger the activation of potassium channels which have an opposite, hyperpolarising effect (Lisman, 2001). This may explain why calcium-dependent plasticity is altered under the influence of nicotine and related substances. Nicotine withdrawal (10 hours) in smokers has also been shown to produce an abolishment of the usual excitability enhancement following

anodal tDCS (Grundey, Thirugnanasambandam, Kaminsky, Drees, Skwirba, Lang… & Nitsche, 2012b). Interestingly, the facilitatory effect of anodal stimulation was reinstated with exposure to nicotine, which indicates that the effects of chronic exposure to nicotine are likely to be qualitatively different to those of acute administration (due to the adaptation of nicotinergic acetylcholine receptors over time). Therefore, asking participants who have identified themselves as smokers to abstain may actually produce unfavourable results and simply including this distinction as a covariate at the analysis stage may be a better approach.

3.6. Conclusions

The present study was unable to provide support for the role of GABAergic or glutamatergic neurotransmission in the generation of anodal stimulation after-effects. While the symmetric suppression sequence produced the most compelling findings with regard to GABA concentration, the lack of statistical significance prevented meaningful conclusions on the specific role of the inhibitory neurotransmitter (in the absence of macromolecules) in the context of tDCS-induced plasticity. Furthermore, interpretation of the evident association between baseline GABA levels and percentage change in response to anodal tDCS was hindered by the emergence of a similar relationship in the sham condition. Individual difference factors are likely to have contributed to these puzzling results and, where possible, should be explicitly accounted for in such studies. Consequently, continued investigation is needed to demonstrate the role of these, and other, neurochemicals in the formation of the effects of tDCS.

4. Experimental Chapter 2

Rising Above the Noise - The Challenge of Combining Transcranial Direct Current Stimulation & Magnetoencephalography

4.1. Abstract

The effects of tDCS are not completely understood in terms of the underlying neurobiology and recent research has become increasingly focused on attempting to explain the underpinnings of the neuromodulation technique. Consequently, researchers have sought the benefits of acquiring neurobiological data via non-invasive neuroimaging modalities. The combination of tDCS and Magnetoencephalography (MEG) is likely to be particularly valuable. Gaining insight into changes in electrophysiological responses that occur during as well as after stimulation is likely to promote a more comprehensive understanding of the underlying neurobiological mechanisms of the method. However, the combination of these techniques is likely to generate magnetic artefacts that could substantially contaminate the data. This chapter documents the initial stages undertaken to implement simultaneous tDCS-MEG and ascertain the extent of these artefacts. Data was acquired prior to and during stimulation. Compared to pre-stimulation recordings, excess noise was observed as an average of all channels and at those individually assessed, during anodal and sham tDCS. The removal of trials corresponding to the current ramp phases largely minimised the evident noise fluctuations. Therefore, the study demonstrates the feasibility of combining tDCS and MEG. This indicates that future research designed to link observable modulations of electrophysiological activity (such as cortical oscillations and evoked responses) to electrical stimulation, should be a viable approach to determine the basis of tDCS.

4.2. Introduction

Research concerning the effects of tDCS has already made progress in delineating potential mechanisms of action (Radman et al., 2009; Ridding & Ziemann, 2010; Medeiros et al., 2012; Krause et al., 2013). The prolonged, polarity-specific change in cortical excitability elicited by the neuromodulation technique is initially thought to arise from alterations in resting membrane potential (Creutzfeldt et al., 1962; Bindman et al., 1964; Purpura & McMurtry, 1965; Nitsche & Paulus, 2001; Funke, 2013). At brief durations of several seconds, the application of anodal stimulation typically leads to transient depolarisation whereas cathodal stimulation results in hyperpolarisation, thus making spontaneous firing more or less likely to occur (Wassermann & Grafman,

2005). Stimulation durations exceeding several minutes have been shown to lead to the archetypical post-stimulation changes in neuroplasticity, which have been reported to mimic long term potentiation and depression (LTP/LTD) (Stagg & Nitsche, 2011; Monte-Silva et al., 2013). Accordingly, a range of pharmacological studies have associated these after-effects with neurotransmitter levels and the engagement of related receptor types, primarily those of glutamate (NMDA) and GABA (A & B subtypes) (Liebetanz et al., 2002; Nitsche et al., 2003b; Nitsche et al., 2004a; Nitsche et al., 2004b; Nitsche et al., 2005). Despite the growing body of literature relating to the basic mechanisms of tDCS, continued research is needed to support these findings.

Since the resurgence of tDCS, far greater emphasis has been placed on conducting multi-modal investigations to establish the underlying principles of the technique (Venkatakrishnan & Sandrini, 2012; Hunter, Coffman, Trumbo & Clark, 2013). Accordingly, renewed focus has been placed on the current lack of suitable computational/physiological models of tDCS function (Bestmann, de Berker & Bonaiuto, 2015). The initial studies that reignited interest in tDCS (Priori et al., 1998; Nitsche & Paulus, 2000/2001) combined the method with Transcranial Magnetic Stimulation (TMS) to elicit motor evoked potentials in order to explicitly measure levels of motor cortex excitability. Short/long interval intracortical inhibition (SICI/LICI), paired-pulse TMS protocols have since been used to probe the involvement of $GABA_A$ and $GABA_B$ subtypes in tDCS after-effects (Antal et al., 2010a; Tremblay et al., 2013). Investigations where DC stimulation has been delivered prior to the acquisition of Magnetic Resonance Spectroscopy (MRS) data have determined the contribution of myoinositol, GABA and the glutamate-glutamine composite, Glx (Rango et al., 2008; Stagg et al., 2009; Clark et al., 2011; Bachtiar et al., 2015). tDCS has also been combined with functional Magnetic Resonance Imaging (fMRI) to investigate modulations of cortico-cortical and thalamo-cortical functional connectivity via resting state activity (Polanía, Paulus & Nitsche, 2012; Sehm, Schäfer, Kipping, Margulies, Conde, Taubert... & Ragert, 2012; Amadi, Ilie, Johansen-Berg & Stagg, 2014). The integration of these methods has undoubtedly allowed for additional insight into the influence of tDCS from a neurobiological perspective. However, while these studies have been instrumental in adding to our comprehension of tDCS mechanisms, MR methods are fundamentally constrained in the time domain. Methods such as fMRI also do not provide direct insights into neuronal function. These are substantial limitations considering the effects of tDCS are thought to evolve over the stimulation

period and engage distinct physiological mechanisms; from an alteration of resting membrane potential to a modulation of synaptic strength (Nitsche et al., 2003b).

Use of electrophysiological methods, such as Electroencephalography (EEG) and MEG, may be particularly advantageous. Combining tDCS with EEG/MEG is particularly appealing because it allows us to directly measure neurophysiological change across the stimulation time course. By characterising the temporal dynamics of tDCS in terms of altered evoked and induced responses, it should provide more comprehensive knowledge to facilitate our understanding of the physiological mechanisms behind the effects of tDCS. Several studies using EEG have already been conducted but largely adopt a pre-post design, which limits the assessment of the temporal evolution of the resulting tDCS effects (Polanía, Nitsche & Paulus, 2011; Jacobson, Ezra, Berger & Lavidor, 2012; Neuling, Rach, Wagner, Wolters & Herrmann, 2012; Spitoni, Cimmino, Bozzacchi, Pizzamiglio & Di Russo, 2013). The concurrent application of these methods offers the advantage of addressing electrophysiological changes that occur during stimulation, to further improve our comprehension of the emergence of tDCS effects. However, a limitation of this approach is that the presence of a DC source is likely to produce noise artefacts on the resulting recordings, although evidence suggests that using robust source reconstruction techniques can overcome the impact of the excess noise (Wirth, Rahman, Kuenecke, Koenig, Horn, Sommer & Dierks, 2011; Sehm, Hoff, Gundlach, Taubert, Conde, Villringer & Ragert, 2013a).

Researchers have also begun to combine tDCS with MEG, which measures the magnetic fields of electric currents generated by post-synaptic potentials of pyramidal cells (Babiloni, Pizzella, Gratta, Ferretti & Romani, 2009). The activity detected by MEG is less susceptible to distortion as it exits the scalp compared to EEG, making source localisation less problematic (Teplan, 2002). Data acquired using EEG, compared to MEG, is also more susceptible to contamination from muscle artefacts (Whitham, Pope, Fitzgibbon, Lewis, Clark, Loveless... & Willoughby, 2007). For these reasons it is often favourable to conduct MEG research where possible, unless the research question primarily involves the detection of radial as opposed to tangential current sources (Ahlfors, Han, Belliveau & Hämäläinen, 2010).

At present, integrative tDCS-MEG research has also largely been confined to using a pre-post design as most researchers have not attempted the simultaneous combination of brain stimulation and neuromagnetic data acquisition (Venkatakrishnan, Contreras-Vidal, Sandrini & Cohen, 2011; Suntrup, Teismann, Wollbrink, Winkels, Warnecke,

Flöel... & Dziewas, 2013). As with concurrent EEG recordings, acquiring a viable MEG dataset having placed an electric current source directly beneath the sensors is not without its challenges. Soekadar, Witkowski, Cossio, Birbaumer, Robinson and Cohen (2013) were the first to report on the feasibility of concurrent tDCS-MEG; documenting the resulting noise levels using a current phantom to assess fluctuations at sensors local to and distant from the active electrode. Noise in sensor space was characterised as being greater at regions corresponding to the active electrode (right motor cortex) and was particularly prominent at lower frequencies. Additionally, DC-induced noise decreased over a distance of 8 cm (anterior and posterior) but was still detectable at distant sites. Using Synthetic Aperture Magnetometry (SAM; Robinson & Vrba, 1999; Vrba & Robinson, 2001), the authors went on to produce source reconstruction estimates for sensorimotor rhythms detected in a sample of five participants, during a finger tapping task: alpha (8-13 Hz), beta (13-30 Hz). This demonstrated the robustness of the SAM beamformer approach to the presence of noise induced by tDCS.

Aside from the impact on recordings, excess noise may also be detrimental to the MEG system itself and has the potential to de-tune or even cause damage to the sensors (SQUIDs). Soekadar et al. (2013) conducted their tDCS-MEG investigation using a 275-channel CTF device (identical to that used within the CUBRIC research facility) and no negative impact on the SQUIDs was documented. The authors also suggested it may be possible to conduct concurrent transcranial alternating current stimulation (tACS)-MEG research, which has recently been implemented successfully (Neuling, Ruhnau, Fuscà, Demarchi, Herrmann & Weisz, 2015). Therefore, this initial study has highlighted the feasibility of integrating tDCS and MEG from a methodological perspective.

The current research aimed to build upon the work of Soekadar et al. (2013) by assessing the noise levels resulting from recordings made using a human subject. While phantom research represents the gold-standard for investigations of source reconstruction, there are obvious limitations to this approach when designing research to be conducted with humans. For example, subjects are able to become fatigued, move in the dewar and exhibit unique conductivity profiles due to the complex organisation of an individual's brain anatomy (Bikson & Datta, 2012; Truong, Magerowski, Blackburn, Bikson, & Alonso-Alonso, 2013; Opitz et al., 2015). It is important to account for each of these factors as they will inevitably impact upon the accuracy of results. For this reason it is essential to assess noise levels in humans as they are ultimately the focus of

prospective research. These noise recordings represent the first step towards achieving the primary aim of addressing aspects of the underlying tDCS mechanisms using MEG. In order to reach this stage, this piece of development work aimed to determine the extent of tDCS-induced magnetic artefacts during concurrent MEG data acquisition within CUBRIC.

4.3. Methods

4.3.1. Subjects

A single subject participated in the research (male, 39 years, right handed). In accordance with local ethical, safety guidelines, the subject was free from all contraindications relating to receiving DC stimulation and entering the MEG environment.

4.3.2. Experimental methods

4.3.2.1. Magnetoencephalography

A 275 channel, radial gradiometer, CTF system (Coquitlam, Canada) was used to acquire whole head MEG recordings with a sample rate of 600 Hz. Recordings from an additional 29 channels were acquired to facilitate noise cancellation. The subject had three electromagnetic head coils attached to landmarks corresponding to the nasion and preauricular points. These coils were localised to the MEG system before and after each of the recordings.

4.3.2.2. Transcranial direct current stimulation

Brain stimulation was delivered using the DC-Stimulator MR device (neuroConn, Germany). The subject was administered active (anodal) and sham stimulation types. Stimulation was delivered for 600 s with a 10 s period corresponding to both the onset and offset of the current, which was gradually ramped up and down. Rubber electrodes, measuring 5x5 cm (25 cm^2), were used to deliver anodal stimulation with a current of 1 mA (current density = 0.04 mA/cm^2). For sham stimulation, the neuroConn device initially ramped up the current to mimic the peripheral effects of active tDCS before ramping down. During the stimulation period, the device discharged current spikes every 550 ms (110 μA over 15 ms) to enable continuous impedance readings. Average current over time was not more than 2 μA.

Due to the need to minimise sources of external magnetic noise within the MEG environment, the tDCS device itself was situated in the adjoining electronics room (outside of the magnetically shielded room; MSR). Device impedance was set to 30 kΩ (compared to the 20 kΩ default, designed for use with behavioural protocols) to compensate for the additional 10 kΩ load placed on the circuit by the shielded components (for an overview of the equipment used, see Figure 4.1). Ten20 paste was used as a conductive medium at the electrode-scalp junction. This approach was favoured to that of using saline soaked sponges to avoid potential impedance issues due to the risk of aeration over time. Saline solution was applied directly to the scalp prior to positioning the electrodes (0.9% concentration). This step was implemented to further decrease impedance, which was found to otherwise exceed the device limit and cause stimulation to cease or fail to initiate.

Figure 4.1. tDCS-MEG components. Top-Bottom, Left-Right: tDCS device, head bands with Velcro attachments, scalp cap, tDCS electrodes (25 cm²), non-shielded filter box (located in electronics room), shielded filter box (located in MSR), connector cables (electrode cable; stimulator cable), extension cable.

A bihemispheric S1 electrode montage was selected in light of evidence suggesting that the use of such configurations may enhance the focality of results (Vines, Cerruti & Schlaug, 2008; Sehm Kipping, Schäfer, Villringer & Ragert, 2013b). For the purpose of this research, focality was increased to attempt to constrain the spread of current with regard to the extent of the effect on the MEG sensors as opposed to achieving greater efficacy of stimulation. Electrode pads measuring 5x5 cm (25 cm²) were chosen to afford enhanced localisation of stimulation compared to that offered using typical 5x7

cm (35 cm²) electrodes (Nitsche et al., 2007). The electrodes were positioned using the 10-10 system at landmarks CP3 (left hemisphere, cathode) and CP4 (right hemisphere, anode), designed to correspond to primary somatosensory cortex (Chatrian et al., 1985). Figure 4.2 illustrates the selected electrode montage.

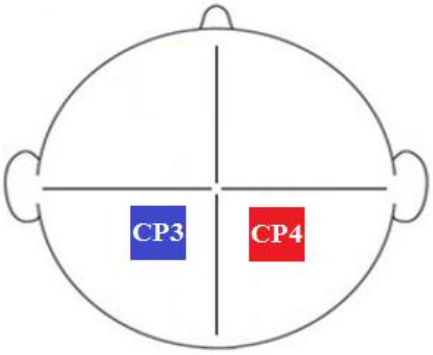

Figure 4.2. Electrode positions. The active electrode (red) was located over site CP4 and the reference electrode (blue) was located above CP3, corresponding to primary somatosensory cortex of each hemisphere (in accordance with the 10-10 system).

4.3.3. Experimental procedure

On entering the MEG suite, the subject was asked to remove all metal-based items. The subject was initially prepared for a standard MEG scan, with only the head localisation coils attached to the fiducial points. Prior to the subject being seated in the MSR, an empty room recording was performed to establish baseline noise levels in the absence of the subject and any additional equipment. Baseline scans consisted of 30 trials, each averaging approximately 1.7 seconds. Once adequately positioned under the dewar, the subject was instructed to relax and remain as still as possible as well as to refrain from blinking excessively or clenching their facial muscles. The subject was asked to rest with their eyes open during all scans, the first of which was acquired to determine the noise level associated with a typical MEG experiment (in the absence of any tDCS components). After the initial scan, the subject was removed from the MSR and prepared for tDCS (as previously specified; see Figure 4.3 for a depiction of a typical tDCS-MEG preparation).

Elements of the tDCS equipment were systematically introduced to the MEG environment. On re-entering the MSR, the tDCS electrode cables were attached to the shielded filter box, which was connected to the tDCS device via an extension cable that was fed between the MSR and the adjoining electronics room. The subject completed scans designed to ascertain noise levels from the addition of the tDCS equipment itself;

when the circuit was completed but the device was switched off (device off) and when it was switched on but not delivering stimulation (device on).

Figure 4.3. tDCS-MEG preparation. The subject is seen here with the MEG head localisation coils attached to the fiducial points (nasion, pre-auricular points) and tDCS electrodes positioned on the scalp, using Ten20 paste and head straps.

As there was no explicit task and the research was not designed to determine the effects of tDCS on neurophysiological or behavioural performance, sham and active stimulation were administered during the same session. The recordings for the stimulation protocols consisted of 400 trials to capture the current onset, plateau and offset phases.

4.3.4. Data analysis

DataEditor, part of the CTF-based software, was used to view the noise recordings with the synthetic third-order gradiometer option selected. The data was visually inspected for evidence of gross artefacts requiring removal, relating to subject movement or muscle activity. The data was then imported into MATLAB (MathWorks, Cambridge) and power spectra were computed using the Periodogram function. This function returns a noise measure in decibels (dB) having performed a Discrete Fourier Transform (DFT), which computes a decomposition of temporally constrained data into activity across frequencies plotted by their respective power. The power spectral density (PSD) estimates for all recordings were visually inspected by comparing the noise levels found during the initial subject scan, representing a standard MEG recording, to the active and sham stimulation protocols. Topographical difference maps were also generated to provide insight into noise levels across the sensor array, created using FieldTrip (Oostenveld, Fries, Maris & Schoffelen, 2010). This data was designed to provide

proof-of-concept information as to whether it would be worthwhile to proceed with combining these methods during future research or whether the generated artefacts would simply be too substantial to allow meaningful inferences to be made.

4.4. Results

Average noise levels across sensors were computed for each recording: Empty Room, Participant + Coils, Device Off, Device On, Sham and Active stimulation (Figure 4.4). Compared to the empty room recording, the addition of the participant and the head localisation coils raised the noise level below 50 Hz. Noise levels appeared to be relatively stable with the addition of the tDCS electrodes and cables, whether the device was switched off or was turned on. However, there was a dramatic broadband increase in noise for sham and active stimulation.

To analyse the noise levels from the previously published paper, Soekadar et al. (2013) adopted the approach of comparing noise at sensors local to and distant from the active electrode. The current study also utilised this method to further address the noise generated at single sensors (Figure 4.5). Having placed the tDCS electrodes in a bihemispheric S1 montage, the position of the active electrode was estimated to correspond to the sensor MRP23. Frontal (MZF02) and occipital (MZO02) sensors were chosen to demonstrate the influence of noise at distant sites. Soekadar et al. (2013) found that sensor disturbance was exhibited directly above the active electrode but noise levels were dramatically attenuated at more remote sites. Performing a similar assessment of individual channels, as expected, the sensor above the active electrode displayed excess disturbance during both sham and active trials, particularly at frequencies below 15 Hz. However, the attenuating effect of sensor position documented in the previous article was not evident in the current data.

Having observed the extent of noise when the trials corresponding to the current onset/offset were incorporated into the PSD plots, these trials were subsequently removed from the respective datasets. In doing so, it was found that the majority of excess noise could be attributed to the transient current onset and offset periods. Accordingly, data relating to the DC plateau appeared to result in much less disruption at the selected sensors (Figure 4.6). This suggests that by removing the trials corresponding to the current onset and offset, a large amount of the fluctuation in noise levels can be removed, therefore, generating much more stable power spectra.

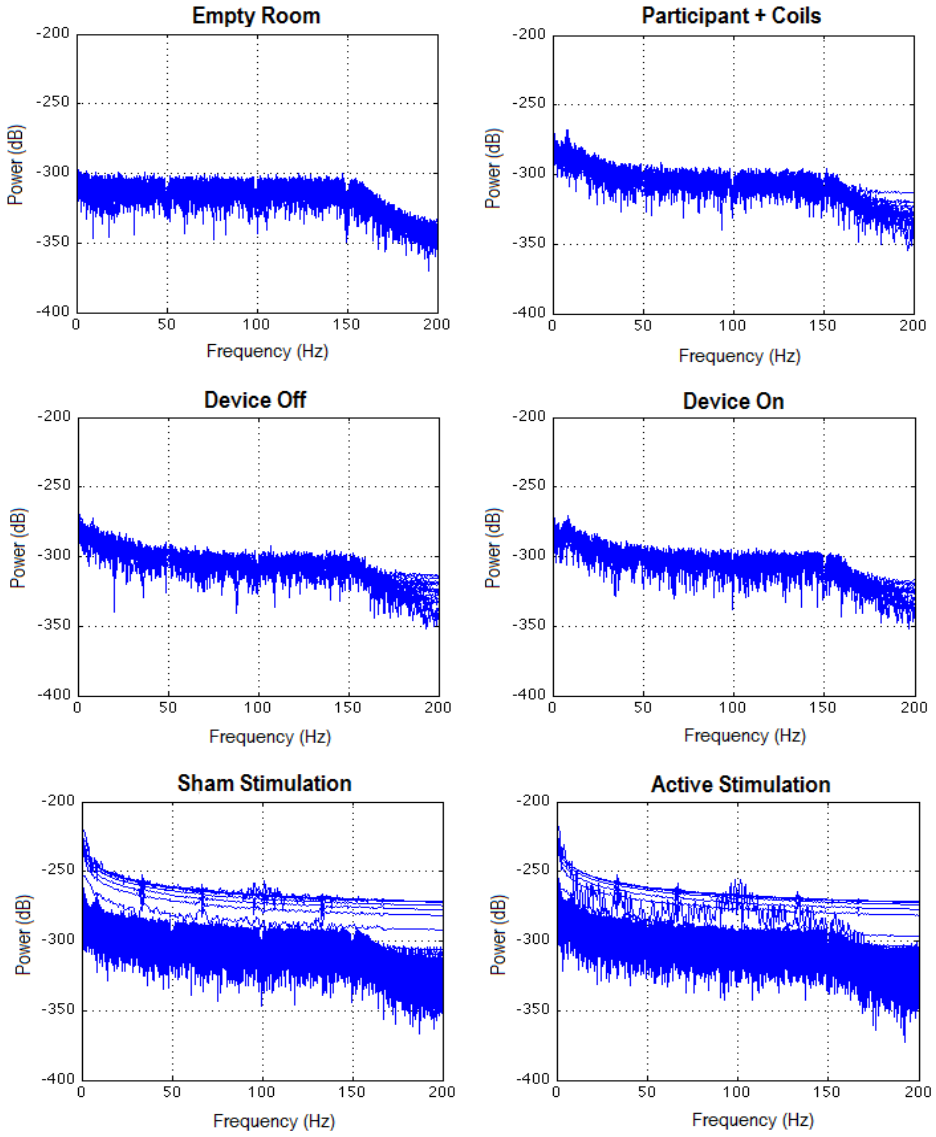

Figure 4.4. Average noise. Power spectra from each recording displayed as an average of noise across the entire sensor array, with trials stacked on top of each other. Sham and active stimulation produced broadband, high amplitude sensor disturbance.

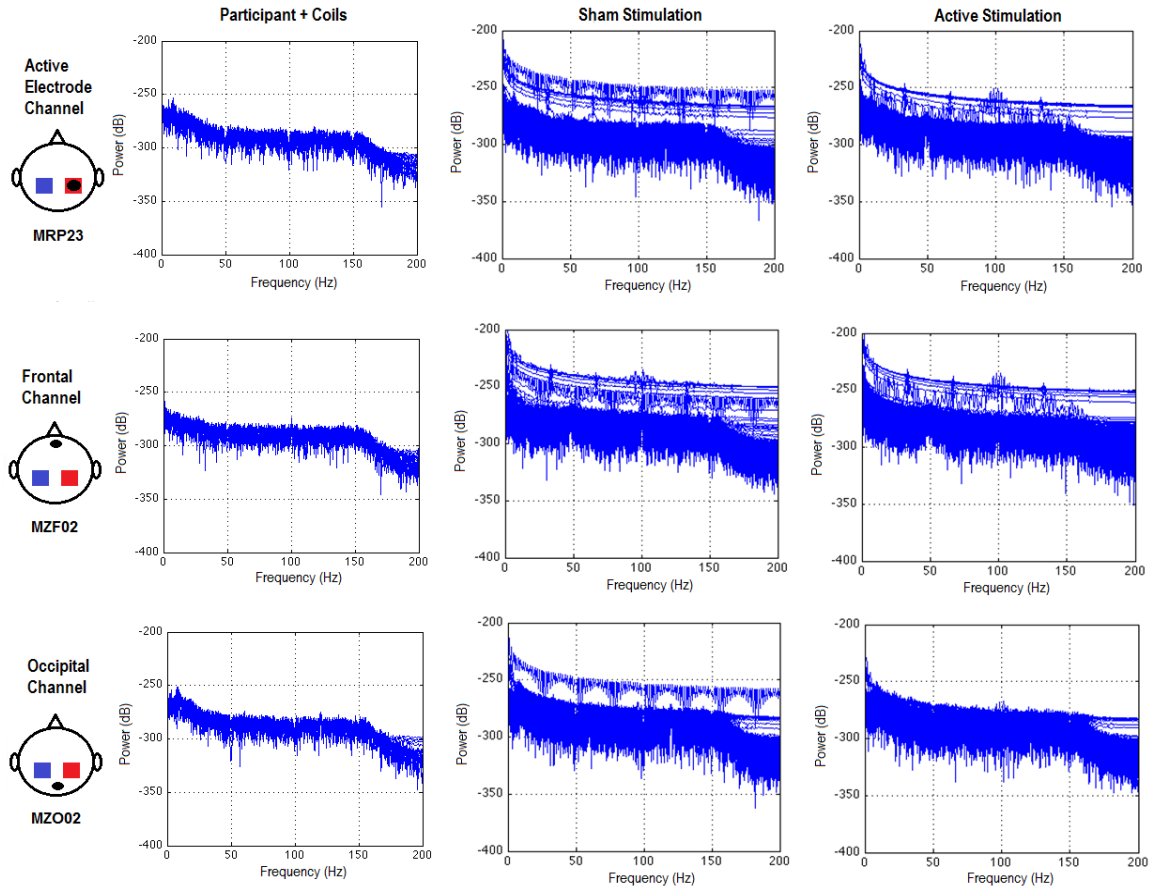

Figure 4.5. tDCS onset/offset noise (single sensor). Power spectra comparing standard noise levels to those of sham and active stimulation at the site of a single sensor. Spectra contain all trials recorded from current onset to offset. The head template images illustrate the approximate position of the active (red) and reference (blue) electrodes as well as the site of the selected sensor (black dot). Several trials appear to have been particularly affected by the addition of tDCS, potentially corresponding to the ramp period(s). The broadband, high amplitude disturbance exhibited across sensors remains present when inspecting noise at individual sites (both local to and distant from the active tDCS electrode).

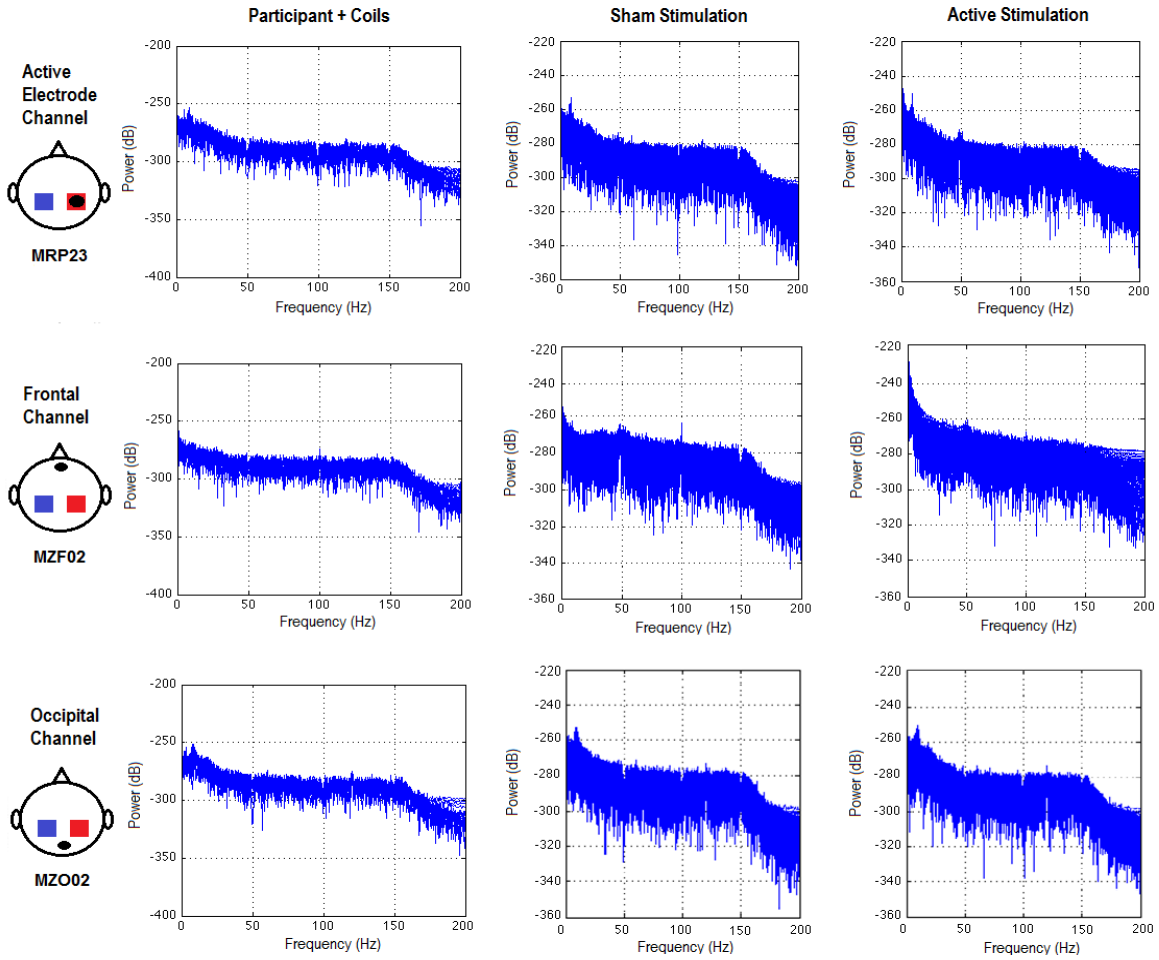

Figure 4.6. Removal of tDCS onset/offset noise (single sensor). Power spectra comparing standard noise levels to those of sham and active stimulation, illustrating noise levels following the removal of trials coinciding with current onset and offset. The head template images illustrate the approximate position of the active (red) and reference (blue) electrodes as well as the site of the selected sensor (black dot). The broadband, high amplitude disturbance exhibited at these individual sensors was vastly attenuated when only the trials from the DC plateau were included in the power spectral density estimate.

This finding was supported by generating topographical difference maps using FieldTrip software. Images representing the difference in sensor-level noise between the stimulation (with and without the ramp period) and standard recordings were produced (Figure 4.7 Sham, Figure 4.8 Active). Each sub-figure highlights regions of sensor disturbance within a specific frequency band: alpha (8-13 Hz), beta (13-30 Hz), low gamma (30-49 Hz), high gamma (51-99 Hz). Mean values were extracted from these maps, representing an average of the noise across all channels and those individually selected as well as the noise present in each frequency range (Table 4.1).

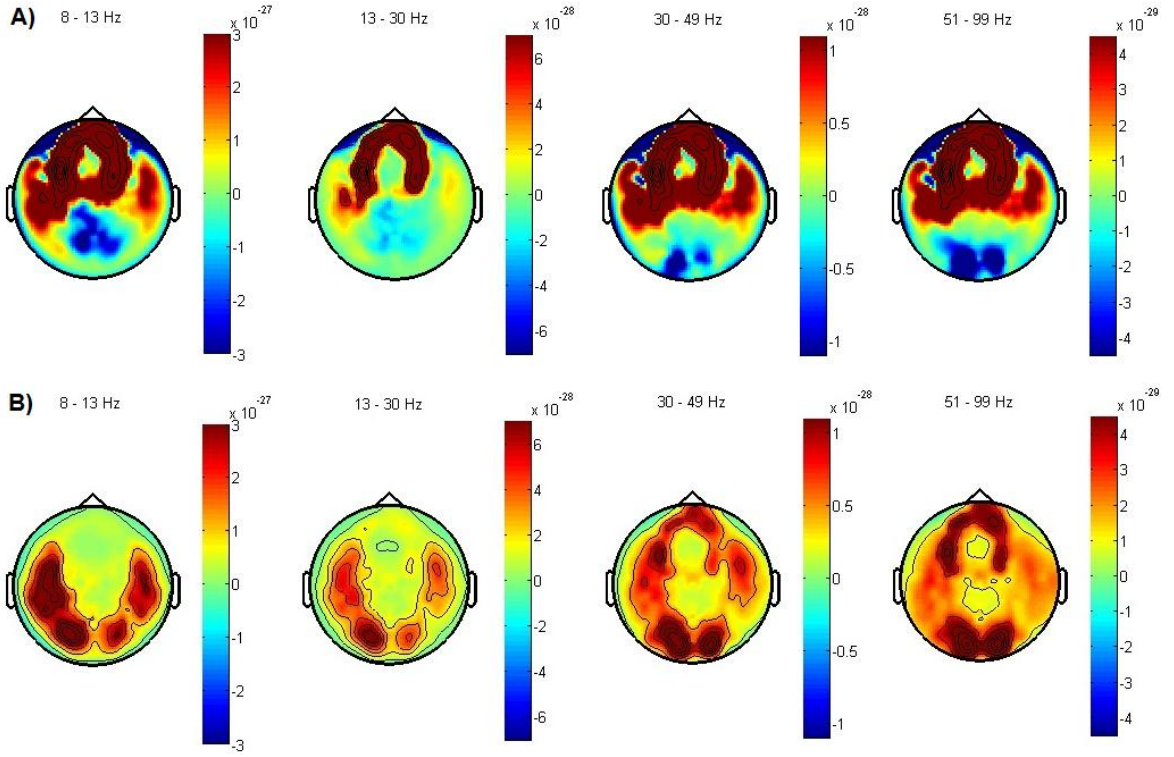

Figure 4.7. Sham condition difference maps. Each sub-figure shows the difference in noise (power) across the respective frequencies, resulting from the following comparisons: A) Sham-Standard, representing residual noise relating to the presence of sham stimulation, B) Plateau Sham-Standard, representing residual noise relating to the presence of sham stimulation without the ramp trials. Noise is reported in Tesla squared (T^2).

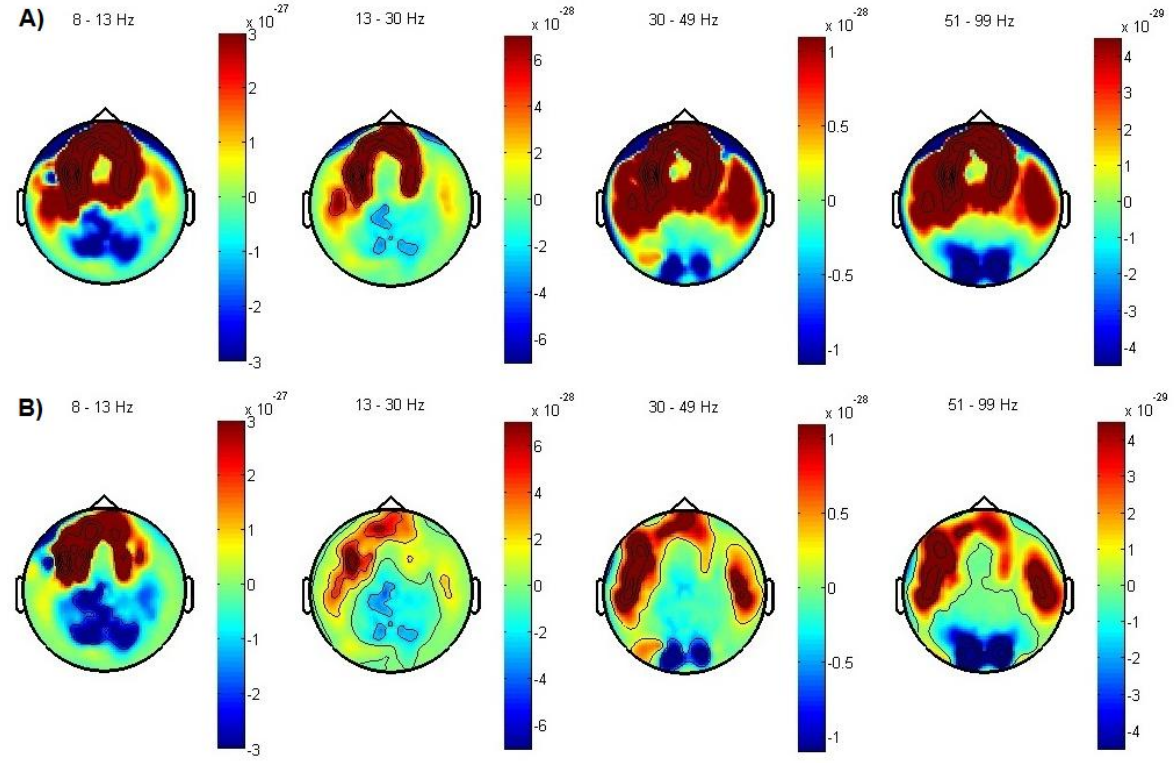

Figure 4.8. Active condition difference maps. Noise (power) across the respective frequencies, resulting from the following comparisons: A) Active-Standard: residual noise relating to the presence of anodal stimulation, B) Plateau Active-Standard: residual noise relating to the presence of anodal stimulation without the ramp trials. Noise is reported in Tesla squared (T^2).

Table 4.1. Mean noise levels derived from the topographical difference maps. The first sub-table shows an average of noise (power; ± SD) for each comparison, across the three selected MEG sensors and as a product of all channels. Subsequent sub-tables demonstrate mean noise values across the three selected MEG sensors and as a product of all channels, for each frequency band. Noise is reported in Tesla squared (T^2).

	Sham-Standard	Plateau Sham-Standard	Active-Standard	Plateau Active-Standard
Electrode	3E-026 ± 2E-25	-3E-028 ± 9E-28	2E-026 ± 1E-25	6E-027 ± 4E-26
Frontal	6E-025 ± 6E-24	-2E-028 ± 1E-27	5E-025 ± 4E-24	8E-026 ± 7E-25
Occipital	4E-028 ± 3E-27	-4E-029 ± 1E-28	2E-027 ± 2E-26	3E-027 ± 2E-26
Total	2E-025 ± 4E-24	-1E-028 ± 7E-28	9E-026 ± 2E-24	2E-026 ± 3E-25

Sham-Standard

	Alpha	Beta	Low Gamma	High Gamma
Electrode	7E-029 ± 1E-27	-1E-028 ± 1E-28	6E-029 ± 2E-28	3E-029 ± 7E-29
Frontal	3E-026 ± 3E-26	1E-027 ± 1E-27	2E-027 ± 5E-27	7E-028 ± 2E-27
Occipital	-3E-028 ± 5E-28	-3E-030 ± 4E-29	-2E-029 ± 1E-29	-2E-029 ± 8E-30
Total	9E-027 ± 2E-26	3E-028 ± 1E-27	6E-028 ± 4E-27	2E-028 ± 1E-27

Plateau Sham-Standard

	Alpha	Beta	Low Gamma	High Gamma
Electrode	-1E-027 ± 1E-27	-2E-028 ± 1E-28	-1E-029 ± 2E-29	-4E-031 ± 3E-30
Frontal	-7E-030 ± 7E-29	1E-029 ± 1E-29	4E-029 ± 8E-29	2E-029 ± 2E-29
Occipital	-4E-028 ± 5E-28	-3E-030 ± 4E-29	-2E-029 ± 9E-30	-2E-029 ± 8E-30
Total	-6E-028 ± 2E-27	-7E-029 ± 2E-28	-7E-030 ± 5E-29	-5E-030 ± 3E-29

Active-Standard

	Alpha	Beta	Low Gamma	High Gamma
Electrode	-3E-028 ± 1E-27	-2E-028 ± 1E-28	6E-029 ± 2E-28	2E-029 ± 5E-29
Frontal	4E-026 ± 5E-26	2E-027 ± 1E-27	3E-027 ± 8E-27	8E-028 ± 2E-27
Occipital	-2E-028 ± 7E-28	6E-030 ± 3E-29	-3E-029 ± 1E-29	-3E-029 ± 9E-30
Total	7E-027 ± 2E-26	2E-028 ± 8E-28	6E-028 ± 4E-27	2E-028 ± 10E-28

Plateau Active-Standard

	Alpha	Beta	Low Gamma	High Gamma
Electrode	-1E-027 ± 1E-27	-2E-028 ± 2E-28	-1E-029 ± 3E-29	-2E-031 ± 6E-30
Frontal	6E-027 ± 4E-27	4E-028 ± 4E-28	1E-028 ± 3E-28	4E-029 ± 1E-28
Occipital	-2E-028 ± 7E-28	9E-030 ± 3E-29	-3E-029 ± 1E-29	-3E-029 ± 9E-30
Total	6E-028 ± 5E-27	-2E-030 ± 3E-28	2E-029 ± 2E-28	5E-030 ± 8E-29

In terms of an average of noise across channels, the comparisons revealed that the active and sham conditions featuring the ramp periods generated more disturbance than the respective plateau trials. The plateau trials produced difference maps that better resembled patterns of resting activity, although residual noise artefacts were present in frontotemporal channels. This is in agreement with the previous PSD plots, where fluctuations in noise were dramatically attenuated following the removal of trials corresponding to the current onset/offset. With regard to frequency, activity in the beta range appears to have been the least affected by the addition of tDCS. Sensor disturbance was anticipated in the alpha band as the previous PSD plots demonstrated excess noise below approximately 15 Hz. Channel disturbance was also prominently observed within the low and high gamma bands but was reduced at the site of the electrode, once the current onset/offset trials had been removed. The topographical plots demonstrate that noise was commonly evident across anterior channels, which may be indicative of a current pathway between electrodes. The noise profile varied at each individual sensor and, surprisingly, the highest noise levels were not consistently found under the electrode pad, particularly for the lower frequency bands.

4.5. Discussion

This development work aimed to examine the noise levels induced by tDCS during simultaneous MEG recordings. Consequently, the research represented a proof-of concept stage in determining the feasibility of conducting combined tDCS-MEG research at CUBRIC. Compared to noise levels present during a standard MEG preparation, the initial investigation of noise as an average across all sensors demonstrated the presence of high amplitude artefacts at low frequencies, during both active and sham stimulation. At the level of individual sensors, the excess noise was present at locations local to and distant from the active electrode. Furthermore, the difference maps indicated that noise levels were not consistently highest at the site of the electrode. This finding stands in contrast to the attenuation of noise at distant sites found by Soekadar et al. (2013). However, while the authors of the previous study conducted their investigation of noise using a current dipole phantom, the present research assessed the induction of artefacts in a human subject. Unlike phantom devices, subjects can become fatigued. Additionally, due to the conductivity profile of human subjects, the spatial pattern of noise is likely to vary in a montage-dependent manner. For example, the bihemispheric montage used in the present study may have been

responsible for producing noise at frontal sensors that may not arise from other configurations. Such differences would not be expected to be evident in a more simplistic, uniform conducting sphere. These issues may go some way to explaining the distinction in findings and illustrate how noise levels are likely to be less predictable, and thus more problematic, in humans. While phantom research is often considered the gold-standard, human subjects will ultimately be the focus of future research endeavours. This research has, therefore, provided insight into the extent of noise to be anticipated during subsequent research.

Crucially, the general presence of the tDCS-induced artefacts appears to be easily reduced. Once the trials that occurred during current onset and offset were removed, there was a visible reduction in high amplitude noise fluctuations in the data. The relative stability of power spectra following the removal of such trials indicates that data acquisition may not be as compromised during the DC plateau. Accordingly, the topographical difference maps revealed less total noise, across all channels, when only the plateau trials were included. However, it should be noted that this reduction of noise did not correspond to each individually assessed channel. For example, in the low and high gamma bands, the residual noise from the active stimulation trials (Active-Standard) was reduced at the electrode sensor (Plateau Active-Standard). In contrast, noise at the frontal channel did not decrease following the removal of trials. The pattern of sensor disturbance at each location indicates that the noise from the onset/offset of the current is likely to impact the sensors surrounding the electrode, whereas the plateau phase is likely to be associated with more distant sites (potentially corresponding to the current pathway). This would explain why removing the ramp trials only improved the noise at the electrode sensor. While this is beneficial for the assessment of local activity, if distant channels become excessively contaminated, investigating the influence of tDCS on remote brain regions may be problematic. Therefore, the influence of trial removal is unlikely to affect the noise profile at all channels in a similar manner and may differ depending on the frequency band(s) of interest.

Nonetheless, the observed enhancement of stability in the generated power spectra - alongside the decrease in total noise and that at the electrode site - should contribute to more accurate estimates of source localisation, which are integral to the inferences that can be made regarding the origin of neural activity. This is because the neuronal responses recorded by MEG exist as measures of magnetic flux in sensor space and sources are not recorded from single sensors in the SQUID array, meaning many

sensors may detect the same source (Baillet et al., 2001). Therefore, to determine the origin of a particular signal in the brain, the data must be reconstructed in source space to provide possible solutions to the inverse problem (Mosher et al., 1999). Facilitating source localisation should, therefore, ensure that meaningful inferences are derived from recordings corresponding to the stimulation period.

Consistent source localisation may be particularly likely to occur if a beamformer approach is utilised because such methods of source reconstruction have been shown to be effective at suppressing noise artefacts (Hillebrand & Barnes, 2005); including those arising from stimulation methods (Adjamian et al., 2009). Such methods should be able to compensate for the evident residual noise of the plateau trials. This is due to the nature of beamforming methods, which act as spatial filters, searching through source space to focus on target activity and suppress activity from other locations. Litvak, Eusebio, Jha, Oostenveld, Barnes, Penny... and Brown (2010) demonstrated that contaminated MEG signals resulting from an implanted Deep Brain Stimulation device could be filtered to reveal "physiologically meaningful information". This is an essential consideration because irresolvable data contamination due to poor separation of the artefacts from the signal would render interpretation, and thus such integrative research, impossible. Crucially, the artefacts in question were of high amplitude as were those associated with tDCS in the present study. Therefore, it should be possible to use a similar source reconstruction technique to remove residual tDCS noise artefacts (e.g. SAM, as shown by Soekadar et al., 2013).

4.6. Conclusions

> "This new method allows for the first time direct measurement of the effects of non-invasive electrical brain stimulation on brain oscillatory activity and behaviour".

This statement by Soekadar et al. (2013) represents the start of an extremely promising future for integrated tDCS-MEG, which will ultimately allow for investigation into the neural underpinnings of the neuromodulation technique itself. The present study has further demonstrated the feasibility of combining tDCS and MEG, which suggests that future research designed to link observable modulations of electrophysiological activity to electrical stimulation, should be a viable approach to determine the neurobiology of tDCS. In doing so, it is hoped that such work will help to establish increasingly refined applications of tDCS in both health and disease.

5. Experimental Chapter 3

From Excitation and Inhibition to Electrophysiology - A Concurrent tDCS-MEG Investigation of the Effects of Brain Stimulation

5.1. Abstract

As a continuation of the development work outlined in the previous chapter, DC stimulation was administered during concurrent MEG data acquisition to assess the neurobiological basis of tDCS. This was achieved using a visuomotor task, which participants performed prior to, during and after DC stimulation. Task-induced responses in the visual gamma band (30-80 Hz) and motor beta band (15-30 Hz) were analysed using Synthetic Aperture Magnetometry (SAM), following the generation of virtual sensors corresponding to the peak voxels observed within primary visual and motor cortices. Consistent estimates of source localisation were obtained from the data; including recordings made during tDCS. A significant reduction in average power in the visual gamma band was observed for anodal stimulation compared to sham. Additionally, aspects of electrode montage selection and tDCS presentation order were found to be contributing factors in determining the frequency and amplitude of induced responses. The magnitude of motor-based evoked responses was also found to be significantly modulated by tDCS. The results provide preliminary evidence that metrics of electrophysiological activity, as measured by MEG, are implicated in the generation of tDCS effects.

5.2. Introduction

Neuroimaging studies have enhanced our understanding of the physiological mechanisms underlying the effects of tDCS on behaviour (Hunter et al., 2013). For example, Magnetic Resonance Imaging (MRI) and Spectroscopy (MRS) have provided insights into alterations of functional connectivity and changes in neurotransmitter concentrations following stimulation (Stagg et al., 2009; Clark et al., 2011; Polanía et al., 2012; Sehm et al., 2013b; Amadi et al., 2014). However, the more prominent use of millisecond-resolution far-field electrophysiological methods, such as Electroencephalography (EEG) and MEG, may be particularly advantageous. To date, the majority of studies combining tDCS and EEG/MEG have not used the techniques concurrently, instead focusing on the changes that occur after the period of stimulation (Polanía et al., 2011; Venkatakrishnan et al., 2011; Jacobson et al., 2012; Neuling et al., 2012; Spitoni et al., 2013). Soekadar et al. (2013) published the first concurrent tDCS-

MEG study, in which a motor paradigm was used to elicit responses in the alpha and beta bands. This work focused on the feasibility of combining the techniques and found no adverse effects of stimulation on the quality of data. Since this first study, the concept of concurrent tDCS-MEG has been promoted as a potential method to study the underpinnings of tDCS' behavioural effects. By linking observable modulations of electrophysiological activity (such as cortical oscillations; Thut, Miniussi & Gross, 2012) to electrical stimulation, this work should help to establish increasingly refined applications of tDCS in both health (through cognitive and behavioural research) and disease (as a treatment option for neurological and psychiatric disorders).

Gamma oscillations (>30 Hz) are an appealing target for tDCS modulation due to current theories linking their generation to the excitation/inhibition balance (Buzsáki & Wang, 2012). For example, fluctuations in gamma oscillations of hippocampal pyramidal cells in rats have recently been shown to rely upon the dynamic modulation of excitation and inhibition (Atallah & Scanziani, 2009). Accordingly, enhancement in the synchrony of pyramidal cell firing is said to be propagated by a release from inhibition exerted by inhibitory post-synaptic currents (IPSCs) on GABAergic interneurons (particularly basket cells: Hasenstaub, Shu, Haider, Kraushaar, Duque & McCormick, 2005; Bartos, Vida & Jonas, 2007). This suggests that pyramidal-interneuron relations are integral to the generation of gamma oscillations (Gonzalez-Burgos & Lewis, 2008).

Pharmacological MEG studies (referred to as pharmaco-MEG; Muthukumaraswamy, 2014) have provided extensive support for this hypothesised role of the excitation/inhibition balance. Firstly, Diazepam (benzodiazepine, $GABA_A$ agonist) has been shown to increase gamma power in the visual cortex via a proposed increase in the efficiency of fast inhibitory processing (Hall, Barnes, Furlong, Seri & Hillebrand, 2010). In a separate study, participants administered alcohol (0.8g/kg) were shown to exhibit an increase in sustained gamma amplitude and a corresponding decrease in the frequency of primary visual cortex responses to a stationary, square-wave grating (compared to results following administration of a placebo; Campbell, Sumner, Singh & Muthukumaraswamy, 2014). These results were proposed to be due to the action of alcohol increasing $GABA_A$ mediated inhibition and diminishing glutamatergic excitation via NMDA receptors. Additionally, alcohol consumption was found to increase the amplitude of gamma oscillations in motor cortex, in response to a finger abduction task (referred to as movement related gamma synchrony, MRGS). In

accordance with the mechanisms set out by Gonzalez-Burgos & Lewis (2008), the slowing of IPSCs induced by alcohol (leading to a decrease in frequency) was said to produce the reduction of inhibition needed to increase the synchronisation of firing (leading to increased response amplitude) via the recruitment of additional pyramidal cells. However, the influence of the GABA Transporter 1 (GAT-1) blocker, Tiagabine, produced no alterations in motor gamma frequency or amplitude following a finger abduction task (Muthukumaraswamy, Myers, Wilson, Nutt, Lingford-Hughes, Singh & Hamandi, 2013a). Tiagabine reportedly inhibits the reuptake of extrasynaptic GABA, thus elevating the overall concentration (Dalby, 2000), whereas substances such as Diazepam and alcohol act at the site of $GABA_A$ receptors to enhance their efficiency (Giusti & Arban, 1993; Roberto, Madamba, Moore, Tallent & Siggins, 2003). Nonetheless, gross increases in GABA concentration seem to correlate with increases in the frequency of both visual (Muthukumaraswamy, Edden, Jones, Swettenham & Singh, 2009) and motor (Gaetz, Edgar, Wang & Roberts, 2011) gamma oscillations. Therefore, GABA concentration changes should be sufficient to modify such brain rhythms (although it should be noted that this evidence derived from MRS has recently been called into question; Cousijn, Haegens, Wallis, Near, Stokes, Harrison & Nobre, 2014). On the whole, the available literature provides a foundation for the influence of the excitation/inhibition balance on the generation of gamma oscillations, indicating a potential role for tDCS-induced modulations.

Oscillations in the beta band (15-30 Hz) have been proposed to be modulated by similar mechanisms to those in the gamma band (Jensen, Pohja, Goel, Ermentrout, Kopell & Hari, 2002; Yamawaki, Stanford, Hall & Woodhall, 2008). Patients with a form of myoclonic epilepsy have been characterised as exhibiting abnormal beta band activity due to reduced intracortical inhibition (Silen, Forss, Jensen & Hari, 2000). Baclofen, which acts at $GABA_B$ receptors, has been reported to enhance beta power (Badr, Matousek & Frederiksen, 1983) and has also been shown to heighten long interval intracortical inhibition (LICI) (McDonnell, Orekhov & Ziemann, 2006). Compelling evidence for the role of excitatory and inhibitory mechanisms in generating the beta rhythm has also been established using pharmaco-MEG. Using a resting paradigm, Diazepam was shown to increase power and decrease beta frequency (Jensen, Goel, Kopell, Pohja, Hari & Ermentrout, 2005). A biophysical network model generated to simulate the data (comprising of 64 pyramidal cells [e] and 16 interneurons [i], predominantly characterised as having i-i or i-e connections), found that the beta band fluctuations could be best explained by an increase in IPSCs on inhibitory neurons as

opposed to those on excitatory cells. While the model favoured an interneuron-based account of beta band activity (interneuron beta; INB, rather than pyramidal-interneuron beta; PINB), it is ultimately the response of excitatory cells that is measured by MEG and, as such, the specific role of inhibition on pyramidal cells is integral. Therefore, the authors concluded that the elevation in beta amplitude was driven by an enhancement in the synchrony of pyramidal cell firing, triggered by increased IPSC delay times that decreased the influence of inhibition and subsequently reduced beta frequency.

To add to this evidence, during the aforementioned Tiagabine study, Muthukumaraswamy et al. (2013a) assessed the influence of the intervention on the frequency and power of event related desynchronisation (ERD) and post movement beta rebound (PMBR) responses. While the ERD was shown to be enhanced by the administration of Tiagabine, the PMBR was diminished, suggesting separate origins for each of these metrics of movement-based activity. The authors comment on the research of Hall and colleagues (2010; Hall, Stanford, Yamawaki, McAllister, Rönnqvist, Woodhall & Furlong, 2011), in which the administration of Diazepam failed to elicit similar changes in PMBR in response to hand contractions or simple button press actions. These opposing findings were attributed to the nature of the pharmacological interventions used. As previously outlined, while both are strictly substances that promote GABAergic efficiency, Tiagabine and Diazepam have very different mechanisms of action. The general increase in endogenous GABA levels afforded by Tiagabine may affect $GABA_A$ and $GABA_B$ receptors, characterising the ERD as a $GABA_A$ specific process and PMBR as a primarily $GABA_B$ mediated response. The fact that fluctuations in the PMBR were measured following an increase in the availability of GABA also explains the observed correlation between PMBR amplitude and GABA concentration (Gaetz et al., 2011).

As a particularly eloquent addition to the pharmaco-MEG literature, Rönnqvist, McAllister, Woodhall, Stanford and Hall (2013) designed a parallel animal and human study to demonstrate the GABAergic underpinnings of beta oscillations. The study found that beta band responses, measured *in vitro* by electrode recordings of slice preparations from rodent M1, were generated by the integrated activity of layer III (supragranular) and layer V (infragranular) pyramidal cells. An assessment of comparative power spectral density (PSD) plots suggested that similar mechanisms were engaged in humans when M1 oscillatory activity was detected during *in vivo* MEG recordings (assessed using a virtual electrode approach to source reconstruction). Of

particular importance, the study compared the effects of relative doses of Zolpidem (a $GABA_A$ agonist with similar mechanisms to benzodiazepines) on slice preparations and human participants, finding that it increased beta power in both samples. Having demonstrated the close correspondence of power changes and underlying physiological mechanisms between animals and humans, highlighting the translational potential of such research, the study provided supporting evidence that beta oscillations are directly affected by GABAergic modulation.

This proposal of causal links between cortical excitation and inhibition and the relative power of beta and gamma oscillations, suggests that oscillatory measures are ideal targets to investigate the effects of direct current stimulation on the brain. As scalp-applied anodal tDCS has been shown to increase glutamatergic transmission (primarily through NMDA receptors) and decrease GABA mediated responses (Liebetanz et al., 2002; Nitsche et al., 2003b; Nitsche et al., 2004a), anodal tDCS should affect gamma and beta band responses measured in MEG. However, compared to the literature highlighting the effects of cortical polarisation on motor (Nitsche & Paulus, 2001), visual (Antal, Kincses, Nitsche, Bartfai & Paulus, 2004a) and somatosensory (Matsunaga, Nitsche, Tsuji & Rothwell, 2004) evoked potentials, few studies have directly investigated the influence of DC stimulation on induced responses. Bikson, Inoue, Akiyama, Deans, Fox, Miyakawa and Jefferys (2004) demonstrated the acute effect of constant current on excitatory activity, measured *in vitro*. Subsequent findings have shown modulations in neuronal population activity, specifically targeting carbachol-induced gamma oscillations (Reato, Rahman, Bikson & Parra, 2010). In a recent extension of this research, Reato, Bikson & Parra (2015) established prolonged modulations of gamma oscillations in hippocampal slice preparations via the application of various DC intensities (10 minutes; -20 V/m to +20 V/m). The authors attributed this finding to alterations in excitatory and inhibitory feedback mechanisms, driven by the modulatory influence of DC stimulation on synaptic plasticity. This study provides compelling evidence that the applied constant current intensities were able to alter ongoing neural activity, beyond the stimulation period (although it should be noted the intensities were far higher than those delivered during human studies; Datta, Bansal, Diaz, Patel, Reato & Bikson, 2009).

Stimulation studies concerning *in vivo* beta and gamma oscillations in humans have also highlighted the potential for tDCS-induced modulations. Antal, Varga, Kincses, Nitsche and Paulus (2004b) determined the prolonged effect of cathodal tDCS on oscillatory

power in visual cortex, which was significantly reduced. Anodal stimulation, however, did not produce any significant modulations but did result in a trend towards increased power (interpreted in the context of the ease of inducing a reduction in excitation as opposed to an increase; Froc, Chapman, Trepel & Racine, 2000). As an illustration of the influence of tDCS on functional connectivity, measured using pre/post EEG, Polanía et al. (2011) found that anodal tDCS was able to increase synchrony between task-relevant connections, in the 60-90 Hz gamma band during a motor-based task. This enhancement affected M1 but also saw the recruitment of premotor and sensorimotor regions, outside of the stimulated area. Additionally, increased intrahemispheric synchrony was accompanied by a decrease in connectivity to the opposite hemisphere, highlighting the local and global influence of tDCS on endogenous rhythms. Finally, in a combined tDCS-EEG study, posterior parietal cortex stimulation was shown to increase power in the beta band at rest during anodal stimulation (1.5 mA, 15 minutes) and for the entire post-stimulation duration (12 minutes), albeit in the absence of any modulation in power with regard to the gamma band (Mangia, Pirini & Cappello, 2014). Although the evidence is limited at present, these *in vitro* and *in vivo* studies suggest that tDCS-induced modulations of beta and gamma rhythms should be observed.

The present study aimed to demonstrate the influence of tDCS on oscillatory activity, using a combined visuomotor task (previously used by Muthukumaraswamy, Carhart-Harris, Moran, Brookes, Williams, Errtizoe... & Nutt, 2013b). This task was used based on its ability to generate robust beta and gamma band responses at spatially separate sources. Consequently, electrode configurations were designed to administer anodal and sham stimulation to primary visual and motor cortices during different sessions. As research investigating links between tDCS and changes in oscillatory power is in its infancy, hypotheses relating to the expected effects of tDCS were generated in accordance with relevant literature (such as the outlined pharmacological-MEG research). With regard to the gamma rhythm, based on literature stating that anodal tDCS produces a decrease in $GABA_A$-mediated inhibition (Stagg & Nitsche, 2011), it was predicted that anodal stimulation, compared to the sham control measure, would have the opposite effect to that found following the consumption of alcohol (known to increase the efficiency of $GABA_A$ receptors and increase inhibition; Campbell et al., 2014). Specifically, the tDCS-induced decline in inhibition was predicted to generate short IPSC durations and sporadic pyramidal cell activity (Hasenstaub et al., 2005), which would produce a decrease in gamma power. In the beta band, it was predicted that anodal stimulation would decrease the power of the ERD response and increase that

of the PMBR, again by reducing GABAergic inhibition. These hypotheses are in accordance with work by Muthukumaraswamy et al. (2013a), which demonstrated that an increase in endogenous GABA levels produced opposite effects in these measures.

5.3. Methods

5.3.1. Subjects

16 subjects took part in the study (10 male). All were aged 23-40 years (*M=27.50, SD=4.65*), had corrected-to-normal vision and were determined to be right-hand dominant (Edinburgh Handedness Inventory, Oldfield, 1971; Appendix 1). Upon expressing an interest in taking part in the study, subjects were screened to determine their eligibility to take part (Appendix 2). Those with any contraindications were excluded from the study. All procedures were carried out with the approval of the local ethics committee.

5.3.2. Visuomotor paradigm

Participants viewed a visual stimulus composed of a vertical, stationary, square-wave grating, presented on a mean luminance background at maximum contrast with a spatial frequency of 3 cycles/degree(°). The visual grating subtended 8 degrees, horizontally and vertically, and featured a green fixation dot at the centre of the stimulus. The stimulus was programmed using the MATLAB Psychophysics Toolbox (Brainard, 1997; Pelli, 1997) and was presented via a Mitsubishi Diamond Pro 2070 monitor. The size of the screen was 1024x768 pixels with a frame rate of 100 Hz. The monitor was positioned outside of the magnetically shielded room (MSR) and was viewed through a gap in the shield, at a distance of 2.15 m. The stimulus duration was set to 1.5-2 s and was followed by a 3 s baseline period, where only the fixation dot was presented (Figure 5.1). Subjects were instructed to attend to the fixation point at all times and to perform an abduction of their right index finger upon stimulus offset. The abduction responses (duration period, 1 s) were recorded via the acquisition computer.

Subjects performed three runs of the visuomotor task during each session: before (Pre), during and after (Post) stimulation. Pre and Post-tDCS runs featured 100 trials, completed in approximately 8 minutes. An additional 50 trials were incorporated during tDCS to accommodate the removal of epochs contaminated by the current ramp phases (where the current was gradually increased to the desired level and subsequently

reduced towards zero on termination), designed to minimise sensor disturbance. These experimental runs lasted for approximately 12 minutes.

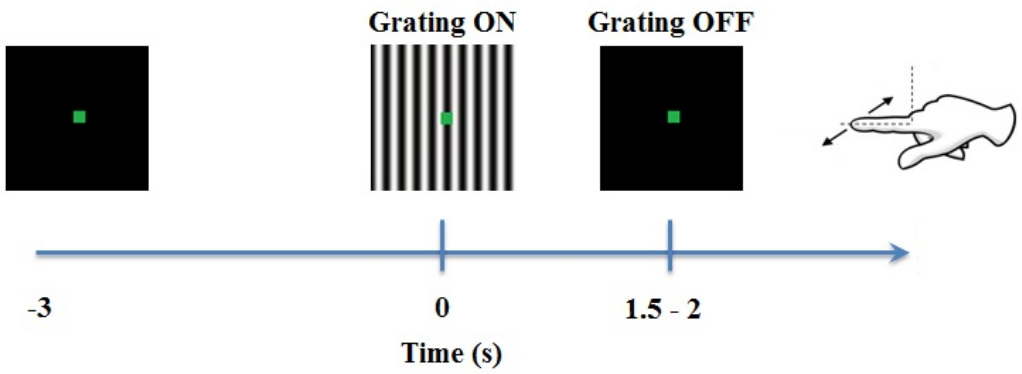

Figure 5.1. A single trial of the visuomotor task. Participants attended to a stationary, square-wave grating for 1.5-2 s prior to making an abduction response with their right index finger at stimulus offset. The grating remained off for 3 s prior to each subsequent trial.

5.3.3. MEG acquisition

Whole head MEG recordings were acquired using a CTF Omega 275 channel, radial gradiometer system, sampled at 600 Hz. Excessive sensor noise necessitated that four of the channels be switched off. The remaining 271 MEG sensors were analysed as synthetic third-order gradiometers (Vrba & Robinson, 2001). An additional 29 channels were used to facilitate noise cancellation. A transistor-transistor logic pulse (TTL) was sent to the MEG system at the start of each stimulus presentation. Subjects had three electromagnetic head coils attached to the nasion and preauricular points, which were continuously localised relative to the MEG system throughout each recording. Vertical and horizontal electroculograms (EOG) were used to record eye movements. The activity of the right first dorsal interosseous (FDI) muscle was monitored via electromyogram (EMG). The finger abductions performed during the visuomotor task were recorded by the MEG system via an optical displacement system (Muthukumaraswamy, 2010).

An anatomical image for each participant was obtained for source localisation. 3D Fast Spoiled Gradient echo (FSPGR) MRI scans were acquired prior to the study, using a 3T General Electric HDx scanner with an eight-channel head coil. Scans were acquired in an axial orientation with 1 mm isotropic voxel resolution. For co-registration of MRI images and MEG data, the positions of the electromagnetic head coils were aligned to the nasion and preauricular points, which were identifiable landmarks on the subjects'

corresponding MRI images. The brain shape of each subject was extracted using FSL's Brain Extraction Tool (BET; Smith, 2002) in order to perform subsequent time-frequency analysis on the data.

5.3.4. Transcranial direct current stimulation

A DC-Stimulator MR device (neuroConn, Germany) was used to deliver direct current stimulation. Subjects were randomly assigned to one of eight session orders, defined by stimulation (Anodal (A) & Sham (S)) and montage (Visual (V) & Motor (M)). The 8 session orders (of a possible 16), were not selected in accordance with a specific rationale; only such that there were orders in which each stimulation/montage type was presented at the start (first two sessions e.g. MMVV, AASS) and end (last two sessions e.g. VVMM, SSAA) of the study and also in an interleaved fashion (e.g. MVMV, ASAS). Each subject participated in 4 sessions. 3 runs of the visuomotor task (pre, during, post-tDCS) were conducted within each of these sessions. Each session took place at least 24 hours apart. Both the researcher and the participant were blinded to the nature of the stimulation that took place during each session. This was made possible using the "study" mode option, in which stimulation parameters were pre-defined and executed using codes for active and sham stimulation. Stimulation duration was set to 600 s for each session, with an additional 10 s onset/offset period. Rubber electrodes, measuring 5x7 cm (35 cm^2), were attached to the scalp using conductive paste. Anodal stimulation was delivered with a current of 1 mA (current density = 0.029 mA/cm^2). For sham stimulation, the neuroConn device initially ramped up the current to mimic the peripheral effects of active tDCS before ramping down. During the stimulation period, the device continued to discharge current spikes every 550 ms (110 μA over 15 ms) to enable continuous impedance readings. The average current over time was not more than 2 μA.

Recent research has demonstrated how the effects of tDCS can extend beyond the region underneath the electrodes, thereby influencing global network dynamics (concerning both resting state and task-specific activity, as shown by Polanía et al., 2011; Amadi et al., 2014). The use of two distinct montages permitted the assessment of both local and global modulations, allowing for potential inferences to be made on regional specificity. For example, the modulation of visual activity could be assessed following stimulation via the alternate, motor montage and vice versa. For the visual montage (Figure 5.2a), the electrodes were positioned at Oz (midline, active) and Cz

(midline, reference), designed to correspond to primary visual cortex (V1) (Chatrian et al., 1985). The motor montage electrodes were situated at C3 (left hemisphere/contralateral to movement, active) and Fp2 (right hemisphere, reference), corresponding to primary motor cortex (M1; Figure 5.2b).

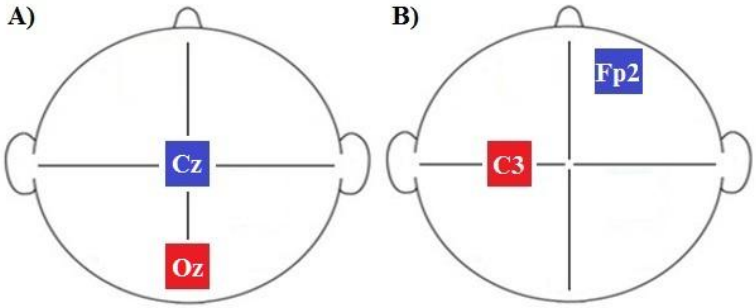

Figure 5.2. Electrode configurations. Electrode positions as referenced to the 10-10 system. A) Visual stimulation montage: Oz (active), Cz (reference). B) Motor stimulation montage: C3 (active), Fp2 (reference).

5.3.5. Experimental procedure

Subjects began each session by completing the necessary consent and screening forms (see Appendix 10 for the study-specific consent form). Pairs of vertical and horizontal EOG electrodes were then attached around the eyes and EMG electrodes positioned over the FDI of the right hand (Figure 5.3). Three electromagnetic head coils were fitted; 1 cm above the nasion and 1 cm anterior of the preauricular points. Scalp measurements were taken to determine accurate positioning of the tDCS electrodes. After the initial preparation phase, subjects were taken into the MSR, seated underneath the dewar in front of the computer monitor and instructed how to use the optical displacement system to perform the finger abduction responses.

Prior to the initial recording, a brief period of stimulation (~10-20 s) was delivered to determine whether impedance levels were sufficient to begin stimulation. Such durations of active stimulation have been shown to produce highly transient changes in cortical excitability, which should have returned to baseline before the onset of the first recording (Bindman et al., 1964; Purpura & McMurtry, 1965; Nitsche et al., 2003b). Three runs of the task were performed per session with a brief interval (~5 minutes) between the during-tDCS and post-tDCS recordings, in order for the participants to give their Adverse Effects Questionnaire (AEQ) responses. The participants stayed within the MSR during this time. Each experimental session lasted approximately 60 minutes.

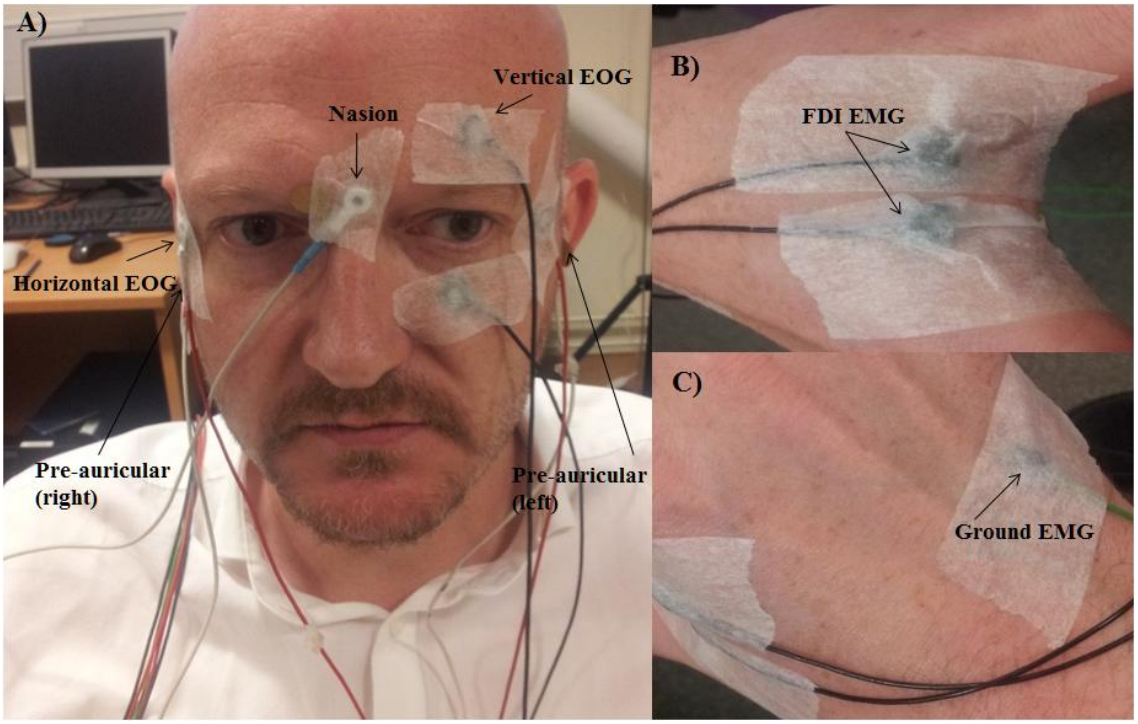

Figure 5.3. Position of electromagnetic head coils, EOG and EMG electrodes. A) The fiducial coils were positioned over the nasion and pre-auricular points, while pairs of EOG sensors were placed horizontally and vertically around the left eye. B) Two EMG electrodes were positioned at either end of the FDI of the right hand. C) The ground electrode for the EMG sensors was placed on the back of the right hand.

5.3.6. MEG data analysis & statistics

The analysis of MEG data was performed using a variety of Linux based software, including viewer and analysis programmes from CTF (DataEditor, MRIViewer), in-house visualisation software (mri3dX; Krish Singh) and analysis scripts written in MATLAB (MathWorks; Cambridge, UK).

The data analysis pipeline was influenced by previous work from the MEG lab at CUBRIC. Analysis of visual and motor data was performed in a similar fashion to that outlined in a recent publication, conducted using an almost identical paradigm (Muthukumaraswamy et al., 2013b). The continuous datasets were epoched based on visual grating onset and EMG markers (-1.5 to 1.5 s visual; -1.5 to 3 s motor). The data were then visually inspected for gross artefacts and epochs were excluded from further analysis based on evidence of excessive eye blinks, muscle clenching and irregular movement displacement. Trials corresponding to the transient current onset/offset periods during concurrent-tDCS were also discarded prior to analysis. On average, ~80% of trials were retained.

Global covariance matrices were generated in the visual gamma band (30-80 Hz) as well as motor gamma (60-90 Hz) and beta (15-30 Hz) bands. Using these covariance matrices, a set of beamformer weights were computed in a voxelwise fashion across the brain at 4 mm isotropic resolution (SAM: Robinson & Vrba 1999; Vrba & Robinson, 2001). For source localisation, a multiple local-spheres forward model (Huang et al., 1999) was implemented. Virtual sensors were created for each beamformer voxel and Student's t-test images were generated to demonstrate source power changes across experimental conditions. As used by Muthukumaraswamy et al. (2013b), the following parameters were defined to determine localisation of visual gamma (-1.5 to 0 s baseline; 0 to 1.5 s active) and motor gamma (-1.3 to 1 s baseline; 0 to 0.3 s active) responses. The following parameters, adapted from Muthukumaraswamy et al. (2013a) and Campbell et al. (2014), were defined to localise motor responses in the beta band: ERD (-1.3 to -0.3 s baseline; -0.3 to 0.3 s active), PMBR (-1.3 to 0 s baseline; 1 to 2.5 s active). To obtain group source localisation estimates, the individual SAM images were concatenated using fslmerge and mean t-images were generated using fslmaths.

The voxels demonstrating the most prominent change for each of the assessed responses were selected and virtual sensors were created for these peak regions. The data was bandpass filtered at 0.5 Hz intervals, from 1 to 100 Hz for visual responses and 1 to 120 Hz for motor responses, to assess the time-frequency response (using an 8 Hz-wide (+/- 4 Hz), third-order Butterworth filter) (Le Van Quyen, Foucher, Lachaux, Rodriguez, Lutz, Martinerie & Varela, 2001). For each frequency interval, the Hilbert transform was used to obtain estimates of the time-varying envelope, which were then averaged across trials. Initially, time-frequency spectrograms were generated using non-baseline corrected, raw spectra to allow analysis of potential differences in the baseline itself. Subsequent analyses reflected changes as a percentage deviation from baseline values.

To complement the investigation of the task-induced activity, changes in the resulting evoked responses were also assessed to provide insight into modulations of activity locked to the onset of the visual stimulus or motor movement (Tallon-Baudry & Bertrand, 1999). This component of the study was largely exploratory as the evoked responses investigated were selected "post-hoc" on the basis of their robustness. The evoked data from the corresponding virtual sensors was plotted to reflect fluctuations in the group response as a product of trial time by source amplitude. These fluctuations were classified in relation to percentage change from baseline values, having baseline-corrected the evoked data. In the motor data, an evoked response that emerged prior to

movement onset and peaked shortly after was observed, followed by a post-movement reversal. The initial peak was characterised as a readiness to respond, reflecting the late stage of the Bereitschaftsfield, while the post-movement deflection signified movement execution (Deecke et al., 1982; Cheyne & Weinberg, 1989; Shibasaki & Hallett, 2006). In accordance with previous literature, these waves are referred to as MF and MEF1, respectively (Kristeva, Cheyne & Deecke, 1991). A large deflection at 100 ms was observed in the visual data (M100), corresponding to the P100 VEP and equivalent VEF (Jeffreys & Axford, 1972a/b; Brenner, Williamson & Kaufman, 1975). The data from each subject was assessed to determine the greatest change in response magnitude for each of the observed waves and the latency at which it occurred. These peaks were derived by searching within a specific time window (the start/end of the deflection). Each response was visually inspected on a subject-by-subject basis to determine the adequate range: MF (-200 – 200 ms), MEF1 (50 – 425 ms), M100 (75 – 150 ms).

SPSS for Windows software (Version 20; IBM, New York) was used to assess significance. As previously outlined, it was predicted that anodal tDCS would reduce power in the gamma band. To test this hypothesis, average power values from the corresponding virtual sensor were entered into a Repeated Measures ANOVA; incorporating the factors, Time (Pre, During, Post), Montage (Visual, Motor) and tDCS (Anodal, Sham). The contribution of the between-subject factors of Montage order (VMVM, MVMV, VVMM, MMVV) and tDCS order (ASAS, SASA, AASS, SSAA) was also analysed. For the beta band, it was predicted that anodal stimulation would decrease the power of the ERD response and increase that of the PMBR. Identical analyses were used to test these hypotheses. While induced oscillatory responses are thought to be signatures of stimulus integration or "binding" and aid information transfer across local and more remote regions (Singer & Gray, 1995; Buzsáki, 2006; Donner & Siegel, 2011; Hipp, Engel & Siegel, 2011), evoked responses have been characterised as specific to a given cortical region and associated stimulus type (Di Russo, Martínez, Sereno, Pitzalis & Hillyard, 2002; Leuthold & Jentzsch, 2002). For this reason, the assessment of the influence of DC stimulation on stimulus-evoked activity was confined to that delivered via the motor montage for motor evoked responses and by the visual montage for visual evoked responses. Therefore, analysis of the peak values reflecting evoked responses did not incorporate the factor of Montage. Greenhouse-Geisser correction was applied where violations of sphericity were apparent. P values less than 0.05 were considered significant.

5.4. Results

Maximum head movement values were assessed in relation to the specific polarity and montage assigned to each session (see Appendix 11 for average head movement values). All statistical outcomes relating to head movement were non-significant, demonstrating consistency throughout the study: Time ($F(1.362,20.432)=3.331$, $p=.072$), Montage ($F(1,15)=.017$, $p=.899$), tDCS ($F(1,15)=.045$, $p=.834$). It should, however, be noted that head movement commonly exceeded the 5 mm threshold (due to the presence of the tDCS electrodes, which made it difficult to position subjects as high in the dewar as would have been normal) but that this was consistent across subjects.

5.4.1. Peripheral effects of tDCS

Impedance values (kΩ) were recorded at the onset of stimulation and classified by stimulation type and montage: Anodal Visual (*M=15.41, SD=0.92*), Anodal Motor (*M=14.53, SD=1.27*), Sham Visual (*M=15.56, SD=1.48*), Sham Motor (*M=14.01, SD=0.64*). No significant differences in impedance were found between tDCS stimulation types ($F(1,15)=1.478$, $p=.243$) or their interaction with each montage (tDCS*Montage: $F(1,15)=2.293$, $p=.151$). However, a significant main effect was established for Montage ($F(1,15)=59.081$, $p=.000$), indicating that impedance for the visual montage was higher than for the motor montage.

Analysis of ratings on the AEQ, corresponding to the period during stimulation, revealed the significant main effects of AEQ item ($F(3.073,46.099)=8.656$, $p=.000$) and tDCS ($F(1,15)=11.575$, $p=.004$). The main effect of Montage was non-significant ($F(1,15)=2.387$, $p=.143$). The AEQ item*tDCS ($F(3.540,53.103)=3.074$, $p=.028$) and AEQ item*Montage ($F(2.243,33.641)=4.563$, $p=.015$) interactions were significant. Further analysis of the AEQ item*tDCS interaction found that anodal stimulation led to higher ratings than the sham condition for the items; Tingling ($t(15)=2.828$, $p=.013$), Itching ($t(15)=3.337$, $p=.004$) and Burning ($t(15)=2.535$, $p=.023$). In relation to the AEQ item*Montage interaction, the motor montage led to higher ratings of Itching ($t(15)=-2.702$, $p=.016$) and the visual montage led to higher rating of tiredness ($t(15)=2.764$, $p=.014$). Impedance and AEQ scores were largely uncorrelated. However, high Tingling ($r(16)=.606$, $p=.013$) and Itching ($r(16)=.674$, $p=.004$) ratings during anodal stimulation of visual cortex were associated with high impedance values. These results indicate that participants may have been aware of the distinction between active and sham stimulation (see Figure 5.4 for AEQ ratings).

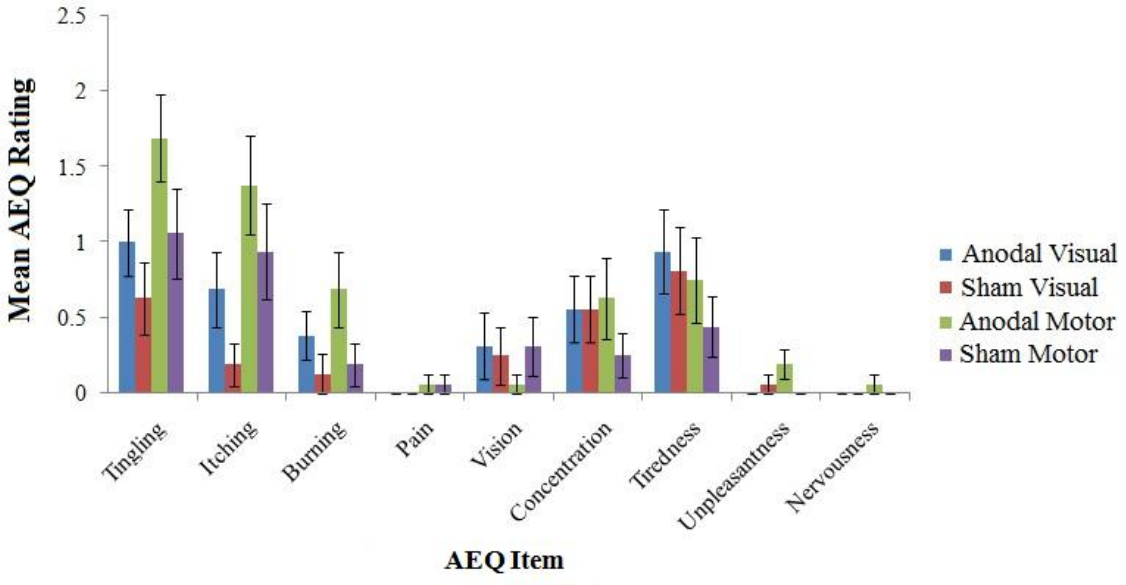

Figure 5.4. Group Adverse Effects Questionnaire ratings. Responses reflect sensations experienced during stimulation. Ratings range from 0 (not experienced) to 1-5 (experienced; higher numbers denote increased severity).

5.4.2. Cortical effects of tDCS

5.4.2.1. Source localisation

Consistent source localisation estimates were derived throughout the study, including those resulting from concurrent tDCS-MEG recordings (Figure 5.5). Prominent bilateral occipital cortex activity was observed in the 30-80 Hz band in response to the visual grating (consistent with the literature: Swettenham et al., 2009; Muthukumaraswamy et al., 2010). Beta band motor responses (15-30 Hz) were largely confined to sensorimotor cortex of the hemisphere contralateral to the finger abduction. The ERD was situated in a posterior location (corresponding to post-central gyrus) compared to the PMBR (pre-central gyrus), as found by Jurkiewicz et al., 2006. Few subjects demonstrated consistent motor gamma responses, prohibiting the analysis of 60-90 Hz activity.

5.4.2.2. Baseline activity

Average power values corresponding to the raw, non-baseline corrected spectra were initially assessed for potential differences introduced by the neuromodulation technique. Repeated Measures ANOVAs produced no significant main effects for the analyses corresponding to the ERD (Time ($F(2,30)=1.737$, $p=.193$); Montage ($F(1,15)=.679$, $p=.423$); tDCS ($F(1,15)=.113$, $p=.741$)), PMBR (Time ($F(2,30)=1.209$, $p=.313$); Montage ($F(1,15)=.229$, $p=.639$); tDCS ($F(1,15)=1.007$, $p=.331$)) or visual gamma

responses (Time (F(2,30)=.813, p=.453); Montage (F(1,15)=3.329, p=.088); tDCS (F(1,15)=.017, p=.899)). All associated interactions were also non-significant.

The lack of significant findings in the period corresponding to the pre-stimulus baseline indicated no statistical influence of the neuromodulation technique. The stability of the pre-stimulus period, with respect to the stimulation, permitted the subsequent representation of the data in terms of relative, percentage change in the active, post-stimulus period with respect to the specified baseline period.

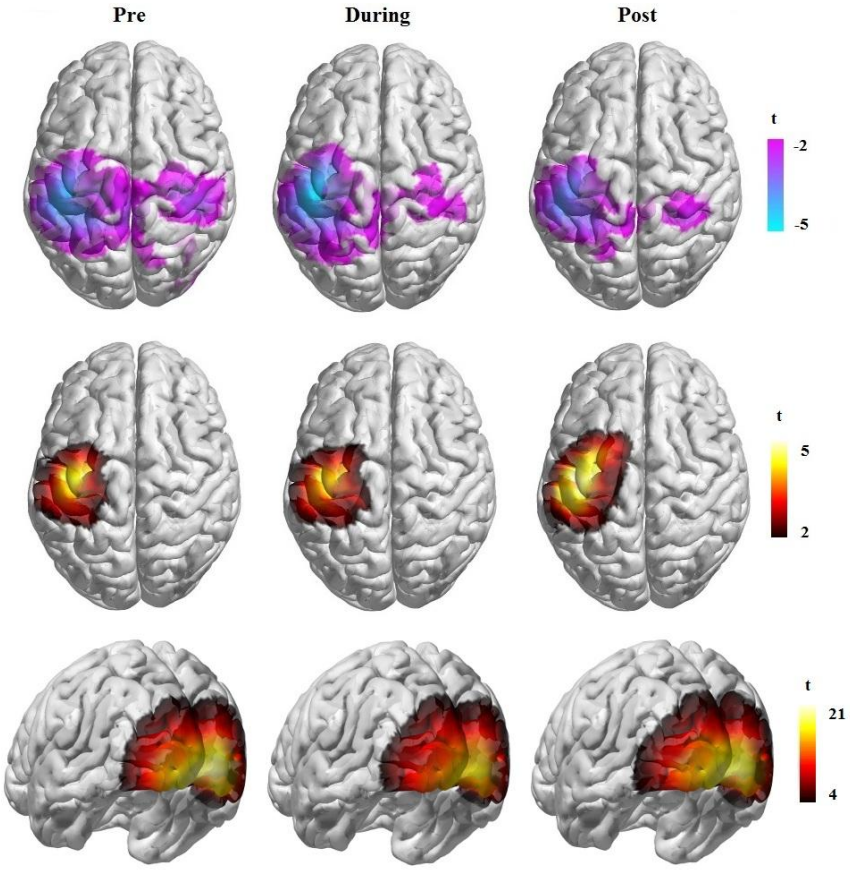

Figure 5.5. Group source localisation. Results of SAM source localisation performed on each response component (top-bottom: beta-ERD, PMBR, visual gamma), across time points (left-right: Pre, During, Post-tDCS). The images show voxelwise group t-statistics, thresholded at $p<0.05$ (uncorrected). These values are indicative of source amplitude changes in regions where activity significantly differed between the active and baseline period of trials. The data depicted corresponds to the experimental runs incorporating anodal stimulation, having been delivered via the visual montage for visual gamma analysis and the motor montage for the analysis of beta band activity. Results were projected onto a template brain using BrainNet Viewer (Xia, Wang & He, 2013).

5.4.2.3. Task-induced responses

An average of source power was computed for the frequency bands of interest to assess modulations of the time-frequency response (see Appendix 12 for average power values).

5.4.2.3.1. Motor beta band response

Figure 5.6 illustrates the time-frequency response for each of the assessed intervals, within the beta band. In relation to the ERD, the factor Time marginally missed significance ($F(2,30)=3.154$, $p=.057$). The main effects of Montage ($F(1,15)=.232$, $p=.637$), tDCS ($F(1,15)=.593$, $p=.453$) and all associated interactions were non-significant. For the analysis of PMBR, Time ($F(2,24)=.341$, $p=.715$) and tDCS ($F(1,12)=1.104$, $p=.314$) were found to be non-significant. There was a significant main effect of Montage ($F(1,12)=10.555$, $p=.007$), coupled with a highly significant Montage*Montage order interaction ($F(3,12)=7.673$, $p=.004$). Further investigation determined that the motor montage resulted in higher average power changes than the visual montage, when subjects performed sessions in the order MVMV ($t(3)=-9.795$, $p=.002$).

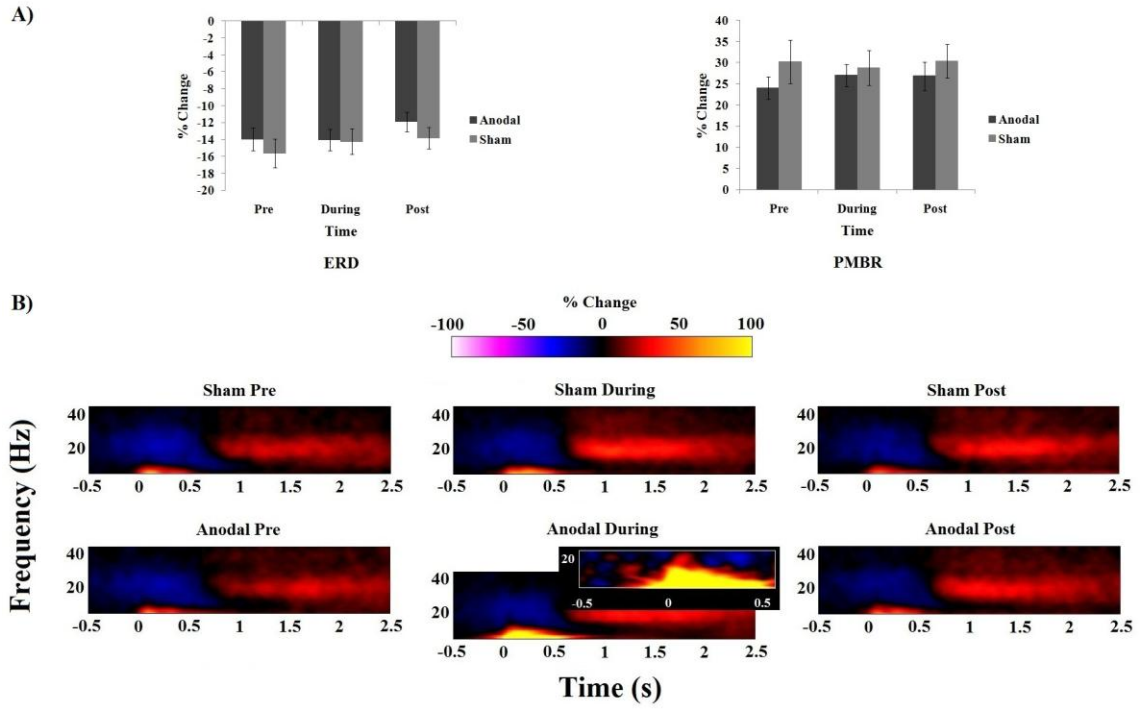

Figure 5.6. Time-frequency response in the beta band. A) Mean percentage change in average power for the ERD and PMBR responses. Error bars represent ± 1 standard error (S.E.M). B) Spectrograms depict motor beta-ERD and PMBR in relation to a finger abduction response (illustrated as percentage change from baseline). Note the onset of 5-12 Hz activity in conjunction with movement onset, during anodal stimulation. The inset within the "Anodal During" panel depicts the time-frequency representation of the corresponding phase-locked component of the data. The identical pattern of movement onset activity suggests the identified 5-12 Hz response reflects an evoked as opposed to induced signal.

5.4.2.3.2. Visual gamma band response

Figure 5.7 demonstrates the time-frequency response within the gamma band. The factor Time ($F(1.430,17.165)=.374$, $p=.624$) was found to be non-significant. Montage ($F(1,12)=9.002$, $p=.011$) and tDCS ($F(1,12)=5.043$, $p=.044$) produced significant main effects. The Montage main effect represented a tendency for the motor montage to result in greater power changes compared to the visual montage. The main effect of tDCS corresponded to a reduction in power in the anodal compared to sham stimulation condition. All within-subject interactions were non-significant, however, there was an interaction for tDCS and the between-subject factor tDCS order ($F(3,12)=4.080$, $p=.033$). A trend was found for the anodal condition to produce a power reduction compared to sham stimulation, with regard to session order SSAA ($t(3)=-3.037$, $p=.056$).

5.4.2.4. Group SAM/Randomisation

In addition to the subject-specific virtual sensor analysis, pairwise comparisons were performed using the average group SAM data in normalised source space. This was achieved using voxelwise permutation testing, implemented via the FMRIB Software Library's (FSL) Randomise tool (Winkler, Ridgway, Webster, Smith & Nichols, 2014). Comparisons were designed to ascertain differences between anodal and sham stimulation conditions. Each comparison required the computation of the positive and negative version of the subtraction (Anodal – Sham; Sham – Anodal) to fulfil the criteria for a two-tailed test. P values greater than 0.975 were considered significant. Appendix 13 illustrates the significant amplitude differences found in task-specific regions of visual and motor cortices. While several significant results were obtained across time points and analysis types, unfortunately, none of the thresholded p values survived correction for multiple comparisons (5000 random-replacement permutations).

5.4.2.5. Transient & sustained visual gamma response

Motor responses from individual subjects often do not exhibit discernable maximum values, and therefore, prohibit the investigation of peak frequency and amplitude. However, the Gaussian shape of the visual gamma response does permit such analysis (see Appendix 14 for peak frequency and amplitude values). The within-subject effects related to peak sustained gamma frequency (0.3-0.8 s after stimulus onset; Koelewijn, Dumont, Muthukumaraswamy, Rich & Singh, 2011) were all non-significant (Time ($F(2,24)=1.926$, $p=.168$); Montage ($F(1,12)=1.801$, $p=.204$); tDCS ($F(1,12)=.288$,

p=.601)). However, the main effect of the between-subjects factor tDCS order was found to be significant (F(3,12)=3.539, p=.048), illustrating that sustained frequency tended to be higher when resulting from tDCS presentation order ASAS (Appendix 15).

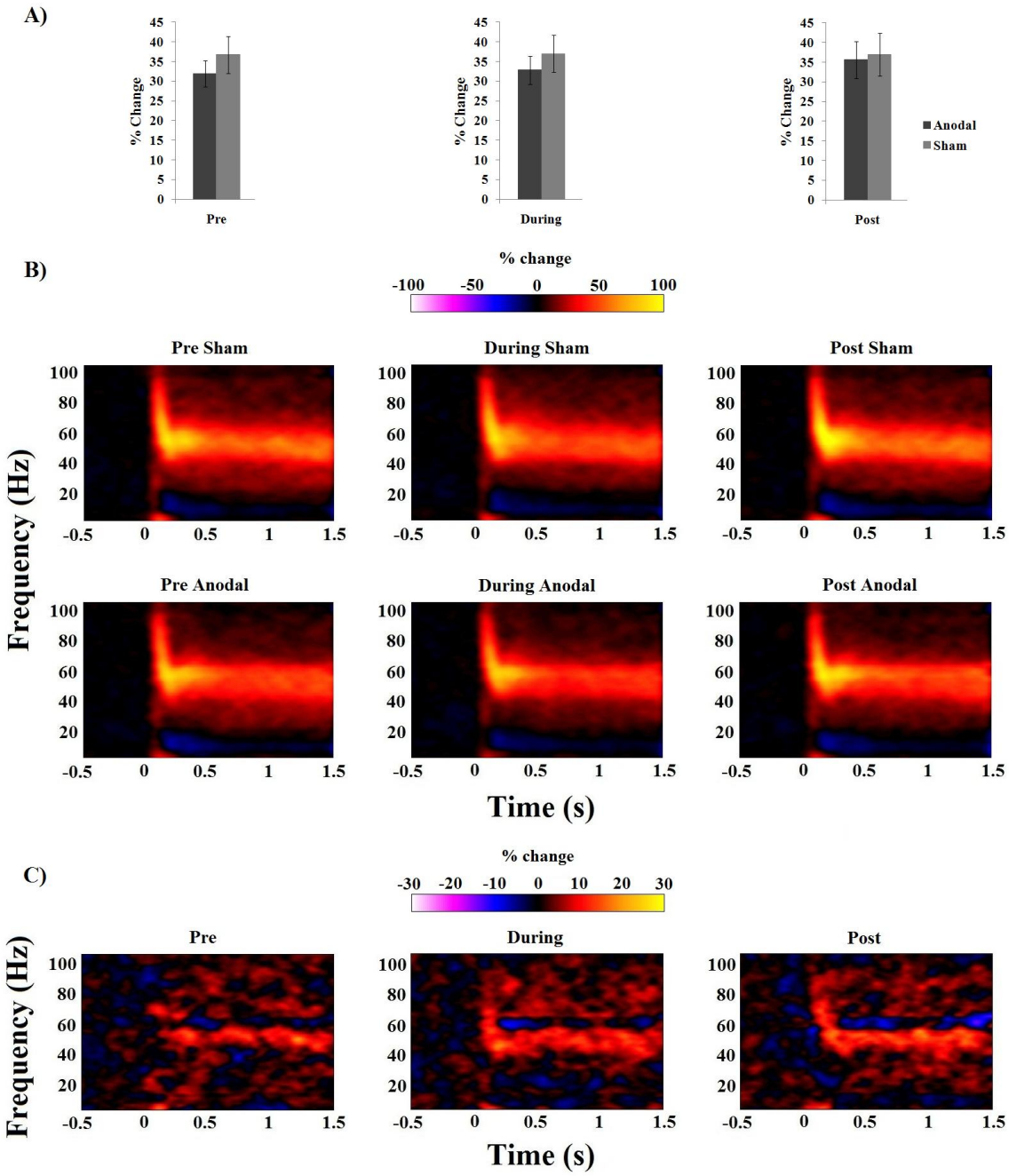

Figure 5.7. Time-frequency response in the gamma band. A) Mean percentage change in average power for the visual gamma response. Error bars represent ± 1 standard error (S.E.M). B) Spectrograms depict visual gamma band responses in relation to a stationary, square-wave grating (illustrated as percentage change from baseline). C) Difference images (Sham-Anodal) demonstrate the strength of the initial gamma 'spike' and the sustained response in the sham condition, indicating that anodal stimulation produced a reduction in power. Anodal stimulation also appears to have produced a more broadband response by elevating the sustained frequency (as illustrated by the negative amplitude change at ~60 Hz).

With regard to peak sustained amplitude, a Repeated Measures ANOVA revealed the non-significant effects of Time ($F(2,30)=.417$, $p=.663$) and tDCS ($F(1,15)=.560$, $p=.466$). The main effect of Montage was significant ($F(1,15)=6.624$, $p=.021$), indicating that the motor montage produced higher peak amplitude values.

For the transient, visual gamma band response (0-0.3 s from stimulus onset) the main effects of Time ($F(1.329,15.948)=1.158$, $p=.317$), Montage ($F(1,12)=.032$, $p=.860$) and tDCS ($F(1,12)=3.743$, $p=.077$) were all non-significant in relation to frequency. Additionally, a 3-way Time*tDCS*tDCS order interaction ($F(6,24)=2.496$, $p=.051$) narrowly missed significance. This most likely demonstrated the trend for the Time*tDCS interaction to approach significance for the presentation order SASA ($F(2,6)=4.154$, $p=.074$), which corresponded to higher transient frequencies being derived from the SASA order during the post- as opposed to pre-stimulation time point of the anodal condition ($t(3)=-6.195$, $p=.008$). With respect to peak transient amplitude, the main effects of Time ($F(1.271,15.249)=1.111$, $p=.326$) and tDCS ($F(1,12)=.716$, $p=.414$) failed to reach significance, while the main effect of Montage ($F(1,12)=6.203$, $p=.028$) was found to be significant. The significant main effect of Montage indicated that higher peak transient amplitude values resulted from the motor compared to visual configuration. A significant main effect was also established for the between-subjects factor tDCS order ($F(3,12)=3.561$, $p=.047$), where transient amplitude tended to be higher when resulting from tDCS presentation order SSAA (Appendix 16).

5.4.2.6. Task-evoked responses

Mean latency and magnitude values for each evoked response are presented in Appendix 17. The data from one participant was removed from the evoked analysis due to the absence of clearly identifiable peak responses.

5.4.2.6.1. Motor evoked response

The MF and MEF1 responses are illustrated in Figures 5.8a and 5.8b, which demonstrate the mean evoked virtual sensor response at the source locations, in motor cortex, identified as having the greatest change in ERD and PMBR, respectively.

Beginning with the analysis of magnitude changes, the MF resulting from the ERD virtual sensor location produced the significant main effect of Time ($F(1.133,15.864)=11.654$, $p=.003$). The main effect of tDCS ($F(1,14)=3.726$, $p=.074$) failed to reach significance. The associated interaction was, however, found to be

significant (Time*tDCS: F(1.026,14.368)=5.554, p=.032). Greater deflections in amplitude were observed for the anodal compared to sham condition during stimulation (t(14)=2.346, p=.034) and during anodal tDCS as opposed to pre- (t(14)=-3.032, p=.009) or post-stimulation (t(14)=2.888, p=.012). Figure 5.6b shows the time-frequency representation of the magnitude change, which corresponds to the burst of activity around 5-12 Hz observed at the time of the ERD. The MF resulting from the PMBR data failed to achieve significance with respect to the main effect of Time (F(1.110,15.547)=4.089, p=.057), tDCS (F(1,14)=1.375, p=.261) and the associated interaction (Time*tDCS: F(1.078, 15.096)=2.546, p=.130).

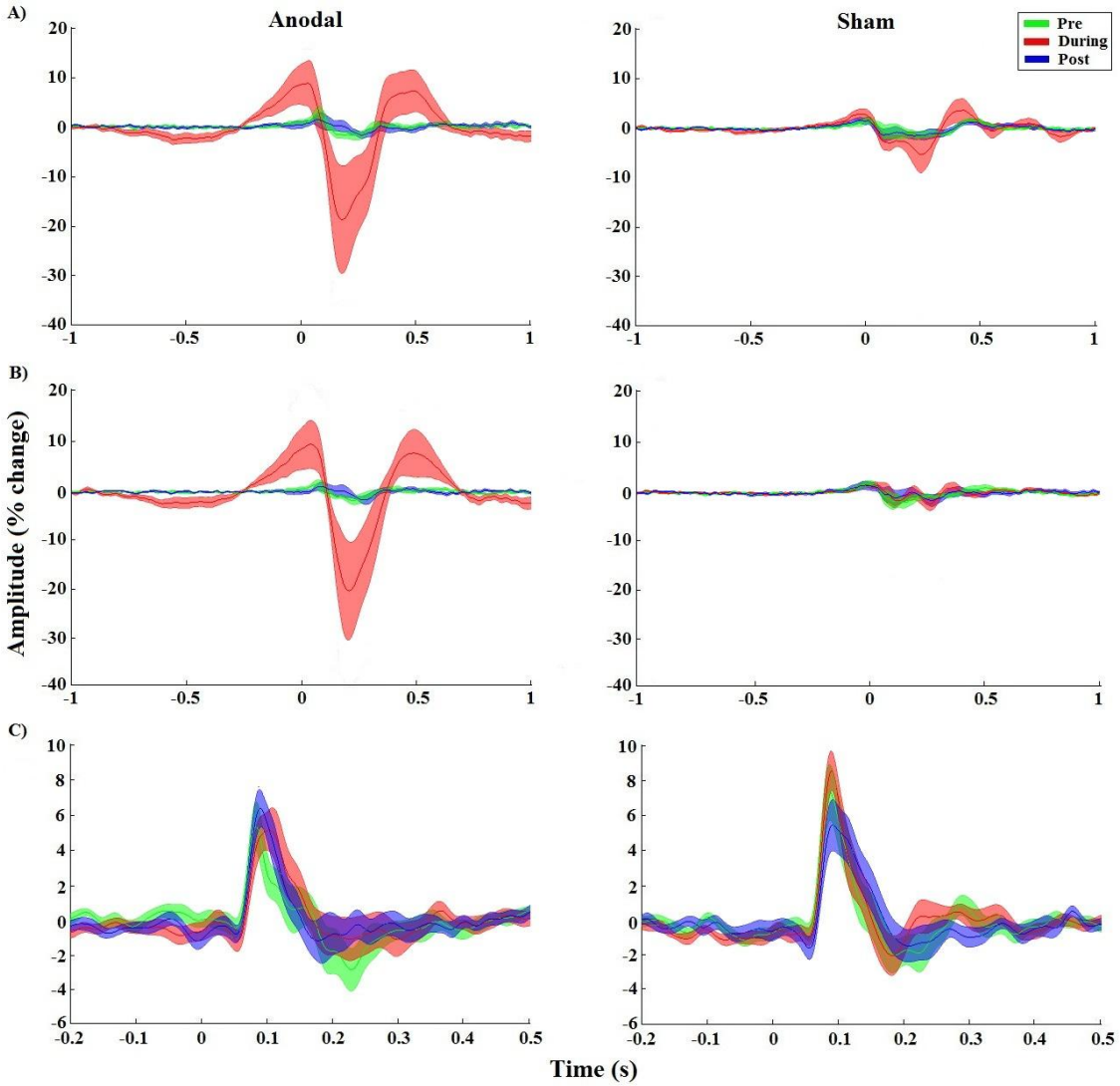

Figure 5.8. Visuomotor evoked responses. Group average evoked responses for anodal (left) and sham (right) stimulation, corresponding to changes in the source amplitude of responses derived from each subject's beta-ERD (A), PMBR (B) and visual gamma (C) virtual sensor. Amplitude change is reflected as percentage change from baseline values. Line colour denotes the factor of Time and line thickness corresponds to ± 1 standard error (S.E.M).

For the MEF1 resulting from the ERD data, the main effect of Time (F(1.014,14.192)=13.280, p=.003), tDCS (F(1,14)=5.439, p=.035) and the associated interaction (Time*tDCS: F(1.010,14.145)=5.380, p=.036) all reached significance. This was due to greater deflections taking place during anodal compared to sham tDCS (t(14)=-2.344, p=.034) and during tDCS as opposed to pre- (t(14)=3.188, p=.007) or post-stimulation (t(14)=-2.999, p=.010). For the MEF1 PMBR data, the main effect of Time (F(1.025,14.346)=4.479, p=.052), tDCS (F(1,14)=2.528, p=.134) and the associated interaction (Time*tDCS: F(1.039,14.543)=3.105, p=.098) did not meet the criteria for significance.

With regard to the latency of evoked responses, analysis of the MF resulting from the ERD virtual sensor did not produce significance for either main effect or the interaction (Time: F(2,28)=2.064, p=.146; tDCS: F(1,14)=.006, p=.939; Time*tDCS: F(2,28)=.641, p=.534). The data relating to the PMBR also failed to reveal a significant main effect of Time (F(1.489,20.845)=2.085, p=.158), tDCS (F(1,14)=.265, p=.615) or the accompanying interaction (Time*tDCS: F(2,28)=.546, p=.585). For the MEF1 resulting from the ERD, the main effect of Time (F(2,28)=2.943, p=.069), tDCS (F(1,14)=.530, p=.478) and the associated interaction (Time*tDCS: F(2,28)=.382, p=.686)) failed to reach significance. For the PMBR data, both main effects and the interaction also failed to meet the criteria for significance (Time: F(2,28)=1.060, p=.360; tDCS: F(1,14)=.025, p=.875; Time*tDCS: F(2,28)=1.228, p=.308).

5.4.2.6.2. Visual evoked response

The M100 evoked response is illustrated in Figure 5.8c, which demonstrates the mean evoked virtual sensor response at the source location, in visual cortex, identified as having the greatest change in gamma synchronisation).

No within-subject main effects or the associated interaction were found to be significant for the M100 visual evoked response, with regard to magnitude (Time: F(2,22)=1.132, p=.341; tDCS: F(1,11)=.990, p=.341; Time*tDCS: F(2,22)=1.304, p=.292). However, the Time*tDCS order interaction was found to be significant (F(6,22)=2.973, p=.028), whereby the significant main effect of Time (F(1.067,3.202)=12.801, p=.033) was established for the stimulation order ASAS. Here, the magnitude of the M100 response was greater during stimulation as opposed to pre- (t(3)=-4.739, p=.018) or post-stimulation (t(3)=4.772, p=.017) time points.

For the analysis of latency changes, the M100 response failed to produce significance

for the main effects of Time ($F(2,28)=.964$, $p=.394$) and tDCS ($F(1,14)=1.064$, $p=.320$) as well as for the associated interaction (Time*tDCS: $F(2,28)=.324$, $p=.726$).

In summary, tDCS was shown to modulate specific evoked and induced oscillatory metrics of visuomotor activity. In relation to the induced responses, average power in the visual gamma band was reduced for the anodal condition. The main effect of Montage was found to be significant during several analyses (both visual and motor), indicating a tendency for enhanced response magnitudes when utilising the motor as opposed to visual montage. Despite the implementation of counterbalanced sessions, Montage order and tDCS order were also shown to affect electrophysiological responses; particularly during the separate analysis of transient and sustained visual gamma. With regard to the evoked responses, the latency of the observed peaks was not significantly affected by tDCS. However, the magnitude of the MF and MEF1 waves was shown to increase during anodal stimulation (predominantly for the ERD virtual sensor location). The M100 visual response was also found to increase in magnitude during the stimulation time point, albeit in conjunction with the order in which the tDCS was presented as opposed to the stimulation itself.

5.5. Discussion

The study aimed to determine whether anodal stimulation could modulate well-characterised markers of brain activity in MEG, in order to address the physiological mechanisms underpinning the neuromodulation technique. Potential modulations of both time-locked and induced responses were assessed before, during and after stimulation. Several aspects of cortical activity were affected by the intervention. Most notably, anodal stimulation produced a reduction of average power in the visual gamma band and an increase in magnitude for the MF and MEF1 responses.

5.5.1. Task-induced responses

While tDCS-specific modulations were not evident for the motor responses, a significant reduction of average power in the visual gamma band was observed for the anodal condition. In accordance with the well-established physiological account of such oscillatory activity, the gamma rhythm is said to allow for insight into the status of the excitation/inhibition balance due to the underlying interplay of GABAergic interneurons and glutamatergic pyramidal cells (Bartos et al., 2007; Gonzalez-Burgos & Lewis, 2008; Buzsáki & Wang, 2012). As previously outlined, anodal tDCS is thought to

perturb the balance of excitation and inhibition by reducing GABAergic neurotransmission and suppressing $GABA_A$ receptor response, while increasing the efficiency of NMDA receptors (Creutzfeldt et al., 1962; Bindman et al., 1964; Liebetanz et al., 2002; Nitsche et al., 2003b; Stagg et al., 2009; Clark et al., 2011). This physiological state is the opposite of that induced by alcohol intake, which has been shown to increase visual gamma amplitude (Campbell et al., 2014). Speculatively, by reducing the influence of GABAergic mechanisms and decreasing inhibitory tone, the release from inhibition that synchronises pyramidal cell response may be relatively absent in the presence of anodal stimulation. This may have led to a suppression of firing and thus a decrease in observed oscillatory power. Such an account explicitly supports the role of GABAergic mechanisms in the generation tDCS effects (Stagg & Nitsche, 2011). However, the reduction in average power was found in the absence of a Time*tDCS interaction, signifying a general outcome as opposed to a specific, temporal expression of the stimulation. In a recent addition to the combined tDCS-MEG literature, Marshall, Esterer, Herring, Bergmann and Jensen (2015) also established a stimulation-based main effect but failed to produce the associated interaction, having used a similar beamformer approach to quantify tDCS-induced changes in visual gamma band activity. Therefore, although the current simultaneous tDCS-MEG literature offers a perspective on the feasibility of recording visual gamma oscillations during tDCS, it has so far been unsuccessful in demonstrating compelling modulations.

Additionally, it should be noted that the reduction in average power does not appear to have been specifically associated with the visual montage (as indicated by the absence of a specific Montage*tDCS interaction), which suggests that stimulation in general, including that of motor cortex, was able to influence visual processing. The position of the cathodal electrode over Cz, close to the motor region, may have been partially responsible for this finding if visuomotor interactions were affected by a hyperpolarisation of neurons in motor cortex. The feasibility of whole-head source reconstruction for tDCS-MEG data has recently been confirmed, which could represent an exciting prospect with regard to examining such modulations that occur in remote regions (Garcia-Cossio, Witkowski, Robinson, Cohen, Birbaumer & Soekadar, 2015).

5.5.2. Task-evoked responses

In contrast to the induced data, only the motor evoked responses were significantly modulated by tDCS. More specifically, the magnitude of the MF and MEF1 responses was shown to be enhanced during anodal stimulation (predominantly at the site of the

peak beamformer voxel from the corresponding beta-ERD analysis). Not surprisingly, the strength of the responses in question was evident in the time-frequency response, represented as a burst of 5-12 Hz activity accompanying the ERD. The functional relevance of the responses affected by the stimulation has previously been demonstrated to correspond to the preparation and subsequent execution of movement (Deecke et al., 1982; Cheyne & Weinberg, 1989; Kristeva et al., 1991; Chen et al., 1998; Chen & Hallett, 1999). Therefore, the presence of DC stimulation appears to have facilitated an increased readiness to respond and engage in task-related movement. Recently, Pellicciari, Brignani and Miniussi (2013) assessed motor cortical reactivity using simultaneous EEG recordings. Similar to the current study, the authors demonstrated a modulation of cortical activity with regard to anodal tDCS. Furthermore, cortical activity was closely associated with changes in corticospinal excitability. These results suggest it is likely that the observed changes in motor evoked responses were linked to alterations in corticospinal activity, which took place while the stimulation was being delivered. This places the results of the current study in accordance with the invasive neurophysiological findings that first determined the neuronal depolarisation and elevation in spontaneous firing associated with anodal tDCS (Creutzfeldt et al., 1962; Bindman et al., 1964; Purpura & McMurtry, 1965) as well as the pioneering human studies that demonstrated the ability of anodal stimulation to increase corticospinal excitability (Nitsche & Paulus, 2000/2001). Taken together, these results further strengthen the available evidence for the influence of anodal polarisation on motor cortex responsivity.

5.5.3. Comparison of modulations in induced and evoked responses

Comparing the response modulations obtained as part of the current study, the most statistically compelling effects of anodal polarisation were those related to the phase-locked, motor evoked components (indicative of basic, low-level processing of perceptual cues and subsequent movement responses; Kristeva et al., 1991). Given that tDCS modulations tend to be more pronounced in motor cortex than posterior regions (Antal et al., 2004a; Lang, Siebner, Chadaide, Boros, Nitsche, Rothwell... & Antal, 2007; Chaieb, Antal & Paulus, 2008; Antal et al., 2010a), the occurrence of alterations in motor responses is not surprising. The prominence of tDCS modulations during the analysis of evoked responses, as opposed to induced rhythms, can be elaborated upon in relation to the distinction between their neurobiological origins (Muthukumaraswamy et al., 2010; Cheyne, 2013). While sustained induced responses are thought to rely upon

complex patterns of global and local connectivity across multiple spatial scales (related to factors that influence synchrony, such as receptor efficiency and neurotransmission), task-evoked responses are thought to arise from transient, spatially-specific changes in cortical excitability (related to the properties of a stimulus innervating a particular sensory system) (Pfurtscheller & Lopes da Silva, 1999). In this instance, it appears that tDCS did not sufficiently modulate the synaptic processes required to alter sustained oscillatory responses but did adjust local, short-lasting cortical reactivity. Accordingly, brief alterations in membrane potential have been observed during anodal polarisation of the cortex, which increase cortical excitability and spontaneous firing rate but do not induce lasting change as evidenced by the lack of after-effects (Purpura & McMurtry, 1965; Nitsche et al., 2003b).

The presence of modulations only during direct current stimulation indicates that this is likely to have been the case for the current study. In the absence of sustained depolarisation and the resulting rise in intracellular sodium and calcium concentration, tDCS would fail to trigger a change in synaptic strength (Liebetanz et al., 2002; Nitsche et al., 2003b; Nitsche et al., 2004b; Fresnoza et al., 2014b). In turn, GABAergic and NMDA receptor efficiency would not be modulated and the balance of excitatory and inhibitory drive thought to underlie gamma and beta oscillatory activity would remain unchanged (Bartos et al., 2007; Yamawaki et al., 2008). An absence of sufficiently consistent modulations to allow changes in synaptic plasticity to emerge may, therefore, explain the relative absence of alterations in task-induced oscillatory activity.

5.5.4. Methodological considerations

Transient changes in cortical excitability are often reported following short durations of DC stimulation (Purpura & McMurtry, 1965; Nitsche et al., 2003b). However, while the duration featured in the current study was comparatively extended, the length of stimulation used may have contributed to the absence of some expected findings. Certain complex cortical responses, such as those requiring neuronal synchronisation, may require extensive (longer than usual) durations of stimulation before modulations can be observed. For example, an increase in fronto-central ERD in the beta band, linked to a finger tapping task, was demonstrated after anodal stimulation of M1 but at twice the duration of the current study (Notturno, Marzetti, Pizzella, Uncini & Zappasodi, 2014). While it should be noted that local and global broadband changes in cortical synchronisation have been found following 10 minutes of sensorimotor

stimulation, this could be attributed to the increased focality of the high-definition tDCS procedure used in the study (Roy, Baxter & He, 2014).

The use of a maximum contrast stimulus may have also contributed to the findings by introducing a 'ceiling effect' (as previously determined by Antal et al., 2004a). To further modulate responses within a system that is already being pushed to the limit of excitation has been shown to be extremely difficult (Froc et al., 2000). Therefore, where neuronal output was likely to have been saturated by the stimulus, this may have restricted the dynamic range of any potential modulations. This would mean that the system would be unable to develop and maintain a consistently altered baseline excitation level. Stimulation would also consequently fail to modify factors, such as the rate of IPSCs on GABAergic interneurons with connections to pyramidal cells, required to alter the synchrony of oscillations (Jensen et al., 2005; Atallah & Scanziani, 2009). Consequently, change in oscillatory activity resulting from tDCS may be more readily observed with lower contrast stimuli, and at longer stimulation durations, to give the modulation of cortical activity additional scope and time to develop.

The position of the electrodes in this investigation changed from that of the initial evaluation of tDCS-induced noise (chapter 4). Should the ability to minimise noise levels be anatomically constrained on the basis of the implemented electrode configuration, this may have had implications for the results of the current study. However, on the basis of source reconstruction of responses in both motor and visual cortex, this does not appear to have been the case. While it is anticipated that the specific pattern of noise will vary with the use of different electrode montages (in line with what is known of changes in the current pathway; Opitz et al., 2015) the noise generated by the configurations used in the present study appears to have been sufficiently minimised to allow consistent source reconstruction estimates to be derived from the data. This would have been problematic where channel disturbance was abundant, particularly during tDCS. Therefore, the presence of reliable source localisation highlights the general applicability of the approach to minimising noise adopted as part of the pilot study, which seems to be independent of the effects of electrode montage – at least where a beamformer technique, such as SAM, is adopted to suppress residual noise.

The current study did not record resting state MEG data, unlike a recent study that found significant modulations of oscillatory activity (Venkatakrishnan et al., 2011). The emergence of resting state effects may be indicative of the state-dependent nature of

tDCS modulations (Benwell, Learmonth, Miniussi, Harvey & Thut, 2015). Behavioural studies have highlighted the reversal or abolishment of typical tDCS effects if stimulation is delivered during task performance, particularly for tasks involving motor actions (Antal, Terney, Poreisz & Paulus, 2007; Horvath, Carter & Forte, 2014). This highlights the fragility of tDCS after-effects and suggests that their emergence may depend on the activity taking place during the stimulation period (Bortoletto, Pellicciari, Rodella & Miniussi, 2015), which may largely underlie the recent finding of inconsistent neurophysiological modulations by tDCS (Horvath, Forte & Carter, 2015b).

Abnormal effects of tDCS have also been demonstrated in relation to the timing of repeated stimulation. Monte-Silva et al. (2013) established that administering subsequent doses of anodal stimulation, with an inter-stimulation interval of 24 hours, produced an abolishment of the expected post-stimulation elevation in motor cortex excitability. As the minimum period between sessions was 24 hours in the current study, such detrimental cumulative effects may have occurred due to subsequent exposure. Furthermore, the effects of stimulation may not emerge immediately. Bindman et al. (1964) demonstrated peak change in firing rate as being approximately 15 minutes after stimulation had ceased. More recently, Pellicciari et al. (2013) observed an increase in alpha power only after 30 minutes had elapsed since the administration of anodal stimulation (although in the absence of an appropriate sham-control condition it is difficult to determine if this was a genuine stimulation effect). Incorporating multiple post-stimulation recordings into future study designs would help to reveal such findings, where present.

Finally, as a potential alternative to the static polarisation delivered via tDCS, tACS could be used to set baseline excitability to synchronise with the dynamics of a desired frequency band. Zaehle, Rach and Herrmann (2010) first demonstrated the influence of tACS on endogenous rhythms, showing entrainment of alpha oscillations in visual cortex. A subsequent study found that tACS at 20 Hz was able to modulate cortical responsivity in M1 and this excitability change was shown to be predicted by related changes in the beta band response (Schutter & Hortensius, 2011). A recent study has also highlighted the feasibility of concurrent tACS-EEG applications and has shown the emergence of synchronisation of alpha oscillations during 10 Hz stimulation (Helfrich et al., 2014). Simultaneous tACS-MEG also appears to be possible (as suggested by Soekadar et al., 2013 and recently implemented by Neuling et al., 2015).

5.5.5. Effects of electrode montage & stimulation order

Aside from the influence of tDCS, the electrode montage used during a given session was demonstrated to determine the nature of average power responses. This occurred in the beta and gamma bands, where the motor montage was associated with enhanced responses compared to the visual montage. This is unlikely to be due to any specific aspect of the stimulation because the montages used were independent of the time points at which average power was assessed and encompassed both active and sham modalities. The greater influence of the motor montage may have been due to lower impedance values resulting from the motor montage, indicating less shunting of the current and more targeted administration to the brain.

Additionally, the reduction of average power in the visual gamma band corresponded to the order in which the tDCS was administered. Specific transient and sustained metrics of visual gamma activity also corresponded to the order in which tDCS was administered, as did the timing of the magnitude change in the visual M100 response. This was surprising as the after-effects of tDCS, following ~10 minutes of stimulation, have been established to return to baseline levels within 90 minutes of the stimulation being terminated (Nitsche & Paulus, 2001). The wash-out interval incorporated between sessions should have also ensured that carry-over effects were unlikely to arise. These order effects were particularly unexpected in the context of the implemented counterbalancing, which should have minimised the confounding influence of stimulation order (providing that any order effects were anticipated to be linear). While persistent effects may occur following several sessions of anodal stimulation and are desirable in a clinical setting (Baker, Rorden & Fridriksson, 2010), specific order effects have not previously been reported where explicitly assessed (Fregni, Boggio, Santos, Lima, Vieira, Rigonatti... & Pascual-Leone, 2006; Boggio, Zaghi, Lopes & Fregni, 2008; Mahmoudi, Haghighi, Petramfar, Jahanshahi, Salehi & Fregni, 2011). However, should these effects be genuine, it raises substantial issues concerning appropriate study design and the transience of stimulation effects.

5.6. Conclusions

Anodal tDCS was shown to modulate electrophysiological activity, primarily evoked responses. As the timing-specific modulation effects were only observed during stimulation, the results are consistent with the influence of tDCS on cortical responsivity via transient as opposed to sustained alterations in membrane potential.

Accordingly, the absence of consistent changes in excitability can account for the lack of prolonged, post-stimulation changes as well as the comparative absence of change with regard to induced responses. Several factors such as stimulus contrast and the execution of motor responses during stimulation may have attenuated the typical tDCS effect. Nonetheless, the study indicates that electrophysiological metrics are likely implicated in the generation of tDCS effects. Future research in this field should focus on establishing optimised stimulation conditions to attempt to address these issues and further investigate the underlying neurobiological mechanisms of DC stimulation.

6. Experimental Chapter 4

Stimulating Somatosensory Psychophysics - A Double-Blind, Sham-Controlled Study of the Neurobiological Mechanisms of Transcranial Direct Current Stimulation

6.1. Abstract

As a neuromodulation technique, tDCS is thought to produce its effects on behaviour by altering cortical excitability. Although the mechanisms underlying the observed effects are thought to rely on the balance of excitatory and inhibitory neurotransmission, the physiological principles of the technique are not completely understood. In this study, the influence of tDCS on vibrotactile adaptation was examined using a simple amplitude discrimination paradigm, which has been shown to exhibit modifications in performance due to changes in inhibitory neurotransmission. The presence of a single-site adaptation (SSA) effect was sought during two pilot studies, in which baseline and adaptation trials (featuring simultaneous, dual-site test stimuli) were presented to subjects as part of a 2AFC task. An identical paradigm was implemented during the main vibrotactile-tDCS study, which also featured a 2IFC sequential version of the baseline task. Double-blind tDCS (Anodal, Sham) of 1 mA was delivered for 600 s to electrodes positioned in a somatosensory/contralateral orbit montage. Stimulation was applied as part of a pre/post design, between blocks of the behavioural tasks. In accordance with previous work, results obtained before the application of tDCS indicated that amplitude discrimination thresholds were significantly worsened during adaptation trials, compared to those achieved at baseline. This was the case even for multiple runs, highlighting the stability of the single-site adaptation effect. Identical findings were present for the pre-tDCS data of the main study. The single-site adaptation task also resulted in higher thresholds than the sequential baseline version. However, tDCS failed to modify amplitude discrimination performance. This non-significant finding was subsequently revealed to constitute substantial evidence for the null hypothesis, using a Bayesian approach. The failure of DC stimulation to alter vibrotactile adaptation thresholds is discussed in the context of several factors that may have confounded the induction of changes in cortical plasticity.

6.2. Introduction

Transcranial direct current stimulation is a neuromodulation technique capable of producing alterations in human behavioural performance, which are thought to rely on region-specific, polarity based changes in cortical excitability (Wassermann & Grafman, 2005; Utz et al., 2010; Paulus, 2011; Krause et al., 2013). Since the advent of the method, a number of studies have attempted to further elucidate the proposed mechanisms by which these changes in behaviour occur. For example, the application of tDCS has been shown to alter the usual response of voltage-gated ion channels responsible for maintaining resting membrane potential (as documented in a recent review; Funke, 2013). When a positive (anodal) current is delivered to the cortex it has been proposed to lead to a depolarisation of underlying neurons and following administration of a negative (cathodal) current, a state of hyperpolarisation is said to be induced. Although this explanation may be greatly over-simplified (de Berker et al., 2013; Radman et al., 2013; Rahman et al., 2013), the induction of spatially-specific depolarisation and hyperpolarisation have been supported by both animal (Creutzfeldt et al., 1962; Bindman et al., 1964; Purpura & McMurty, 1965) and human studies (Nitsche, Schauenburg, Lang, Liebetanz, Exner, Paulus & Tergau, 2003c).

As well as demonstrating polarity specific effects, the influence of tDCS has been shown to vary as a function of the duration of stimulation. Transient changes in membrane excitability have been observed during stimulation, where a DC current is administered for short durations in the range of seconds, whereas persistent alterations beyond cessation appear to occur following several minutes of exposure (Stagg & Nitsche, 2011). Neuroimaging and pharmacological interventions have demonstrated that modulations observed at short durations appear to be dependent on changes in the action of sodium and calcium channels (Nitsche et al., 2003b), whereas more persistent adjustments in excitability involve the action of N-methyl-D-aspartate (NMDA) and γ-aminobutyric acid (GABA) receptors (Liebetanz et al., 2002; Nitsche et al., 2004a; Nitsche et al., 2004b; Nitsche et al., 2005; Tremblay et al., 2013) as well as related changes in the concentration of excitatory and inhibitory neurotransmitters (Stagg et al., 2009; Clark et al., 2011; Stagg et al., 2011b; Bachtiar et al., 2015). As such, the polarity specific effects of tDCS have been compared to LTP/LTD (Ridding & Ziemann, 2010; Brunoni, Fregni & Pagano, 2011b; Monte-Silva et al., 2013).

Although the existing literature has provided compelling findings, continued research is needed to advance our understanding of the underpinnings of tDCS. To further address the possible mechanisms underlying the stimulation effects, a non-invasive behavioural approach could be utilised. This would be particularly beneficial should the chosen paradigm be established to have similar underlying physiology to tDCS. However, the majority of studies investigating the neurobiological mechanisms underlying tDCS have either not used an explicit behavioural task (instead using MEPs to investigate tDCS effects) or have been measured 'at rest' (e.g. studies incorporating neuroimaging methods). Those that have used a behavioural task have employed higher-level cognitive paradigms where it is often difficult to conceptualise behavioural change in terms of alterations in membrane potentials.

Of the few studies concerning the effects of tDCS on somatosensory processing, behavioural tactile perception studies have largely focused on Quantitative Sensory Testing (QST; Bachmann et al., 2010; Grundmann et al., 2011; Jürgens et al., 2012) and aspects of spatial discrimination (Ragert et al., 2008; Fujimoto et al., 2014; Yau et al., 2014). tDCS has also been found to modulate vibrotactile frequency discrimination ability, both during and after stimulation (Rogalewski et al., 2004). These studies highlight the links between direct current stimulation and task performance. They do not in general, however, provide a detailed model of the underlying neurobiology supporting the tactile behaviour itself. One approach to resolve this problem is to use a behavioural paradigm that is understood more completely at the neurophysiological level and, furthermore, thought to rely upon similar physiological mechanisms to the stimulation method. It would thus be anticipated that integrating tDCS into such an intervention would modify behavioural performance in a predictable manner. By focusing on simpler paradigms, a more comprehensive understanding of the mechanisms underlying tDCS should result, which should lead to the use of the method in a more optimised way as a potential treatment for neurological and psychiatric disorders (for a review of the clinical applications of tDCS, see Brunoni et al., 2012).

Sensory psychophysics has been used extensively to benchmark links between neurostimulation methods and behaviour (Ruff, Blankenburg, Bjoertomt, Bestmann, Freeman, Haynes... & Driver, 2006; Lee, Jacobs, Asmussen, Zapallow, Tommerdahl & Nelson, 2013). To further investigate the neurobiology of tDCS in a similar fashion, a vibrotactile adaptation paradigm was selected; where prolonged stimulus exposure has been demonstrated to induce short-term changes in perceptual processing (for an

extensive review of vibrotactile adaptation; see Kohn & Whitsel, 2002). The paradigm, known as single-site adaptation (SSA), involves the administration of an adapting stimulus to a single digit (prior to a dual-site amplitude discrimination task) and has been shown to dramatically increase (i.e. worsen) discrimination thresholds (difference limen; DL) compared to those achieved at baseline (Tannan, Simons, Dennis & Tommerdahl, 2007; Zhang, Francisco, Holden, Dennis & Tommerdahl, 2009). Tannan et al. (2007) gathered data from multiple runs of a single-site adaptation protocol, which varied in adaptor duration (0.2-2 s). As the duration of the adaptor increased, there was a systematic decrease in performance capability evident from an increase in DL values (23 μm at baseline, compared to 37 μm and 104 μm at 0.2 s and 2 s, respectively). Puts, Edden, Wodka, Mostofsky and Tommerdahl (2013) recently replicated the expected effect of single-site adaptation, demonstrating an average performance decrement of 36% following a 1s adaptor stimulus.

The mechanisms underlying the response to vibrotactile adaptation have been studied extensively in cats and non-human primates (O'Mara et al., 1988; Whitsel et al., 2000; Chen et al., 2003; Whitsel et al., 2003) and also via electroencephalography in humans (Kelly & Folger, 1999). From this research, it is thought that only the primary somatosensory neurons at the test site are permitted to habituate to the initial adaptor stimulus, which causes a perceptual imbalance in the context of which the two subsequent test stimuli are compared. Due to the reduction in the perceived intensity at the site of the test stimulus, it becomes difficult to distinguish the test from the standard stimulus, which leads to degraded performance compared to baseline. These results are in accordance with predictions made by Gescheider, Santoro, Makous and Bolanowski (1995), which state that detection thresholds increase with stimulus duration and such threshold increases are likely to be evident in the presence of adapting stimuli.

To further illustrate this concept, Folger et al. (2008) demonstrated that test stimuli of at least 170 μm would need to be presented to subjects in order to be perceived as different from a standard stimulus of 100 μm, under adaptation conditions. This is in comparison to the baseline condition where, without the influence of adaptation, subjects were capable of discriminating between the 100 μm standard and test stimuli of just 120 μm. Exposure to adaptation stimuli appears to lead to a mismatch between the actual intensity of the stimulus delivered and the subject's perceptual experience of it, thus preventing finer discriminations due to the mechanisms underlying the reduction in perceived intensity at the test site.

Changes in the concentration of the major inhibitory and excitatory central nervous system (CNS) neurotransmitters, GABA and glutamate, as well as the action of related post-synaptic receptors ($GABA_A$, NMDA) have been suggested to underlie vibrotactile adaptation (Lee et al., 1992; Lee & Whitsel, 1992). The role of the excitation/inhibition balance has also been emphasised during subsequent animal-based, optical intrinsic signal imaging (OIS) investigations, in which local competitive interactions between minicolumns appear to be essential in moulding the response to repetitive stimuli (Tommerdahl et al., 2002; Chiu et al., 2005; Simons et al., 2005; Simons et al., 2007). Accordingly, increased absorbance (a marker of neuronal activity) at the site of the stimulus has been observed alongside inhibition of the surrounding region, supporting the role of GABAergic, lateral inhibition in vibrotactile adaptation.

The proposed role of GABAergic inhibition has also been determined via the assessment of performance in a range of human subject populations, including those with Autism Spectrum Disorder (ASD), concussion, migraines and alcohol dependence (Tannan et al., 2008; Zhang, Francisco, Holden, Dennis & Tommerdahl, 2011a; Nguyen, Ford, Calhoun, Holden, Gracely & Tommerdahl, 2013a; Nguyen, Gillen, Garbutt, Kampov-Polevoi, Holden, Francisco & Tommerdahl, 2013b). The expected single-site adaptation effect demonstrated by healthy controls is notably absent in these samples, despite achieving largely similar baseline scores. This discrepancy in performance is thought to emerge from the presence of altered CNS sensitivity in the respective samples. For example, evidence suggests that individuals with ASD are likely to exhibit abnormal cortical excitability levels due to a reduction in inhibitory neurotransmission (Casanova et al., 2002; Casanova et al., 2003; Uhlhaas & Singer, 2006; Uhlhaas & Singer, 2012). This suggests that a loss of normal inhibitory function – possibly mediated by GABAergic mechanisms - is likely to produce an atypical response to adaptation.

The work of Folger et al. (2008) extends support for the interpretation of the clinical population studies. Healthy control subjects given Dextromethorphan (DXM), an NMDAR antagonist, were found to achieve similar baseline performance to those given a placebo but failed to demonstrate the usual decline in single-site adaptation performance. Here, the suppression of glutamatergic mechanisms via administration of DXM meant that subjects were unaffected by the adaptor. In the absence of normal excitatory activity, the magnitude of the initial response to the adaptor was likely reduced as was the inhibition needed to tune responses to repetitive stimuli, meaning the

action of GABAergic processes, such as lateral inhibition, also decreased. Therefore, DXM was proposed to facilitate a release from inhibition. Accordingly, NMDAR activation has been shown to provide a significant drive in facilitating GABAergic transmission in interneurons (Xue, Masuoka, Gong, Chen, Yanagawa, Law & Konishi, 2011), meaning its blockade should greatly reduce inhibitory transmission. Studies such as this indicate that the decrease in performance following the single-site adaptor cannot be attributed to a simple addition of noise or the presence of a distraction and that the engagement of CNS processes is integral to the adaptation effect (Kohn & Whitsel, 2002). Furthermore, such a reduction in GABAergic 'tone' has been proposed to underlie the effects of anodal tDCS (Stagg et al., 2009; Bachtiar et al., 2015) (in addition to the established role of glutamatergic, NMDA receptors; Nitsche et al., 2003b). On the basis of the outlined GABA modulation, comparable results to the DXM study may be obtained post-stimulation. Therefore, the neurobiological similarity between vibrotactile adaptation and tDCS meant that the paradigm represented an ideal starting point from which to examine the proposed GABAergic contribution to the effects of tDCS.

This chapter documents the progress made in assessing the neurobiological basis of tDCS via the SSA paradigm: from pilot studies designed to clarify the reliability of the metric to its incorporation with the neuromodulation technique. Initial predictions were that vibrotactile thresholds would be higher following SSA than baseline trials, as found in the literature. Integrating anodal and sham tDCS into the vibrotactile paradigm, initial predictions were that active tDCS would not produce changes in discrimination thresholds for the baseline task whereas a decrease in threshold values (i.e. an improvement) would be observed for the SSA condition. In the presence of anodal stimulation, it was proposed that resting membrane potential would be elevated (via a release from inhibition, i.e. increased NMDA efficiency and decreased GABAergic neurotransmission) such that the cortical excitability profile of subjects should mimic that proposed for individuals with altered CNS sensitivity. While baseline thresholds in such populations have been established as similar to those of healthy controls, such individuals do not appear to be susceptible to the influence of adapting stimuli. Therefore, during the adaptation version of the task, subjects were predicted to obtain better performance measures (lower discrimination thresholds) following anodal compared to sham tDCS.

6.3. Methodology & Results

6.3.1. Experiment 1: Single-Site Adaptation & Amplitude Discrimination

Before adopting the task for use alongside tDCS, a pilot study was conducted to determine the ability of the protocol to produce the expected results. The parameters chosen to test the single-site protocol were largely similar to those that feature in the published literature (Tannan et al., 2007; Zhang et al., 2009; Puts et al., 2013). However, the adaptor amplitude was matched to that of the standard stimulus as opposed to the initial test amplitude. The vibrotactile adaptation literature states that the evoked adaptation response is most prominent when the adaptor amplitude is matched to that of the subsequent standard (Goble & Hollins, 1993). This offers the maximum potential for the test stimulus to be perceived as novel because the response of the neurons to the standard will be reduced following an identical adaptor stimulus. In the case where the adaptor amplitude is matched to that of the initial test stimulus, the adaptor would not consistently correspond to any of the following stimuli because the nature of the test stimulus means it is constantly changing as it tracks performance levels. The rationale behind matching the adaptor and test amplitude is to evoke the maximum reduction in gain (perceived intensity) at the test site, such that the test phase stimuli cannot be easily discriminated and a more pronounced adaptation effect is likely to arise. However, this approach has implications for the term "adaptation", which may be misleading in contexts where the adaptor and subsequent stimuli are not identical. Nevertheless, it should be reiterated that during SSA the digit that receives the adapting stimulus will always receive the test stimulus and will never be exposed to the standard, which may mean that the matching of amplitudes is not particularly crucial for SSA.

The use of an adaptor of the lowest amplitude possible, while still eliciting the expected behavioural response, is likely to be favourable because it ensures that the following stimuli are not overshadowed by the strength of the adaptor. For example, Goble and Hollins (1993) also indicated that the selection of an adapting stimulus of higher amplitude than the standard will automatically make it virtually undetectable due to a related boost in DL values (reduced detection ability). In selecting the stimulus parameters, it was the desire of the current study not to degrade performance by making it impossible to perform the task by virtue of the selected stimulus parameters but to subtly modify the stimuli enough to perturb the underlying mechanisms integral to the paradigm. Using a lower amplitude adaptor should mean that a reliable adaptation effect is elicited but also that standard and test stimuli are able to be detected and

discriminated between. For this reason and in the interest of maintaining consistency between stimuli featured in the adaptor and test phase, matching the adaptor to the standard stimulus appeared to be the most scientifically valid approach.

6.3.1.1. Subjects

To determine the ideal sample size, baseline and adaptation values from several studies were acquired from the lab of a collaborator (Prof. Mark Tommerdahl). Power calculations were performed using G*Power Version 3.1 (University of Dusseldorf, Germany; Faul et al., 2007). Sample sizes ranging from N=9 to N=23 have been quoted in the literature, however, based on the effect size of the existing data the calculations recommended a sample size of N=9 (assuming one-tailed significance, Appendix 18).

12 predominantly right-handed subjects, aged 22-28 years took part in the study (7 female; *M=24.64, SD=1.80*). All procedures were carried out with the approval of the local ethics committee.

6.3.1.2. Vibrotactile task

Subjects completed two versions of a 2AFC task, designed to test their ability to discriminate between vibrations of differing amplitudes. Stimuli were delivered to the index and middle finger (digits 2 and 3) of the left hand, using a vibrotactile stimulation device capable of delivering dual-site stimuli (CM5; Cortical Metrics, North Carolina).

Each subject completed baseline and SSA runs. During the baseline task, subjects were asked to determine which of two simultaneously delivered stimuli felt more intense. In the SSA task, subjects were instructed to ignore a single vibration before making the same intensity judgement on the subsequent pair (see Figure 6.1a for a schematic representation of each phase of the task). It is important to note that the stimulus configuration of the SSA task could potentially bias responses should subjects' recognise that the correct choice will always correspond to the initially adapted digit. However, SSA scores are typically much higher than those achieved at baseline and no uniform improvement is seen across entire subject samples.

Responses on each task were tracked using an adaptive staircase method (reviewed in Leek, 2001). The first half of trials was executed in a 1up/1down protocol. The amplitude of the test stimulus selected for the subsequent trial was adjusted in accordance with the response accuracy of the previous trial. The final half of trials was conducted using a 2up/1down protocol, in which two correct responses were required

before performance was classified to have improved and the amplitude of the test stimulus was reduced. Step size was maintained at 20 μm across all trials and experimental runs. All vibrotactile pulses were sinusoidal and were delivered at 25 Hz (defined as flutter stimulation). Adaptor amplitude was 200 μm, which was identical to that of the proceeding standard stimulus. The test stimulus varied between 205-400 μm. The duration of the adaptor was 1000 ms, with a 500 ms interval for the test phase. Standard and test pulses were delivered simultaneously and their location was randomised across trials.

Figure 6.1. Vibrotactile Trials. A) Trial stimulation: 25 Hz sinusoidal stimuli were delivered to D2 and D3 of the left hand. Adaptation trials consisted of a single pulse delivered to one digit (in this instance D3). During the test phase, stimuli were delivered simultaneously to D2 and D3. Subjects were required to determine which stimulus was of the highest amplitude. Baseline trials consisted only of the test phase. B) Trial timing: Adaptation trials began with the presentation of a single pulse to the selected digit (A; 1000 ms), followed by an interval between the adaptor and test stimuli (1000 ms) before the standard and test stimuli were simultaneously delivered (S/T; 500 ms). Subjects were given an unrestricted response interval (RI) to indicate which digit they thought had received the stimulus of highest amplitude, after which an interval signalled the onset of the next trial (5000 ms) (figure adapted from Tannan et al., 2007).

6.3.1.3. Experimental procedure

Subjects were seated in front of a computer monitor with the vibrotactile stimulation device positioned on their left-hand side. They were instructed to lightly rest their digit tips over the corresponding finger pads. Each subject completed two experimental runs of each task version (20 trials per run), which lasted approximately 15 minutes.

Adaptation trials began with a period of single-site stimulation, which was to be ignored. This was followed by an interval before the test phase, in which a period of dual-site stimulation was delivered. Baseline trials incorporated only the test phase (see Figure 6.1b for stimulus timings). Subjects had an unrestricted interval to make the required intensity discrimination and responded with their right-hand, using the left and right mouse buttons. A left click corresponded to D3 and a right click corresponded to D2. Subjects were provided with visual cues to guide their responses. These were in the form of "IGNORE!" and "TEST!" statements that appeared on screen.

6.3.1.4. Data analysis & statistics

The data were plotted using MATLAB (Version 7.4.0; MathWorks, Cambridge) to derive performance curves for each experimental run (Figure 6.2). These were visually

inspected for evidence of adequate performance capability (standard task progression and final DL values within the expected range) and threshold stabilisation. Excessive noise in the data constituted grounds for exclusion. One particular run posed cause for concern (Figure 6.3) and the dataset for this subject was removed due to a lack of threshold stability.

Statistical analyses were computed for the remaining subjects using SPSS for Windows software (Version 20; IBM, New York). Data were compared with regard to differences between baseline and adaptation trials. The DL value for each run, representing the average test stimulus value from the final five trials, was entered separately into a two-way, Repeated Measures ANOVA analysis with the following variables; Condition (Baseline, SSA) and Run (1, 2). Where appropriate, Greenhouse-Geisser correction was used to compensate for violations of sphericity. P values were considered significant if they reached the level of less than 0.05.

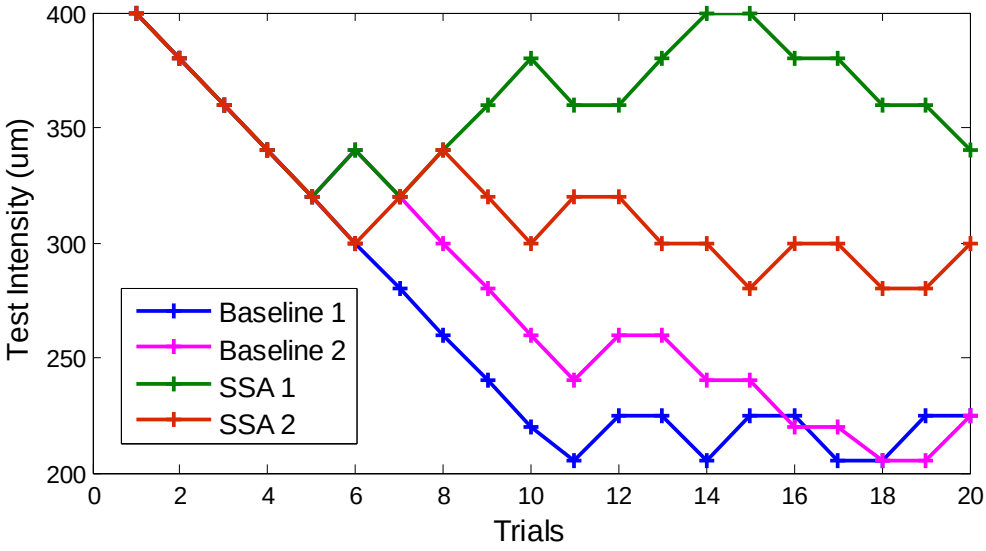

Figure 6.2. Pilot study task performance. Performance curves from a single subject. All conditions exhibit the expected response pattern (initial rapid improvement in discrimination capacity) and progression to threshold stabilisation towards the end of each run.

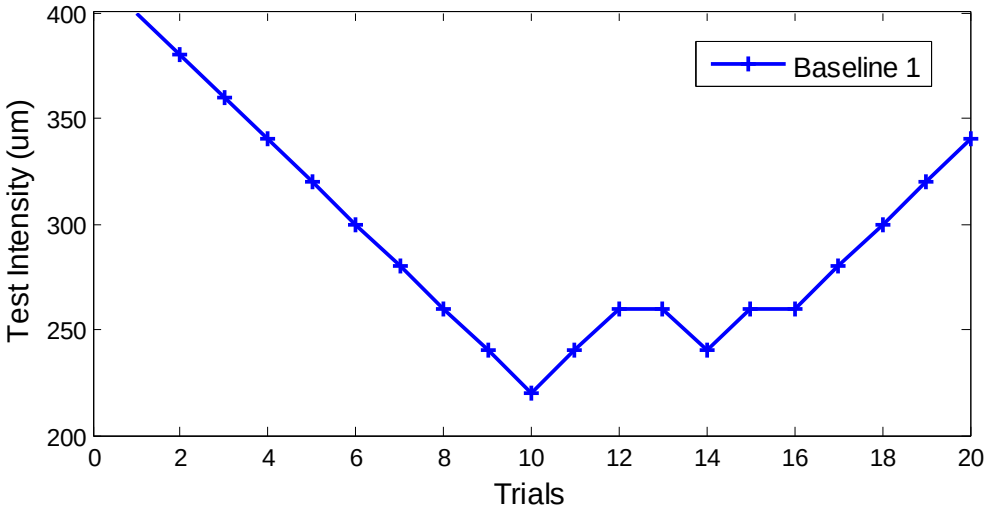

Figure 6.3. Pilot study atypical task performance. Performance curves from a single subject, obtained during Baseline run 1. The absence of standard threshold stabilisation indicated a lack of ability to consistently perform the task. The data from this subject was excluded from further analysis.

6.3.1.5. Results

Average DL values were computed across subjects for each condition and run: Baseline Run 1 (*M=56.91, SD =24.76*), Baseline Run 2 (*M=59.73, SD =30.44*), SSA Run 1 (*M=108.73, SD =46.16*), SSA Run 2 (*M=74.91, SD =35.88*). Figure 6.4 illustrates higher DL values for SSA trials than those of the baseline condition during Run 1, with a less prominent distinction emerging for Run 2.

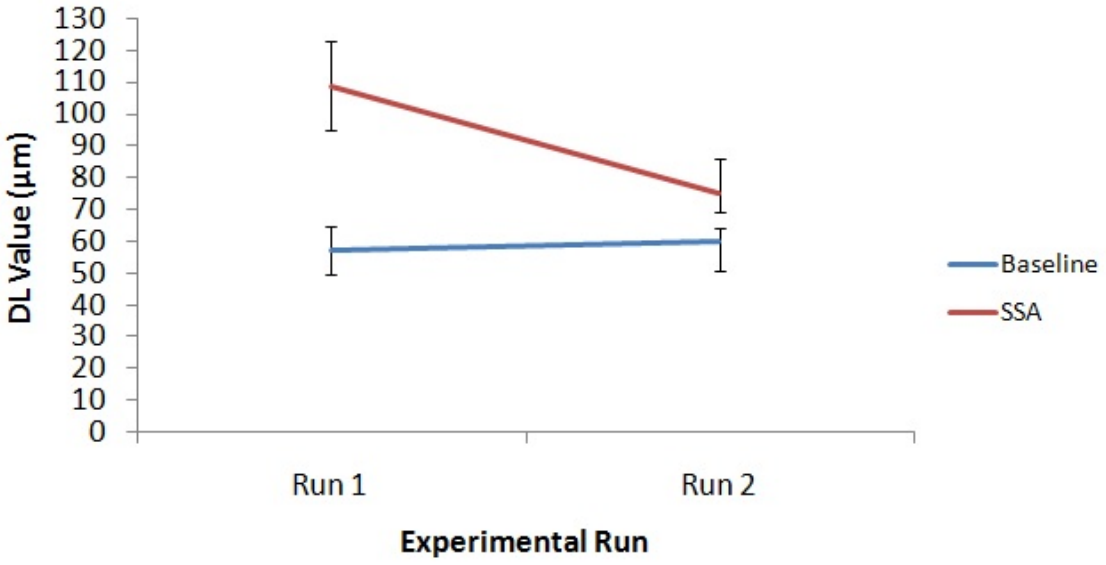

Figure 6.4. Pilot study thresholds. Average DL values obtained during baseline and SSA conditions. Error bars represent ± 1 standard error (S.E.M).

The 2x2 ANOVA produced a significant main effect for Condition ($F(1,10)=9.261$, $p=.012$). The main effect of Run was non-significant ($F(1,10)=1.636$, $p=.230$) as was the interaction between Condition and Run ($F(1,10)=2.670$, $p=.133$). As expected, the results indicate that subjects achieved higher amplitude discrimination thresholds during SSA than baseline trials. Despite the marked decrease in scores for the SSA condition in Run 2, these findings also suggest that subjects obtained similar thresholds during each experimental run.

6.3.2. Experiment 2: Repeatability of the Single-Site Adaptation Effect

While the main effect of Run was non-significant in Experiment 1, the dramatic attenuation in the magnitude of the adaptation effect during the second run warranted further investigation. This would be detrimental to any studies in which the task was implemented in conjunction with tDCS, where multiple runs would be conducted across several sessions. To determine whether responses were likely to be a product of repeated exposure to the task, a follow-up pilot study was carried out.

Eight subjects aged 24-32 (4 male; *M=26.38, SD=2.56*) were asked to complete four runs of each task. All details pertaining to the task, procedure and statistical analysis were identical to the initial study. All data obtained was suitable for analysis.

6.3.2.1. Results

Average DL values were computed across subjects for each condition and run. The overall mean was also calculated for each condition: Baseline (*M=43.06, SD =26.30*) and SSA (*M=100.19, SD =53.71*). Figure 6.5 illustrates the distinction between conditions, with SSA runs consistently producing much higher thresholds than those derived from the baseline trials. While the baseline scores appear to have been fairly uniform, there was a trend for SSA scores to systematically increase across runs.

A 2x4 ANOVA incorporating the factors Condition (Baseline, SSA) and Run (1, 2, 3, 4) established a significant main effect for Condition ($F(1,7)=16.263$, $p=.005$). The main effect of Run failed to reach significance ($F(1.847,12.932)=.661$, $p=.585$), as did the interaction between Condition and Run ($F(2.099,14.693)=.698$, $p=.520$). These results suggest the SSA condition produced significantly higher thresholds compared to baseline, which confirms the expected adaptation effect finding present in Experiment 1. Furthermore, the non-significant main effect of Run indicates that subjects' scores

did not fluctuate between runs, meaning that the scores derived provide a stable measure of performance and do not appear to be highly susceptible to the effects of repeat exposure. In summary, the pilot studies presented here provided evidence to suggest that the SSA paradigm produced consistent results and was suitable for continued use.

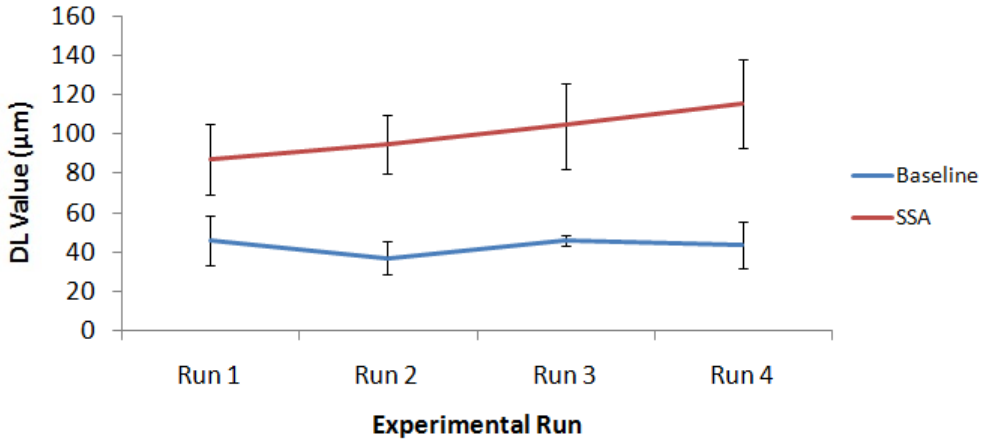

Figure 6.5. Extended pilot study thresholds. Average DL values obtained from multiple runs of the baseline and SSA tasks. Error bars represent ± 1 standard error (S.E.M).

6.3.3. Experiment 3: tDCS & Amplitude Discrimination Performance

Having established repeatable results, the SSA paradigm was combined with tDCS to further investigate the underpinnings of the neuromodulation technique.

6.3.3.1. Subjects

12 subjects took part in the study (7 female). The sample number was based upon earlier power calculations for the behavioural tasks (Appendix 18), in the absence of adequate tDCS data on which to base tDCS sample size calculations due to the novelty of the study. However, many tDCS studies use such sample sizes and achieve significant modulations of their selected paradigms (Elmer, Burkard, Renz, Meyer & Jancke, 2009; Ladeira, Fregni, Campanhã, Valasek, De Ridder, Brunoni & Boggio, 2011; Spiegel, Hansen, Byblow & Thompson, 2012; Tang & Hammond, 2013; Pavlova, Kuo, Nitsche & Borg, 2014). Subjects were aged 19-31 years (*M=24.08, SD=3.34*) and right-hand dominant, determined by the short-form Edinburgh Handedness Inventory (Oldfield, 1971; Appendix 1). Upon expressing an interest in taking part in the study, subjects were issued with a screening form to determine their eligibility (Appendix 2). Those with any of the contraindications listed were excluded from the study. All procedures were carried out with approval of the local ethics committee.

6.3.3.2. Vibrotactile task

Subjects performed identical versions of the tasks to those described above, as part of the pilot studies. A 2IFC dual-site sequential version of the simple, baseline task was also introduced for comparison against the simultaneous version (Figure 6.6). During the sequential task, subjects were required to perform the same amplitude intensity judgement as in the simultaneous version. The key difference was that instead of presenting the standard and test stimuli at the same time; each vibration was delivered during a separate interval. The presentation of trails was randomised across D2 and D3, however, every trial was performed within a single digit. This was to ensure there were no differences with regard to the peripheral receptors and neuronal populations engaged by either baseline task. The 2IFC task was incorporated in order to facilitate the exploration of the inhibitory underpinnings of tDCS because the simultaneous and sequential tasks are thought to differ in terms of their inhibitory processing demands. Accordingly, performance of the sequential task relies upon lateral inhibitory processes only operating at a single site as opposed to between digits. Meanwhile, sensory information corresponding to the digit receiving the weaker stimulus must be suppressed as the sensation at the site of the stronger stimulus is localised, during the simultaneous task. By concurrently stimulating two digits, they become synchronised and isolating the more intense sensation to a digit-specific receptor population becomes more difficult because the resulting percept is unified. This is especially relevant for adjacent neuronal ensembles, such as those corresponding to D2/D3. Holden, Nguyen, Francisco, Zhang, Dennis and Tommerdahl (2012) found this to be the case during a temporal order judgement task, where localisation errors were particularly prominent for D2 and D3 compared to D2 and D4 or D2 and D5. The baseline tasks may, therefore, differ in terms of their typical thresholds for post-tDCS trials. The aforementioned literature documenting amplitude discrimination capacity in subjects with altered CNS sensitivity has not reported changes in simultaneous baseline thresholds (Folger et al., 2008; Tannan et al., 2008; Zhang, Zolnoun, Francisco, Holden, Dennis & Tommerdahl, 2011b; Nguyen et al., 2013b). For this reason, anodal tDCS was not predicted to alter performance at baseline. However, any changes in the efficacy of inhibitory processing would be predicted to have a greater influence on the performance of the simultaneous as opposed to the sequential task - due to the increased demand for GABAergic lateral inhibition, which is thought to be suppressed by anodal tDCS.

Figure 6.6. Sequential Trials. A) Trial stimulation: 25 Hz sinusoidal stimuli were randomly delivered to either D2 or D3 of the left hand (in this instance D2). For a given trial, the alternate digit received no stimulation (in this instance D3, indicated by the flat line representing that no sinusoidal stimuli were delivered). Trials consisted only of the test phase, in which the two stimuli were delivered in separate time intervals. Subjects were required to determine whether the stimulus delivered in the first or second interval was of the highest amplitude. B) Trial timing: Trials began with the presentation of a single vibration to the randomly selected digit (1st; 500 ms), followed by an inter-stimulus interval (1000 ms) before another single vibration was delivered to the same digit (2nd; 500 ms). Subjects were given an unrestricted response interval (RI) to indicate which digit they believed received the highest amplitude stimuli, after which an interval signalled the onset of the next trial (5000 ms) (figure adapted from Tannan et al., 2007).

6.3.3.3. Transcranial direct current stimulation

Brain stimulation was delivered via a DC-Stimulator Plus device (neuroConn, Germany). Subjects participated in two sessions defined by stimulation type: Anodal (A) and Sham (S). Each session took place at least one week apart. Both the researcher and the subject were naive to the nature of the stimulation that took place during each session. This was made possible using the device's "study" mode option, in which stimulation parameters were pre-defined and executed using codes for active and sham stimulation. Stimulation duration was set to 600 s for each session, with a 10 s current ramp up/down period. Rubber electrodes, measuring 5x7 cm (35 cm^2), enclosed in saline soaked sponges (0.9% concentration) were used to deliver anodal stimulation with a current of 1 mA (current density = 0.029 mA/cm^2). For sham stimulation, the current was initially ramped up over 10 s to mimic the peripheral effects of tDCS before being ramped down. During the course of the designated stimulation period, the device continued to discharge minute current spikes every 550 ms (110 μA over 15 ms) to enable continuous impedance readings. The average current over time is not more than 2 μA, which the device documentation describes as having no therapeutic effect. A right hemisphere somatosensory/contralateral orbit montage was selected as the most commonly used configuration for somatosensory stimulation (Nitsche et al., 2008). Electrodes were positioned using the 10-10 system at landmarks Fp1 (left hemisphere, cathode) and CP4 (right hemisphere/contralateral to the stimulus, anode), designed to correspond to primary somatosensory cortex (S1) (Chatrian et al., 1985). The electrode placement configuration is illustrated in Figure 6.7.

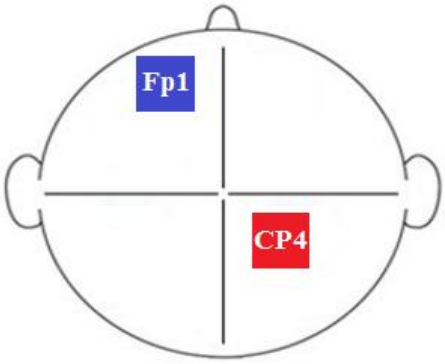

Figure 6.7. Electrode montage. Electrodes were positioned at locations CP4 (right hemisphere/contralateral to the stimulus, anode) and Fp1 (left hemisphere, cathode) of the 10-10 system.

6.3.3.4. Experimental procedure

All procedural details relating to the vibrotactile tasks were identical to those of the pilot studies (Experiment 1 & 2). Subjects began each session by completing one block of the three vibrotactile tasks. It was anticipated that implementing single runs may reduce power and precision by introducing more noise into the data. However, as the factor of Run had been shown to be non-significant during both pilot studies, it was deemed to be sufficient to acquire one run for each task per block. For the two simultaneous tasks, responses were identical to those previously documented. For the sequential baseline task, subjects used the left and right mouse buttons to indicate whether the first or second interval, respectively, contained the more intense stimulus.

After completing the initial runs, subjects were prepared for tDCS. The presentation of each task order and stimulation type was fully counterbalanced (Appendix 19). Following DC stimulation, two more blocks of the vibrotactile tasks were completed. The first block took place 5 minutes after stimulation (5-15 minutes post-tDCS; Post 1) and the second block was executed after twenty minutes had elapsed since the end of stimulation (20-30 minutes post-tDCS; Post 2). The first post-tDCS block was designed to detect the presence of post-stimulation effects of tDCS while the second block was included to gain insight into the duration of any evident effects. Between the first and second post-tDCS blocks, subjects answered an adverse effects questionnaire (AEQ) to assess the presence of any side-effects related to stimulation (Appendix 4). Subjects were also given the questionnaire before each subsequent session to assess side-effects of prolonged duration and/or delayed onset. Experimental sessions lasted approximately 60 minutes in total (see Figure 6.8 for a chronological overview).

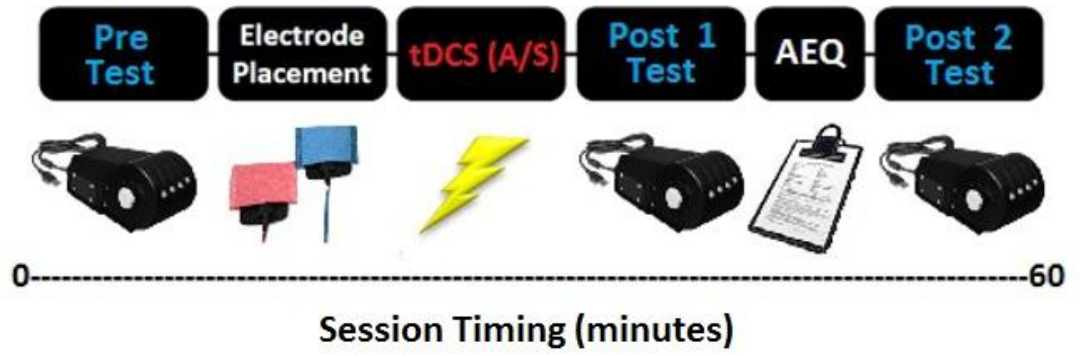

Figure 6.8. Experimental design. Subjects initially completed one run of each of the vibrotactile tasks before receiving anodal or sham stimulation. This was followed by another two blocks of the tasks, post-stimulation. Subjects completed an adverse effects questionnaire between post-stimulation task blocks.

6.3.3.5. Data analysis & statistics

As during the pilot studies, the data were visually examined for adequate performance capability and threshold stabilisation. Excessive noise in the data constituted grounds for exclusion. Following visual inspection, the majority of subjects' performance curves exhibited stabilisation similar to those obtained during Experiment 1 (see Figure 6.2). However, two subject's data was declared unsuitable for analysis (Figure 6.9). These subjects were subsequently removed and two additional subjects, of a similar demographic to the initial subjects, were recruited: 12 subjects (7 female), aged 19-31 years (*M=23.50, SD=3.63*). Initial analyses focused on establishing the presence of an adaptation effect by assessing pre-tDCS scores for comparison against the previously obtained pilot data. Paired t-tests were used to define these results. Subsequently, to assess the influence of tDCS stimulation across time and conditions, all scores were entered into a three-way, Repeated Measures ANOVA, including the following variables; Condition (Simultaneous; SIM, Sequential; SEQ; Single-Site Adaptation; SSA), tDCS (Anodal, Sham) and Time (Pre, Post1, Post2). Where appropriate, Greenhouse-Geisser correction was used to compensate for violations of sphericity. P values were considered significant if they reached the level of less than 0.05.

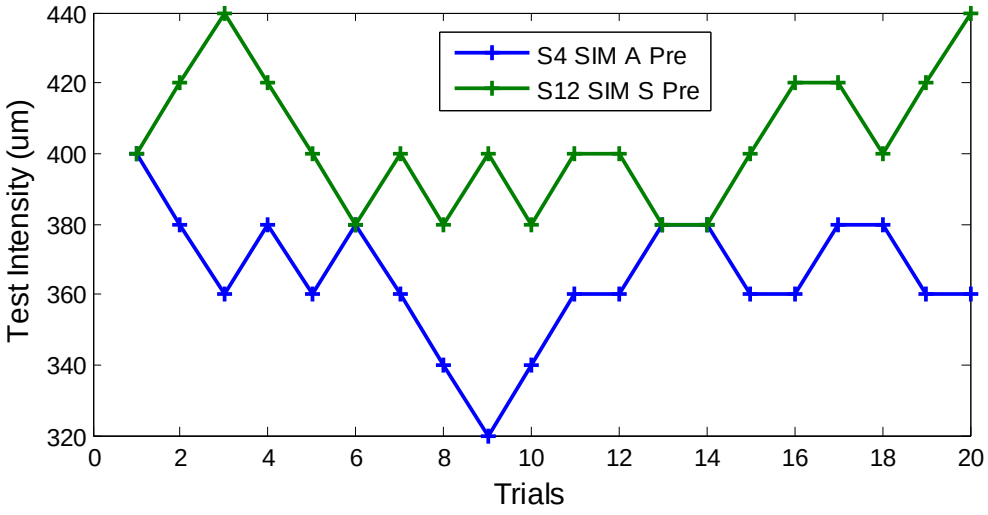

Figure 6.9. Pre-tDCS atypical task performance. Performance curves from two subjects. Data from these subjects was not suitable for analysis due to lack of typical performance progression and high DL values.

6.3.3.6. Results

6.3.3.6.1. Pre-tDCS data

Average DL values were computed across subjects for each condition (Table 6.1). The overall pre-tDCS mean values were also calculated by averaging data across sessions: SIM (*M=50.92, SD=27.43*), SEQ (*M=31.67, SD=20.14*), SSA (*M=132.33, SD=70.96*).

Table 6.1. Pre-tDCS threshold values. DL values corresponding to each of the conditions by session.

	SIM S1	**SIM S2**	**SEQ S1**	**SEQ S2**	**SSA S1**	**SSA S2**
Mean	56.58	45.25	36.50	26.83	139.67	125.00
SD	30.30	24.20	24.97	13.16	78.98	64.59

Figure 6.10 demonstrates that the lowest thresholds appear to have been achieved during the SEQ condition, followed closely by those related to the SIM condition. In comparison to the baseline conditions, threshold values obtained during the SSA condition were not only the highest but were also the most variable. It is important to note that these results are predicated on a change in sensitivity – however, it is equally possible that a change in bias may produce a similar pattern. To qualitatively assess this, results of the SIM and SSA tasks were visually inspected. This is typically achieved by fitting a psychometric function to the data. However, having been generated via a staircase method, each of the intensity values delivered was not equally represented and the data did not possess an adequate spread of values to support the formation of

psychometric curves. However, with the caveat of uneven numbers of trials, percentage correct values were generated for the sampled intensities and these figures were entered into scatterplots to visualise the data. The majority of subjects displayed a rightward-shift in performance on the SSA task in comparison to the SIM version (Figure 6.11a). This can be characterised in relation to constant error or loss of accuracy because the pattern of performance was largely similar but was likely subject to a systematic misjudgement in intensity.

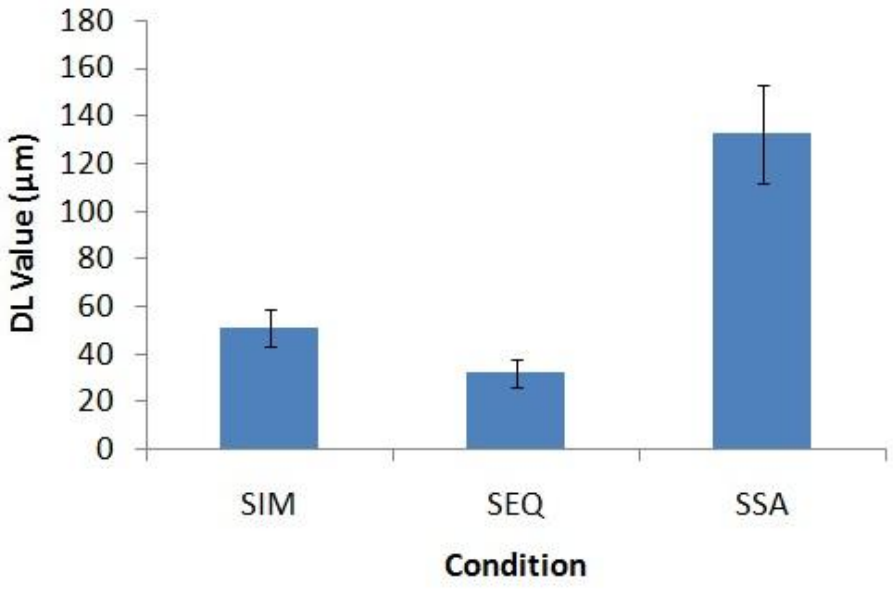

Figure 6.10. Pre-tDCS amplitude discrimination thresholds. Average DL values for each task condition, obtained prior to DC stimulation. Error bars represent ± 1 standard error (S.E.M).

Some participants also demonstrated deviations from baseline performance and increased response variability within the SSA task (Figure 6.11b). The transition from harder to easier trials was not as smooth as that established in the baseline task, indicating the presence of variable error or loss of precision in such instances. In the context of the percentage correct values, it is important to note that due to the limited spread of data and the small number of trials presented, any such variability would have led to exaggerated performance differences. Additionally, unlike MOCS in which trials are randomised and stimulus intensities are set in advance, errors of this nature within staircase procedures define future performance and automatically make it more challenging for the participant to maintain a standard progression pattern. This makes it extremely difficult to draw firm conclusions but the available evidence does suggest that SSA task performance primarily reflects a consistent decrement in the ability of participants to accurately discriminate between stimuli. This is likely due to the induced

perceptual imbalance proposed in the literature (Folger et al., 2008), which seems to create uniform inaccuracies in the perception of the test stimulus following adaptation.

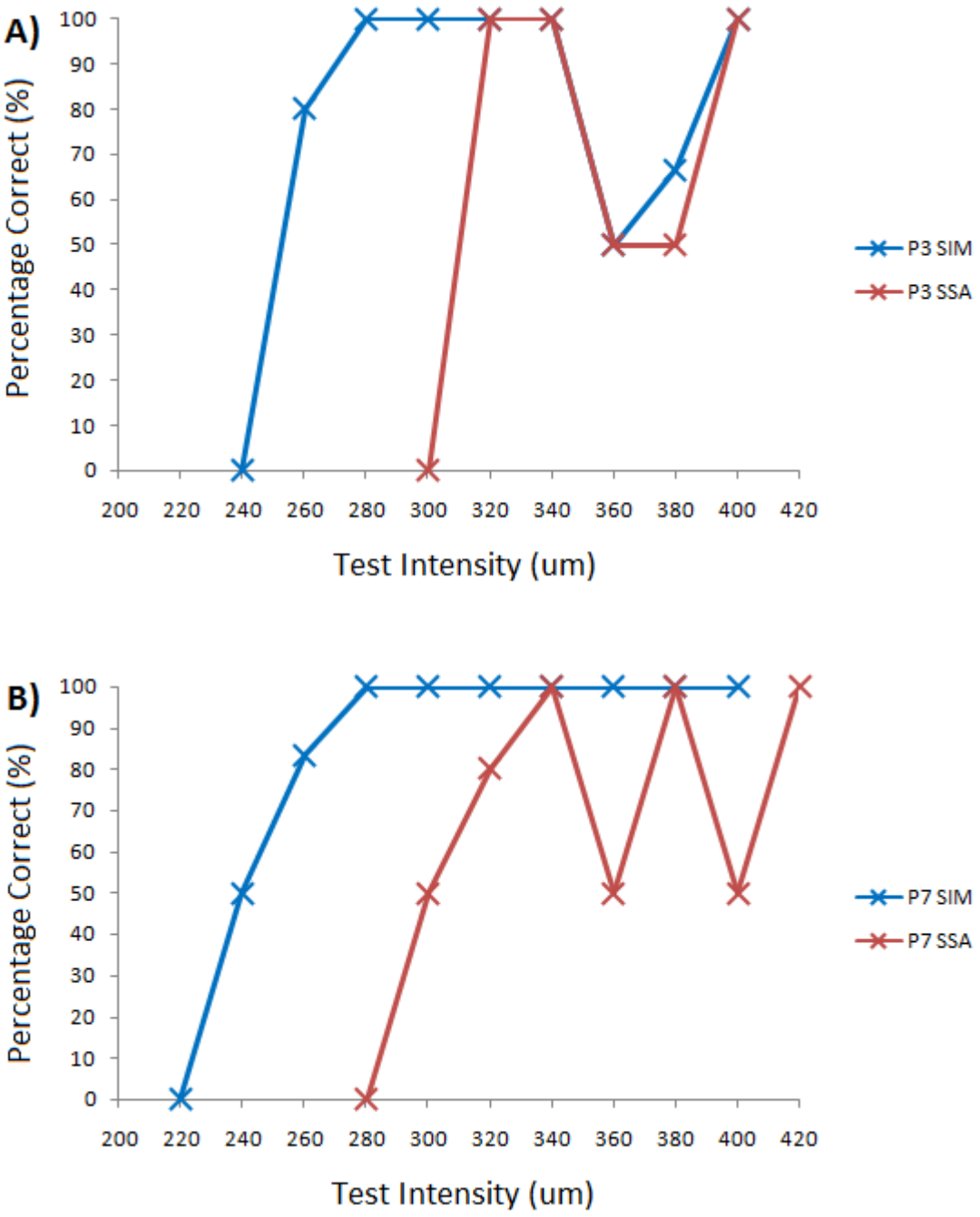

Figure 6.11. Characterisation of performance error. Scatterplots representing data produced by single subjects for the baseline and adaptation conditions, which display alterations in the A) accuracy and B) precision of responses between tasks.

Table 6.1 also indicates that DL values resulting from the first session were higher than those of the second session. For this reason, rather than using a one-way ANOVA to analyse the DL values by condition, the data were entered into a Repeated Measures ANOVA (Condition, Session) to assess the potential influence of repeated exposure.

The 3x2 ANOVA produced a significant main effect for Condition ($F(1.331,14.641)=28.236$, $p=.000$). The main effect of Session failed to reach significance ($F(1,11)=1.288$, $p=.280$). As did the interaction between Condition and Session ($F(2,22)=.026$, $p=.975$). Subsequent paired t-tests determined the significant difference between conditions largely existed between SIM/SSA and SEQ/SSA as opposed to SIM/SEQ task types: SIM/SEQ S1 ($t(11)=1.386$, $p=.193$), SIM/SEQ S2 ($t(11)=2.139$, $p=.056$), SIM/SSA S1 ($t(11)=-4.316$, $p=.001$), SIM/SSA S2 ($t(11)=-4.505$, $p=.001$), SEQ/SSA S1 ($t(11)=-4.199$, $p=.001$), SEQ/SSA S2 ($t(11)=-4.911$, $p=.000$).

The results in relation to Condition were as expected: the SSA condition threshold values were significantly higher than those of either baseline measure. Amplitude discrimination performance did not significantly differ between baseline tasks (SIM, SEQ). The lack of significant difference between sessions also indicates that repeat exposure to the tasks did not produce a substantial change in threshold values.

6.3.3.6.2. Post-tDCS data

During stimulation, impedance levels were on average 6.27 kΩ: Anodal *(M=6.61, SD=2.84)*, Sham *(M=5.93, SD=1.71)*. Subjects reported minor adverse effects, including mild to moderate itching and tingling sensations under the electrodes. Slight tiredness and difficulty concentrating were also documented, as was a mild burning sensation at current onset. A single subject described the incidence of a warming sensation to their upper body and a general feeling of contentment and relaxation. Only mild itching and tiredness persisted beyond the end of each session and all subjects responded positively to participating in further tDCS studies (Figure 6.12). Assessing the AEQ ratings obtained during stimulation for differences between tDCS conditions, the main effect of AEQ item was found to be statistically significant ($F(2.054,22.593)=13.220$, $p=.000$). This indicated that some items (e.g. Itching, Tingling) were experienced more readily and with more severity than others (e.g. Concentration problems). The main effect of tDCS ($F(1,11)=6.217$, $p=.030$) was significant, while the associated interaction (AEQ item*tDCS: $F(2.603,28.637)=1.149$, $p=.342$) was non-significant. Only the difference between stimulation conditions for the Itching item ($t(11)=2.171$, $p=.053$) approached significance, suggesting participants largely experienced similar peripheral sensations during both anodal and sham tDCS.

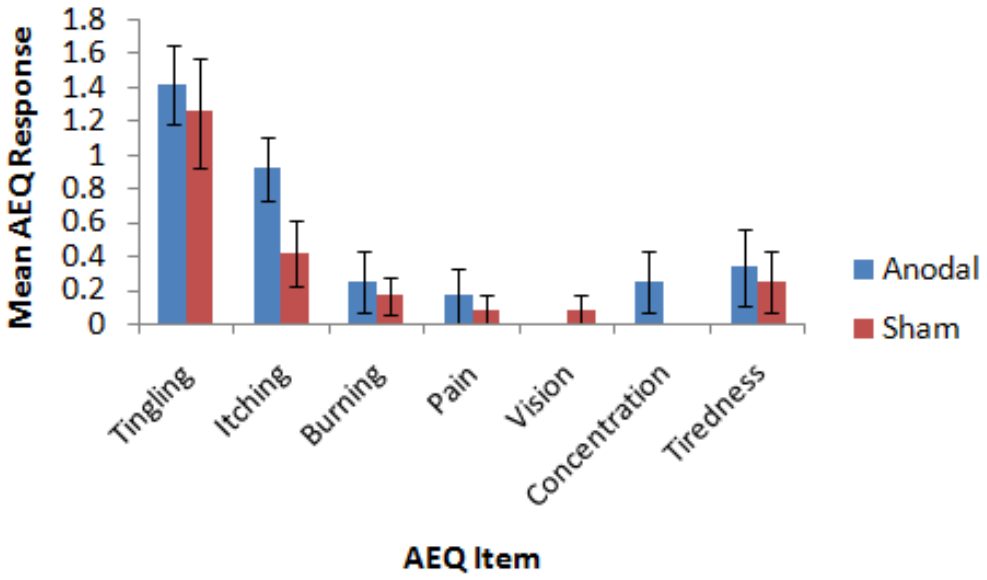

Figure 6.12. AEQ Responses. Average responses to the questionnaire items experienced during stimulation. The scale of responses ranged from 0 (not experienced) to 1-5, indicating heightened severity of the sensation experienced. Error bars represent ± 1 standard error (S.E.M).

Average DL values were computed for each condition, as a product of tDCS and Time. Figure 6.13 illustrates that the SSA thresholds were consistently higher than those of the baseline measures. Thresholds also appeared lower in the SIM condition related to anodal stimulation as compared to sham (but subsequent analysis showed that no significant differences were present for each of the conditions; see Appendix 20).

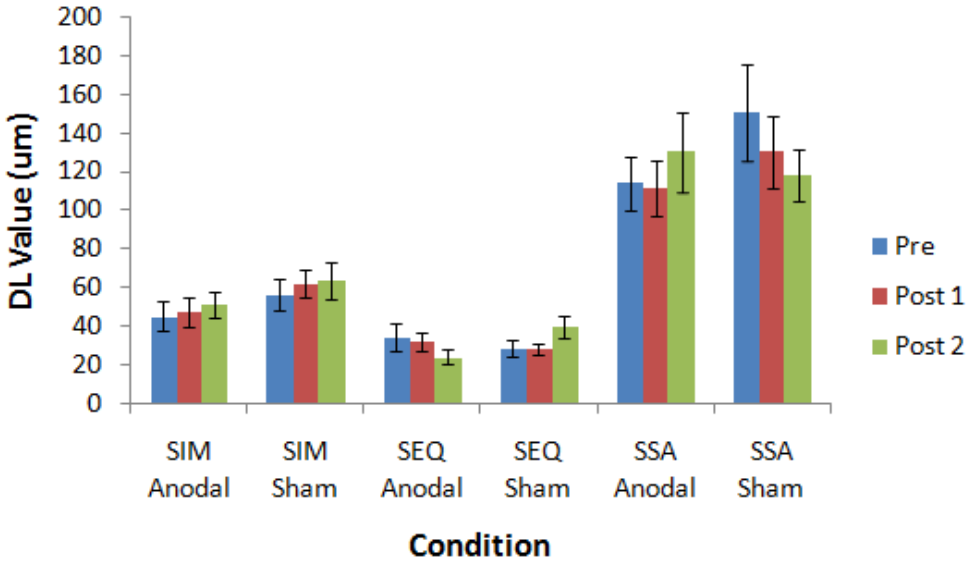

Figure 6.13. Post-tDCS amplitude discrimination thresholds. Average DL values obtained before and after tDCS, for each task condition in relation to the assessed stimulation modes. Error bars represent ± 1 standard error (S.E.M).

A 3x2x3 Repeated Measures ANOVA incorporating the factors Condition (SIM, SEQ, SSA), tDCS (Anodal, Sham) and Time (Pre, Post 1, Post 2) established a significant main effect for Condition ($F(1.406,14.056)=66.751$, $p=.000$). The main effects of tDCS ($F(1,10)=2.244$, $p=.165$) and Time ($F(2,20)=.224$, $p=.801$) failed to reach significance, as did all of the associated within-subject variable interactions. The influence of the between-subjects factor tDCS order (Anodal/Sham, Sham/Anodal) was assessed and found to be significant ($F(1,10)=7.340$, $p=.022$) as was the Condition*tDCS order interaction ($F(1.406,14.056)=9.236$, $p=.005$). The additional role of the between-subjects variable Task order (SIM/SEQ/SSA, SIM/SSA/SEQ, SEQ/SIM/SSA, SEQ/SSA/SIM, SSA/SIM/SEQ, SSA/SEQ/SIM) was non-significant ($F(5,6)=.168$, $p=.966$).

A series of paired t-tests established that the significant difference between conditions largely existed between SIM/SSA and SEQ/SSA as opposed to SIM/SEQ task types, as was the case for the pre-tDCS data (Appendix 21). Independent t-tests demonstrated that the Condition*tDCS order interaction appeared to stem from a general tendency for DL values to be lower when subjects experienced anodal prior to sham stimulation, which was particularly evident for the SSA scores (Appendix 22). This tendency was further tested using a Repeated Measures ANOVA with factors of Time (Pre, Post 1, Post 2), tDCS order (Anodal/Sham, Sham/Anodal) and Session (1, 2) to analyse each of the task conditions separately. A significant main effect of tDCS order was demonstrated only for the SSA condition (SIM ($F(1,5)=2.216$, $p=.197$); SEQ ($F(1,5)=1.598$, $p=.262$); SSA ($F(1,5)=7.590$, $p=.040$)). These results confirmed the previous suggestion that only the data from the SSA condition was significantly influenced by stimulation order. The main effect of Session for each of the conditions was non-significant (SIM ($F(1,5)=3.883$, $p=.106$); SEQ ($F(1,5)=1.819$, $p=.235$); SSA ($F(1,5)=.251$, $p=.637$)). Additionally, analysis of the SSA condition resulted in a Time*tDCS order*Session interaction that narrowly failed to reach significance ($F(2,10)=4.049$, $p=.051$). While DL values did not appear to have fluctuated between sessions in general (for any of the conditions), the interaction found for the SSA data suggests that there may be a more subtle influence of tDCS order at a specific time point for a particular session. Such an outcome may manifest as a carry-over effect, in which the influence of tDCS order (particularly A/S) would be shown to lead to a distinction in DL scores across sessions.

Although the non-significant main effect of Session for all conditions suggested the influence of repeated task exposure could be ruled out, unfortunately, due to the design of the study, any such carry-over effect could still be largely confounded by familiarity with the task. To address the trend established by the interaction, while minimising the effect of practice, scores from the Pre time point were assessed across sessions for each tDCS order. This approach allowed for insight into task performance prior to any stimulation in the first session, while assessing any residual effect of having previously undergone a single application of either anodal (A/S group) or sham (S/A group) tDCS at the start of the second session.

Paired samples t-tests revealed a significant difference in subjects' DL values for the SSA condition during the first session, which corresponded to lower scores for the A/S order ($t(5)=-2.695$, $p=.043$). This indicated a pre-existing difference in performance, irrespective of tDCS stimulation, most likely illustrating initial ability to execute the task. The same comparison was performed on data from session 2, following a single application of tDCS, was found to be non-significant ($t(5)=-.671$, $p=.532$). Therefore, each group produced statistically similar thresholds at the Pre time point during session 2. Assessing each stimulation order separately, neither groups' performance altered between sessions: A/S ($t(5)=-.524$, $p=.622$), S/A ($t(5)=1.975$, $p=.105$). This illustrates that the stimulation given in the first session was unlikely to have influenced scores during the second session, thus opposing a carry-over effect.

While traditional, Neyman-Pearson statistics permit the acceptance of experimental hypotheses where criteria for a significant p value have been fulfilled, they do not allow for valid inferences to be made on the acceptance of the null hypothesis (in light of established non-significant differences between conditions: Wagenmakers, 2007; Kruschke, 2010; Dienes, 2011). Such support for the null hypothesis can be derived using Bayesian statistics (Dienes, 2014), an approach which has become increasingly popular in recent years (for examples of use, see Verbruggen, Adams, van't Wout, Stevens, McLaren & Chambers, 2013; Greve, Cooper & Henson, 2014). Opposing models typically representing the experimental and null hypotheses are compared to generate a Bayes factor (*B*), which constitutes a ratio of the likelihood of each model being true. By computing a Bayes factor, one of three outcomes can be achieved based on the generated value. A *B* value of less than a third corresponds to strong support for the null hypothesis, a value of between a third and 3 relates to insubstantial evidence for a firm conclusion and values above 3 indicate evidence for the alternative hypothesis

(Jeffreys, 1961). Therefore, a Bayesian analysis framework was adopted to investigate whether the results of the current study genuinely reflected that tDCS had no effect on task performance. This was specifically targeted towards the SSA condition, where the alternative hypothesis stated that a decrease in discrimination thresholds should have been evident following anodal compared to sham stimulation.

A half-normal distribution model was chosen in light of the directionality of the prediction (Dienes, 2014). The model specifies that the theoretical variance for the population can be estimated (e.g. establishing a value to represent the standard deviation of a given sample). While the effect size of tDCS has previously been shown to be similar in magnitude to that of a corresponding behavioural intervention (Harty, Robertson, Miniussi, Sheehy, Devine, McCreery & O' Connell, 2014), it does not seem reasonable to expect that the application of tDCS should be as effective as the difference between behavioural conditions in all instances (considering tDCS-driven effect sizes appear to be mediated by factors such as electrode placement and montage selection: Mathys, Loui, Zheng & Schlaug, 2010; Schambra, Abe, Luckenbaugh, Reis, Krakauer & Cohen, 2011). In the absence of existing tDCS effect size data for the vibrotactile paradigm, the present study estimated that a tDCS modulation of the behavioural effect would be equivalent to half the magnitude of the established mean behavioural difference (between the SSA and SIM task conditions). To reduce the results into a single vector, the Post 2 data was removed to facilitate a more simplistic pre/post design (having proposed that any observed tDCS influence would be most evident as a distinction between the Pre and Post 1 as opposed to Pre and Post 2 runs).

The data was assessed using the MATLAB version of an online Bayes calculator (http://www.lifesci.sussex.ac.uk/home/Zoltan_Dienes/inference/bayes_factor.swf).
Sample mean (*M=-17.75*) and sample size corrected, standard error values (*SEM=21.40*) were calculated. The population mean was set to zero and the likely population standard deviation was defined as being half that of the observed behavioural effect size (as specified above). This was derived from the pre-tDCS data as the mean difference of the grand average SSA value and that of the SIM condition ((132.33-50.92)/2=40.71). The corresponding Bayes factor was *0.28*. The analysis indicated strong support for the null hypothesis that tDCS did not have an effect on the performance of the vibrotactile adaptation task.

To summarise, these results suggest the SSA condition consistently produced significantly higher thresholds compared to those of SIM and SEQ baseline tasks, which

parallels the findings present in the pre-tDCS analysis and the previous pilot studies. The non-significant findings relating to tDCS show that subjects' DL values did not fluctuate between anodal and sham sessions, demonstrating that tDCS failed to modify amplitude discrimination performance. Furthermore, the significance of the between-subjects variable tDCS order and the Condition*tDCS order interaction were determined not to constitute a carry-over effect as initially speculated. The Bayesian analysis produced substantial evidence for the null hypothesis to confirm that tDCS did not have an effect on the performance of the vibrotactile adaptation task.

6.4. Discussion

The current research aimed to investigate the role of modifications in cortical plasticity on amplitude discrimination performance, with the wider aim of further investigating the physiological underpinnings of tDCS after-effects. As predicted, the results of the initial pilot studies (Experiment 1 & 2) indicated that in the presence of adaptation stimuli, amplitude discrimination thresholds were vastly degraded compared to baseline trials. Subsequent analysis of pre-stimulation trials in the vibrotactile-tDCS study also demonstrated this adaptation effect. However, the main study (Experiment 3) failed to establish threshold changes following the application of anodal tDCS.

6.4.1. Vibrotactile pilot studies

The results of the pilot studies provide evidence that the presence of short duration, adaptation stimuli is sufficient to produce changes in information processing, which in turn, are substantial enough to influence behavioural performance. During both pilot studies, SSA scores were significantly higher than those at baseline. These findings parallel those of other studies using healthy control subjects to investigate the influence of single-site adaptation on amplitude discrimination (Tannan et al., 2007; Zhang et al., 2009; Puts et al., 2013). Furthermore, Experiment 2 provided novel evidence for the stability of the adaptation effect across multiple runs. Compared to the results of Puts et al. (2013), in which a 36% difference between baseline and SSA thresholds was established, the percentage difference derived from Experiment 1 was identical. Puts et al. (2013) also adopted an adaptor value matching that of the standard stimulus as opposed to that of the initial test value. Despite adopting a similar approach to stimulus presentation, Puts et al. (2013) used an adaptor amplitude of 100 μm compared to the 200 μm adaptor stimulus incorporated into the current study. In Experiment 2, the extended pilot study yielded much higher percentage differences (47% Run 1, 61% Run

2, 56% Run 3, 62% Run 4; 57% average). The results of Experiment 2 are more in line with what is known of the influence of stimulus intensity with regard to adaptation. The magnitude of the adaptation response has been shown to vary simply as a product of adaptor amplitude. From a physiological perspective, stimuli of heightened amplitude produce more pronounced cortical responses (Chiu et al., 2005; Chiu, 2006). During an optical imaging study, Simons et al. (2005) discovered increased absorbance (classified as increased firing rate) at regions 3b and 1 of primary somatosensory cortex following 400 μm compared to 50 μm stimulation. Although the spatial extent of activation remained the same, a decrease in absorbance was detected at neighbouring regions, which signifies the lateral inhibition of unrelated neuronal populations via an increase in the responsiveness of GABAergic processes. By using a higher amplitude adaptor stimulus in the present study, there was a potential for the resulting reduction in perceived intensity to be more dramatic than previously established. Therefore, an increase in the prominence of the observed adaptation effect was to be anticipated due to a resulting increase in the magnitude of cortical response elicited as well as the better defined development of an inhibitory surround area.

Simons et al. (2007) have subsequently shown that increasing the duration of an adapting stimulus also produces a tuning effect and a change in the response of receptive fields. Stimulus durations equal to or below 0.5 s have been described to evoke weak and diffuse cortical responses, whereas durations above 0.5 s produce the aforementioned inhibition of surrounding regions as well as enhanced filtering evident from a reduction in spatial extent. The use of an adaptor duration of 1s does appear to produce an adequate change in the CNS response of the adapted digit, such that the adaptor had the anticipated detrimental influence on perceived intensity and subsequent task performance. As the adaptor was of a brief duration, this indicates that adaptation within the context of the current study occurred via CNS mechanisms. Therefore, the study provides extended support for the notion of CNS mediated short-term plasticity and behavioural change (Nguyen et al, 2013a; Nguyen et al, 2013b; Zhang et al, 2011b).

The CNS mediation of vibrotactile adaptation is likely to predominantly occur at the level of S1, where sharpening of the responses of individual neurons and synchronisation of population level firing have been demonstrated, following repetitive vibrotactile stimuli (Whitsel et al., 2003). The refinement of S1 response extends to behavioural performance via changes in gain and contrast, linked to lateral inhibition processes as previously outlined (Lee et al., 1992; Tommerdahl et al., 2002). As the

current results are in accordance with those of previous studies, a similar approach to account for the results of the pilot studies is adopted here. Consequently, the role of local competitive interactions between minicolumns remains the likely dominant factor in the modification of short-term plasticity and task performance (Tannan et al., 2007).

6.4.2. Vibrotactile-tDCS study

6.4.2.1. Pre-tDCS findings

As predicted SSA scores were considerably higher than those achieved during the SIM baseline. The emergence of this behavioural effect following a single run of each condition suggests that sufficient data was acquired without reducing power and introducing excess noise. The study also revealed the novel finding of a similar distinction in performance between SSA and SEQ baseline DL values. The fact that SIM and SEQ baseline thresholds did not differ indicates that both conditions represent similar measures of simple amplitude discrimination performance. Therefore, a distinction between baseline conditions in relation to their recruitment of lateral inhibition processes does not appear to be evident at a behavioural level (Holden et al., 2012). Percentage differences in performance were 62% for the SIM condition and 76% for the SEQ condition with respect to the average SSA threshold value. In parallel with the pilot studies, the figures for both baseline conditions were higher than the 36% stated by Puts et al. (2013). This is likely to be due to variations in adaptor amplitude between studies as explained above (Chiu et al., 2005; Simons et al., 2005). Furthermore, as illustrated during Experiment 2, the pre-tDCS results of Experiment 3 do not seem to be influenced by repeat exposure to the task conditions. To summarise, the results corresponding to the pre-tDCS runs were similar to those of the aforementioned pilot studies, further supporting the detrimental influence of single-site adaptation stimuli on behavioural performance.

6.4.2.2. Post-tDCS findings

The SSA studies conducted using clinical populations (e.g. ASD, Tannan et al., 2008) and pharmacological interventions (e.g. DXM, Folger et al., 2008) emphasise the role of inhibitory processing in adaptation performance. Although the ASD population are largely studied from the perspective of CNS hyperexcitability, this may be driven by abnormal minicolumn structure which impairs GABAergic inhibition (Casanova et al., 2002; Casanova et al., 2003; Uhlhaas & Singer, 2006; Uhlhaas & Singer, 2012).

Similarly, while the administration of DXM provides insight into hypoexcitability via reduced NMDA receptor efficiency, the resulting reduction of excitation is hypothesised to lead to a decrease in the recruitment of associated inhibitory processes. Therefore, both sets of studies infer that reduced inhibition is integral to the finding that those with altered CNS sensitivity do not respond to the presence of adapting stimuli in the typical manner. As anodal tDCS is also thought to be dependent on an alteration of the efficacy of inhibitory, GABAergic mechanisms (Stagg & Nitsche, 2011), performance changes for the SSA task following tDCS were expected to occur (in line with those who are GABA deficient). Unfortunately, this was not the case as anodal tDCS had no influence on amplitude discrimination performance in any condition, compared to sham (as shown in Figure 6.13 and supported by a series of paired t-tests in Appendix 20). While threshold alterations were not predicted for the baseline conditions, this result was surprising in the context of the adaptation task.

Although the significant influence of tDCS order suggests that lower thresholds were established when subjects' were exposed to anodal stimulation in their first session, this is unlikely to be a product of the stimulation itself. Instead, it may be more plausibly explained by the variation in thresholds of the SSA condition. For example, with regard to the potential carry-over effect, the S/A group scores decreased between sessions (DL 188.67 to 137.33), which would not be expected for the sham group because it represents an inactive mode of stimulation. However, the opposite pattern was observed for the A/S group, where scores increased (DL 90.67 to 112.67). General practice effects that could be used to interpret the S/A group decrease evidently did not emerge in the A/S group as might be expected, meaning the results are most likely due to the instability of SSA scores. The implementation of Bayesian statistics allowed for further insight into the non-significant effect of DC stimulation by resulting in a Bayes factor that provided substantial evidence for the null hypothesis. This implies that there were no differences between thresholds derived following anodal compared to sham stimulation for the SSA condition. Additionally, despite the sample size being optimised towards the detection of the desired behavioural effect, the outcome of the Bayesian analysis suggests that the study was sufficiently powered to provide substantial evidence with regard to the outcome of the tDCS intervention.

The question remains that, considering the substantial overlap in the proposed physiological mechanisms of anodal tDCS and vibrotactile adaptation – why were there no changes in the observed SSA thresholds, to the extent that the null hypothesis could

be supported? Crucially, do the proposed mechanisms underlying tDCS, or perhaps those relating to the vibrotactile task, need to be revised? Focusing on the efficacy of the stimulation method itself, there are several factors which may have contributed to the lack of observed tDCS effect on amplitude discrimination performance. Individual differences have been shown to influence cortical plasticity, which may create possible sources of variance and dramatically impact upon results (Ridding & Ziemann, 2010). In a recent study, Wiethoff et al. (2014) determined that approximately 75% of responses to anodal tDCS, delivered to motor cortex, were facilitatory but the remaining responses were of an inhibitory nature. While variability will inevitably differ between studies for many reasons (e.g. those related to the stimulation protocol), such inter-subject variation may present a significant confound such that analysis on an individual rather than group level may be warranted (as illustrated in a recent review; Horvath et al., 2014). Several studies investigating the influence of tDCS on responses to Quantitative Sensory Testing (QST) further emphasise the impact of inter-subject variation (Bachmann et al., 2010; Grundmann et al., 2011; Jürgens et al., 2012). Despite incorporating similar sample populations and sensorimotor montages as well as identical current intensities, durations and electrode sizes, the results of each study differed dramatically.

A potential source of variance is represented by the unique nature of an individual's brain anatomy, which is likely to produce differences in the current density levels at the target brain region (Bikson & Datta, 2012; Russell, Goodman, Pierson, Shepherd, Wang, Groshong & Wiley, 2013; Kim, Kim, Chang, Kim, Kim & Im, 2014; Opitz et al., 2015). A recent simulation study has illustrated that the highest current densities may often be produced 2-4 cm from the target region under the electrodes, falling in a region between the active and reference electrodes (Rampersad, Janssen, Lucka, Aydin, Lanfer, Lew... & Oostendorp, 2014). In relation to the montage adopted as part of the current study, peak current strength may have been situated over the Vertex (Cz) which could explain the lack of tDCS effects as this region is presumed to be functionally inert. Although establishing realistic head models of current pathways is computationally demanding, these studies highlight their importance when considering the influence of tDCS on task performance.

The results may also have been confounded due to gender differences. Research suggests that females are susceptible to hormone fluctuations linked to GABAergic neurotransmission levels and that there is a general stability of crucial excitatory and

inhibitory processes in men compared to women (Kuo, Paulus & Nitsche, 2006; Chaieb, Antal & Paulus, 2008). At specific points of the menstrual cycle, females experience stages of greater GABAergic neurotransmission via increased progesterone levels (Epperson, Haga, Mason, Sellers, Gueorguieva & Zhang, 2002; Smith, Adams, Schmidt, Rubinow & Wassermann, 2002). This fluctuation was not controlled for as part of the study. Recruiting females at different cycle stages may have led to any general neuromodulatory effects being cancelled out. This would be further compounded when coupled with the GABA stability in male subjects, who may elicit an attenuated response compared to females. Future research to define the nature of tDCS after-effects in both male and female-only samples is needed to clarify whether sex differences present a realistic confound.

The impact of genetic contributions on the efficacy of neurostimulation techniques has previously been demonstrated. Brain-Derived Neurotrophic Factor (BDNF) has been implicated in LTP and has a profound effect on pre-synaptic glutamate release and post-synaptic NMDA receptor function (Nathan, Cobb, Lu, Bullmore & Davies, 2011). Accordingly, the presence of the Val66Met polymorphism, which impairs the action of BDNF and therefore glutamate release, has been proposed to influence cortical plasticity. This could dramatically impact on the effect of stimulation methods, such as rTMS and tDCS (Cheeran, Talelli, Mori, Koch, Suppa, & Edwards, 2008; Fritsch, Reis, Martinowich, Schambra, Ji & Cohen, 2010), although not all studies have reported the expected detrimental association between the Val66Met polymorphism and tDCS-induced plasticity (Antal, Chaieb, Moliadze, Monte-Silva, Poreisz & Thirugnanasambandam, 2010b). Similarly, Puri, Hinder, Fujiyama, Gomez, Carson and Summers (2015) discovered that Met carriers exhibited greater responses to anodal tDCS, particularly at longer stimulation durations (e.g. 20 as opposed to 10 minutes). This indicates that response variability may well be attributable to genetic factors. However, as the study focused on older adults and plasticity declines across the lifespan, in this respect the results suggest that the greatest tDCS-induced gains may be achieved by those who most need them.

Additional factors that have been reported to affect cortical plasticity include advancing age, which reduces plasticity (Fathi, Ueki, Mima, Koganemaru, Nagamine & Tawfik, 2010) and regular exercise, which increases plasticity (Cirillo, Lavender, Ridding & Semmler, 2009). The time of day at which subjects are tested may also produce variable effects with evidence suggesting that cortical plasticity is enhanced in the afternoon

(Sale, Ridding & Nordstrom, 2007). However, a Magnetic Resonance Spectroscopy (MRS) study on the influence of time of day on GABA levels failed to document any significant fluctuations (Evans et al., 2010), indicating that altered cortical plasticity may not be due directly to the measure of GABAergic inhibition derived by MRS (e.g. related specifically to neurotransmission and extrasynaptic tone; Stagg, 2014).

It is also entirely plausible that while the influence of tDCS was not visible at a behavioural level, physiological changes may have still been induced. Suntrup, Teismann, Wollbrink, Winkels, Warnecke and Flöel (2013) demonstrated a significant event-related desynchronisation (ERD) in the theta band, following tDCS, for a task of moderate difficulty. However, the study failed to establish any pre/post differences using a behavioural metric for the same task. Only the more difficult version of the task produced significant behavioural results. As the current study did not measure any index of physiological modulation it is impossible to draw conclusions as to whether such alterations took place. Nonetheless, it appears that the nature of the task as well as its inherent level of difficulty may not have been sufficient for tDCS modulation to occur at the level of behaviour. In relation to task difficulty, the use of a staircase method prevents researcher control of complexity because stimulus presentation is based entirely on an individual's performance, which is unique to their particular threshold. Although establishing an individual's threshold should involve trials becoming progressively more difficult, those who perform well will inevitably experience the tasks as less challenging thus creating a bias in the sample. Use of a method of constant stimuli approach (Leek, 2001), in which the stimuli to be presented are set a-priori, may offer some insight into the role of task difficulty.

With regard to the nature of the task used in the current study, it may be possible that the use of a purely perceptual task without an explicit learning component may have contributed to the lack of an observed tDCS effect. The use of anodal stimulation protocols coupled with motor learning tasks has highlighted the potential of the neuromodulation technique to induce predictable, performance enhancements (Nitsche et al., 2003c; Stagg et al., 2011b; Kim, Stephenson, Morris & Jackson, 2014). While such tasks have been hypothesised to recruit LTP-like mechanisms, research into the underpinnings of amplitude discrimination has primarily focused on altered lateral inhibition processes (Tommerdahl et al., 2002; Chiu et al., 2005). However, a balance between glutamatergic excitation and GABAergic inhibition is required for LTP to take place (Trepel & Racine, 2000). Although the close biochemical coupling of GABA and

glutamate suggests that a change in GABA is likely to be accompanied by a correlated change in glutamate, the precise role of glutamatergic neurotransmission in amplitude discrimination is largely unknown. Like the aforementioned motor learning tasks, *in vitro* responses to repetitive stimulation have also been characterised in terms of LTP (Lee et al., 1992). Supporting findings have been established *in vivo,* where NMDA receptor antagonists were able to attenuate the cortical adaptation response (Lee & Whitsel, 1992). However, the stimuli used in relation to these animal studies were directly delivered to the brain and were in the duration of minutes rather than seconds as commonly used in modern human studies. It may, therefore, be the case that the necessary reduction in inhibition and parallel increase in NMDA receptor efficiency may not have occurred during the task as performed in human subjects, making it difficult for tDCS to modify behavioural performance.

It may have been the case that aspects of the adopted stimulation protocol could have prevented the emergence of a tDCS effect. Rogalewski et al. (2004) demonstrated a modulation of performance on a vibrotactile frequency discrimination task via cathodal stimulation, while no effect of anodal stimulation was observed. The present study did not employ cathodal stimulation and as such may have failed to report a stimulation-induced alteration in task performance for this reason. Additionally, Rogalewski et al. (2004) demonstrated that the observed reduction in correct responses related to cathodal tDCS began during the stimulation period and Ragert et al. (2008) established a facilitatory effect of anodal tDCS on spatial discrimination ability, which also emerged during the stimulation period. There is much debate with regard to the ideal point at which to administer tDCS. Quartarone, Morgante, Bagnato, Rizzo, Sant'Angelo, Aiello… and Girlanda (2004) demonstrated that the completion of a motor imagery task, after DC stimulation, was able to diminish the influence of anodal tDCS but extended that of cathodal tDCS. Conversely, Antal et al. (2007) reported a reversal of the expected influence of anodal stimulation, thus mimicking cathodal effects, following the performance of a simple motor task administered during stimulation. Therefore, to boost the likelihood of inducing plasticity changes, it has yet to be established whether it is advantageous to attempt to synchronise the onset of stimulation with that of the task by adopting an "online" stimulation approach.

This may largely be dependent on the nature of the plasticity induced, with reference to state-dependent effects (Huang, Colino, Selig & Malenka, 1992; Abraham & Bear, 1996; Ziemann & Siebner, 2008; Cosentino, Fierro, Paladino, Talamanca, Vigneri,

Palermo… & Brighina, 2012). An alternative may be to alter the typical pre/post stimulation pattern. For example, Bastani and Jaberzadeh (2014) reported that several within-session doses of tDCS, with extended intervals between each subsequent exposure, may be the key to enhancing cortical excitability (also emphasised by Goldsworthy, Pitcher & Ridding, 2015). As this study employed a classic pre/post design, such potential effects may have been missed. Lastly, it is of relevance that the expected duration of effects following somatosensory stimulation has also yet to be determined. This makes it difficult to know what constitutes a typical response, such that establishing the optimal structure of post-stimulation task blocks is problematic. For example, Rogalewski et al. (2004) demonstrated short-lasting after effects of 7 minutes, whereas those observed by Ragert et al. (2008) persisted for 40 minutes. The distinction between these studies may reflect differences in stimulation duration, polarity, and/or current density; the effects of which are less appreciated outside of motor cortex (as discussed by Chaieb et al., 2008).

6.5. Conclusions

The study supported previous findings that single-site adaptation stimuli are capable of producing robust decrements in vibrotactile amplitude discrimination thresholds, compared to those established at baseline. Despite evidence suggesting a similarity in terms of the neurobiological mechanisms underlying the behavioural and neurostimulation methods, anodal tDCS was unable to modulate the observed adaptation effect at a behavioural level. Refinement of the stimulation protocol (e.g. trialling an alternative montage, delivering stimulation during the task) may be beneficial in determining whether it was the parameters of the current study that prevented the emergence of the expected tDCS effect. Additionally, to better understand the mechanisms underlying the task in humans as well as the influence of tDCS, future research could integrate the behavioural paradigm with measurements of neuronal function and neurotransmission (e.g. MEG and MRS, utilised in experimental chapters 3 and 5) to assess the prospect of modulations in neurobiological activity that were beyond the scope of the current study.

7. Experimental Chapter 5

Modulation of Use-Dependent Plasticity in Primary Somatosensory Cortex - A Double-Blind, Sham-Controlled Transcranial Direct Current Stimulation Study

7.1. Abstract

tES techniques, such as tDCS, have commonly been paired with behavioural tasks in order to modulate performance. However, these paradigms are often not understood at the level of physiology. This prevents any modification of behavioural effects translating to valuable inferences on the neurobiological basis of the stimulation technique itself. To circumvent this issue, the study addressed the underpinnings of tDCS by utilising the principles of vibrotactile adaptation. Importantly, the mechanisms sub-serving vibrotactile adaptation have been confirmed in several animal studies and, analogous to tDCS, are proposed to rely upon changes in inhibitory neurotransmission. Vibrotactile stimulation was delivered in the form of a 2AFC dual-site amplitude discrimination task, where adaptation stimuli have been shown to improve performance (in contrast to the paradigm used in chapter 6). The presence of this adaptation effect was sought during a pilot study, in which baseline and adaptation trials were presented to subjects. An identical task was implemented during the main vibrotactile-tDCS study. Double-blind tDCS (Anodal/Cathodal/Sham) of 1 mA was delivered for 600 s to electrodes organised in a bihemispheric primary somatosensory cortex montage, between blocks of each task in a pre/post design. In accordance with the previous literature, the pilot study results indicated that amplitude discrimination thresholds were significantly lower for adaptation than baseline trials. The pre-tDCS results from the main study showed no such distinction between conditions. However, cathodal tDCS lowered adaptation DL values compared to sham; such that they were sufficiently reduced enough to produce the expected distinction between conditions. Using Bayesian statistics, these findings were confirmed. Conversely, Bayes factors generated to reveal the effect of anodal stimulation supported the null hypothesis. The data suggest that the vibrotactile adaptation effect is likely to be dependent on specific elements of the adopted recruitment criteria e.g. sample population, task expertise. The individual post-tDCS results and the distinction between polarities are reviewed in the context of interactions between the task and stimulation as well as aspects of the stimulation protocol, such as the implemented bihemispheric montage.

7.2. Introduction

tDCS has been shown to produce polarity-specific changes in cortical excitability and behavioural performance (Wassermann & Grafman, 2005; Utz et al., 2010; Paulus, 2011; Krause et al., 2013). Underlying these changes, our current understanding of the technique suggests that short stimulation durations typically lead to alterations in membrane excitability, characterised by changes in the usual response of voltage-gated ion channels that regulate the flow of sodium and calcium (Creutzfeldt et al., 1962; Bindman et al., 1964; Purpura & McMurty, 1965; Funke, 2013). Extended stimulation intervals have been demonstrated to produce the more prolonged effects associated with tDCS, linked to modifications of neurotransmitter systems that influence synaptic plasticity (Liebetanz et al., 2002; Nitsche et al., 2003b; Nitsche et al., 2004a; Nitsche et al., 2004b; Nitsche et al., 2005; Stagg et al., 2009; Clark et al., 2011; Monte-Silva et al., 2013; Tremblay et al., 2013). One approach to further address the possible origins of these tDCS effects is to adopt behavioural tasks that have common physiological elements to DC stimulation. Where there are evident modulations of task performance, such alterations could be reliably attributed to their shared neurobiological mechanisms.

Chapter 6 addressed the combination of tDCS and single-site adaptation, a vibrotactile adaptation paradigm thought to engage GABAergic lateral inhibition processes within primary somatosensory cortex (S1) (O'Mara et al., 1988; Kelly & Folger, 1999; Whitsel et al., 2000; Tommerdahl et al., 2002; Chen et al., 2003; Whitsel et al., 2003). In relation to task performance, the SSA paradigm typically degrades performance compared to baseline because of the perceptual imbalance in perceived intensity between adaptation and test stimuli (Tannan et al., 2007; Folger et al., 2008; Zhang et al., 2009; Puts et al., 2013). Local competitive interactions between minicolumns, therefore, appear to be essential in shaping the response to such repetitive stimuli (Lee et al., 1992; Lee & Whitsel, 1992; Chiu et al., 2005; Simons et al., 2005; Simons et al., 2007). Comparable explanations have also been put forward to account for the pattern of human behavioural performance that arises following dual-site vibrotactile adaptation. However, in this instance, the ability of a participant to engage in the task is often improved. This suggests that stimulus processing is optimised by applying adaptation stimuli under the conditions of the dual-site paradigm (Kohn & Whitsel, 2002).

As for SSA, one such example originates from tasks probing amplitude discrimination capacity, in which subjects are asked to determine which of two, otherwise similar,

stimuli is of the highest amplitude (perceived as most intense). During simultaneous presentation of 1 s adaptation stimuli to D2 and D3, Tannan et al. (2007) discovered that their subjects experienced a pronounced reduction in difference limen (DL), from 23 to 13 μm. This indicates that they were better able to discriminate between smaller differences in standard and test stimulus amplitudes than they were in the absence of pre-exposure to the stimuli. The performance improvement was accounted for in terms of S1 response, characterised as a dramatic change in gain and contrast mechanisms. The identical adaptation stimuli delivered to each digit was said to produce an improvement in gain, described as enhanced neuronal tuning, resulting from a reduction in perceived intensity at each site. Subsequently delivered stimuli with similar characteristics are, therefore, likely to elicit an attenuated response. However, the perception of a novel stimulus produces a more distinctive response, such that there is an accompanying increase in contrast via enhanced GABAergic lateral inhibition. The attenuation of stimuli with similar attributes (in this case, amplitude) typically leads to such observations of enhanced discrimination capacity following adaptation (Tannan et al., 2007; Puts et al., 2013). Similar explanations have since been put forward to account for a range of findings arising from measures of amplitude discrimination (Folger et al., 2008; Francisco, Tannan, Zhang, Holden & Tommerdahl, 2008; Zhang et al., 2011a; Zhang et al., 2011b; Nguyen et al., 2013a; Nguyen et al., 2013b; Francisco, Holden, Zhang, Favorov & Tommerdahl, 2011). Therefore, lateral inhibition, as governed by the balance of excitatory/inhibitory neurotransmission, appears to be the driving force behind these performance improvements. The dual-site paradigm should, therefore, represent a useful tool with which to explore our current understanding of tDCS mechanisms.

The investigation was primarily intended to strengthen the existing understanding of prolonged tDCS effects, afforded by the knowledge relating to the physiology of vibrotactile adaptation. Consequently, the study was designed to ascertain the effect of tDCS-modulated cortical excitability on the influence of adaptation stimuli, with regard to subjects' dual-site amplitude discrimination capacity. With respect to the incorporated electrode montage, the study is also novel in its use of a bihemispheric configuration specifically designed to probe the dynamics of primary somatosensory cortex. Previous research has shown that such electrode montages have the potential to alter interhemispheric inhibition (IHI). This serves to facilitate depolarisation under the anode, while inducing hyperpolarisation under the cathode (located over the homologue of the opposite hemisphere) (Ragert, Nierhaus, Cohen & Villringer, 2011). The

approach should, therefore, produce a more focal effect compared to unihemispheric montages (Vines et al., 2008; Sehm et al., 2012).

To establish the existence of the expected adaptation effect, an initial behavioural pilot study was conducted prior to the introduction of tDCS stimulation. The main study incorporated the use of double-blind, sham-controlled tDCS to determine the effect of variations in neuromodulation on the established behavioural outcome. In light of the available evidence, it was predicted that the presence of adaptation stimuli would enhance subjects' performance on the amplitude discrimination task, compared to baseline trials. Given the novelty of the tDCS intervention, it was difficult to anticipate the nature of the results. However, with regard to what is known of the polarity-specific effects, compared to sham stimulation, it was predicted that tDCS would enhance (anodal) and reduce (cathodal) typical amplitude discrimination ability during adaptation trials.

7.3. Methodology & Results

7.3.1. Experiment 1: Vibrotactile Pilot Study

7.3.1.1. Subjects

12 subjects took part in the study (7 males). Subjects were aged 21-27 years (*M=24.25*, *SD=1.48*) and were predominantly right-handed. All procedures were carried out with approval of the local ethics committee.

7.3.1.2. Vibrotactile task

Subjects completed two versions of a 2AFC task, designed to test their ability to discriminate between vibratory stimuli of differing amplitudes. Stimuli were delivered to the index and middle finger (digits 2 and 3) of the left hand, using a vibrotactile stimulation device capable of delivering dual-site stimuli (CM5; Cortical Metrics, North Carolina). The device featured adjustable 5 mm probe tips and sufficient contact with the skin was ensured via a closed-loop algorithm.

Each subject completed baseline and adaptation versions of the task. During the baseline task, subjects were asked to determine which of two simultaneously delivered stimuli felt more intense. In the adaptation task, subjects were instructed to ignore an initial pair of stimuli before making the same intensity judgement on the subsequent

pair, as they did in the baseline task (see Figure 7.1a for a schematic representation of the stimuli).

Responses on each task were tracked, using an adaptive staircase method (Leek, 2001). The first half of trials was executed in a 1up/1down protocol. The amplitude of the test stimulus selected for the subsequent trial was adjusted in accordance with the response accuracy of the previous trial. The final half of trials was conducted using a 2up/1down protocol, in which two correct responses were required before performance was classified to have improved and the amplitude of the test stimulus was reduced. Step size was maintained at 20 μm across all trials and experimental runs. All vibrotactile pulses delivered were classified as sinusoidal, 25 Hz flutter stimulation. The adaptor stimuli (200 μm) and the standard (200 μm) and test (205-400 μm) stimuli were delivered simultaneously within each pair of pulses. The location of the standard and test stimuli was randomised across trials.

7.3.1.3. Experimental procedure

Subjects were seated in front of a computer monitor, with the vibrotactile stimulation device positioned on their left-hand side. Subjects were instructed to lightly rest their digit tips over the corresponding pads on the device. All sessions began with two runs of each version of the task. Each run consisted of a series of initial training trials. Correct responses on three consecutive training trails were required to progress to the next stage.

Due to the elusive nature of the dual-site adaptation effect (mentioned by Prof. Mark Tommerdahl and Dr. Nicolaas Puts, personal communication), alternate adapt and test phase intervals were trialled to optimise the likelihood of achieving a reliable effect. The following task parameters were chosen, having been established to elicit a more consistent effect (during six separate runs) than the standard values reported in the literature (adapt/test: 1000/500 ms). Adaptation trials began with an initial period of dual-site stimulation lasting 520 ms, which was to be ignored by subjects. This was followed by an interval of 1000 ms before the test phase, in which another period of dual-site stimulation was delivered for 160 ms. After the test stimuli had been presented, subjects had an unrestricted amount of time to make the required intensity discrimination. Trials were followed by a 5000 ms inter-trial interval. Baseline trials incorporated only the test phase (see Figure 7.1b for a schematic representation of each

trial type). The presentation of each version of the vibrotactile task was fully counterbalanced.

Figure 7.1. Vibrotactile Trials. A) Trial stimulation: 25 Hz sinusoidal stimuli were delivered simultaneously to D2 and D3 of the left hand. Adaptation trials consisted of an initial pair of stimuli, identical in amplitude, which were followed by an amplitude discrimination test, in which one stimulus was of higher amplitude than the other (in this instance, D3). Baseline trials consisted only of the test phase. B) Trial timing: Adaptation trials began with the presentation of identical paired pulses (A; 520 ms), followed by an interval (1000 ms) before the standard and test stimuli were simultaneously delivered (S/T; 160 ms). Subjects then responded during an unrestricted period of time (RI), after which an interval signalled the onset of the next trial (5000 ms) (images adapted from Tannan et al., 2007).

Subjects made their responses by using the left and right mouse buttons. A left click corresponded to the middle finger (D3) and a right click corresponded to the index finger (D2). Subjects were provided with visual cues to guide their responses. These were in the form of "IGNORE!" and "TEST!" statements that appeared on screen during the respective stimulation periods. Visual feedback was provided during training trials, in the form of positive or negative animated facial expressions. The training phase was followed by the main task, which comprised of 32 trials. During the main task, the amplitude of the test stimulus was tracked following the protocol outlined in the previous section. Subjects completed one block, containing two runs of each task, which lasted approximately 20 minutes.

7.3.1.4. Data analysis & statistics

The data were plotted using MATLAB (Version 7.4.0; MathWorks, Cambridge) to derive performance curves for each experimental run (for example data, see Figure 7.2). These were visually inspected for evidence of threshold stabilisation. Excessive noise in the data constituted grounds for exclusion. All datasets were found to be suitable for further analysis.

Statistical analyses were computed using SPSS for Windows software (Version 20; IBM, New York). Data were compared with regard to differences between adaptation and baseline trials. The DL value for each run, representing the average test stimulus value from the final 5 trials, was entered separately into a two-way, Repeated Measures ANOVA analysis with the following variables; Condition (Baseline, Adaptation) and Run (1, 2). P values were considered significant if they were less than 0.05.

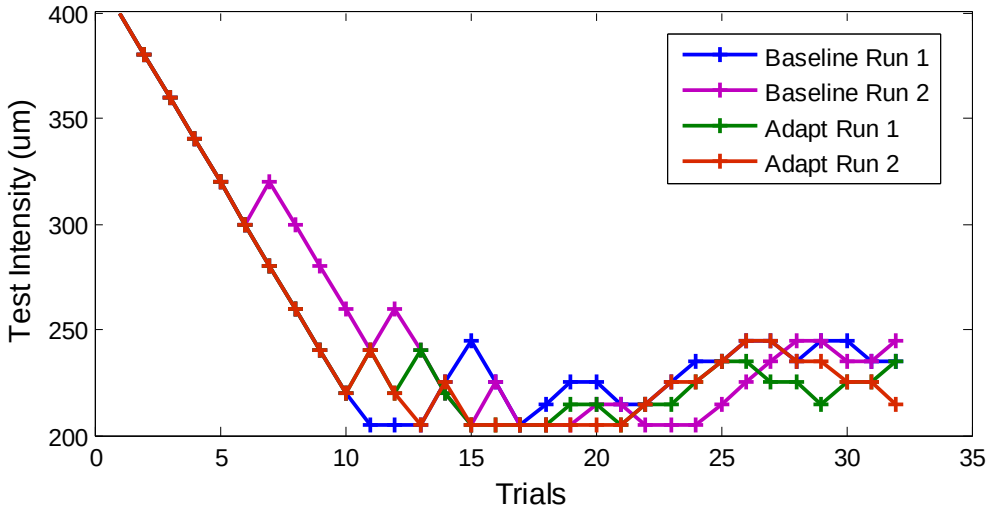

Figure 7.2. Pilot study task performance. Performance curves from a single subject. All conditions exhibit the expected response pattern (initial rapid improvement in discrimination capacity) and progression to threshold stabilisation towards the end of each run.

7.3.1.5. Results

Average DL values were computed across subjects for each condition and run: Baseline Run 1 (*M=59.62, SD =38.51*), Baseline Run 2 (*M=40.33, SD =21.47*), Adapt Run 1 (*M=37.83, SD =12.97*) and Adapt Run 2 (*M=26.00, SD =12.87*). Mean scores illustrate lower DL values for adapt trials than those of the baseline condition and an improvement in performance between Runs 1 and 2, for both trial types (Figure 7.3).

The two-way ANOVA produced a significant main effect for Condition ($F(1,11)=6.500$, $p=.027$). The main effect for Run failed to reach significance ($F(1,11)=4.385$, $p=.060$). The interaction between Condition and Run was also non-significant ($F(1,11)=.597$, $p=.456$).

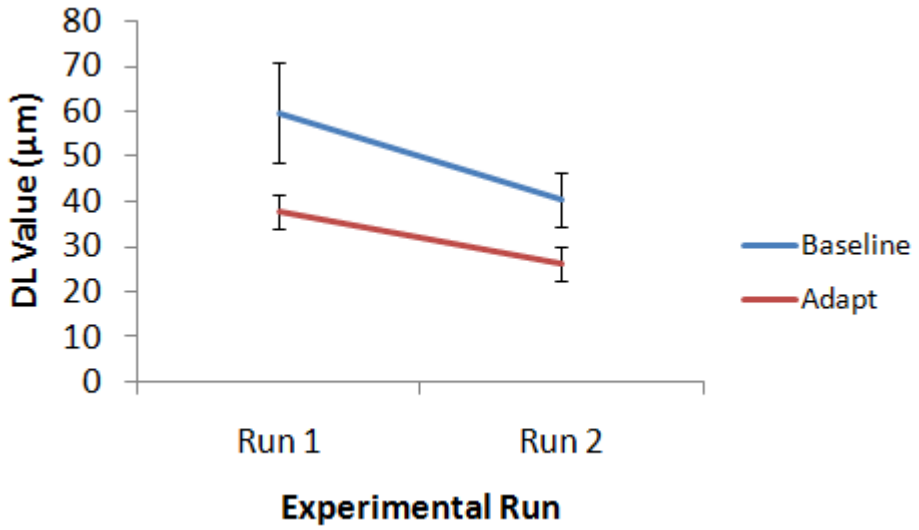

Figure 7.3. Pilot study thresholds. Average DL values obtained across runs on an amplitude discrimination task in the baseline and adapt trial versions. Error bars represent ± 1 standard error (S.E.M).

The results indicate that subjects were able to achieve substantially lower amplitude discrimination thresholds during adapt than baseline trials. Despite the evident trend, these findings also suggest that subjects obtained similar thresholds during each experimental run.

To assess the thresholds by gender (performed retrospectively, after the vibrotactile-tDCS study; see Discussion section) DL values were divided into those derived from male and female subjects. As is evident in Figure 7.4, both groups demonstrated the expected response pattern while female subjects exhibited a trend for more prominent differences between adapt and baseline scores. Incorporating the between-subjects factor Gender into the two-way, Repeated Measures ANOVA revealed significant main effects for Condition ($F(1,10)=7.197$, $p=.023$) and Run ($F(1,10)=7.985$, $p=.018$). Gender alone was not found to be significant ($F(1,10)=.274$, $p=.612$). However, there was a significant Run*Gender interaction ($F(1,10)=5.361$, $p=.043$). Paired samples t-tests demonstrated the tendency for Run 2 to result in lower threshold values than Run 1, for female ($t(4)=2.765$, $p=.051$) compared to male ($t(6)=.480$, $p=.648$) subjects. The Condition*Gender interaction failed to reach significance ($F(1,10)=1.011$, $p=.338$), although analysis of the data from female subjects ($t(4)=2.347$, $p=.079$) approached the criteria for a significant difference between baseline and adaptation trials (lower for adaptation), compared to that of the male subjects ($t(6)=1.325$, $p=.233$). Therefore, both genders achieved a comparable performance on each trial type but females differed with regard to their performance between runs.

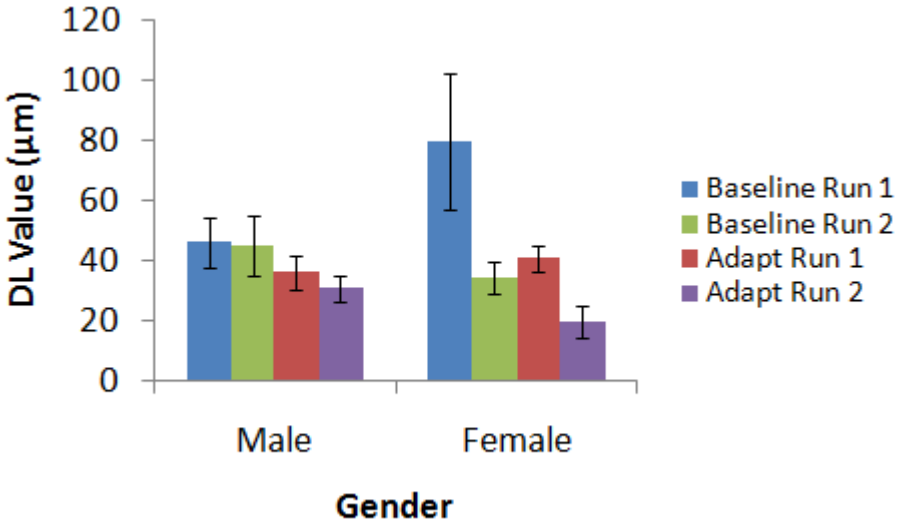

Figure 7.4. Gender-based pilot study thresholds. Average DL values obtained from male (N=7) and female (N=5) subjects on an amplitude discrimination task during the baseline and adapt trial versions. Error bars represent ± 1 standard error (S.E.M).

7.3.2. Experiment 2: Dual-Site, Vibrotactile-tDCS Study

Having established the desired dual-site adaptation effect, a period of DC stimulation was integrated between runs to determine whether the neuromodulation technique could alter behavioural performance.

7.3.2.1. Subjects

18 subjects took part in the study. All subjects were male, aged 22-34 years (*M=25.17*, *SD=3.94*) and right-hand dominant (determined by the short-form Edinburgh Handedness Inventory, Appendix 1; Oldfield, 1971). A purely male sample was recruited in light of evidence of sex differences in the after-effects produced by brain stimulation techniques, such as rTMS and tDCS (Hausmann, Tegenthoff, Sänger, Janssen, Güntürkün & Schwenkreis, 2006; Kuo, Paulus & Nitsche, 2006; Chaieb et al., 2008). These differences have been associated with changes in GABA levels due to hormone fluctuations during the menstrual cycle. Specifically, at certain points of the menstrual cycle, females experience stages of greater GABAergic neurotransmission via increased progesterone levels (Epperson et al., 2002; Smith et al., 2002). As GABA is thought to underpin the physiological effect of DC stimulation, this potential source of variability was eliminated by excluding female subjects from the study. Upon expressing an interest in taking part in the study, subjects were issued with a screening form to determine their eligibility (Appendix 2). Those with any of the contraindications

listed were excluded from the study. All procedures were carried out with approval from the local ethics committee.

7.3.2.2. Vibrotactile task

Subjects performed identical versions of the pilot study tasks, described above.

7.3.2.3. Transcranial direct current stimulation

Brain stimulation was delivered via the DC-Stimulator Plus device (neuroConn, Germany). Subjects participated in three sessions defined by stimulation type: Anodal (A), Cathodal (C) and Sham (S). Each session took place at least one week apart. Both the researcher and the subjects were naive to the nature of the stimulation that took place during each session. This was made possible using the device's "study" mode option, in which stimulation parameters were pre-defined and executed using codes for active and sham stimulation. Stimulation duration was set to 600 s for all sessions, with a 10 s current ramp period at the beginning and end of the stimulation interval. Rubber electrodes, measuring 5x5 cm (25 cm^2), enclosed in saline soaked sponges (0.9% concentration) were used to deliver anodal stimulation with a current of 1 mA (current density = 0.04 mA/cm^2). This electrode size was chosen to offer increased focality compared to that offered using electrodes of a 5x7 cm (35 cm^2) design (Nitsche et al, 2007). The polarity was reversed for cathodal stimulation (-1 mA), ensuring the montage used was identical across sessions. For sham stimulation, the current was initially ramped up for 10 s to mimic the peripheral effects associated with tDCS. During the course of the designated stimulation period, the device continued to discharge current spikes to enable continuous impedance readings. A bihemispheric S1 montage was selected in light of evidence proposing a reduction in IHI and improved focality of results (Ragert et al., 2011; Vines et al., 2008; Sehm et al., 2012). Electrodes were positioned using the 10-10 system at landmarks CP3 (left hemisphere, cathode) and CP4 (right hemisphere/contralateral to the stimulus, anode), designed to correspond to primary somatosensory cortex (Chatrian et al., 1985). These sites are located 10% posterior of 10-20 positions C3 and C4 (primary motor cortex) (Figure 7.5).

7.3.2.4. Experimental procedure

All procedural details relating to the vibrotactile tasks were identical to the pilot study.

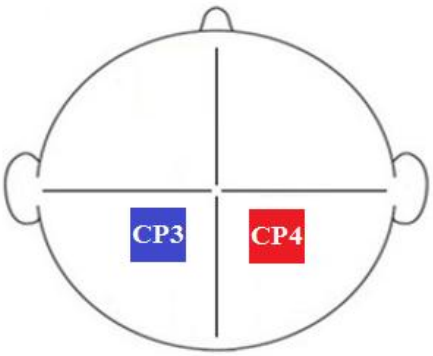

Figure 7.5. Electrode montage. The bihemispheric somatosensory montage was achieved by positioning the electrodes, using the 10-10 system, at landmarks CP3 (left hemisphere, cathode) and CP4 (right hemisphere/contralateral to the stimulus, anode).

As in the pilot study, subjects began each session by completing one block of the vibrotactile tasks. After completing the initial block, subjects were prepared for tDCS. The presentation of each stimulation type was fully counterbalanced. Task order and stimulation type were pseudo-randomised to ensure an equal amount of combinations were presented (Appendix 23). Following DC stimulation, two more blocks of the tasks were completed. The first block took place immediately after stimulation (0-20 minutes post-tDCS) and the second block was executed after twenty minutes had elapsed since the end of stimulation (20-40 minutes post-tDCS). All subjects completed these blocks within the designated time periods. After the second block was completed, subjects answered an adverse effects questionnaire (AEQ) to assess the presence of any side-effects related to stimulation (Appendix 4). Subjects were also given the questionnaire before each subsequent session to assess side-effects of prolonged duration and/or delayed onset. Sessions lasted approximately 90 minutes (Figure 7.6).

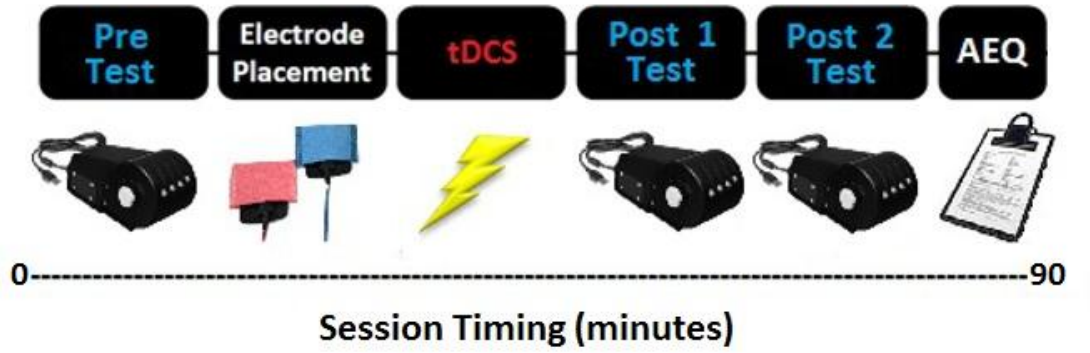

Figure 7.6. Session overview. Subjects initially completed one block of the vibrotactile tasks (two runs of each version), before 600 s of anodal, cathodal or sham stimulation. This was immediately followed by another two blocks of the tasks. Subjects documented any adverse effects that they had experienced during and/or after the stimulation, once experimental data collection had finished.

7.3.2.5. Data analysis & statistics

As during the pilot study, the data were visually examined for threshold stabilisation and excessive noise in the data constituted grounds for exclusion. Following visual inspection, the majority of subjects' performance curves exhibited stabilisation similar to those obtained during the pilot study. However, three subject's data was declared unsuitable for future analysis (for example data, see Figure 7.7). Preliminary analyses focused on establishing the presence of an adaptation effect using the pre-tDCS data, for comparison against the previously obtained pilot data. For each participant the DL value for each run was entered separately into a two-way Repeated Measures ANOVA, featuring the variables Condition (Baseline, Adaptation) and Run (1, 2), with data collapsed across the tDCS factor (Anodal, Cathodal, Sham). Subsequently, to assess the influence of tDCS stimulation across time and conditions, scores were entered into a four-way, Repeated Measures ANOVA, including the following variables; tDCS, Time (Pre, Post1, Post2), Run and Condition. The between-subjects factor of tDCS order (ACS, ASC, CAS, CSA, SAC, SCA) was also assessed. Where appropriate, Greenhouse-Geisser correction was used to compensate for violations of sphericity. P values were considered significant if they were less than 0.05.

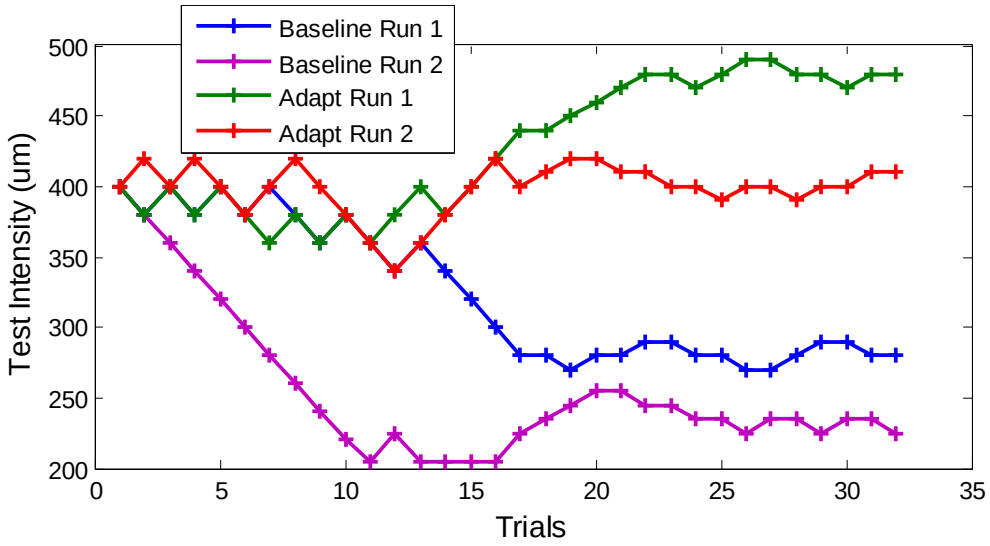

Figure 7.7. Vibrotactile-tDCS study atypical task performance. Performance curves from a single subject, obtained during the pre-tDCS trials of Session 1. The lack of standard performance pattern during Baseline run 1 as well as Adaptation runs 1 and 2 indicated a lack of ability to sufficiently perform the task. Data representing such atypical performance was excluded from further analysis.

7.3.2.6. Results

7.3.2.6.1. Pre-tDCS data

Average DL values were computed within the pre-tDCS time point for each condition and experimental run completed: Baseline Run 1 (*M=39.18, SD =17.33*), Baseline Run 2 (*M=38.31, SD =15.27*), Adapt Run 1 (*M=36.78, SD =11.01*) and Adapt Run 2 (*M=32.42, SD =6.53*). These scores illustrate lower DL values for adapt trials than those of the baseline condition. An improvement in performance between Runs 1 and 2 was demonstrated for adapt trials only (Figure 7.8).

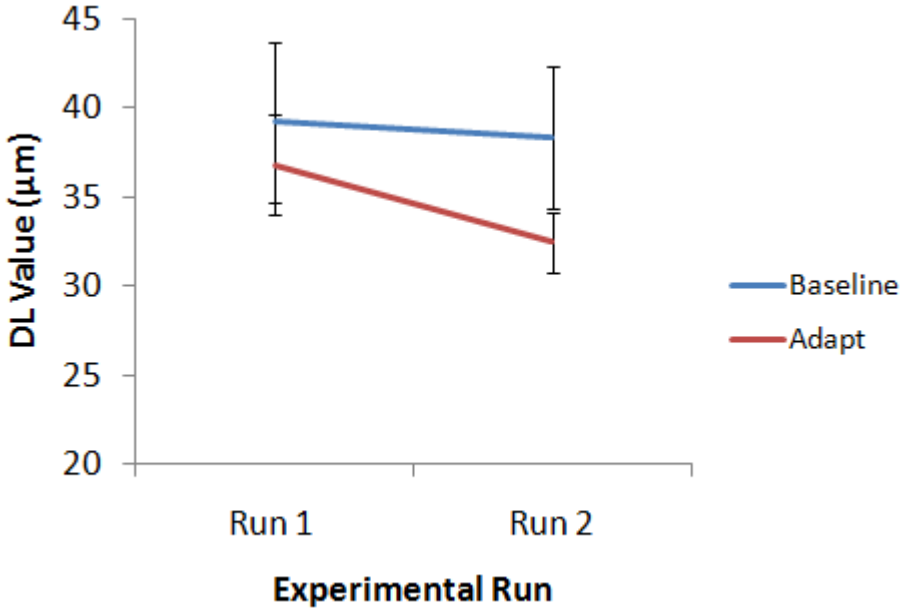

Figure 7.8. Pre-tDCS thresholds. Average DL values obtained prior to tDCS, across runs, on an amplitude discrimination task in baseline and adapt trials. Error bars represent ± 1 standard error (S.E.M).

The two-way Repeated Measures ANOVA failed to produce significant main effects for Condition ($F(1,14)=.926$, $p=.352$) or Run ($F(1,14)=1.039$, $p=.325$). The Condition and Run interaction was also not found to be significant ($F(1,14)=.316$, $p=.583$). These results indicate that although there was a trend in line with the expected adaptation effect, in this instance, the difference between conditions failed to reach significance.

7.3.2.6.2. Post-tDCS data

Mean impedance levels (kΩ) were derived for Anodal *(M=8.27, SD=3.13)*, Cathodal *(M=8.09, SD=3.42)* and Sham stimulation *(M=7.90, SD=3.52).* During stimulation, subjects reported minor adverse effects, including mild to moderate itching and tingling sensations under the electrodes. Slight tiredness and difficulty concentrating were also documented. A single subject described the incidence of a pulsing sensation corresponding to the area beneath the electrodes once stimulation had terminated. Only mild itching was persistent beyond the end of each session. Several subjects rated the

experience as marginally unpleasant, however, all subjects responded positively to participating in further tDCS studies (see Figure 7.9 for mean AEQ responses). Assessing the AEQ ratings obtained during stimulation for differences between tDCS conditions, the main effect of AEQ item was found to be statistically significant ($F(2.743,38.397)=7.650$, $p=.001$). This indicated that some items (e.g. Itching) were experienced more readily and with more severity than others (e.g. Pain). Importantly, the main effect for tDCS ($F(2,28)=.534$, $p=.592$) and the associated interaction (AEQ item*tDCS ($F(3.049,42.685)=1.233$, $p=.310$)) were non-significant, suggesting participants experienced similar peripheral sensations in all conditions.

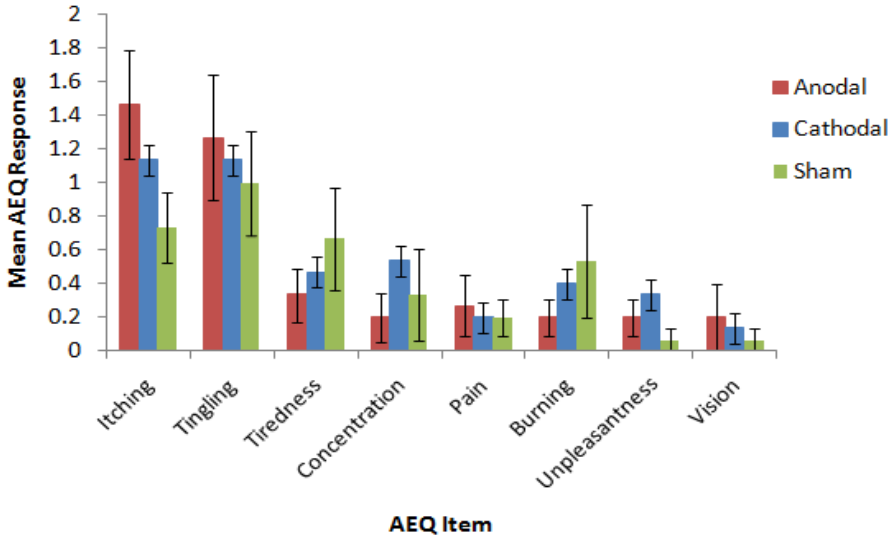

Figure 7.9. AEQ Responses. Average responses to the questionnaire items experienced during stimulation. The scale of responses ranged from 0 (not experienced) to 1-5, indicating heightened severity of the sensation experienced. Error bars represent ± 1 standard error (S.E.M).

To assess the influence of tDCS over time, scores were entered into a four-way Repeated Measures ANOVA. The DL values for each stimulation type are shown in Figure 7.10. No discernable differences between levels of each variable were visible. The between-subjects factor of tDCS order was non-significant ($F(5,9)=.555$, $p=.732$). The within-subject main effects for tDCS ($F(2,28)=.931$, $p=.406$), Time ($F(2,28)=.414$, $p=.665$), Run ($F(1,14)=3.710$, $p=.075$) and Condition ($F(1,14)=.758$, $p=.399$) were also non-significant. All possible interactions failed to reach significance, with the exception of a three-way interaction between tDCS, Time and Condition ($F(4,56)=2.881$, $p=.031$).

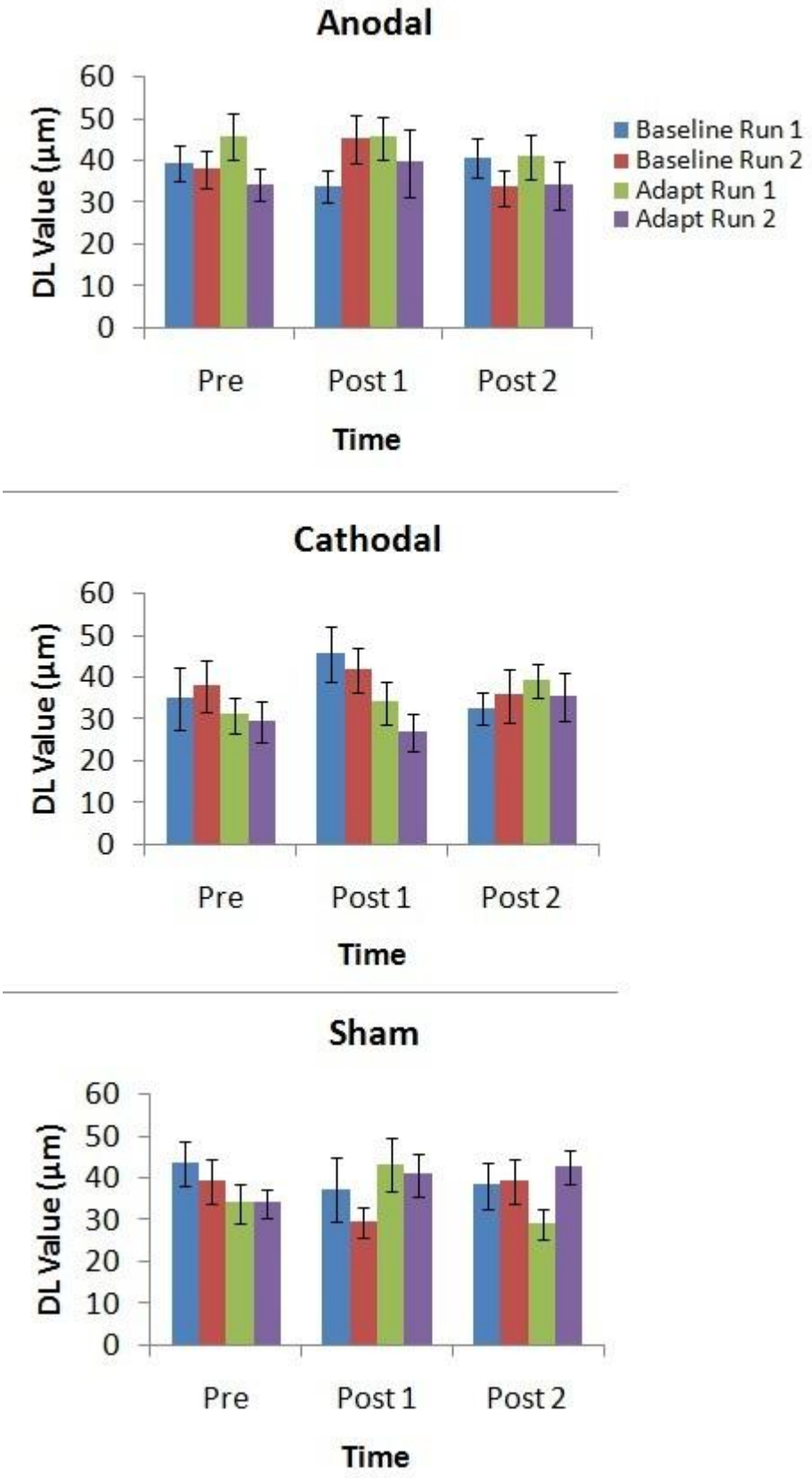

Figure 7.10. Vibrotactile-tDCS thresholds. Average DL values obtained for each stimulation type (Anodal, Cathodal, Sham) for an amplitude discrimination task during baseline and adapt trials. Error bars represent ± 1 standard error (S.E.M).

To discover the source of the three-way interaction, scores were collapsed across levels of the Run variable and a simple effects analysis was performed using a series of two-way repeated measures ANOVAs. A significant two-way interaction was produced for tDCS and Condition ($F(2,28)=5.283$, $p=.011$), corresponding to trials occurring at the Post 1 time point only e.g. immediately after stimulation.

Using a series of paired samples t-tests, it was determined that the significant differences occurred between cathodal and sham stimulation for the adaptation trials ($t(14)=-2.187$, $p=.046$) and between baseline and adaptation trials with respect to cathodal stimulation ($t(14)=3.138$, $p=.007$). As visible in Figure 7.11, these differences correspond to lower mean DL values for cathodal compared to sham stimulation for the adaptation trials and lower thresholds for the adaptation compared to baseline task corresponding to cathodal condition, immediately after stimulation.

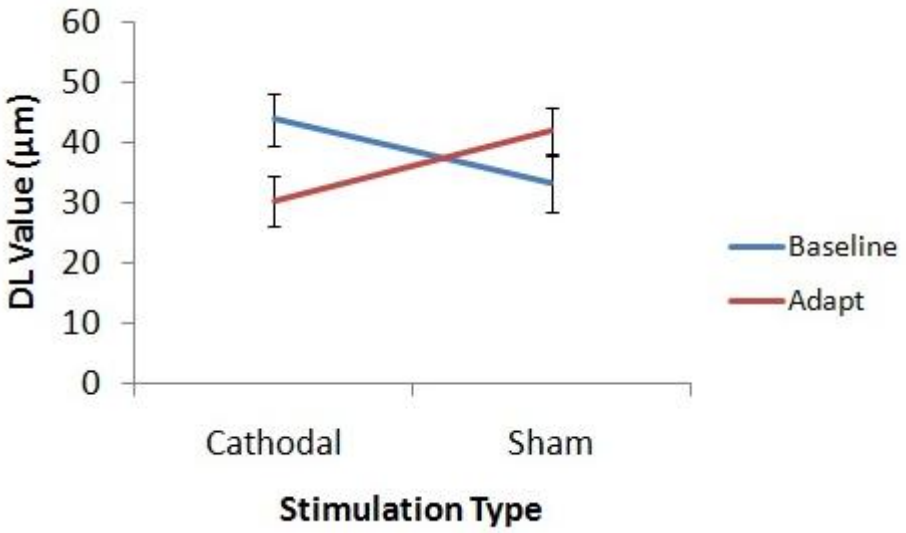

Figure 7.11. tDCS*Time*Condition Interaction. Average DL values obtained by collapsing across the variable 'Run'. Data represents trials performed during the Post 1 time point, immediately after stimulation. Error bars represent ± 1 standard error (S.E.M).

In contrast to the pilot data, the pre-tDCS results indicate that subjects achieved similar amplitude discrimination thresholds during both conditions. With regard to tDCS stimulation, no significant effects on discrimination thresholds were evident during the initial analysis. This did not differ as a product of tDCS order. However, subsequent analysis in light of the three-way interaction revealed a facilitation effect, whereby cathodal tDCS reduced DL values compared to sham when adaptation stimuli preceded the test phase and also produced the expected adaptation effect of lower DL values during adaptation trials, compared to those at baseline.

In addition to the frequentist analysis, a Bayesian analysis framework was adopted to further investigate the influence of cathodal tDCS at the Post 1 time point. In light of the present findings, the direction of the predicted outcome for cathodal tDCS was reversed when constructing the models for comparison - the alternative hypothesis, therefore, specified a decrease in DL values. Additionally, support for the null hypothesis was sought with respect to anodal tDCS. Here, the alternative hypothesis outlined at the outset of the study was retained.

The data was assessed using the MATLAB version of an online Bayes calculator (http://www.lifesci.sussex.ac.uk/home/Zoltan_Dienes/inference/bayes_factor.swf). A half-normal distribution model was chosen in light of the directionality of the predictions (Dienes, 2011; Dienes, 2014). In the absence of existing tDCS effect size data for the vibrotactile paradigm, the present study estimated that a tDCS modulation of the behavioural effect would be equivalent to half the magnitude of the established mean behavioural difference (between the Adapt and Baseline task conditions of the pilot data (50-32/2=18)). This formed the basis of the population standard deviation for each of the analyses. The population mean was set to zero for each model comparison. Sample mean and sample-size corrected, standard error values were calculated for the Adaptation condition (Sham-Anodal: *M=-0.53, S.E.M= 6.13*; Sham-Cathodal: *M=11.50, S.E.M=5.78*), for the Anodal condition (Baseline-Adapt: *M=-2.97, S.E.M=6.00*) and for the Cathodal condition (Baseline-Adapt: *M=13.4, S.E.M=4.70*).

The corresponding Bayes factors were as follows: Sham-Anodal (*B=0.30*), Sham-Cathodal (*B=3.57*), Baseline-Adapt (Anodal; *B=0.23*), Baseline-Adapt (Cathodal; *B=22.63*). In line with the accepted interpretation of these values (Jeffreys, 1961), the analyses indicate support for the null hypotheses which stated that anodal tDCS did not have an effect on the performance of the vibrotactile adaptation task. Conversely, strong support was evident for the alternative hypotheses in relation to the opposite polarity. This confirmed that the application of cathodal tDCS produced a reduction in adaptation thresholds, in comparison to those obtained following sham stimulation and also to those achieved during the baseline task.

7.4. Discussion

The current research aimed to investigate the role of modifications in cortical plasticity on amplitude discrimination performance. The study was also conducted with the wider aim of further investigating the physiological underpinnings of tDCS after-effects.

Results of the initial pilot study indicated that in the presence of dual-site adaptation stimuli, amplitude discrimination thresholds were vastly improved compared to baseline trials. However, the subsequent analysis of pre-tDCS trials in the main study failed to demonstrate this adaptation effect. The main study also failed to establish changes in task performance following the application of anodal tDCS. However, cathodal tDCS was shown to produce the expected adaptation effect and reduce adaptation thresholds compared to sham stimulation.

7.4.1. Vibrotactile pilot study

The results of the pilot study provide evidence that the presence of short duration, pre-exposure stimuli is sufficient to produce changes in information processing, which in turn, are substantial enough to influence behavioural performance. As suggested during a review of somatosensory dynamics (Kohn & Whitsel, 2002), the existence of the adaptation effect appears to facilitate the processing of vibrotactile stimuli. In the case of dual-site amplitude discrimination, this enhancement manifested as lower thresholds derived from adaptation trials. This finding parallels those of other studies investigating the dynamics of amplitude discrimination (Goble & Hollins, 1993; Delemos & Hollins, 1996; Tannan et al., 2007; Folger et al., 2008; Francisco et al., 2008; Francisco et al., 2011). Furthermore, this result was established with a pre-exposure duration of 520 ms, regarded as capable of engaging centrally mediated as opposed to peripherally mediated processing mechanisms (Whitsel et al., 2000; Bensmaia et al., 2005; Leung et al., 2005). Therefore, the study provides extended support to the notion of CNS mediated short-term plasticity and behavioural change (Zhang et al., 2011b; Nguyen et al., 2013a; Nguyen et al., 2013b). The CNS mediation of vibrotactile adaptation is likely to predominantly occur at the level of S1, where sharpening of the responses of individual neurons and synchronisation of population level firing have been demonstrated, following repetitive vibrotactile stimuli (Whitsel et al., 2003). The refinement of S1 response extends to behavioural performance via changes in gain and contrast, linked to lateral inhibition processes (Lee et al., 1992; Tommerdahl et al., 2002). As the current results are in accordance with those of previous studies, a similar approach to account for the results of the pilot study is adopted here. Consequently, the role of local competitive interactions between minicolumns remains the likely dominant factor in the modification of short-term plasticity and task performance (Tannan et al., 2007).

The pilot data also provides insight on the extent of the adaptation effect. With regard to the results of Tannan et al. (2007), improved DL values from 23 to 13 μm were

demonstrated following adaptation trials of 1 s duration. Taking an average of DL values from runs 1 and 2 of each task version, thresholds resulting from the current study were reduced from 50 to 32 μm, when subjects' were presented with 520 ms adaptation stimuli. While a similar pattern of results was observed, scores from the present study were considerably higher. As previously established in the animal literature, the funnelling of responses at the level of S1 is greatly influenced by duration, with larger performance improvements taking place with 5 s compared to 0.5 s periods (Simons et al., 2007). Improved amplitude discrimination ability has also been documented following 1-2 s as opposed to 0.5 s adaptation durations (Chiu, 2006). This has been associated with the time required for the evolving spatial pattern of S1 response to move beyond an enhancement in magnitude and extend to the inhibition of surrounding regions. Therefore, while the adaptation trials were subject to improvement, as expected, the shortened exposure duration in the present study may not have allowed for such a pronounced effect as previously established in the literature. However, the current research utilised standard and test values of 200-400 μm whereas the aforementioned study incorporated much lower amplitudes of 100-200 μm. This increased amplitude should have produced an enhanced adaptation effect, in accordance with the available animal literature (Chiu et al., 2005; Simons et al., 2005). However, on further inspection, this may not be the case. Francisco et al. (2008) demonstrated the effect of increasing amplitude using standard values ranging from 50-800 μm. In relation to the percentage difference of DL values obtained compared to the standard, values of 50-300 μm saw a dramatic improvement but the effect stabilised thereafter. Consequently, the improvements offered by increasing amplitude do not appear to exceed 300 μm and may, alongside the deviation in duration, account for the seemingly attenuated adaptation effect found by the current study.

7.4.2. Vibrotactile-tDCS study

7.4.2.1. Pre-tDCS findings

As illustrated by the pilot results and existing literature, the extent of the effect elicited by dual-site adaptation stimuli can vary considerably. Furthermore, the very existence of a dual-site adaptation effect can be extremely elusive (Prof. Mark Tommerdahl and Dr. Nicolaas Puts, personal communication). This can be conceptualised in relation to a ceiling effect, where it is difficult to establish a significant improvement in performance, particularly if discrimination capacity is already excellent at baseline. In

addition, there are several methodological factors that may also account for the distinction between pilot and pre-tDCS results.

Firstly, the sample population with respect to gender is likely to have contributed to the distinction between pilot and pre-tDCS results. On examining the pre-tDCS results, a collaborator (Prof. Mark Tommerdahl) remarked that a similar pattern had emerged in their lab when a group of male subjects had been tested by a female experimenter. The male subjects had exerted excessive force onto the vibrotactile stimulation device in an attempt to improve performance, which would have saturated their fine discrimination ability and made them worse at the task. This elimination of the beneficial influence of dual-site adaptation was restored in later sessions, which also seems to have occurred in the current study (if the data are considered chronologically as opposed to by tDCS type; Session 1= Baseline 40.7/Adapt 38.7, Session 2=38.9/39.1, Session 3= 36.6/26 μm). On the basis of this insight, the main effect of condition found in the pilot data was re-analysed by gender, as previously documented in the Results section. Given the size of the groups, meaningful inferences are difficult to make. However, when performance was assessed as a product of each run, female subjects were found to have statistically improved thresholds for the last of the two blocks (albeit in the presence of high variability on the first baseline run). It does appear that there was also a larger difference between conditions (indicative of the adaptation effect) for females than males. The pilot results derived from the female subjects suggest that their data contributed towards the overall significance of the main effect of condition more so than those of the male group, as the results of the female group approached significance. Given a larger number of subjects, which would be better able to discern group differences, this distinction between genders may have been significant. This is an important consideration as the performance of different genders may be a driving factor in the overall magnitude of results.

Additionally, differences in hormone regulation across genders may have contributed to the observed distinction in the pilot and pre-tDCS data. The performance of female subjects on vibrotactile detection measurements has been shown to fluctuate in accordance with the menstrual cycle (Gescheider & Verrillo, 1984). The thresholds of female subjects were found to vary across the course of the cycle, in response to stimulus frequencies of 250 Hz as opposed to 15 Hz (perhaps only implicating responses to vibratory stimuli governed by the Pacinian as opposed to Meissner corpuscles, which would not be relevant to the low-frequency stimuli administered in

the current study). Nonetheless, those taking oral contraceptives demonstrated stable thresholds, suggesting the documented effects can be associated specifically with the regulation of hormones. However, there is a lack of general consensus on the role of gender in determining vibrotactile thresholds as the limited results have not been consistent (see Goff, Rosner, Detre & Kennard, 1965; Verrillo, 1979; Ye & Griffin, 2011). With regard to the more complex demands of amplitude discrimination capacity, at present there are no known gender differences in performance per-se, with or without adaptation, regardless of experimenter gender (Jameson Holden, personal communication). Therefore, further studies would be required to verify the results of the current study in mixed and single sex samples, which should also incorporate a range of combinations reflecting the gender of the experimenter.

In addition to the effects of sample and experimenter gender, the majority of the sample population forming the initial study comprised of individuals' from the School of Psychology, who had gained experience of the tasks prior to taking part in the documented pilot study. This is in comparison to the tDCS study sample, largely recruited via external methods. Although the main effect of experimental run was determined to be non-significant, the enhanced performance found during the second compared to the initial run of the pilot study (especially for females) illustrates that the impact of increased familiarity with the task may be quite substantial. Introducing additional training trials, to stabilise individual thresholds and reduce within-subject variability, could filter out noise that may mask any true effects. Excessive exposure to the task, on the part of the author, may also have caused the task to become over-optimised. The task utilised an adaptation duration of half that commonly found in the literature and may be too difficult for most naive subjects. This does not appear to have been the case in relation to the pilot study data, however, in this instance it is possible that the benefit of prior experience may have attenuated the effects of task difficulty.

7.4.2.2. Post-tDCS findings

While the adaptation effect failed to manifest prior to the application of tDCS, cathodal stimulation was shown to produce lower adaptation thresholds compared to baseline. The effect of cathodal tDCS on adaptation thresholds was also evident compared to that of the sham condition. On the basis of the known neurobiological underpinnings of the behavioural paradigm and DC stimulation, the following explanation of results is proposed. Firstly, cathodal tDCS is likely to have led to a prolonged hyperpolarisation of the underlying neurons, forcing resting membrane potential away from the threshold

for action potential discharge (Creutzfeldt et al., 1962; Bindman et al., 1964; Purpura & McMurty, 1965; Nitsche et al., 2003c; de Berker et al., 2013; Radman et al., 2013; Rahman et al., 2013). This would have subsequently resulted in a shift towards inhibitory as opposed to excitatory cortical drive (Nitsche & Paulus, 2001; Nitsche et al., 2003b; Nitsche et al., 2004a), thus facilitating the efficiency of GABAergic, lateral inhibition required for optimal tactile processing to take place (Tommerdahl et al., 2002; Chiu et al., 2005; Simons et al., 2005; Simons et al., 2007). These effects of cathodal tDCS were present immediately after stimulation (Post 1) but not at the extended time point (Post 2), indicating that any alteration in cortical excitability failed to last more than 20 minutes (substantially shorter than reported for motor cortex; Nitsche & Paulus, 2001). However, a previously reported effect of cathodal stimulation on tactile frequency discrimination was only reported to last 7 minutes once stimulation had ceased (Rogalewski et al., 2004). This lack of sustained influence on task performance may be due to the proposed reduction of excitability in regions posterior to motor cortex (Antal et al., 2004a; Lang et al., 2007).

As evidenced by the lack of beneficial effect on baseline thresholds, the effect of cathodal tDCS had the greatest advantage on adaptation trials (where cues, in the form of variations in perceived stimulus intensity, were able to guide responses). This stimulation-induced boost to inhibitory processing capacity may have been necessary to adjust the normally consistent performance of male subjects, explaining the absence of the pre-tDCS adaptation effect in the all male sample. This is in accordance with the comparative lack of adaptation effect for males as opposed to females during the pilot study. Speculatively, this may be related to GABA levels in male subjects compared to females (Epperson et al., 2002; Smith et al., 2002), as has been proposed to account for the performance of those with ASD (thought to demonstrate a GABAergic deficiency; Tannan et al., 2008; Casanova et al., 2002; Casanova et al., 2003; Uhlhaas & Singer, 2006; Uhlhaas & Singer, 2012). Lower levels and/or the stability of GABA are likely to prevent male subjects from typically attaining levels of performance found in females, however, in this instance cathodal tDCS was able to produce the optimised GABA levels required for male subjects to harness the advantage of adaptation stimuli. Future research to define the nature of the tDCS after-effects in both male and female-only samples is needed to clarify whether sex differences present a realistic source of variability. If this is the case, it is important that more studies begin to take these gender effects into consideration. As a potential solution to allow mixed-gender studies, female

subjects could be recruited to participate at a given stage of their cycle, when oestrogen and progesterone are relatively stable (e.g. during the initial 7 days).

It is important to note that the observed effect of cathodal tDCS differs from that initially predicted. Although the demonstrated facilitation effect is compelling from a mechanistic perspective, the influence of cathodal stimulation was expected to result in a decrement in task performance - in line with the commonly cited "anodal/excitation, cathodal/inhibition" perspective on stimulation polarity. The results of the current study suggest this approach is likely to be greatly over-simplified. Accordingly, the effects are often non-linear within-polarity (when considering differences in stimulation time and intensity; Bastani & Jaberzadeh, 2013; Batsikadze, Moliadze, Paulus, Kuo & Nitsche, 2013; Monte-Silva et al., 2013; Fresnoza et al., 2014b). Furthermore, research with pharmacological agents has highlighted how anodal and cathodal stimulation should not necessarily be considered as polar opposites from a mechanistic perspective. Interventions often alter the effects of anodal stimulation, while the same substances have no influence on the brief and/or prolonged effects of cathodal stimulation (Nitsche et al., 2003b; Nitsche et al., 2004a). Therefore, the resulting effect of a given stimulation protocol is likely to be highly specific to the stimulation parameters and paradigm in question (Benwell et al., 2015; Bortoletto et al., 2015).

In the context of the cathodal results, anodal tDCS may have been expected to worsen adaptation performance on the basis of a decrease in GABAergic processing efficiency. This would have been biologically plausible due to the greater dynamic range with which positive current stimulation would have had to degrade performance as opposed to the limited scope negative current stimulation had to improve performance. However, an explanation for the relative absence of an anodal stimulation effect can be derived by considering the specifics of the current study. Pirulli, Fertonani and Miniussi (2014) placed the emergence of cathodal facilitation effects in the context of localised cortical depression, which other regions dynamically respond to. These additional regions are, therefore, proposed to contribute to the observed effect of cathodal stimulation, which is rooted in the adaptive response of the cortex. An ideal region to respond to such excitability changes would be the homologue of the opposite hemisphere. Accordingly, recent evidence has highlighted the existence of direct interhemispheric connections between S1 regions (Ragert et al., 2011) and the functional importance of the ipsilateral hemisphere in processing tactile information (for a review of human and non-human primate studies; see Tommerdahl, Favorov & Whitsel, 2010).

Crucially, both S1 regions were stimulated via the bihemispheric montage adopted by the current study. Speculatively, inducing cortical depression in the hemisphere contralateral to the stimulus and elevating excitability in the opposite, ipsilateral hemisphere (to which the tactile stimuli were delivered) may have resulted in the enhanced influence of ipsilateral S1, which is normally engaged in stimulus processing albeit to a lesser extent than the contralateral hemisphere. This unique circumstance of altering the recruitment demands of both hemispheres via cathodal tDCS is likely to have led to optimised performance - particularly if the cortical inhibition of the contralateral hemisphere was of a beneficial nature, as previously discussed. If this was the case, elevating excitability in the hemisphere contralateral to the stimulus (as predicted for anodal stimulation) would be considered detrimental to performance. However, as the ipsilateral hemisphere had undergone cortical depression, resources may have been diverted between hemispheres to regulate excitation, which attenuated what would have otherwise produced a maladaptive effect due to the contralateral excitability enhancement. Therefore, although the study cannot explicitly comment on physiological task mechanisms, this explanation may account for why behavioural performance was not significantly altered following anodal stimulation. Importantly, adopting a different electrode configuration (e.g. S1/contralateral orbit) may change the resulting effects due to the altered influence of DC stimulation on somatosensory network-level interactions. It is these interactions that appear to be crucial in the generation of the observed results as opposed to the impact of tDCS on isolated regions.

Lastly, it should be noted that despite the seemingly beneficial influence of the bihemispheric montage during the current study, there have been mixed results on their efficacy (Vines et al., 2008; Mordillo-Mateos, Turpin-Fenoll, Millán-Pascual, Núñez-Pérez, Panyavin, Gómez-Argüelles... & Oliviero, 2012; Sehm et al., 2012; Fusco, De Angelis, Morone, Maglione, Paolucci, Bragoni & Venturiero, 2013; Kidgell, Goodwill, Frazer & Daly, 2013; Sehm et al., 2013b). Selecting a bihemispheric montage will often mean the electrodes are positioned closer together than is typical and there is evidence to suggest this may lead to an excessive amount of the current being shunted through the scalp rather than entering the cortex (Datta, Elwassif, Battaglia & Bikson, 2008). Taking the potential issues surrounding electrode proximity and position into account, the effects of bihemispheric montages are evidently not yet properly understood.

7.5. Conclusions

In relation to the vibrotactile adaptation tasks, it is likely that the variation in male and female performance was the driving factor underlying the distinction between pilot and pre-tDCS results. As such, gender differences may go some way to explaining the elusiveness of the dual-site adaptation effect. With regard to tDCS, its effect on vibrotactile adaptation performance varied between polarities. While cathodal tDCS improved adaptation thresholds, anodal tDCS had no effect on behaviour (although this is not to say an effect was not present at a physiological level, beyond the scope of the study). These findings most likely occurred as a combination of the physiological underpinnings of the task and the implemented bihemispheric montage. Beyond the task and stimulation parameters, the study indicates that the effects of tDCS are likely dependent on the individual capacity of participants. Male subjects failed to demonstrate an adaptation effect prior to stimulation, potentially due to the stability of the GABAergic system that governs task-specific lateral inhibition mechanisms. It appears that cathodal tDCS heightened the efficiency of these mechanisms and ultimately optimised performance, by enabling subjects to fully utilise adaptation cues. As such, the results highlight how the effects of tDCS are likely to be more complex than previously anticipated. This will undoubtedly have implications for existing models outlining the mechanisms of action of the neuromodulation technique, which should be adapted accordingly to account for such observations.

8. General Discussion

The research aimed to investigate the neurobiological basis of tDCS. Each experimental chapter was designed to probe the previously proposed mechanisms by focusing on distinct outcome measures. Neuroimaging techniques were utilised to measure resulting fluctuations in key neurochemicals and neuromagnetic responses, while behavioural paradigms were used to detect stimulation-induced changes in task performance. The spectroscopy study failed to demonstrate the anticipated significant decrease in GABA and increase in Glx concentration. However, in line with our expectations, the optimised GABA acquisition presented the most promising findings, providing modest support for the role of inhibitory neurotransmission in the generation of tDCS effects. With regard to the concurrent tDCS-MEG research, the amplitude of transient motor evoked responses was shown to be enhanced during active compared to sham tDCS. Additionally, power in the visual gamma band was found to be reduced with respect to the active condition. These results support and extend findings that suggest tDCS is able to modulate resting membrane potential (particularly cortical excitability of the motor region) but definitive evidence for prolonged, synaptic change was not evident. Finally, the behavioural research highlighted the specificity of tDCS effects; where active stimulation was shown to improve performance on the dual-site adaptation paradigm, with no effect on the single-site version of the task. These studies implicate the importance of variations in stimulation parameters and how they likely interact with the physiological underpinnings of an administered task. Taken together, adopting the approach of conducting innovative behavioural and neuroimaging research has led to novel insights into the underlying mechanisms of the effects of tDCS.

8.1. Neuroimaging Studies

The neuroimaging component of the research was designed to provide insight into the neurobiological mechanisms underlying responses to tDCS. Magnetic resonance spectroscopy was utilised to study the role of key excitatory and inhibitory neurochemicals, while Magnetoencephalography was employed to investigate the generation of tDCS effects via changes in induced and evoked neuromagnetic responses.

8.1.1. Magnetic Resonance Spectroscopy

The lack of significant findings regarding changes in GABA and Glx was unexpected, given the available evidence (Stagg et al., 2009; Stagg et al., 2011b; Clark et al., 2011;

Kim, Stephenson, Morris & Jackson, 2014; Hunter et al., 2015; Bachtiar et al., 2015). While the existing literature converges on the occurrence of anodal tDCS effects arising from a prolonged increase in cortical excitability (thus implicating the function of glutamatergic pyramidal cells and GABAergic interneurons: Stagg & Nitsche, 2011; Medeiros et al., 2012), the current study was unable to corroborate this.

With regard to GABA, the results were unlikely to be related to any major methodological issues as the study largely replicated the design of that used by Stagg et al. (2009). However, the preceding study may have benefitted from the explicit assessment of cortical excitability before and after tDCS, via measurement of MEPs, to ensure that the stimulation had had the desired effect. It is likely that anodal stimulation did alter excitability levels in some participants, as the main effect of tDCS came close to reaching significance in the GABA' analysis, but the degree of inter-individual variation observed indicated that differences in response to tDCS were particularly prominent. It has recently been proposed that approximately 25% of subjects may not have the expected response, which should be acknowledged when determining the ideal sample size (Wiethoff et al., 2014). The figure for the current study was in the region of ~33%, such that the extent of variance most likely played a contributing role in the non-significance of the results. Significant changes in Glx, following anodal stimulation, have only thus far been noted where the stimulation intensity and duration have far exceeded that of typical studies and the sequence used was optimised to detect glutamate (Clark et al., 2011), which may account for the absence of such an effect in this instance. In future, it is advised that studies of this nature should endeavour to investigate a single neurochemical of interest. This would simplify the design and ensure that sequences can be tailored appropriately to increase the likelihood of accurate quantification.

Combined tDCS-spectroscopy studies have provided insight into the nature of stimulation-induced after-effects, however, the most compelling findings (that suggest tDCS effects are dependent on GABAergic and glutamatergic function) have come from pharmacological interventions, which are able to directly influence synaptic activity (Liebetanz et al., 2002; Nitsche et al., 2003b; Nitsche et al., 2004a; Nitsche et al., 2004b; Kuo et al., 2008; Monte-Silva et al., 2013; Fresnoza et al., 2014b). MRS is unable to specifically quantify synaptic concentrations, meaning such changes may be largely beyond the scope of the technique. Despite its lack of specificity, MRS is currently the only means of non-invasively addressing neurochemical change *in vivo*

and advances in methodology are likely to assist in circumventing this issue (Puts & Edden, 2012).

Instead of utilising MRS in isolation, a more advantageous approach may be to integrate the method into studies featuring a pharmacological component. As previously stated, the existing pharmacological tDCS literature has provided the most persuasive findings but incorporating spectroscopic measures of neurotransmission could provide a direct perspective on the nature of tDCS-induced change at a neurochemical level, as opposed to simply measuring MEPs as an index of cortical excitability. For example, by assessing change in MEPs alongside potential fluctuations in the neurochemical of interest, a range of tDCS protocols could be implemented to determine under what circumstances stimulation-based changes are able to be quantified from unspecified pools of the neurochemical as opposed to engaging receptor-specific, synaptic activity. Agents designed to target neuromodulators, such as dopamine and serotonin (shown to influence response to tDCS; Kuo et al., 2008; Nitsche et al., 2009; Fresnoza et al., 2014b) could also be administered, with excitatory and inhibitory neurotransmission acting as surrogate markers as these chemicals cannot be directly imaged with MRS.

8.1.2. Magnetoencephalography

Anodal stimulation was found to reduce average power in the visual gamma band. Accordingly, the release from inhibition that is thought to synchronise pyramidal cell response may have been relatively absent in the presence of anodal stimulation (Bartos et al., 2007; Gonzalez-Burgos & Lewis, 2008; Buzsáki & Wang, 2012). This could have led to a suppression of firing and thus a decrease in oscillatory power. Such an account would strengthen the evidence for the role of GABAergic mechanisms in the generation tDCS effects. However, much like the promising but non-significant results of the GABA' analysis from the spectroscopy study, because the Time*tDCS interaction was not significant this finding must be interpreted with caution. Consequently, the MEG study also failed to produce definitive evidence for the emergence of prolonged, synaptic alterations as a result of tDCS.

Pilot work was conducted to determine whether simultaneous stimulation and neuromagnetic recordings could take place as part of the study. In accordance with Soekadar et al. (2013), concurrent tDCS-MEG was found to be feasible. Therefore, unlike the MRS study, the MEG research featured an "online" component, where electrophysiological change could be established during stimulation. This is where an

increase in the magnitude of the MF and MEF1 evoked responses was found, emphasising the benefit of such study designs. These responses have been shown to correspond to the preparation and subsequent execution of movement (Deecke et al., 1982; Cheyne & Weinberg, 1989; Kristeva et al., 1991; Chen et al., 1998; Chen & Hallett, 1999). The presence of DC stimulation, therefore, appears to have facilitated an increased readiness to respond and engage in task-related movement. These alterations in evoked motor responses are in accordance with the literature that has found evidence of neuronal depolarisation and elevation in spontaneous firing associated with anodal tDCS (Creutzfeldt et al., 1962; Bindman et al., 1964; Purpura & McMurtry, 1965) as well as studies that have demonstrated the ability of anodal stimulation to increase corticospinal excitability (Nitsche & Paulus, 2000/2001). Therefore, this aspect of the MEG study was able to support the existing knowledge of the influence of anodal polarisation on motor cortex responsivity.

The presence of modulations only during direct current stimulation indicates that aspects of the stimulation protocol or study design are likely to have prevented the sustained depolarisation and resulting rise in intracellular sodium and calcium concentration needed to trigger a change in synaptic strength (Liebetanz et al., 2002; Nitsche et al., 2003b; Nitsche et al., 2004b). The stimulation duration may have not been sufficient for changes in neuronal synchronisation to take place (Notturno et al., 2014). The use of a maximum contrast stimulus may have also contributed to the findings by introducing a 'ceiling effect' (Antal et al., 2004a). Additionally, typical tDCS effects have been shown to be altered if stimulation is delivered during task performance, particularly for tasks involving motor actions such as that utilised by the present study (Antal et al., 2007; Horvath et al., 2014). This makes it especially difficult to know when to administer stimulation in conjunction with a behavioural task or whether to simply address the effects of tDCS on resting state activity in order to avoid this issue. The importance of conducting pilot investigations to determine the likelihood of these outcomes should be emphasised as part of future research, such that the induction of neuroplastic change is not disrupted by aspects of methodological design.

8.2. Behavioural Studies

The behavioural component of the research aimed to investigate the role of modifications in cortical plasticity on vibrotactile amplitude discrimination performance, with the wider aim of further investigating the physiological underpinnings of tDCS after-effects.

8.2.1. Single-site adaptation

The expected degradation of task performance was established during pre-stimulation, baseline trials of the single-site adaptation task (Tannan et al., 2007; Zhang et al., 2009; Puts et al., 2013). However, no change was evident following anodal compared to sham tDCS. This was confirmed with a Bayesian analysis approach, having derived a Bayes factor for the SSA task that provided substantial evidence for the null hypothesis. As proposed for the MRS study, inter-individual differences in the response to tDCS may have contributed to the lack of observed change in SSA thresholds. In support of this notion, several Quantitative Sensory Testing (QST) studies adopting identical stimulation protocols have established dramatically different results (Bachmann et al., 2010; Grundmann et al., 2011; Jürgens et al., 2012). Additionally, the electrode montage used may have meant that the maximum current was focused over the vertex rather than S1 (as indicated by a recent simulation study; Rampersad et al., 2014). This emphasises the importance of estimating the current flow for each implemented electrode configuration. Such a computational modelling approach to derive realistic head models will no doubt become increasingly integral to future tDCS studies (Bikson & Datta, 2012; Russell et al., 2013; Kim, Kim, Chang, Kim, Kim & Im, 2014).

The nature of the task (as it did not feature an explicit learning component, unlike the paradigms used by Nitsche, Schauenburg, Lang, Liebetanz, Exner, Paulus & Tergau, 2003c; Stagg et al., 2011b; Kim, Stephenson, Morris & Jackson, 2014) may have prevented the necessary reduction in inhibition and parallel increase in NMDA receptor efficiency for LTP to take place, making it difficult for tDCS to modify behavioural performance. It should also be acknowledged that while no behavioural change was evident after stimulation, this does not rule out the possibility that excitability changes may have taken place during stimulation (as observed by Rogalewski et al., 2004; Ragert et al., 2008).

Unlike the MEG study, the behavioural research was conducted in a pre/post design, such that the ‘online’ effects of stimulation were unknown. As previously documented, there is on-going debate in the literature relating to the ideal point at which stimulation should be administered (Horvath et al., 2014) and consequently, delivering tDCS at rest is associated with both benefits and limitations. By delivering stimulation at rest, physiological responses to tDCS that require temporal evolution to support extended modifications of performance are able to develop without potentially being abolished by responses associated with a particular task e.g. finger movements (Antal et al., 2007).

The online protocol adopted during the MEG study may have influenced the development of longer-lasting modifications in plasticity in this manner. Alternatively, administering stimulation prior to task performance can be extremely detrimental, as evidenced by Stagg and colleagues in a series of experiments conducted into motor learning. Performance relating to such paradigms appears to benefit from the delivery of anodal stimulation during the task but administering stimulation at rest, before the task, can abolish or even reverse any positive effect (Stagg, Jayaram, Pastor, Kincses, Matthews & Johansen-Berg, 2011d). This is likely related to the regulation of synaptic plasticity, whereby the successive presentation of two separate sources capable of LTP-induction typically results in LTD (Abraham, 2008). Recent evidence suggests that this effect is likely driven by the engagement of $GABA_A$ receptors (Amadi, Allman, Johansen-Berg & Stagg, 2015). Delivery of tDCS before the task translated to a decrease in learning, suggested to take place via blockade of further LTP-induction due to increased inhibitory synaptic activity (determined using a 2.5 ms SICI protocol). Therefore, where an explicit learning component is engaged it is unlikely that delivering stimulation prior to the task will be beneficial. Ultimately, it appears that the utility of performing online or offline protocols will be determined by the nature of the task in question and whether it is also able to induce prolonged changes in the response of the underlying neurons.

Physiological alterations may have been evident but were not indexed as part of the SSA study (Suntrup et al., 2013). This is a distinct advantage of combining behavioural paradigms with neuroimaging (Hunter et al., 2013). However, simplistic designs are likely to be the most effective with regard to establishing and adequately interpreting the effects of stimulation, as documented in the MEG section. By incorporating multiple components into a single study, the added complexity of the methodology may obscure the likelihood of revealing compelling findings to begin with.

8.2.2. Dual-site adaptation

During the mixed-gender pilot study, amplitude discrimination thresholds were vastly improved compared to baseline trials in the presence of dual-site adaptation stimuli (Kohn & Whitsel, 2002; Tannan et al., 2007). However, in the male-only tDCS experiment, the adaptation effect was not demonstrated for the pre-stimulation trials. As with MRS-derived measures of GABA (Epperson et al., 2002) and responses to tDCS (Chaieb et al., 2008), the performance of female subjects on vibrotactile tasks has been shown to fluctuate in accordance with the menstrual cycle (Gescheider, Verrillo,

McCain & Aldrich, 1984). In this instance, females were shown to outperform males and thus greatly contribute towards the observed adaptation effect, providing the rationale for the distinction between pilot and pre-tDCS findings.

As in the SSA study, anodal tDCS failed to alter responses to dual-site adaptation stimuli, however, more promising findings were observed with respect to cathodal stimulation. The adaptation effect was reinstated and adaptation thresholds were reduced compared to sham stimulation but this finding only emerged having reduced the complexity of the statistical design. This point echoes the previously outlined need to conduct simple experiments as multi-factorial analyses complicate the interpretation of basic effects. The outcome of cathodal stimulation was also in the opposite direction to that initially predicted. This highlights the need for caution when adopting the standard "anodal/improvement, cathodal/decrement" perspective on stimulation polarity, as this account appears to be greatly over-simplified. Cathodal tDCS is likely to have forced resting membrane potential away from the threshold for action potential discharge (Creutzfeldt et al., 1962; Bindman et al., 1964; Purpura & McMurty, 1965; Radman et al., 2013; Rahman et al., 2013). This would have resulted in a shift towards inhibitory as opposed to excitatory cortical drive (Nitsche & Paulus, 2001; Nitsche et al., 2003b; Nitsche et al., 2004a), thus facilitating the efficiency of GABAergic, lateral inhibition required for optimal tactile processing to take place (Tommerdahl et al., 2002; Chiu et al., 2005; Simons et al., 2005; Simons et al., 2007). This stimulation-induced boost to inhibitory processing capacity may have been necessary to adjust the normally consistent performance of males, due to the stability of GABA in male subjects compared to females (Smith et al., 2002). Therefore, this account proposes that male subjects are less likely to benefit from adaptation cues than females and that cathodal tDCS produced the optimised GABA levels required to harness the advantage of such stimuli.

The success of the dual-site adaptation study may simply be explained by the use of the cathodal polarity, which did not feature in any of the other investigations due to the inherent increase in the number of required experimental sessions. However, the use of a bihemispheric montage could have also had a substantial contribution. Cathodal facilitation effects have previously been placed in the context of localised cortical depression, which other regions dynamically respond to due to the adaptive nature of the cortex (Pirulli et al., 2014). In this instance, the presence of direct interhemispheric connections between S1 regions (Ragert et al., 2011) could have meant that the

homologue region of the opposite hemisphere was involved in tactile information processing to a greater extent, following cathodal tDCS, which appears to have been highly beneficial. Therefore, the dual-site adaptation study demonstrated the importance of engaging a cortical network with a given stimulation intervention, as opposed to targeting isolated regions. The bihemispheric montage may have been the key to observing a tDCS effect in this instance and would explain why the SSA study was unsuccessful, as it implemented a unihemispheric configuration.

It should also be considered that the results of the behavioural studies may reflect the use of strategies. Rather than responses being a product of altered sensitivity due to adaptation and/or tDCS, there is a possibility that participants adopted certain strategies to better enable them to perform the tasks. For example, comparing the intensity of the test stimulus to that of the preceding adaptation stimulus as opposed to the standard stimulus or referencing the test stimulus against an internal representation of average test intensity. In the context of the former, where the adaptation and standard are identical, it may be presumed that the temporal segregation between the adaptor and the test could aid response accuracy. Whereas in the latter, subjects likely presume that test stimuli are made up of more and less extreme values and so determine the likely average, responding to the current test item on the basis of whether it is more or less intense than this perceived mean value.

In the SSA study, being able to separate the comparison stimuli from the context of the presumed perceptual imbalance (that is said to occur following adaptation), would have undoubtedly been beneficial and may have meant DL values remained similar to those achieved at baseline. This could have been accomplished using either of the strategies outlined above; referencing the test stimulus to the strength of the temporally distant adaptor stimulus or comparing the test stimulus to an internal, rather than a directly perceived, standard. However, the adaptor was still able to produce an increase in DL, indicating that no such strategy was implemented (at least not successfully). No statistically significant difference was noted between the SEQ and SIM versions of the baseline task, which differ in their presentation of stimuli in terms of relative timing. This also serves to highlight how adopting a strategy based on temporal segregation was unlikely to be successful in this instance.

These strategies may be more applicable to the DSA task, in which performance did improve following adaptation and cathodal tDCS. However, this should be considered unlikely because the internal standard would need to be constantly updated as new test

amplitudes were delivered and also be extremely accurate to avoid chance levels of performance. The gains of adopting this strategy, therefore, would not outweigh the costs in relation to effort and maintenance. It is also unlikely to be the dominant reason for the decrease in DL values on the basis of pharmacological evidence. Folger et al. (2008) demonstrated that dual-site adaptation task performance (in addition to that of the single-site version) was modified by consumption of Dextromethorphan (DXM). More specifically, dual-site performance was degraded in the active substance group compared to those who had been given a placebo. Task performance under DXM was proposed to mimic that observed in those with ASD, which in this instance meant that subjects were unable to tune neural responses and reduce their thresholds having been exposed to the adaptation stimulus. Had subjects been primarily relying upon strategies as opposed to responding based on altered CNS sensitivity, the pharmacological intervention may not have produced significantly different results compared to baseline. Accordingly, to provide exclusive support for the strategy explanation, discrimination thresholds would need to be maintained at pre-drug levels in those assigned to the active substance group of such a pharmacological intervention study. Therefore, while the potential for strategies to be implemented in addition to the aforementioned change in physiological processes cannot be ruled out entirely, the available evidence suggests that adaptation performance must be based to a large extent on transient changes in use-dependent plasticity. To enhance knowledge regarding subject responses, participants could be asked to provide details on any consciously adopted strategies that were implemented during the experiment.

Taken together, the amplitude discrimination results suggest that the effects of tDCS may not always emerge at the level of behaviour and when they do it is likely to reflect an interaction between the chosen stimulation parameters, the underlying mechanisms of the implemented task and potentially even participant strategies. For this reason, it is crucial that more behavioural-tDCS research is conducted using paradigms where their physiological underpinnings are already well-established or can be investigated using neuroimaging techniques.

8.3. General Limitations & Future Directions

Several themes emerged from this series of studies that should be viewed as general concerns surrounding tES research. Firstly, the issue of achieving sufficient statistical power is prevalent throughout the fields of neuroscience and psychology (Button, Ioannidis, Mokrysz, Nosek, Flint, Robinson & Munafò, 2013) but is a particular

concern where studies are novel, such as those conducted here. tES research has seen a resurgence in the past 10-15 years and an increasing amount of studies incorporating tDCS, tACS and/or tRNS have been published each year. Subsequently, the interest surrounding these neuromodulation techniques has seen them applied to a multitude of domains with an even more substantial variety of stimulation protocols. Although the wide remit of the research conducted thus far has demonstrated the scope of applications, this diversity has propagated a lack of coherent themes and replication of studies, which is detrimental when attempting to determine adequate sample sizes.

As prime examples, a-priori power calculations were conducted for the MRS study and the single-site adaptation study but both resulted in non-significant results. The spectroscopy study sample was based on data from an almost identical investigation that had successfully established the outcome we predicted (Stagg et al., 2009), which should have meant the sample was sufficient to detect effects. However, the presence of individual differences in participant responses to tDCS meant that the estimated sample size was likely inadequate. This highlights the uncertainty surrounding estimates of power that are based on single studies. Had more studies of this kind been previously conducted, such variability would likely have been reflected in the estimated sample size. Given the strength of evidence for the role of neurotransmission (Stagg & Nitsche, 2011), it is not thought that our non-significant results represent an accurate perspective of the effects of tDCS. It is, therefore, predicted that the results do not truly reflect the null hypothesis. Consequently, had there been less variability in the sample or additional subjects been recruited, it is likely there would have been a significant decrease in GABA' following anodal tDCS.

For the SSA study, the sample size estimate was based on the effect size related to the behavioural tasks in the absence of past tDCS-oriented data. Therefore, the initial number of participants required for an observable tDCS effect to arise could have been underestimated. The variability in task responses, particularly for the SSA version, could have also compounded this issue. However, significant tDCS effects have previously been shown to emerge in samples of this size (Elmer, Burkard, Renz, Meyer & Jancke, 2009; Ladeira, Fregni, Campanhã, Valasek, De Ridder, Brunoni & Boggio, 2011; Spiegel, Hansen, Byblow & Thompson, 2012; Tang & Hammond, 2013; Pavlova, Kuo, Nitsche & Borg, 2014) and the dual-site adaptation task (chapter 7) resulted in a significant cathodal tDCS effect with an equivalent number of subjects given the

additional tDCS mode. This suggests that it is entirely possible to derive tDCS effects from such samples (while also considering the caveat of false positives).

Further analysis using a Bayesian approach revealed sufficient evidence for the null hypothesis, supporting the assumption of the frequentist statistics that tDCS had no influence on SSA amplitude discrimination thresholds. It is possible that it was the specific set of circumstances that generated the null finding in this particular instance but it is unlikely that simply increasing the number of participants to enhance power would address this. The DSA study highlighted how tDCS effects are likely to be extremely dependent on the target of stimulation (isolated regions vs. network-level engagement) as well as the demands of each task and the nature of the adaptation cue (beneficial or detrimental to information processing), suggesting the fundamental details of the investigation are likely to have led to the outcome of the SSA study as opposed to the results representing a false negative. However, the issue remains that power calculations are of little use if they aren't based on sufficient data and there is a basic need for a larger volume of similar studies (in relation to the methods, paradigms and stimulation protocols adopted) that can be used to generate more accurate sample-size calculations. Without such a wealth of studies to draw upon, accurate assessment of the efficacy of tDCS is prevented and recent reviews of this topic (Horvath et al., 2015a/2015b) have been criticised for basing meta-analyses on such diverse data (Nitsche, Bikson & Bestmann, 2015). Nonetheless, the need to establish consistent findings will undoubtedly have to be emphasised in future if the effects of tES are to be validated, such that the outlook for the field can represent 'significant progress and promise for the future' (Bikson, Edwards & Kappenman, 2014).

Aside from the variety of research conducted, there is also a tendency for tES methods to be paired with complex cognitive tasks, in an attempt to assess how cognition can be boosted (Cohen Kadosh, Soskic, Iuculano, Kanai & Walsh, 2010) or applied as a potential treatment for a given neurological or psychiatric condition (Brunoni et al., 2012). In contrast, there are relatively few investigations into the underlying neurobiology of the technique and the mechanisms by which the desired after-effects actually emerge. Studies concerning the systematic adjustment of stimulation parameters - for example, the influence of longer durations or increases in current density and distinctions between administering 'online' or 'offline' stimulation - are also largely absent. Consequently, even subtle variations in stimulation protocols can make interpreting results from different studies extremely difficult. These are all issues

that need to be tackled prior to more elaborate, application-oriented studies taking place. It can, therefore, be said that those involved in tES research often attempt to 'run before they can walk'. The studies conducted here attempted to address this issue and have shown that pilot studies to optimise stimulation parameters are crucial (as also emphasised by Kuo, Paulus & Nitsche, 2014). For this reason, continued investigations are needed into the basic principles of tDCS effects before such therapeutic aims can be properly addressed.

The role of individual differences has been proposed to be a prominent factor in the results of tDCS research and may also be seen to undermine our understanding of the method and its therapeutic validity (Horvath et al., 2014; Krause & Cohen Kadosh, 2014). A number of specific types of between-subject variability, ranging from gender to genetics, are outlined as potential influences with regard to the findings presented within this thesis. To account for typical and atypical results, participants are often characterised as responders or non-responders, indicating that tDCS is unlikely to have the same effect on every individual. This shouldn't change our understanding of the underlying physiological mechanisms but suggests not everyone has the same potential to experience tDCS-induced changes in plasticity. For example, responses to tDCS among young and older adults as well as healthy older adults and those diagnosed with Alzheimer's disease are thought to differ on the basis of changes that determine plasticity, such as decreasing levels of GABA and glutamate (Hsu, Ku, Zanto & Gazzaley, 2014). Therefore, such studies acknowledge that individual differences in response to tDCS across the lifespan are apparent but highlight that this variability is likely due to alterations in the precise physiological mechanisms proposed to drive the effects of the stimulation method.

In a clinical capacity, individual differences inevitably have implications for the validity of tDCS as a universal treatment. However, it should be noted that this is often the case and interventions, whether pharmacological or psychological, do not have maximal success rates. Disorders where tDCS has been trialled often have complex aetiologies (e.g. schizophrenia) that are only partly understood and differ in each patient, which is why tDCS should be seen to represent one of many options and should not be regarded as a miracle intervention. There is a definite need for researchers to consider whether the known mechanisms of tDCS align with those of their chosen clinical target to maximise the likelihood of discovering a viable treatment. This makes it increasingly important to refine the application of tDCS towards the most neurobiologically relevant

disorders, such as those requiring regulation of excitatory and inhibitory signalling. This is most likely why tDCS continues to be so successful in stroke rehabilitation (Allman, Amadi, Winkler, Wilkins, Filippini, Kischka... & Johansen-Berg, 2016).

Additionally, instances where tDCS has been proposed to be of benefit but has yet to be shown to have an effect may simply reflect the need to use different parameters. Although the technique doesn't appear to act in an entirely predictable linear fashion (Batsikadze et al., 2013), considering the needs of a specific population or individual may be the key to achieving the desired outcomes. With regard to the ageing population, older participants have been shown to benefit from longer stimulation periods as mechanisms of synaptic plasticity become less efficient (with variability in this observation being attributed to related genetic factors; Puri et al., 2015). Consequently, as reflected upon in a recent article, attributing generic labels such as "tES is good for all" or "tES is not good at all" fails to take all of these complexities into account (Fertonani & Miniussi, 2016). Moving forward, future studies should be encouraged to acknowledge these individual difference factors by controlling for their influence or seeking to find ways in which to circumvent the impact of diversity.

Of particular importance to the clinical efficacy of tDCS, is the ability of the method to offer sustained benefits across sessions and with repeated doses. This has been shown in samples with stroke (Lefebvre, Dricot, Laloux, Gradkowski, Desfontaines, Evrard… & Vandermeeren, 2015), chronic pain (Concerto, Al Sawah, Chusid, Trepal, Taylor, Aguglia & Battaglia, 2015) and Alzheimer's dementia (Boggio, Ferrucci, Mameli, Martins, Martins, Vergari… & Priori., 2012; Khedr, El Gamal, El-Fetoh, Khalifa, Ahmed, Ali… & Karim, 2014) and infers that the continued delivery of stimulation will eliminate the transience of the after-effects produced (at least until the implemented follow-up test period, typically at 4 weeks). A given stimulation pattern may, therefore, produce carry-over effects that translate to between-session as opposed to within-session benefits. However, beyond the typical 4 week follow-up, habituation to DC protocols may arise with continued exposure that would place limits on the extent of their therapeutic ability. In a similar state-dependent manner that tDCS is able to modulate responses to rTMS (Cosentino, Fierro, Paladino, Talamanca, Vigneri, Palermo… & Brighina, 2012), implementing tACS or tRNS prior to administering tDCS may facilitate maximal benefits in homeostatic plasticity and prevent adaptation from occurring (Abraham, 2008; Silvanto, Muggleton & Walsh, 2008).

It is important to note that such cumulative or carry-over effects may equally be observed with detrimental outcomes. In one particular study, an inter-session interval of 24 hours abolished the expected rise in motor cortex excitability after anodal tDCS (Monte-Silva et al., 2013). Conversely, two doses of cathodal tDCS (10 minutes apart) have been shown to improve working memory capacity (Carvalho, Boggio, Gonçalves, Vigário, Faria, Silva… & Leite, 2015). While conducting anodal and cathodal sessions within 4 hours of each other produced no discernable change in baseline resting motor thresholds or MEPs and no order/carry-over effects were found with respect to post-stimulation MEP amplitudes (Pellicciari et al., 2013). Unlike the series of studies presented within this thesis, the aforementioned study - like many others in the literature - did not incorporate a sham condition, which would have represented a valuable baseline measure given the close proximity of the active conditions. Additionally, it did not adopt a double-blind approach to remove aspects of researcher bias; another general theme amongst the existing research, which the studies conducted here also aimed to address.

Despite adopting these regulatory control measures, counterbalancing and wash-out periods (of 24 hours and 7 days, respectively), order effects were observed in both the MEG and single-site adaptation studies. This may have been coincidental but nonetheless it is not clear what patterns of repeated stimulation are likely to produce any kind of lasting effect, be it beneficial or detrimental, on the outcome of subsequent sessions. These results likely represent the inherent issues of performing statistical tests on sub-groups within already limited sample sizes. The issue of statistical power is once again pertinent because it is unlikely that there is sufficient power to support the detection of true effects in such cases. Any effects that do emerge could be the product of Type 1 error, constituting 'false positive' findings, and equally the absence of an effect may simply be due to 'false negative' results or Type 2 error. When basing an analysis on a small number of observations, differences can be artificially inflated or there may not be enough diversity in the data to isolate meaningful differences, which lead to a lack of precision in the findings. This means the emerging results need to be interpreted with extreme caution, whether they are confirmatory or contradictory. While acknowledging these limitations, should the results represent a genuine effect of stimulation order, research into the minimum period of time to constitute a sufficient inter-session interval (incorporating double-blind and sham control measures) should be conducted in order to verify future findings.

8.4. Closing Remarks

With respect to the underlying mechanisms of tDCS, the research did not find compelling statistical evidence to support the involvement of sustained neuroplastic change, as assessed via concentrations of sensorimotor GABA and Glx as well as motor beta and visual gamma oscillations. These outcomes were likely due to methodological factors and so it is not proposed that these mechanisms are not, in fact, involved in the generation of after-effects. The MEG study was, however, able to corroborate the influence of tDCS on resting membrane potential and motor cortical excitability; showing how anodal stimulation was capable of transiently enhancing the amplitude of evoked responses during simple finger movements. The behavioural results highlighted how cathodal tDCS was able to facilitate performance on a dual-site adaptation task, while modulations following anodal stimulation were not evident for this task or a single-site version of the paradigm. These findings demonstrated the importance of considering the effects of each polarity in conjunction with knowledge of the task mechanisms. This section of the research was able to enhance the existing literature in the somatosensory domain, stating that tDCS-induced modulations of vibrotactile task performance can be observed, given the appropriate polarity and electrode configuration. Aside from the use of innovative research methodology, the studies conducted here have also set a precedent in terms of the research standards adopted – incorporating counterbalancing, double-blind designs and sham-control measures – but there is certainly additional scope for improvement. Emphasising the importance of basic science alongside rigorously designed and optimised studies will undoubtedly pave the way for increasingly valid insights, which will ultimately lead to the refined application of tDCS in a variety of contexts.

9. References

Abraham, W. C. (2008). Metaplasticity: tuning synapses and networks for plasticity. *Nature Reviews Neuroscience*, *9(5)*, 387-399.

Abraham, W. C. & Bear, M. F. (1996). Metaplasticity: the plasticity of synaptic plasticity. *Trends in Neurosciences*, *19(4)*, 126-130.

Adjamian, P., Worthen, S. F., Hillebrand, A., Furlong, P. L., Chizh, B. A., Hobson, A. R... & Barnes, G. R. (2009). Effective electromagnetic noise cancellation with beamformers and synthetic gradiometry in shielded and partly shielded environments. *Journal of Neuroscience Methods*, *178(1)*, 120-127.

Agarwal, S. M., Shivakumar, V., Bose, A., Subramaniam, A., Nawani, H., Chhabra, H... & Venkatasubramanian, G. (2013). Transcranial direct current stimulation in schizophrenia. *Clinical Psychopharmacology and Neuroscience*, *11(3)*, 118-125.

Ahlfors, S. P., Han, J., Belliveau, J. W. & Hämäläinen, M. S. (2010). Sensitivity of MEG and EEG to source orientation. *Brain Topography*, *23(3)*, 227-232.

Ahonen, A. I., Hämäläinen, M. S., Kajola, M. J., Knuutila, J. E. T., Laine, P. P., Lounasmaa, O. V... & Tesche, C. D. (1993). 122-channel SQUID instrument for investigating the magnetic signals from the human brain. *Physica Scripta*, *T49A*, 198.

Albert, D. J. (1966a). The effects of polarizing currents on the consolidation of learning. *Neuropsychologia*, *4(1)*, 65-77.

Albert, D. J. (1966b). The effect of spreading depression on the consolidation of learning. *Neuropsychologia*, *4(1)*, 49-64.

Amadi, U., Allman, C., Johansen-Berg, H. & Stagg, C. J. (2015). The homeostatic interaction between anodal transcranial direct current stimulation and motor learning in humans is related to GABA A activity. *Brain Stimulation*, *8(5)*, 898-905.

Amadi, U., Ilie, A., Johansen-Berg, H. & Stagg, C. J. (2014). Polarity-specific effects of motor transcranial direct current stimulation on fMRI resting state networks. *Neuroimage*, *88*, 155-161.

Allman, C., Amadi, U., Winkler, A. M., Wilkins, L., Filippini, N., Kischka, U... & Johansen-Berg, H. (2016). Ipsilesional anodal tDCS enhances the functional benefits of rehabilitation in patients after stroke. *Science Translational Medicine*, *8(330).*

Antal, A., Brepohl, N., Poreisz, C., Boros, K., Csifcsak, G. & Paulus, W. (2008). Transcranial Direct Current Stimulation Over Somatosensory Cortex Decreases Experimentally Induced Acute Pain Perception. *The Clinical Journal of Pain*, *24(1)*, 56-63.

Antal, A., Chaieb, L., Moliadze, V., Monte-Silva, K., Poreisz, C., Thirugnanasambandam, N... & Paulus, W. (2010b). Brain-derived neurotrophic factor (BDNF) gene polymorphisms shape cortical plasticity in humans. *Brain Stimulation*, *3(4)*, 230-237.

Antal, A., Kincses, T. Z., Nitsche, M. A., Bartfai, O. & Paulus, W. (2004a). Excitability changes induced in the human primary visual cortex by transcranial direct current stimulation: direct electrophysiological evidence. *Investigative Ophthalmology & Visual Science, 45(2),* 702-707.

Antal, A. & Paulus. W. (2008). Transcranial direct current stimulation and visual perception. *Perception, 37,* 367-374.

Antal, A. & Paulus, W. (2013). Transcranial alternating current stimulation (tACS). *Frontiers in Human Neuroscience, 7*.

Antal, A., Paulus, W. & Nitsche, M. A. (2011). Electrical stimulation and visual network plasticity. *Restorative Neurology and Neuroscience, 29(6),* 365-374.

Antal, A., Terney, D., Kühnl, S. & Paulus, W. (2010a). Anodal transcranial direct current stimulation of the motor cortex ameliorates chronic pain and reduces short intracortical inhibition. *Journal of Pain and Symptom Management, 39(5),* 890-903.

Antal, A., Terney, D., Poreisz, C. & Paulus, W. (2007). Towards unravelling task-related modulations of neuroplastic changes induced in the human motor cortex. *European Journal of Neuroscience, 26(9),* 2687-2691.

Antal, A., Varga, E. T., Kincses, T. Z., Nitsche, M. A. & Paulus, W. (2004b). Oscillatory brain activity and transcranial direct current stimulation in humans. *Neuroreport, 15(8),* 1307-1310.

Atallah, B. V. & Scanziani, M. (2009). Instantaneous modulation of gamma oscillation frequency by balancing excitation with inhibition. *Neuron, 62(4),* 566-577.

Babiloni, C., Pizzella, V., Gratta, C. D., Ferretti, A. & Romani, G. L. (2009). Fundamentals of electroencefalography, magnetoencefalography, and functional magnetic resonance imaging. *International Review of Neurobiology, 86,* 67-80.

Bachmann, C. G., Muschinsky, S., Nitsche, M. A., Rolke, R., Magerl, W., Treede, R. D... & Happe, S. (2010). Transcranial direct current stimulation of the motor cortex induces distinct changes in thermal and mechanical sensory percepts. *Clinical Neurophysiology, 121(12),* 2083-2089.

Bachtiar, V., Near, J., Johansen-Berg, H. & Stagg, C. J. (2015). Modulation of GABA and resting state functional connectivity by transcranial direct current stimulation. *eLife, 4,* e08789.

Bachtiar, V. & Stagg, C. J. (2014). The role of inhibition in human motor cortical plasticity. *Neuroscience, 278,* 93-104.

Badr, G. G., Matousek, M. & Frederiksen, P. K. (1983). A quantitative EEG analysis of the effects of baclofen on man. *Neuropsychobiology, 10(1),* 13-18.

Baillet, S., Mosher, J. C. & Leahy, R. M. (2001). Electromagnetic brain mapping. *Signal Processing Magazine, IEEE, 18(6),* 14-30.

Baker, J. M., Rorden, C. & Fridriksson, J. (2010). Using transcranial direct-current stimulation to treat stroke patients with aphasia. *Stroke, 41(6),* 1229-1236.

Barnes, G. R. & Hillebrand, A. (2003). Statistical flattening of MEG beamformer images. *Human Brain Mapping, 18,* 1-12.

Bartos, M., Vida, I. & Jonas, P. (2007). Synaptic mechanisms of synchronized gamma oscillations in inhibitory interneuron networks. *Nature Reviews Neuroscience, 8(1),* 45-56.

Bastani, A. & Jaberzadeh, S. (2013). Differential modulation of corticospinal excitability by different current densities of anodal transcranial direct current stimulation. *PloS One, 8(8),* e72254.

Bastani, A. & Jaberzadeh, S. (2014). Within-session repeated a-tDCS: the effects of repetition rate and inter-stimulus interval on corticospinal excitability and motor performance. *Clinical Neurophysiology, 125(9),* 1809-1818.

Batsikadze, G., Moliadze, V., Paulus, W., Kuo, M. F. & Nitsche, M. A. (2013). Partially non-linear stimulation intensity-dependent effects of direct current stimulation on motor cortex excitability in humans. *The Journal of Physiology, 591(7),* 1987-2000.

Batsikadze, G., Paulus, W., Grundey, J., Kuo, M. F. & Nitsche, M. A. (2014). Effect of the nicotinic α4β2-receptor partial agonist varenicline on non-invasive brain stimulation-induced neuroplasticity in the human motor cortex. *Cerebral Cortex*, bhu126.

Behar, K. L., den Hollander, J. A., Stromski, M. E., Ogino, T., Shulman, R. G., Petroff, O. A. & Prichard, J. W. (1983). High-resolution 1H nuclear magnetic resonance study of cerebral hypoxia in vivo. *Proceedings of the National Academy of Sciences, 80(16),* 4945-4948.

Bejjani, A., O'Neill, J., Kim, J. A., Frew, A. J., Yee, V. W., Ly, R... & Levitt, J. G. (2012). Elevated glutamatergic compounds in pregenual anterior cingulate in pediatric autism spectrum disorder demonstrated by 1H MRS and 1H MRSI. *PLoS One, 7(7),* e38786.

Bensmaia, S. J., Leung, Y. Y., Hsiao, S. S. & Johnson, K. O. (2005). Vibratory adaptation of cutaneous mechanoreceptive afferents. *Journal of Neurophysiology, 94(5),* 3023-3036.

Benwell, C. S., Learmonth, G., Miniussi, C., Harvey, M. & Thut, G. (2015). Non-linear effects of transcranial direct current stimulation as a function of individual baseline performance: Evidence from biparietal tDCS influence on lateralized attention bias. *Cortex, 69,* 152-165.

Berger, H. (1929). Uber das elektroenkephalogram des menchen. *Archiv fur Psychiatrie und Nervenkrankheiten, 87,* 527−570.

Best, J. G., Stagg, C. J. & Dennis, A (2014). Other Significant Metabolites: Myo-Inositol, GABA, Glutamine and Lactate. In C. J. Stagg & D. Rothman (Eds.) *"Magnetic Resonance Spectroscopy: Tools for Neuroscience Research and Emerging Clincal Applications"*(pp. 122-140). Academic Press.

Bestmann, S., de Berker, A. O. & Bonaiuto, J. (2015). Understanding the behavioural consequences of noninvasive brain stimulation. *Trends in Cognitive Sciences*, *19(1),* 13-20.

Bhattacharyya, P. K. (2014). Macromolecule contamination in GABA editing using MEGA-PRESS should be properly accounted for. *Neuroimage, 84,* 1111-1112.

Bhattacharyya, P. K., Lowe, M. J. & Phillips, M. D. (2007). Spectral quality control in motion-corrupted single-voxel J-difference editing scans: An interleaved navigator approach. *Magnetic Resonance in Medicine, 58(4),* 808-812.

Bhattacharyya, P. K., Phillips, M. D., Stone, L. A., Bermel, R. A. & Lowe, M. J. (2013). Sensorimotor cortex gamma-aminobutyric acid concentration correlates with impaired performance in patients with MS. *American Journal of Neuroradiology, 34(9),* 1733-1739.

Bikson, M. & Datta, A. (2012). Guidelines for precise and accurate computational models of tDCS. *Brain Stimulation, 5(3),* 430-431.

Bikson, M., Edwards, D. & Kappenman, E. (2014). The outlook for non-invasive electrical brain stimulation. *Brain Stimulation, 7(6),* 771.

Bikson, M., Inoue, M., Akiyama, H., Deans, J. K., Fox, J. E., Miyakawa, H. & Jefferys, J. G. (2004). Effects of uniform extracellular DC electric fields on excitability in rat hippocampal slices in vitro. *The Journal of Physiology, 557(1),* 175-190.

Bindman, L. J., Lippold, O. C. J. & Redfearn, J. W. T. (1964). The action of brief polarizing currents on the cerebral cortex of the rat (1) during current flow and (2) in the production of long-lasting after-effects. *The Journal of Physiology, 172(3),* 369-382.

Bjartmar, C., Kidd, G., Mörk, S., Rudick, R. & Trapp, B. D. (2000). Neurological disability correlates with spinal cord axonal loss and reduced N-acetyl aspartate in chronic multiple sclerosis patients. *Annals of Neurology*, *48(6),* 893-901.

Bliss, T. V. & Lømo, T. (1973). Long-lasting potentiation of synaptic transmission in the dentate area of the anaesthetized rabbit following stimulation of the perforant path. *The Journal of Physiology*, *232(2),* 331-356.

Bloch, F., Hansen, W. W. & Packard, M. (1946). Nuclear magnetic resonance. *Physical Review, 70(7-8),* 460-474.

Bloembergen, N., Purcell, E. M. & Pound, R. V. (1948). Relaxation effects in nuclear magnetic resonance absorption. *Physical Review, 73(7),* 679-712.

Boggio, P. S., Ferrucci, R., Mameli, F., Martins, D., Martins, O., Vergari, M... & Priori, A. (2012). Prolonged visual memory enhancement after direct current stimulation in Alzheimer's disease. *Brain Stimulation*, *5(3),* 223-230.

Boggio, P. S., Zaghi, S., Lopes, M. & Fregni, F. (2008). Modulatory effects of anodal transcranial direct current stimulation on perception and pain thresholds in healthy volunteers. *European Journal of Neurology*, *15(10),* 1124-1130.

Bogner, W., Gruber, S., Doelken, M., Stadlbauer, A., Ganslandt, O., Boettcher, U... & Hammen, T. (2010). In vivo quantification of intracerebral GABA by single-voxel 1 H-MRS—How reproducible are the results?. *European Journal of Radiology*, *73(3)*, 526-531.

Bolanowski, S. J., Gescheider, G. A., Verrillo, R. T. & Checkosky, C. M. (1988). Four channels mediate the mechanical aspects of touch. *The Journal of the Acoustical society of America*, *84(5)*, 1680-1694.

Bortoletto, M., Pellicciari, M. C., Rodella, C. & Miniussi, C. (2015). The interaction with task-induced activity is more important than polarization: a tDCS study. *Brain Stimulation*, *8(2)*, 269-276.

Bottomley, P. A. (1987). Spatial localization in NMR spectroscopy in vivo. *Annals of the New York Academy of Sciences*, *508(1)*, 333-348.

Bottomley, P. A., Edelstein, W. A., Foster, T. H. & Adams, W. A. (1985). In vivo solvent-suppressed localized hydrogen nuclear magnetic resonance spectroscopy: a window to metabolism?. *Proceedings of the National Academy of Sciences*, *82(7)*, 2148-2152.

Boy, F., Evans, C. J., Edden, R. A., Lawrence, A. D., Singh, K. D., Husain, M. & Sumner, P. (2011). Dorsolateral prefrontal γ-aminobutyric acid in men predicts individual differences in rash impulsivity. *Biological Psychiatry*, *70(9)*, 866-872.

Brainard, D. H. (1997). The psychophysics toolbox. *Spatial Vision*, *10*, 433-436.

Brenner, D., Williamson, S. J. & Kaufman, L. (1975). Visually evoked magnetic fields of the human brain. *Science*, *190*, 480–482.

Brix, M. K., Ersland, L., Hugdahl, K., Grüner, R., Posserud, M. B., Hammar, Å... & Beyer, M. K. (2015). Brain MR spectroscopy in autism spectrum disorder—the GABA excitatory/inhibitory imbalance theory revisited. *Frontiers in Human Neuroscience*, *9*.

Brodmann, K. (1909). Vergleichende Lokalisationslehre der Groβ-hirnrinde in ihren Prinzipien dargestellt auf Grund des Zellenbaues. Leipzig, Barth, JA.

Brookes, M. J., Woolrich, M., Luckhoo, H., Price, D., Hale, J. R., Stephenson, M. C... & Morris, P. G. (2011). Investigating the electrophysiological basis of resting state networks using magnetoencephalography. *Proceedings of the National Academy of Sciences*, *108(40)*, 16783-16788.

Brunoni, A. R., Amadera, J., Berbel, B., Volz, M. S., Rizzerio, B. G. & Fregni, F. (2011a). A systematic review on reporting and assessment of adverse effects associated with transcranial direct current stimulation. *International Journal of Neuropsychopharmacology*, *14(8)*, 1133-1145.

Brunoni, A. R., Fregni, F. & Pagano, R. L. (2011b). Translational research in transcranial direct current stimulation (tDCS): a systematic review of studies in animals. *Reviews in the Neurosciences*, *22(4)*, 471-481.

Brunoni, A. R., Kemp, A. H., Shiozawa, P., Cordeiro, Q., Valiengo, L. C. L., Goulart, A. C... & Benseñor, I. M. (2013). Impact of 5-HTTLPR and BDNF polymorphisms on response to sertraline versus transcranial direct current stimulation: implications for the serotonergic system. *European Neuropsychopharmacology*, *23(11)*, 1530-1540.

Brunoni, A. R., Nitsche, M. A., Bolognini, N., Bikson, M., Wagner, T., Merabet, L... & Fregni, F. (2012). Clinical research with transcranial direct current stimulation (tDCS): challenges and future directions. *Brain Stimulation*, *5(3)*, 175-195.

Button, K. S., Ioannidis, J. P., Mokrysz, C., Nosek, B. A., Flint, J., Robinson, E. S. & Munafò, M. R. (2013). Power failure: why small sample size undermines the reliability of neuroscience. *Nature Reviews Neuroscience*, *14(5)*, 365-376.

Buzsáki, G. (2006). *Rhythms of the Brain*. Oxford University Press.

Buzsáki, G. & Wang, X. J. (2012). Mechanisms of gamma oscillations. *Annual Review of Neuroscience*, *35*, 203-225.

Cai, K., Nanga, R. P., Lamprou, L., Schinstine, C., Elliott, M., Hariharan, H... & Epperson, C. N. (2012). The impact of gabapentin administration on brain GABA and glutamate concentrations: a 7T 1H-MRS study. *Neuropsychopharmacology*, *37(13)*, 2764-2771.

Callaway, E. M. (2004). Feedforward, feedback and inhibitory connections in primate visual cortex. *Neural Networks*, *17(5)*, 625-632.

Campbell, A. E., Sumner, P., Singh, K. D. & Muthukumaraswamy, S. D. (2014). Acute effects of alcohol on stimulus-induced gamma oscillations in human primary visual and motor cortices. *Neuropsychopharmacology*, *39(9)*, 2104-2113.

Cardin, J.A., Carlen, M., Meletis, K., Knoblich, U., Zhang, F., Deisseroth, K… & Moore, C. I. (2009). Driving fast-spiking cells induces gamma rhythm and controls sensory responses. *Nature*, *459*, 663-667.

Carvalho, S., Boggio, P. S., Gonçalves, Ó. F., Vigário, A. R., Faria, M., Silva, S... & Leite, J. (2015). Transcranial Direct Current Stimulation Based Metaplasticity Protocols in Working Memory. *Brain Stimulation*, *8(2)*, 289-294.

Casanova, M. F., Buxhoeveden, D. & Gomez, J. (2003). Disruption in the inhibitory architecture of the cell minicolumn: implications for autisim. *The Neuroscientist*, *9(6)*, 496-507.

Casanova, M. F., Buxhoeveden, D. P., Switala, A. E. & Roy, E. (2002). Minicolumnar pathology in autism. *Neurology*, *58(3)*, 428-432.

Cavassila, S., Deval, S., Huegen, C., Van Ormondt, D. & Graveron-Demilly, D. (2001). Cramer–Rao bounds: an evaluation tool for quantitation. *NMR in Biomedicine*, 14(4), 278-283.

Cerletti, U. (1950). Old and new information about electroshock. *American Journal of Psychiatry*, *107(2)*, 87-94.

Chaieb, L., Antal, A. & Paulus, W. (2008). Gender-specific modulation of short-term neuroplasticity in the visual cortex induced by transcranial direct current stimulation. *Visual Neuroscience, 25(1),* 77-81.

Chatrian, G. E., Lettich, E. & Nelson, P. L. (1985). Ten percent electrode system for topographic studies of spontaneous and evoked EEG activity. *American Journal of EEG Technology, 25,* 83-92.

Cheeran, B., Talelli, P., Mori, F., Koch, G., Suppa, A., Edwards, M... & Rothwell, J. C. (2008). A common polymorphism in the brain-derived neurotrophic factor gene (BDNF) modulates human cortical plasticity and the response to rTMS. *The Journal of Physiology, 586(23),* 5717-5725.

Chen, L. M., Friedman, R. M. & Roe, A. W. (2003). Optical imaging of a tactile illusion in area 3b of the primary somatosensory cortex. *Science, 302,* 881–885.

Chen, R. & Hallett, M. (1999). The time course of changes in motor cortex excitability associated with voluntary movement. *The Canadian Journal of Neurological Sciences, 26(3),* 163-169.

Chen, R., Yaseen, Z., Cohen, L. G. & Hallett, M. (1998). Time course of corticospinal excitability in reaction time and self-paced movements. *Annals of Neurology, 44(3),* 317-325.

Chen, W., Zhu, X. H., Thulborn, K. R. & Ugurbil, K. (1999). Retinotopic mapping of lateral geniculate nucleus in humans using functional magnetic resonance imaging. *Proceedings of the National Academy of Sciences, 96(5),* 2430-2434.

Cheyne, D. O. (2013). MEG studies of sensorimotor rhythms: a review. *Experimental Neurology, 245,* 27-39.

Cheyne, D., Bells, S., Ferrari, P., Gaetz, W. & Bostan, A. C. (2008). Self-paced movements induce high-frequency gamma oscillations in primary motor cortex. *Neuroimage, 42(1),* 332-342.

Cheyne, D. & Weinberg, H. (1989). Neuromagnetic fields accompanying unilateral finger movements: pre-movement and movement-evoked fields. *Experimental Brain Research, 78(3),* 604-612.

Chiu, J. S. (2006). Characterization of Minicolumnar Patterns in SI Cortex [Dissertation]. Chapel Hill: University of North Carolina at Chapel Hill.

Chiu, J. S., Tommerdahl, M., Whitsel, B. L. & Favorov, O. V. (2005). Stimulus-dependent spatial patterns of response in SI cortex. *BMC Neuroscience, 6(1),* 47-60.

Cirillo, J., Lavender, A. P., Ridding, M. C. & Semmler, J. G. (2009). Motor cortex plasticity induced by paired associative stimulation is enhanced in physically active individuals. *The Journal of Physiology, 587,* 5831–5842.

Clark, V. P., Coffman, B. A., Mayer, A. R., Weisend, M. P., Lane, T. D., Calhoun, V. D... & Wassermann, E. M. (2012). TDCS guided using fMRI significantly accelerates learning to identify concealed objects. *Neuroimage, 59(1),* 117-128.

Clark, V.P., Coffman, B. A., Trumbo, M. C. & Gasparovic, C. (2011). Transcranial direct current stimulation (tDCS) produces localized and specific alterations in neurochemistry: A 1H magnetic resonance spectroscopy study. *Neuroscience Letters, 500(1),* 67-71.

Cleve, M., Gussew, A. & Reichenbach, J. R. (2015). In vivo detection of acute pain-induced changes of GABA+ and Glx in the human brain by using functional 1 H MEGA-PRESS MR spectroscopy. *Neuroimage, 105,* 67-75.

Cobb, S. R., Buhl, E. H., Halasy, K., Paulsen, O. & Somogyi, P. (1995). Synchronization of neuronal-activity in hippocampus by individual gabaergic interneurons. *Nature, 378,* 75–78.

Cohen, D. (1972). Magnetoencephalography: detection of the brain's electrical activity with a superconducting magnetometer. *Science, 175(4022),* 664-666.

Cohen Kadosh, R., Soskic, S., Iuculano, T., Kanai, R. & Walsh, V. (2010). Modulating neuronal activity produces specific and long-lasting changes in numerical competence. *Current Biology, 20(22),* 2016-2020.

Concerto, C., Al Sawah, M., Chusid, E., Trepal, M., Taylor, G., Aguglia, E. & Battaglia, F. (2015). Anodal transcranial direct current stimulation for chronic pain in the elderly: a pilot study. *Aging Clinical and Experimental Research,* 1-7.

Cosentino, G., Fierro, B., Paladino, P., Talamanca, S., Vigneri, S., Palermo, A... & Brighina, F. (2012). Transcranial direct current stimulation preconditioning modulates the effect of high-frequency repetitive transcranial magnetic stimulation in the human motor cortex. *European Journal of Neuroscience, 35(1),* 119-124.

Cousijn, H., Haegens, S., Wallis, G., Near, J., Stokes, M. G., Harrison, P. J. & Nobre, A. C. (2014). Resting GABA and glutamate concentrations do not predict visual gamma frequency or amplitude. *Proceedings of the National Academy of Sciences, 111(25),* 9301-9306.

Creutzfeldt, O. D., Fromm, G. H. & Kapp, H. (1962). Influence of transcortical dc currents on cortical neuronal activity. *Experimental Neurology, 5(6),* 436-452.

Dalby, N. O. (2000). GABA-level increasing and anticonvulsant effects of three different GABA uptake inhibitors. *Neuropharmacology, 39(12),* 2399-2407.

Damadian, R. (1971). Tumor detection by nuclear magnetic resonance. *Science, 171(3976),* 1151-1153.

Datta, A., Bansal, V., Diaz, J., Patel, J., Reato, D. & Bikson, M. (2009). Gyri-precise head model of transcranial direct current stimulation: improved spatial focality using a ring electrode versus conventional rectangular pad. *Brain Stimulation, 2(4),* 201-207.

Datta, A., Elwassif, M., Battaglia, F. & Bikson, M. (2008). Transcranial current stimulation focality using disc and ring electrode configurations: FEM analysis. *Journal of Neural Engineering, 5,* 163–174.

de Berker, A. O., Bikson, M. & Bestmann, S. (2013). Predicting the behavioural impact of transcranial direct current stimulation. *Frontiers in Human Neuroscience, 7.*

de Bondt, T., de Belder, F., Vanhevel, F., Jacquemyn, Y. & Parizel, P. M. (2015). Prefrontal GABA concentration changes in women—Influence of menstrual cycle phase, hormonal contraceptive use, and correlation with premenstrual symptoms. *Brain Research, 1597,* 129-138.

Deecke, L., Weinberg, H. & Brickett, P. (1982). Magnetic fields of the human brain accompanying voluntary movement: Bereitschaftsmagnetfeld. *Experimental Brain Research, 48(1),* 144-148.

de Graaf, R. A. (2013). *In vivo NMR spectroscopy: principles and techniques*. John Wiley & Sons.

Delemos, K.A. & Hollins, M. (1996). Adaptation-induced enhancement of vibrotactile amplitude discrimination: The role of adapting frequency. *The Journal of the Acoustical Society of America, 99(1),* 508-516.

Demanuele, C., James, C. J. & Sonuga-Barke, E. J. (2007). Distinguishing low frequency oscillations within the 1/f spectral behaviour of electromagnetic brain signals. *Behavioral and Brain Functions, 3:*62.

Denker, M., Roux, S., Lindén, H., Diesmann, M., Riehle, A. & Grün, S. (2011). The local field potential reflects surplus spike synchrony. *Cerebral Cortex, 21(12),* 2681-2695.

Dienes, Z. (2011). Bayesian versus orthodox statistics: Which side are you on? *Perspectives on Psychological Science, 6(3),* 274-290.

Dienes, Z. (2014). Using Bayes to get the most out of non-significant results. *Frontiers in Psychology, 5*.

Di Russo, F., Martínez, A., Sereno, M. I., Pitzalis, S. & Hillyard, S. A. (2002). Cortical sources of the early components of the visual evoked potential. *Human Brain Mapping, 15(2),* 95-111.

Donner, T. H. & Siegel, M. (2011). A framework for local cortical oscillation patterns. *Trends in Cognitive Sciences, 15(5),* 191-199.

Dreher, W. & Leibfritz, D. (2005). New method for the simultaneous detection of metabolites and water in localized in vivo 1H nuclear magnetic resonance spectroscopy. *Magnetic Resonance in Medicine, 54(1),* 190-195.

Dum, R. P. & Strick, P. L. (2002). Motor areas in the frontal lobe of the primate. *Physiology & Behavior, 77(4),* 677-682.

Durst, C. R., Michael, N., Tustison, N. J., Patrie, J. T., Raghavan, P., Wintermark, M. & Velan, S. S. (2015). Noninvasive evaluation of the regional variations of GABA using magnetic resonance spectroscopy at 3 Tesla. *Magnetic Resonance Imaging, 33(5),* 611-617.

Dymond, A. M., Coger, R. W. & Serafetinides, E. A. (1975). Intracerebral current levels in man during electrosleep therapy. *Biological Psychiatry, 10(1),* 101-104.

Eagleman, D. M. (2004). The where and when of intention. *Science, 303,* 1144–1146.

Eckhorn, R., Bauer, R., Jordan, W., Brosch, M., Kruse, W., Munk, M. & Reitboeck, H. J. (1988). Coherent oscillations: A mechanism of feature linking in the visual cortex?. *Biological Cybernetics, 60(2),* 121-130.

Edden, R. A., Intrapiromkul, J., Zhu, H., Cheng, Y. & Barker, P. B. (2012b). Measuring T2 in vivo with J-difference editing: Application to GABA at 3 tesla. *Journal of Magnetic Resonance Imaging, 35(1),* 229-234.

Edden, R. A., Puts, N. A. & Barker, P. B. (2012a). Macromolecule-suppressed GABA-edited magnetic resonance spectroscopy at 3T. *Magnetic Resonance in Medicine, 68(3),* 657-661.

Edden, R. A., Puts, N. A., Harris, A. D., Barker, P. B. & Evans, C. J. (2014). Gannet: A batch-processing tool for the quantitative analysis of gamma-aminobutyric acid–edited MR spectroscopy spectra. *Journal of Magnetic Resonance Imaging, 40(6),* 1445-1452.

Elbert, T., Lutzenberger, W., Rockstroh, B. & Birbaumber, N. (1981). The influence of low-level transcortical DC-currents on respones speed in humans. *International Journal of Neuroscience, 14,* 101–114.

Ellisman, M. H., Rash, J. E., Staehelin, L. A. & Porter, K. R. (1976). Studies of excitable membranes. II. A comparison of specializations at neuromuscular junctions and nonjunctional sarcolemmas of mammalian fast and slow twitch muscle fibers. *The Journal of Cell Biology, 68(3),* 752-774.

Elmer, S., Burkard, M., Renz, B., Meyer, M. & Jancke, L. (2009). Direct current induced short-term modulation of the left dorsolateral prefrontal cortex while learning auditory presented nouns. *Behavioral and Brain Functions, 5:*29.

Engel, S. A., Glover, G. H. & Wandell, B. A. (1997). Retinotopic organization in human visual cortex and the spatial precision of functional MRI. *Cerebral Cortex, 7(2),* 181-192.

Epperson, C. N., Haga, K., Mason, G. F., Sellers, E., Gueorguieva, R., Zhang, W... & Krystal, J.H. (2002). Cortical {gamma}-aminobutyric acid levels across the menstrual cycle in healthy women and those with Premenstrual Dysphoric Disorder: a proton magnetic resonance spectroscopy study. *Archives of General Psychiatry, 59(9),* 851-858.

Epperson, C. N., O'Malley, S., Czarkowski, K. A., Gueorguieva, R., Jatlow, P., Sanacora, G... & Mason, G. F. (2005). Sex, GABA, and nicotine: the impact of smoking on cortical GABA levels across the menstrual cycle as measured with proton magnetic resonance spectroscopy. *Biological Psychiatry, 57(1),* 44-48.

Erne, S. N. (1983). Shielded rooms. In Williamson, J. R., Romani, G. L., Kaufman, L., Modena, I. (eds). *Biomagnetism, an interdisciplinary approach*. Plenum Press, New York.

Evans, C. J., McGonigle, D. J. & Edden, R. A. E. (2010). Diurnal stability of γ-aminobutyric acid concentration in visual and sensorimotor cortex. *Journal of Magnetic Resonance Imaging, 31(1),* 204-209.

Evans, C. J., Puts, N. A., Robson, S. E., Boy, F., McGonigle, D. J., Sumner, P... & Edden, R. A. (2013). Subtraction artifacts and frequency (Mis-) alignment in J-difference GABA editing. *Journal of Magnetic Resonance Imaging, 38(4),* 970-975.

Evarts, E. V. (1968). Relation of pyramidal tract activity to force exerted during voluntary movement. *Journal of Neurophysiology, 31,* 14-27.

Falmagne, J. C. (1986). Psychophysical measurement and theory. In Boff, K. R., Kaufman, L., & Thomas, J. P. (Eds.) *"Handbook of perception and human performance".* New York: John Wiley & Sons.

Fathi, D., Ueki, Y., Mima, T., Koganemaru, S., Nagamine, T., Tawfik, A... & Fukuyama, H. (2010). Effects of aging on the human motor cortical plasticity studied by paired associative stimulation. *Clinical Neurophysiology, 121,* 90–93.

Faul, F., Erdfelder, E., Lang, A. G. & Buchner, A. (2007). G* Power 3: A flexible statistical power analysis program for the social, behavioral, and biomedical sciences. *Behavior Research Methods, 39(2),* 175-191.

Fechner, G. T. (1860). *Elemente der Psychophysik.* English translation: Howes, D. H. & Boring, E. C. (eds) and Adler, H. E. (transl.) (1966). New York: Holt (Rinehart & Winston).

Ferrucci, R., Bortolomasi, M., Vergari, M., Tadini, L., Salvoro, B., Giacopuzzi, M... & Priori, A. (2009). Transcranial direct current stimulation in severe, drug-resistant major depression. *Journal of Affective Disorders, 118(1),* 215-219.

Fertonani, A. & Miniussi, C. (2016). Transcranial Electrical Stimulation: What We Know and Do Not Know About Mechanisms. *The Neuroscientist, 1,* 15.

Filler, R. & Saha, R. (2009). Fluorine in medicinal chemistry: a century of progress and a 60-year retrospective of selected highlights. *Future Medicinal Chemistry, 1(5),* 777-791.

Fleiss, J. L. (1971). Measuring nominal scale agreement among many raters. *Psychological Bulletin, 76(5),* 378–382.

Floyer-Lea, A., Wylezinska, M., Kincses, T. & Matthews, P. M. (2006). Rapid modulation of GABA concentration in human sensorimotor cortex during motor learning. *Journal of Neurophysiology, 95,* 1639–1644.

Folger, S., Tannan, V., Zhang, Z., Holden, J. & Tommerdahl, M. (2008). Effects of the N-methyl-D-Aspartate receptor antagonist dextromethorphan on vibrotactile adaptation. *BMC Neuroscience, 9(1),* 87-95.

Frahm, J., Merboldt, K. D., Hänicke, W. & Haase, A. (1985). Stimulated echo imaging. *Journal of Magnetic Resonance, 64(1),* 81-93.

Francis, S. T., Kelly, E. F., Bowtell, R., Dunseath, W. J. R., Folger, S. E. & McGlone, F. (2000). fMRI of the responses to vibratory stimulation of digit tips. *Neuroimage, 11(3),* 188-202.

Francisco, E., Holden, J., Zhang, Z., Favorov, O. & Tommerdahl, M. (2011). Rate dependency of vibrotactile stimulus modulation. *Brain Research, 1415,* 76-83.

Francisco, E., Tannan, V., Zhang, Z., Holden, J. & Tommerdahl, M. (2008). Vibrotactile amplitude discrimination capacity parallels magnitude changes in somatosensory cortex and follows Weber's Law. *Experimental Brain Research, 191(1),* 49-56.

Fregni, F., Boggio, P. S., Santos, M. C., Lima, M., Vieira, A. L., Rigonatti, S. P... & Pascual-Leone, A. (2006). Noninvasive cortical stimulation with transcranial direct current stimulation in Parkinson's disease. *Movement Disorders, 21(10),* 1693-1702.

Fresnoza, S., Paulus, W., Nitsche, M. A. & Kuo, M. F. (2014b). Nonlinear Dose-Dependent Impact of D1 Receptor Activation on Motor Cortex Plasticity in Humans. *The Journal of Neuroscience, 34(7),* 2744-2753.

Fresnoza, S., Stiksrud, E., Klinker, F., Liebetanz, D., Paulus, W., Kuo, M. F. & Nitsche, M. A. (2014a). Dosage-dependent effect of dopamine D2 receptor activation on motor cortex plasticity in humans. *The Journal of Neuroscience, 34(32),* 10701-10709.

Friedman, L. & Glover, G. H. (2006). Report on a multicenter fMRI quality assurance protocol. *Journal of Magnetic Resonance Imaging, 23,* 827–839.

Fries, P. (2005). A mechanism for cognitive dynamics: neuronal communication through neuronal coherence. *Trends in Cognitive Sciences, 9,* 474-480.

Fries, P. (2009). Neuronal gamma-band synchronization as a fundamental process in cortical computation. *Annual Review of Neuroscience, 32,* 209-224.

Fritsch, B., Reis, J., Martinowich, K., Schambra, H. M., Ji, Y., Cohen, L. G... & Lu, B. (2010). Direct current stimulation promotes BDNF-dependent synaptic plasticity: potential implications for motor learning. *Neuron, 66(2),* 198-204.

Froc, D. J., Chapman, C. A., Trepel, C. & Racine, R. J. (2000). Long-term depression and depotentiation in the sensorimotor cortex of the freely moving rat. *The Journal of Neuroscience, 20(1),* 438-445.

Fujimoto, S., Yamaguchi, T., Otaka, Y., Kondo, K. & Tanaka, S. (2014). Dual-hemisphere transcranial direct current stimulation improves performance in a tactile spatial discrimination task. *Clinical Neurophysiology, 125(8),* 1669-1674.

Funke, K. (2013). Quite simple at first glance–complex at a second: modulating neuronal activity by tDCS. *The Journal of Physiology, 591(16),* 3809-3809.

Fusco, A., De Angelis, D., Morone, G., Maglione, L., Paolucci, T., Bragoni, M. & Venturiero, V. (2013). The ABC of tDCS: Effects of Anodal, Bilateral and Cathodal Montages of Transcranial Direct Current Stimulation in Patients with Stroke—A Pilot Study. *Stroke Research and Treatment.*

Fylan, F., Holliday, I. E., Singh, K. D., Anderson, S. J. & Harding, G. F. (1997). Magnetoencephalographic investigation of human cortical area V1 using color stimuli. *Neuroimage, 6(1),* 47-57.

Gaetz, W., Edgar, J. C., Wang, D. J. & Roberts, T. P. (2011). Relating MEG measured motor cortical oscillations to resting γ-aminobutyric acid (GABA) concentration. *Neuroimage, 55(2),* 616-621.

Gaiarsa, J. L., Caillard, O. & Ben-Ari, Y. (2002). Long-term plasticity at GABAergic and glycinergic synapses: mechanisms and functional significance. *Trends in Neurosciences, 25(11),* 564-570.

Gaiarsa, J. L., Kuczewski, N. & Porcher, C. (2011). Contribution of metabotropic GABA B receptors to neuronal network construction. *Pharmacology & Therapeutics, 132(2),* 170-179.

Garcia-Cossio, E., Witkowski, M., Robinson, S. E., Cohen, L. G., Birbaumer, N. & Soekadar, S. R. (2015). Simultaneous transcranial direct current stimulation (tDCS) and whole-head magnetoencephalography (MEG): assessing the impact of tDCS on slow cortical magnetic fields. *Neuroimage*.

Georgopoulos, A. P., Kalaska, J. F., Caminiti, R. & Massey, J. T. (1982) On the relations between the direction of two dimensional arm movements and cell discharge in primate motor cortex. *The Journal of Neuroscience, 2,* 1527–1537.

Gescheider, G. A. (2013). *Psychophysics: The Fundamentals*. Psychology Press.

Gescheider, G. A., Bolanowski, S. J. & Verrillo, R. T. (2004). Some characteristics of tactile channels. *Behavioural Brain Research, 148(1),* 35-40.

Gescheider, G. A., Santoro, K. E., Makous, J. C. & Bolanowski, S. J. (1995). Vibrotactile forward masking: effects of the amplitude and duration of the masking stimulus. *The Journal of the Acoustical Society of America, 98(6),* 3188-3194.

Gescheider, G. A., Verrillo, R. T., McCain, J. T. & A1drich, E. M. (1984). Effects of the menstrual cycle on vibrotactile sensitivity. *Perception and Psychophysics, 36(6),* 586-592.

Geyer, S., Schleicher, A. & Zilles, K. (1999). Areas 3a, 3b, and 1 of human primary somatosensory cortex: 1. Microstructural organization and interindividual variability. *Neuroimage, 10(1),* 63-83.

Gilbert, C. D. (1996). Plasticity in visual perception and physiology. *Current Opinion in Neurobiology, 6(2),* 269-274.

Giusti, P. & Arban, R. (1993). Physiological and pharmacological bases for the diverse properties of benzodiazepines and their congeners. *Pharmacological Research, 27(3),* 201-216.

Goble, A. K. & Hollins, M. (1993). Vibrotactile adaptation enhances amplitude discrimination. *The Journal of the Acoustical Society of America, 93(1),* 418-424.

Goble, A. K. & Hollins, M. (1994). Vibrotactile adaptation enhances frequency discrimination. *The Journal of the Acoustical Society of America, 96(2),* 771-780.

Goddard, A. W. (2016). Cortical and subcortical gamma amino acid butyric acid deficits in anxiety and stress disorders: Clinical implications. *World Journal of Psychiatry, 6(1),* 43.

Goff, G. D., Rosner, B. S., Detre, T. & Kennard, D. (1965). Vibration perception in normal man and medical patients. *Journal of Neurology, Neurosurgery, and Psychiatry, 28(6),* 503-509.

Goldsworthy, M. R., Pitcher, J. B. & Ridding, M. C. (2015). Spaced Noninvasive Brain Stimulation Prospects for Inducing Long-Lasting Human Cortical Plasticity. *Neurorehabilitation and Neural Repair,* 29*(8),* 714-721.

Gonzalez-Burgos, G. & Lewis, D. A. (2008). GABA neurons and the mechanisms of network oscillations: implications for understanding cortical dysfunction in schizophrenia. *Schizophrenia Bulletin, 34(5),* 944-961.

Gray, C. M. & Singer, W. (1989). Stimulus-specific neuronal oscillations in orientation columns of cat visual cortex. *Proceedings of the National Academy of Sciences, 86(5),* 1698-1702.

Greve, A., Cooper, E. & Henson, R. (2014). No evidence that 'fast-mapping' benefits novel learning in healthy older adults. *Neuropsychologia, 60,* 52-59.

Gross, J., Kujala, J., Hämäläinen, M., Timmermann, L., Schnitzler, A. & Salmelin, R. (2001). Dynamic imaging of coherent sources: studying neural interactions in the human brain. *Proceedings of the National Academy of Sciences, 98(2),* 694-699.

Grundey, J., Thirugnanasambandam, N., Kaminsky, K., Drees, A., Skwirba, A. C., Lang, N... & Nitsche, M. A. (2012a). Rapid effect of nicotine intake on neuroplasticity in non-smoking humans. *Frontiers in Pharmacology, 3.*

Grundey, J., Thirugnanasambandam, N., Kaminsky, K., Drees, A., Skwirba, A. C., Lang, N... & Nitsche, M. A. (2012b). Neuroplasticity in cigarette smokers is altered under withdrawal and partially restituted by nicotine exposition. *The Journal of Neuroscience, 32(12),* 4156-4162.

Grundmann, L., Rolke, R., Nitsche, M. A., Pavlakovic, G., Happe, S., Treede, R. D... & Bachmann, C. G. (2011). Effects of transcranial direct current stimulation of the primary sensory cortex on somatosensory perception. *Brain Stimulation, 4(4),* 253-260.

Gustafsson, B., Wigstrom, H., Abraham, W. C. & Huang, Y. Y. (1987). Long-term potentiation in the hippocampus using depolarizing current pulses as the conditioning stimulus to single volley synaptic potentials. *The Journal of Neuroscience, 7(3),* 774-780.

Haase, A., Frahm, J., Hanicke, W. & Matthaei, D. (1985). 1H NMR chemical shift selective (CHESS) imaging. *Physics in Medicine and Biology, 30(4),* 341-344.

Hahn, E. L. (1950). Spin echoes. *Physical Review, 80(4),* 580-602.

Hains, D. E. (2007). *Neuroanatomy: An atlas of structures, sections and systems* (7th ed). Lippincott Williams & Wilkins, New York.

Hall, S. D., Barnes, G. R., Furlong, P. L., Seri, S. & Hillebrand, A. (2010). Neuronal network pharmacodynamics of GABAergic modulation in the human cortex determined using pharmaco-magnetoencephalography. *Human Brain Mapping, 31(4),* 581-594.

Hall, S. D., Stanford, I. M., Yamawaki, N., McAllister, C. J., Rönnqvist, K. C., Woodhall, G. L. & Furlong, P. L. (2011). The role of GABAergic modulation in motor function related neuronal network activity. *Neuroimage, 56(3),* 1506-1510.

Halsband, U., Matsuzaka, Y. & Tanji, J. (1994). Neuronal activity in the primate supplementary, pre-supplementary and premotor cortex during externally and internally instructed sequential movements. *Neuroscience Research, 20(2),* 149-155.

Hämäläinen, M., Hari, R., Ilmoniemi, R. J., Knuutila, J. & Lounasmaa, O. V. (1993). Magnetoencephalography—theory, instrumentation, and applications to noninvasive studies of the working human brain. *Reviews of Modern Physics, 65(2),* 413-497.

Harada, M., Kubo, H., Nose, A., Nishitani, H. & Matsuda, T. (2011). Measurement of variation in the human cerebral GABA level by in vivo MEGA-editing proton MR spectroscopy using a clinical 3 T instrument and its dependence on brain region and the female menstrual cycle. *Human Brain Mapping, 32(5),* 828-833.

Hari, R. & Salmelin, R. (2012). Magnetoencephalography: from SQUIDs to neuroscience. *Neuroimage, 61(2),* 386-396.

Harris, A. D., Puts, N. A., Barker, P. B. & Edden, R. A. (2014). Spectral-editing measurements of GABA in the human brain with and without macromolecule suppression. *Magnetic Resonance in Medicine.*

Hartline, H. K. (1938). The response of single optic nerve fibers of the vertebrate eye to illumination of the retina. *The American Journal of Physiology, 121 (1938),* 400-415.

Harty, S., Robertson, I. H., Miniussi, C., Sheehy, O. C., Devine, C. A., McCreery, S. & O'Connell, R. G. (2014). Transcranial Direct Current Stimulation over Right Dorsolateral Prefrontal Cortex Enhances Error Awareness in Older Age. *The Journal of Neuroscience, 34(10),* 3646-3652.

Hasenstaub, A., Shu, Y., Haider, B., Kraushaar, U., Duque, A. & McCormick, D. A. (2005). Inhibitory postsynaptic potentials carry synchronized frequency information in active cortical networks. *Neuron, 47(3),* 423-435.

Hausmann, M., Tegenthoff, M., Sänger, J., Janssen, F., Güntürkün, O. & Schwenkreis, P. (2006). Transcallosal inhibition across the menstrual cycle: a TMS study. *Clinical Neurophysiology, 117(1),* 26-32.

Helfrich, R. F., Schneider, T. R., Rach, S., Trautmann-Lengsfeld, S. A., Engel, A. K. & Herrmann, C. S. (2014). Entrainment of brain oscillations by transcranial alternating current stimulation. *Current Biology, 24(3),* 333-339.

Hellerbach, A., Schuster, V., Jansen, A. & Sommer, J. (2013). MRI phantoms–are there alternatives to agar. *PloS One, 8(8),* e70343.

Hellwag, C. F. & Jacobi, M. (1802). Erfahrungen uber die Heilkrafte des Galvanismus und Betrachtungen uber desselben chemische und physiologische Wirkungen. Friedrich Perthes: Hamburg, Germany.

Henry, P. G., Dautry, C., Hantraye, P. & Bloch, G. (2001). Brain GABA editing without macromolecule contamination. *Magnetic Resonance in Medicine, 45(3),* 517-520.

Hess, G. & Donoghue, J. P. (1994). Long-term potentiation of horizontal connections provides a mechanism to reorganize cortical motor maps. *Journal of Neurophysiology, 71(6),* 2543-2547.

Hess, G. & Donoghue, J. P. (1996). Long-term depression of horizontal connections in rat motor cortex. *European Journal of Neuroscience, 8(4),* 658-665.

Hillebrand, A. & Barnes, G. R. (2002). A quantitative assessment of the sensitivity of whole-head MEG to activity in the adult human cortex. *Neuroimage, 16,* 638–650.

Hillebrand, A. & Barnes, G. R. (2005). Beamformer analysis of MEG data. *International Review of Neurobiology, 68,* 149-171.

Hillebrand, A., Fazio, P., De Munck, J. C. & Van Dijk, B. W. (2013). Feasibility of clinical magnetoencephalography (MEG) functional mapping in the presence of dental artefacts. *Clinical Neurophysiology, 124(1),* 107-113.

Hipp, J. F., Engel, A. K. & Siegel, M. (2011). Oscillatory synchronization in large-scale cortical networks predicts perception. *Neuron, 69(2),* 387-396.

Holden, J. K., Nguyen, R. H., Francisco, E. M., Zhang, Z., Dennis, R. G. & Tommerdahl, M. (2012). A novel device for the study of somatosensory information processing. *Journal of Neuroscience Methods, 204(2),* 215-220.

Holland, R., Leff, A. P., Josephs, O., Galea, J. M., Desikan, M., Price, C. J... & Crinion, J. (2011). Speech facilitation by left inferior frontal cortex stimulation. *Current Biology, 21(16),* 1403-1407.

Hone-Blanchet, A., Edden, R. A. & Fecteau, S. (in press). Online effects of transcranial direct current stimulation in real time on human prefrontal and striatal metabolites. *Biological Psychiatry*.

Hoogenboom, N., Schoffelen, J. M., Oostenveld, R., Parkes, L. M. & Fries, P. (2006). Localizing human visual gamma-band activity in frequency, time and space. *Neuroimage, 29(3),* 764-773.

Horvath, J. C., Carter, O. & Forte, J. D. (2014). Transcranial direct current stimulation: five important issues we aren't discussing (but probably should be). *Frontiers in Systems Neuroscience, 8.*

Horvath, J. C., Forte, J. D. & Carter, O. (2015a). Quantitative review finds no evidence of cognitive effects in healthy populations from single-session transcranial direct current stimulation (tDCS). *Brain Stimulation,* 8*(3),* 535-550.

Horvath, J. C., Forte, J. D. & Carter, O. (2015b). Evidence that transcranial direct current stimulation (tDCS) generates little-to-no reliable neurophysiologic effect beyond MEP amplitude modulation in healthy human subjects: A systematic review. *Neuropsychologia, 66,* 213-236.

Hoshi, E. & Tanji, J. (2004). Differential Roles of Neuronal Activity in the Supplementary and Presupplementary Motor Areas: From Information Retrieval to Motor Planning and Execution. *The Journal of Physiology, 92,* 3482-3499.

Hsu, W. Y., Ku, Y., Zanto, T. P. & Gazzaley, A. (2015). Effects of noninvasive brain stimulation on cognitive function in healthy aging and Alzheimer's disease: a systematic review and meta-analysis. *Neurobiology of Aging, 36(8),* 2348-2359.

Huang, M. X., Mosher, J. C. & Leahy, R, M. (1999). A sensor-weighted overlapping-sphere head model and exhaustive head model comparison for MEG. *Physics in Medicine and Biology, 44,* 423–440.

Huang, Y. Y., Colino, A., Selig, D. K. & Malenka, R. C. (1992). The influence of prior synaptic plasticity on the induction of long-term potentiation. *Science, 255(5045),* 730-733.

Hubel, D. H. & Wiesel, T. N. (1974). Sequence regularity and geometry of orientation columns in the monkey striate cortex. *Journal of Comparative Neurology, 158(3),* 267-293.

Hubel, D. H. & Wiesel, T. N. (1963). Shape and arrangement of columns in cat's striate cortex. *The Journal of Physiology, 165(3),* 559-568.

Hudspeth, A. J. & Logothetis, N. K. (2000). Sensory systems. *Current Opinion in Neurobiology, 10(5),* 631-641.

Hund-Georgiadis, M. & von Cramon, D. Y. (1999). Motor-learning-related changes in piano players and non-musicians revealed by functional magnetic-resonance signals. *Experimental Brain Research, 125,* 417–425.

Hunter, M. A., Coffman, B. A., Gasparovic, C., Calhoun, V. D., Trumbo, M. C. & Clark, V. P. (2015). Baseline effects of transcranial direct current stimulation on glutamatergic neurotransmission and large-scale network connectivity. *Brain Research, 1594,* 92-107.

Hunter, M. A., Coffman, B. A., Trumbo, M. C. & Clark, V. P. (2013). Tracking the neuroplastic changes associated with transcranial direct current stimulation: a push for multimodal imaging. *Frontiers in Human Neuroscience, 7.*

Hupe, J. M., James, A. C., Payne, B. R., Lomber, S. G., Girard, P. & Bullier, J. (1998). Cortical feedback improves discrimination between figure and background by V1, V2 and V3 neurons. *Nature, 394(6695),* 784-787.

Iwamura, Y. (1998). Hierarchical somatosensory processing. *Current Opinion in Neurobiology, 8(4),* 522-528.

Iyer, M. B., Mattu, U., Grafman, J., Lomarev, M., Sato, S. & Wassermann, E. M. (2005). Safety and cognitive effect of frontal DC brain polarization in healthy individuals. *Neurology, 64(5),* 872-875.

Jacobson, L., Ezra, A., Berger, U. & Lavidor, M. (2012). Modulating oscillatory brain activity correlates of behavioral inhibition using transcranial direct current stimulation. *Clinical Neurophysiology, 123(5),* 979-984.

Jeffreys, D. A. & Axford, J. G. (1972a). Source locations of pattern-specific components of human visual evoked potentials. I. Component of striate cortical origin. *Experimental Brain Research, 16(1),* 1-21.

Jeffreys, D. A. & Axford, J. G. (1972b). Source locations of pattern-specific components of human visual evoked potentials. II. Components of extra-striate cortical origin. *Experimental Brain Research, 16(1),* 22-40.

Jeffreys, H. (1961). *Theory of probability* (3rd ed.). Oxford: Oxford University Press, Clarendon Press.

Jenkinson, M. & Smith, S. (2001). A global optimisation method for robust affine registration of brain images. *Medical Image Analysis, 5(2),* 143-156.

Jensen, O., Goel, P., Kopell, N., Pohja, M., Hari, R. & Ermentrout, B. (2005). On the human sensorimotor-cortex beta rhythm: sources and modeling. *Neuroimage, 26(2),* 347-355.

Jensen, O., Pohja, M., Goel, P., Ermentrout, B., Kopell, N. & Hari, R. (2002). On the physiological basis of the 15–30 Hz motor-cortex rhythm. In *Proceedings of the 13th International Conference on Biomagnetism* (pp. 313-315). VDE Verlag GMBH, Berlin.

Johansson, R. S. & Valbo, A. B. (1979). Tactile sensibility in the human hand: relative and absolute densities of four types of mechanoreceptive units in the glabrous skin. *The Journal of Physiology, 186,* 283-300.

Johnson, K. O. (2001). The roles and functions of cutaneous mechanoreceptors. *Current Opinion in Neurobiology, 11(4),* 455-461.

Joundi, R. A., Jenkinson, N., Brittain, J. S., Aziz, T. Z. & Brown, P. (2012). Driving oscillatory activity in the human cortex enhances motor performance. *Current Biology, 22(5),* 403-407.

Juchem, C., Nixon, T. W., Diduch, P., Rothman, D. L., Starewicz, P. & de Graaf, R. A. (2010). Dynamic shimming of the human brain at 7 T. *Concepts in Magnetic Resonance Part B: Magnetic Resonance Engineering, 37(3),* 116-128.

Jürgens, T. P., Schulte, A., Klein, T. & May, A. (2012). Transcranial direct current stimulation does neither modulate results of a quantitative sensory testing protocol nor ratings of suprathreshold heat stimuli in healthy volunteers. *European Journal of Pain, 16(9),* 1251-1263.

Jurkiewicz, M. T., Gaetz, W. C., Bostan, A. C. & Cheyne, D. (2006). Post-movement beta rebound is generated in motor cortex: evidence from neuromagnetic recordings. *Neuroimage, 32(3),* 1281-1289.

Kakei, S., Hoffman, D. S. & Strick, P. L. (1999). Muscle and movement representations in the primary motor cortex. *Science, 285(5436),* 2136-2139.

Kalaska, J. F., Scott, S. H., Cisek, P. & Sergio, L. E. (1997). Cortical control of reaching movements. *Current Opinion in Neurobiology, 7(6),* 849-859.

Kamali, A., Kramer, L. A., Butler, I. J. & Hasan, K. M. (2009). Diffusion tensor tractography of the somatosensory system in the human brainstem: initial findings using high isotropic spatial resolution at 3.0 T. *European Radiology, 19(6),* 1480-1488.

Karni, A., Meyer, G., Rey-Hipolito, C., Jezzard, P., Adams, M. M., Turner, R. & Ungerleider, L. G. (1998). The acquisition of skilled motor performance: fast and slow experience-driven changes in primary motor cortex. *Proceedings of the National Academy of Sciences, 95(3),* 861-868.

Kastner, S., Schneider, K. A. & Wunderlich, K. (2006). Beyond a relay nucleus: neuroimaging views on the human LGN. *Progress in Brain Research, 155*, 125-143.

Kaufman, D. L., Houser, C. R. & Tobin, A. J. (1991). Two forms of the γ-aminobutyric acid synthetic enzyme glutamate decarboxylase have distinct intraneuronal distributions and cofactor interactions. *Journal of Neurochemistry, 56(2),* 720-723.

Kellaway, P. (1946). The part played by electric fish in the early history of bioelectricity and electrotherapy. *Bulletin of the History of Medicine, 20(2),* 112-137.

Kelly, E. F. & Folger, S. E. (1999). EEG evidence of stimulus-directed response dynamics in human somatosensory cortex. *Brain Research, 815(2),* 326-336.

Khedr, E. M., El Gamal, N. F., El-Fetoh, N. A., Khalifa, H., Ahmed, E. M., Ali, A. M... & Karim, A. A. (2014). A double-blind randomized clinical trial on the efficacy of cortical direct current stimulation for the treatment of Alzheimer's disease. *Frontiers in Aging Neuroscience, 6.*

Kidgell, D. J., Goodwill, A. M., Frazer, A. K. & Daly, R. M. (2013). Induction of cortical plasticity and improved motor performance following unilateral and bilateral transcranial direct current stimulation of the primary motor cortex. *BMC Neuroscience, 14:*64.

Kilavik, B. E., Zaepffel, M., Brovelli, A., MacKay, W. A. & Riehle, A. (2013). The ups and downs of beta oscillations in sensorimotor cortex. *Experimental Neurology, 245*, 15-26.

Kim, J. H., Kim, D. W., Chang, W. H., Kim, Y. H., Kim, K., & Im, C. H. (2014). Inconsistent outcomes of transcranial direct current stimulation may originate from anatomical differences among individuals: Electric field simulation using individual MRI data. *Neuroscience Letters, 564,* 6-10.

Kim, S., Stephenson, M. C., Morris, P. G. & Jackson, S. R. (2014). tDCS-induced alterations in GABA concentration within primary motor cortex predict motor learning and motor memory: A 7 Tesla magnetic resonance spectroscopy study. *Neuroimage, 99*, 237-243.

Kingdom, F. A. A. & Prins, N. (2009). *Psychophysics: A Practical Introduction*. London: Academic Press.

Klein, S. A. (2001). Measuring, estimating, and understanding the psychometric function: A commentary. *Perception & Psychophysics, 63(8),* 1421-1455.

Kleschevnikov, A. M. & Routtenberg, A. (2001). PKC activation rescues LTP from NMDA receptor blockade. *Hippocampus, 11(2),* 168-175.

Koch, S. P., Habermehl, C., Mehnert, J., Schmitz, C. H., Holtze, S., Villringer, A... & Obrig, H. (2010). High-resolution optical functional mapping of the human somatosensory cortex. *Frontiers in Neuroenergetics, 2*.

Koelewijn, L., Dumont, J. R., Muthukumaraswamy, S. D., Rich, A. N. & Singh, K. D. (2011). Induced and evoked neural correlates of orientation selectivity in human visual cortex. *Neuroimage, 54(4),* 2983-2993.

Kohn, A. (2007). Visual adaptation: physiology, mechanisms, and functional benefits. *Journal of Neurophysiology, 97(5),* 3155-3164.

Kohn, A. & Whitsel, B. L. (2002). Sensory cortical dynamics. *Behavioural Brain Research, 135(1),* 119-126.

Kornhuber, H. H. & Deecke, L. (1964). Hirnpotentialanderungen beim Menschen vor und nach Willkurbewegungen, dargestellt mit Magnetband-Speiche-rung und Ruckwartsanalyse. *Pflugers Archiv European Journal of Physiology, 281*, 52.

Korsakov, I. A. & Matveeva, L. V. (1982). Psychophysical characteristics of perception and of brain electrical activity during occipital micropolarization. *Human Physiology, 8,* 259-266.

Kourtzi, Z., Tolias, A. S., Altmann, C. F., Augath, M. & Logothetis, N. K. (2003). Integration of local features into global shapes: monkey and human FMRI studies. *Neuron, 37(2),* 333-346.

Krause, B. & Cohen Kadosh, R. (2014). Not all brains are created equal: the relevance of individual differences in responsiveness to transcranial electrical stimulation. *Frontiers in Systems Neuroscience, 8,* 25.

Krause, B., Márquez-Ruiz, J. & Cohen Kadosh, R. (2013). The effect of transcranial direct current stimulation: a role for cortical excitation/inhibition balance? *Frontiers in Human Neuroscience, 7.*

Kreis, R., Ernst, T. & Ross, B. D. (1993). Absolute quantitation of water and metabolites in the human brain. II. Metabolite concentrations. *Journal of Magnetic Resonance, Series B, 102(1),* 9-19.

Kristeva, R., Cheyne, D. & Deecke, L. (1991). Neuromagnetic fields accompanying unilateral and bilateral voluntary movements: topography and analysis of cortical sources. *Electroencephalography and Clinical Neurophysiology/Evoked Potentials Section, 81(4),* 284-298.

Kruschke, J. K. (2010). Bayesian data analysis. *Wiley Interdisciplinary Reviews: Cognitive Science, 1(5),* 658-676.

Kuffler, S. W. (1953). Discharge patterns and functional organization of mammalian retina. *Journal of Neurophysiology, 16(1),* 37-68.

Kuo, M. F., Paulus, W. & Nitsche, M. A. (2006). Sex differences in cortical neuroplasticity in humans. *Neuroreport, 17(16),* 1703-1707.

Kuo, M. F., Paulus, W. & Nitsche, M. A. (2008). Boosting focally-induced brain plasticity by dopamine. *Cerebral Cortex, 18(3),* 648-651.

Kuo, M. F., Paulus, W. & Nitsche, M. A. (2014). Therapeutic effects of non-invasive brain stimulation with direct currents (tDCS) in neuropsychiatric diseases. *Neuroimage, 85*, 948-960.

Kurth, R., Villringer, K., Mackert, B. M., Schwiemann, J., Braun, J., Curio, G... & Wolf, K. J. (1998). fMRI assessment of somatotopy in human Brodmann area 3b by electrical finger stimulation. *Neuroreport, 9(2),* 207-209.

Ladeira, A., Fregni, F., Campanhã, C., Valasek, C. A., De Ridder, D., Brunoni, A. R. & Boggio, P. S. (2011). Polarity-dependent transcranial direct current stimulation effects on central auditory processing. *PloS One, 6(9),* e25399.

Lally, N., Nord, C. L., Walsh, V. & Roiser, J. P. (2013). Does excitatory fronto-extracerebral tDCS lead to improved working memory performance?. *F1000Research, 2*.

Landis, J. R. & Koch, G. G. (1977). The measurement of observer agreement for categorical data. *Biometrics, 33,* 159–174.

Lang, N., Siebner, H. R., Chadaide, Z., Boros, K., Nitsche, M. A., Rothwell, J. C... & Antal, A. (2007). Bidirectional modulation of primary visual cortex excitability: a combined tDCS and rTMS study. *Investigative Ophthalmology & Visual Science, 48(12),* 5782-5787.

Leahy, R. M., Mosher, J. C., Spencer, M. E., Huang, M. X. & Lewine, J. D. (1998). A study of dipole localization accuracy for MEG and EEG using a human skull phantom. *Electroencephalography and Clinical Neurophysiology, 107(2),* 159-173.

Lee, K. G., Jacobs, M. F., Asmussen, M. J., Zapallow, C. M., Tommerdahl, M. & Nelson, A. J. (2013). Continuous theta-burst stimulation modulates tactile synchronization. *BMC Neuroscience, 14:*89.

Lee, C. J. & Whitsel, B. L. (1992). Mechanisms underlying somatosensory cortical dynamics. I. In vivo studies. *Cerebral Cortex, 2,* 81–106.

Lee, C. J., Whitsel, B. L. & Tommerdahl, M. (1992). Mechanisms underlying somatosensory cortical dynamics: II. In vitro studies. *Cerebral Cortex, 2,* 107-133.

Leek, M. R. (2001). Adaptive procedures in psychophysical research. *Attention, Perception, & Psychophysics, 63(8),* 1279-1292.

Lefebvre, S., Dricot, L., Laloux, P., Gradkowski, W., Desfontaines, P., Evrard, F... & Vandermeeren, Y. (2015). Neural substrates underlying stimulation-enhanced motor skill learning after stroke. *Brain, 138(1),* 149-163.

Lennie, P. (2003). Receptive fields. *Current Biology, 13,* 216-219.

Leung, Y. Y., Bensmaia, S. J., Hsiao, S. S. & Johnson, K. O. (2005). Time-course of vibratory adaptation and recovery in cutaneous mechanoreceptive afferents. *Journal of Neurophysiology, 94(5),* 3037-3045.

Leuthold, H. & Jentzsch, I. (2002). Distinguishing neural sources of movement preparation and execution: An electrophysiological analysis. *Biological Psychology, 60(2),* 173-198.

Le Van Quyen, M., Foucher, J., Lachaux, J., Rodriguez, E., Lutz, A., Martinerie, J. & Varela, F. J. (2001). Comparison of Hilbert transform and wavelet methods for the analysis of neuronal synchrony. *Journal of Neuroscience Methods, 111,* 83-98.

Levine, A. J., Lewallen, K. A. & Pfaff, S. L. (2012). Spatial organization of cortical and spinal neurons controlling motor behavior. *Current Opinion in Neurobiology, 22(5),* 812-821.

Levitt, H. (1970). Transformed up-down methods in psychoacoustics. *Journal of the Acoustical Society of America, 33,* 467–476.

Leyton, S. S. F. & Sherrington, C. S. (1917). Observations on the excitable cortex of the chimpanzee, orangutan and gorilla. *Quarterly Journal of Experimental Physiology, 11*, 135–222.

Liebetanz, D., Nitsche, M. A., Tergau, F. & Paulus, W. (2002). Pharmacological approach to the mechanisms of transcranial DC-stimulation-induced after-effects of human motor cortex excitability. *Brain, 125(10),* 2238-2247.

Liepert, J., Miltner, W. H. R., Bauder, H., Sommer, M., Dettmers, C., Taub, E. & Weiller, C. (1998). Motor cortex plasticity during constraint-induced movement therapy in stroke patients. *Neuroscience Letters, 250(1),* 5-8.

Liepert, J., Schwenkreis, P., Tegenthoff, M. & Malin, J. P. (1997). The glutamate antagonist riluzole suppresses intracortical facilitation. *Journal of Neural Transmission, 104(11-12),* 1207-1214.

Lisman, J. E. (2001). Three Ca2+ levels affect plasticity differently: the LTP zone, the LTD zone and no man's land. *The Journal of Physiology, 532(2),* 285-285.

Litvak, V., Eusebio, A., Jha, A., Oostenveld, R., Barnes, G. R., Penny, W. D... & Brown, P. (2010). Optimized beamforming for simultaneous MEG and intracranial local field potential recordings in deep brain stimulation patients. *Neuroimage, 50(4),* 1578-1588.

Lømo, T. (1966). Frequency potentiation of excitatory synaptic activity in the dentate area of the hippocampal formation. *Acta Physiologica, 68,* 128.

Loo, C. K., Martin, D. M., Alonzo, A., Gandevia, S., Mitchell, P. B. & Sachdev, P. (2011). Avoiding skin burns with transcranial direct current stimulation: preliminary considerations. *International Journal of Neuropsychopharmacology, 14(3),* 425-426.

Lopes da Silva, F. (2011). Biophysical aspects of EEG and magnetoencephalogram generation. In Schomer, D. L. and Lopes da Silva, F. (eds), *Niedermeyer's Electroencephalography*. 6th Edition ed. Philadelphia, USA: Lippincott Williams and Wilkins.

Luppi, P. H., Peyron, C. & Fort, P. (2016). Not a single but multiple populations of GABAergic neurons control sleep. *Sleep Medicine Reviews*.

Lynch, G., Larson, J., Kelso, S., Barrionuevo, G. & Schottler, F. (1983). Intracellular injections of EGTA block induction of hippocampal long-term potentiation. *Nature, 305(5936),* 719-721.

Madison, D. V., Malenka, R. C. & Nicoll, R. A. (1991). Mechanisms underlying long-term potentiation of synaptic transmission. *Annual Review of Neuroscience, 14(1),* 379-397.

Mahmoudi, H., Haghighi, A. B., Petramfar, P., Jahanshahi, S., Salehi, Z. & Fregni, F. (2011). Transcranial direct current stimulation: electrode montage in stroke. *Disability & Rehabilitation, 33,* 1383-1388.

Malenka, R. C., Kauer, J. A., Zucker, R. S. & Nicoll, R. A. (1988). Postsynaptic calcium is sufficient for potentiation of hippocampal synaptic transmission. *Science, 242(4875),* 81-84.

Mangia, A. L., Pirini, M. & Cappello, A. (2014). Transcranial direct current stimulation and power spectral parameters: a tDCS/EEG co-registration study. *Frontiers in Human Neuroscience, 8*.

Mansfield, P. (1977). Multi-planar image formation using NMR spin echoes. *Journal of Physics Condensed Matter: Solid State Physics, 10(3),* 55-58.

Manto, M., Bower, J. M., Conforto, A. B., Delgado-García, J. M., da Guarda, S. N. F., Gerwig, M... & Timmann, D. (2012). Consensus paper: roles of the cerebellum in motor control—the diversity of ideas on cerebellar involvement in movement. *The Cerebellum, 11(2),* 457-487.

Marshall, T. R., Esterer, S., Herring, J. D., Bergmann, T. O. & Jensen, O. (2015). On the relationship between cortical excitability and visual oscillatory responses—A concurrent tDCS–MEG study. *Neuroimage*.

Mathys, C., Loui, P., Zheng, X. & Schlaug, G. (2010). Non-invasive brain stimulation applied to Heschl's gyrus modulates pitch discrimination. *Frontiers in Psychology, 1*.

Matsunaga, K., Nitsche, M. A., Tsuji, S. & Rothwell, J. C. (2004). Effect of transcranial DC sensorimotor cortex stimulation on somatosensory evoked potentials in humans. *Clinical Neurophysiology, 115(2),* 456-460.

Matsuzaka, Y., Picard, N. & Strick, P. L. (2007). Skill representation in the primary motor cortex after long-term practice. *Journal of Neurophysiology, 97(2),* 1819-1832.

McCormick, D. A. (1989). GABA as an inhibitory neurotransmitter in human cerebral cortex. *Journal of Neurophysiology, 62(5),* 1018-1027.

McDonnell, M. N., Orekhov, Y. & Ziemann, U. (2006). The role of GABAB receptors in intracortical inhibition in the human motor cortex. *Experimental Brain Research, 173(1),* 86-93.

McDonnell, M. N., Orekhov, Y. & Ziemann, U. (2007). Suppression of LTP-like plasticity in human motor cortex by the GABAB receptor agonist baclofen. *Experimental Brain Research, 180(1),* 181-186.

McGonigle, D. J. (2004). Somesthetic Function. In Frackowiak, R. S., Ashburner, J. T., Penny, W. D., Zeki, S., Friston, K. J., Frith, C. D., Dolan, R. J. & Price, C. J. (Eds.), *Human Brain Function* (pp. 75-104). Academic Press.

McGonigle, D. J., Aston, P., Josephs, O. & Frackowiak, R. S. J. (1998). Somatotopy of vibrotactile stimulation in SI: an fMRI study. *Neuroimage, 7.*

McIlwain, H. (1985). *Biochemistry and the Central Nervous System* (5th ed.). Edinburgh: Churchill Livingstone.

McKeefry, D. J. & Zeki, S. (1997). The position and topography of the human colour centre as revealed by functional magnetic resonance imaging. *Brain, 120(12),* 2229-2242.

McRobbie, D. W., Moore, E. A., Graves, M. J. & Prince, M. R. (2006). *MRI from Picture to Proton*. Cambridge University Press.

Medeiros, L. F., de Souza, I. C. C., Vidor, L. P., de Souza, A., Deitos, A., Volz, M. S... & Torres, I. L. (2012). Neurobiological effects of transcranial direct current stimulation: a review. *Frontiers in Psychiatry, 3.*

Mekle, R., Mlynárik, V., Gambarota, G., Hergt, M., Krueger, G. & Gruetter, R. (2009). MR spectroscopy of the human brain with enhanced signal intensity at ultrashort echo times on a clinical platform at 3T and 7T. *Magnetic Resonance in Medicine, 61(6),* 1279-1285.

Merchant, H., Naselaris, T. & Georgopoulos, A. P. (2008). Dynamic sculpting of directional tuning in the primate motor cortex during three-dimensional reaching. *The Journal of Neuroscience, 28(37),* 9164-9172.

Merkl, A., Schubert, F., Quante, A., Luborzewski, A., Brakemeier, E. L., Grimm, S... & Bajbouj, M. (2011). Abnormal cingulate and prefrontal cortical neurochemistry in major depression after electroconvulsive therapy. *Biological Psychiatry, 69(8),* 772-779.

Mescher, M., Merkle, H., Kirsch, J., Garwood, M. & Gruetter, R. (1998). Simultaneous in vivo spectral editing and water suppression. *NMR in Biomedicine, 11,* 266-272.

Mescher, M., Tannus, A., Johnson, M. N. & Garwood, M. (1996). Solvent suppression using selective echo dephasing. *Journal of Magnetic Resonance, Series A, 123(2),* 226-229.

Mikkelsen, M., Singh, K. D., Sumner, P. & Evans, C. J. (2015). Comparison of the repeatability of GABA-edited magnetic resonance spectroscopy with and without macromolecule suppression. *Magnetic Resonance in Medicine*.

Miranda, P. C., Lomarev, M. & Hallett, M. (2006). Modeling the current distribution during transcranial direct current stimulation. *Clinical Neurophysiology, 117(7),* 1623-1629.

Moore, C. I., Stern, C. E., Corkin, S., Fischl, B., Gray, A. C., Rosen, B. R. & Dale, A. M. (2000). Segregation of somatosensory activation in the human rolandic cortex using fMRI. *Journal of Neurophysiology, 84(1),* 558-569.

Mondino, M., Bennabi, D., Poulet, E., Galvao, F., Brunelin, J. & Haffen, E. (2014). Can transcranial direct current stimulation (tDCS) alleviate symptoms and improve cognition in psychiatric disorders?. *The World Journal of Biological Psychiatry, 15(4),* 261-275.

Monte-Silva, K., Kuo, M. F., Hessenthaler, S., Fresnoza, S., Liebetanz, D., Paulus, W. & Nitsche, M. A. (2013). Induction of late LTP-like plasticity in the human motor cortex by repeated non-invasive brain stimulation. *Brain Stimulation, 6(3),* 424-432.

Mordillo-Mateos, L., Turpin-Fenoll, L., Millán-Pascual, J., Núñez-Pérez, N., Panyavin, I., Gómez-Argüelles, J. M... & Oliviero, A. (2012). Effects of simultaneous bilateral tDCS of the human motor cortex. *Brain Stimulation, 5(3),* 214-222.

Mori, F., Nicoletti, C. G., Kusayanagi, H., Foti, C., Restivo, D. A., Marciani, M. G. & Centonze, D. (2013). Transcranial direct current stimulation ameliorates tactile sensory deficit in multiple sclerosis. *Brain Stimulation, 6(4),* 654-659.

Mosher, J.C., Leahy, R. M. & Lewis, P. S. (1999). EEG and MEG: Forward solutions for inverse methods. *IEEE Transactions on Biomedical Engineering, 46,* 245–259.

Mountcastle, V. B. (1957). Modality and topographic properties of single neurons of cat's somatic sensory cortex. *Journal of Neurophysiology, 20,* 408–434.

Mountcastle, V. B. (2005). *The sensory hand: neural mechanisms of somatic sensation*. Cambridge, MA: Harvard University Press.

Mullins, P. G., McGonigle, D. J., O'Gorman, R. L., Puts, N. A., Vidyasagar, R., Evans, C. J. & Edden, R. A. (2014). Current practice in the use of MEGA-PRESS spectroscopy for the detection of GABA. *Neuroimage, 86,* 43-52.

Murakami, S. & Okada, Y. (2006). Contributions of principal neocortical neurons to magnetoencephalography and electroencephalography signals. *The Journal of Physiology, 575,* 925–936.

Mushiake, H., Inase, M. & Tanji, J. (1991). Neuronal activity in the primate premotor, supplementary, and precentral motor cortex during visually guided and internally determined sequential movements. *Journal of Neurophysiology, 66(3),* 705-718.

Muthukumaraswamy, S. D. (2010). Functional properties of human primary motor cortex gamma oscillations. *Journal of Neurophysiology, 104(5),* 2873-2885.

Muthukumaraswamy, S. D. (2014). The use of magnetoencephalography in the study of psychopharmacology (pharmaco-MEG). *Journal of Psychopharmacology*.

Muthukumaraswamy, S. D., Carhart-Harris, R. L., Moran, R. J., Brookes, M. J., Williams, T. M., Errtizoe, D... & Nutt, D. J. (2013b). Broadband cortical desynchronization underlies the human psychedelic state. *The Journal of Neuroscience, 33(38),* 15171-15183.

Muthukumaraswamy, S. D., Edden, R. A., Jones, D. K., Swettenham, J. B. & Singh, K. D. (2009). Resting GABA concentration predicts peak gamma frequency and fMRI amplitude in response to visual stimulation in humans. *Proceedings of the National Academy of Sciences, 106(20),* 8356-8361.

Muthukumaraswamy, S. D., Myers, J. F. M., Wilson, S. J., Nutt, D. J., Lingford-Hughes, A., Singh, K. D. & Hamandi, K. (2013a). The effects of elevated endogenous GABA levels on movement-related network oscillations. *Neuroimage, 66,* 36-41.

Muthukumaraswamy, S. D. & Singh, K. D. (2013). Visual gamma oscillations: the effects of stimulus type, visual field coverage and stimulus motion on MEG and EEG recordings. *Neuroimage, 69,* 223-230.

Muthukumaraswamy, S. D., Singh, K. D., Swettenham, J. B. & Jones, D. K. (2010). Visual gamma oscillations and evoked responses: variability, repeatability and structural MRI correlates. *Neuroimage, 49(4),* 3349-3357.

Myers, J. F., Evans, C. J., Kalk, N. J., Edden, R. A. & Lingford-Hughes, A. R. (2014). Measurement of GABA using J-difference edited 1H-MRS following modulation of synaptic GABA concentration with tiagabine. *Synapse, 68(8),* 355-362.

Nakamura, A., Yamada, T., Goto, A., Kato, T., Ito, K., Abe, Y... & Kakigi, R. (1998). Somatosensory homunculus as drawn by MEG. *Neuroimage, 7(4),* 377-386.

Naressi, A., Couturier, C., Castang, I., De Beer, R. & Graveron-Demilly, D. (2001). Java-based graphical user interface for MRUI, a software package for quantitation of in vivo/medical magnetic resonance spectroscopy signals. *Computers in Biology and Medicine, 31(4),* 269-286.

Nathan, P. J., Cobb, S. R., Lu, B., Bullmore, E. T. & Davies, C. H. (2011). Studying synaptic plasticity in the human brain and opportunities for drug discovery. *Current Opinion in Pharmacology, 11(5),* 540-548.

Nauhaus, I., Busse, L., Carandini, M. & Ringach, D. L. (2009). Stimulus contrast modulates functional connectivity in visual cortex. *Nature Neuroscience, 12,* 70–76.

Near, J. (2014). Spectral Quantification and Pitfalls in Interpreting Magnetic Resonance Spectroscopy Data: What to Look Out For. In C. J. Stagg & D. Rothman (Eds.) *"Magnetic Resonance Spectroscopy: Tools for Neuroscience Research and Emerging Clincal Applications"*(pp. 49-70). Academic Press.

Near, J., Ho, Y. C. L., Sandberg, K., Kumaragamage, C. & Blicher, J. U. (2014). Long-term reproducibility of GABA magnetic resonance spectroscopy. *Neuroimage, 99,* 191-196.

Nelson, A. J. & Chen, R. (2008). Digit somatotopy within cortical areas of the postcentral gyrus in humans. *Cerebral Cortex, 18(10),* 2341-2351.

Neuling, T., Rach, S., Wagner, S., Wolters, C. H. & Herrmann, C. S. (2012). Good vibrations: Oscillatory phase shapes perception. *Neuroimage, 63(2),* 771-778.

Neuling, T., Ruhnau, P., Fuscà, M., Demarchi, G., Herrmann, C. S. & Weisz, N. (2015). Friends, not foes: Magnetoencephalography as a tool to uncover brain dynamics during transcranial alternating current stimulation. *Neuromage, 118,* 406-413.

Nichols, T. E. & Holmes, A. P. (2002). Nonparametric permutation tests for functional neuroimaging: a primer with examples. *Human Brain Mapping, 15(1),* 1-25.

Nitsche, M. A., Bikson, M. & Bestmann, S. (2015). On the use of meta-analysis in neuromodulatory non-invasive brain stimulation. *Brain Stimulation, 8(3),* 666-667.

Nitsche, M. A., Cohen, L. G., Wassermann, E. M., Priori, A., Lang, N., Antal, A... & Pascual-Leone, A. (2008). Transcranial direct current stimulation: State of the art 2008. *Brain Stimulation, 1(3),* 206-223.

Nitsche, M. A., Doemkes, S., Karakoese, T., Antal, A., Liebetanz, D., Lang, N... & Paulus, W. (2007). Shaping the effects of transcranial direct current stimulation of the human motor cortex. *Journal of Neurophysiology, 97(4),* 3109-3117.

Nitsche, M. A., Fricke, K., Henschke, U., Schlitterlau, A., Liebetanz, D., Lang, N... & Paulus, W. (2003b). Pharmacological modulation of cortical excitability shifts induced by transcranial direct current stimulation in humans. *The Journal of Physiology, 553(1),* 293-301.

Nitsche, M.A., Jaussi, W., Liebetanz, D., Lang, N., Tergau, F. & Paulus, W. (2004b). Consolidation of human motor cortical neuroplasticity by D-cycloserine. *Neuropsychopharmacology, 29(8),* 1573-1578.

Nitsche, M. A., Kuo, M. F., Karrasch, R., Wächter, B., Liebetanz, D. & Paulus, W. (2009). Serotonin Affects Transcranial Direct Current–Induced Neuroplasticity in Humans. *Biological Psychiatry, 66(5),* 503-508.

Nitsche, M. A., Lampe, C., Antal, A., Liebetanz, D., Lang, N., Tergau, F. & Paulus, W. (2006). Dopaminergic modulation of long-lasting direct current-induced cortical excitability changes in the human motor cortex. *European Journal of Neuroscience, 23,* 1651–1657.

Nitsche, M. A., Liebetanz, D., Lang, N., Antal, A., Tergau, F. & Paulus, W. (2003a). Modulation of cortical excitability by weak direct current stimulation–technical, safety and functional aspects. *Supplements to Clinical Neurophysiology, 56(3),* 255-276.

Nitsche, M. A., Liebetanz, D., Schlitterlau, A., Henschke, U., Fricke, K., Frommann, K... & Tergau, F. (2004a). GABAergic modulation of DC stimulation-induced motor cortex excitability shifts in humans. *European Journal of Neuroscience, 19(10),* 2720-2726.

Nitsche, M. A. & Paulus, W. (2000). Excitability changes induced in the human motor cortex by weak transcranial direct current stimulation. *The Journal of Physiology, 527(3),* 633-639.

Nitsche, M. A. & Paulus, W. (2001). Sustained excitability elevations induced by transcranial DC motor cortex stimulation in humans. *Neurology, 57,* 1899–1901.

Nitsche, M. A., Schauenburg, A., Lang, N., Liebetanz, D., Exner, C., Paulus, W. & Tergau, F. (2003c). Facilitation of implicit motor learning by weak transcranial direct current stimulation of the primary motor cortex in the human. *Journal of Cognitive Neuroscience, 15,* 619–626.

Nitsche, M. A., Seeber, A., Frommann, K., Klein, C. C., Rochford, C., Nitsche, M. S... & Tergau, F. (2005). Modulating parameters of excitability during and after transcranial direct current stimulation of the human motor cortex. *The Journal of Physiology, 568(1),* 291-303.

Nguyen, R. H., Ford, S., Calhoun, A. H., Holden, J. K., Gracely, R. H. & Tommerdahl, M. (2013a). Neurosensory assessments of migraine. *Brain Research, 1498,* 50-58.

Nguyen, R. H., Gillen, C., Garbutt, J. C., Kampov-Polevoi, A., Holden, J. K., Francisco, E. M. & Tommerdahl, M. (2013b). Centrally-mediated sensory information processing is impacted with increased alcohol consumption in college-aged individuals. *Brain Research, 1492,* 53-62.

Nolte, J. & Sundsten, J. (2002). *The human brain: an introduction to its functional anatomy* (Vol. 5, p. 650). St. Louis: Mosby.

Notturno, F., Marzetti, L., Pizzella, V., Uncini, A. & Zappasodi, F. (2014). Local and remote effects of transcranial direct current stimulation on the electrical activity of the motor cortical network. *Human Brain Mapping, 35(5),* 2220-2232.

Nowak, H. (1998). Biomagnetism. In Andrai, W., Nowak, H. (eds). *Magnetism in Medicine*. Wiley, Berlin.

Nudo, R. J., Milliken, G. W., Jenkins, W. M. & Merzenich, M. M. (1996). Use-dependent alterations of movement representations in primary motor cortex of adult squirrel monkeys. *The Journal of Neuroscience, 16(2),* 785-807.

Nunez, P. L. & Silberstein, R. B. (2000). On the relationship of synaptic activity to macroscopic measurements: does co-registration of EEG with fMRI make sense?. *Brain Topography, 13(2),* 79-96.

O'Gorman, R. L., Michels, L., Edden, R. A., Murdoch, J. B. & Martin, E. (2011). In vivo detection of GABA and glutamate with MEGA-PRESS: Reproducibility and gender effects. *Journal of Magnetic Resonance Imaging, 33(5),* 1262-1267.

Oldfield, R. C. (1971). The assessment and analysis of handedness: the Edinburgh inventory. *Neuropsychologia, 9(1),* 97-113.

O'Mara, S., Rowe, M. J. & Tarvin, R. P. (1988). Neural mechanisms in vibrotactile adaptation. *Journal of Neurophysiology, 59,* 607–622.

Oostenveld, R., Fries, P., Maris, E. & Schoffelen, J. M. (2010). FieldTrip: open source software for advanced analysis of MEG, EEG, and invasive electrophysiological data. *Computational Intelligence and Neuroscience*.

Opitz, A., Paulus, W., Will, S., Antunes, A. & Thielscher, A. (2015). Determinants of the electric field during transcranial direct current stimulation. *Neuroimage, 109,* 140-150.

O'Shea, J., Boudrias, M. H., Stagg, C. J., Bachtiar, V., Kischka, U., Blicher, J. U. & Johansen-Berg, H. (2014). Predicting behavioural response to TDCS in chronic motor stroke. *Neuroimage, 85*, 924-933.

Overduin, S. A. & Servos, P. (2008). Symmetric sensorimotor somatotopy. *PloS One, 3(1),* e1505.

Pantev, C., Bertrand, O., Eulitz, C., Verkindt, C., Hampson, S., Schuierer, G. & Elbert, T. (1995). Specific tonotopic organizations of different areas of the human auditory cortex revealed by simultaneous magnetic and electric recordings. *Electroencephalography and Clinical Neurophysiology, 94(1),* 26-40.

Parent, A. (2004). Giovanni Aldini: from animal electricity to human brain stimulation. *The Canadian Journal of Neurological Sciences, 31(4),* 576-584.

Parrish, T. B., Gitelman, D. R., LaBar, K. S. & Mesulam, M. (2000). Impact of signal-to-noise on functional MRI. *Magnetic Resonance in Medicine, 44(6),* 925-932.

Paulus, W. (2011). Transcranial electrical stimulation (tES–tDCS; tRNS, tACS) methods. *Neuropsychological Rehabilitation, 21(5),* 602-617.

Pavlova, E., Kuo, M. F., Nitsche, M. A. & Borg, J. (2014). Transcranial direct current stimulation of the premotor cortex: Effects on hand dexterity. *Brain Research, 1576,* 52-62.

Pelli, D. G. (1997). The VideoToolbox software for visual psychophysics: transforming numbers into movies. *Spatial Vision, 10,* 437–442.

Pellicciari, M. C., Brignani, D. & Miniussi, C. (2013). Excitability modulation of the motor system induced by transcranial direct current stimulation: a multimodal approach. *Neuroimage, 83,* 569-580.

Penfield, W. & Rasmussen, T. (1950). *The cerebral cortex of man; a clinical study of localization of function.* New York: NY, MacMillan.

Pfurtscheller, G., Graimann, B., Huggins, J. E., Levine, S. P. & Schuh, L. A. (2003). Spatiotemporal patterns of beta desynchronization and gamma synchronization in corticographic data during self-paced movement. *Clinical Neurophysiology, 114(7),* 1226-1236.

Pfurtscheller, G. & Lopes da Silva, F. (1999). Event-related EEG/MEG synchronization and desynchronization: basic principles. *Clinical Neurophysiology, 110(11),* 1842-1857.

Pirulli, C., Fertonani, A. & Miniussi, C. (2014). Is neural hyperpolarization by cathodal stimulation always detrimental at the behavioral level?. *Frontiers in Behavioral Neuroscience, 8*.

Pleger, B. & Villringer, A. (2013). The human somatosensory system: from perception to decision making. *Progress in Neurobiology, 103,* 76-97.

Ploner, M., Schmitz, F., Freund, H. J. & Schnitzler, A. (2000). Differential organization of touch and pain in human primary somatosensory cortex. *Journal of Neurophysiology, 83(3),* 1770-1776.

Polanía, R., Nitsche, M. A. & Paulus, W. (2011). Modulating functional connectivity patterns and topological functional organization of the human brain with transcranial direct current stimulation. *Human Brain Mapping, 32(8),* 1236-1249.

Polanía, R., Paulus, W. & Nitsche, M. A. (2012). Modulating cortico-striatal and thalamo-cortical functional connectivity with transcranial direct current stimulation. *Human Brain Mapping, 33(10),* 2499-2508.

Pollard, T. D. & Cooper, J. A. (2009). Actin, a central player in cell shape and movement. *Science, 326(5957),* 1208-1212.

Porcu, P., Sogliano, C., Cinus, M., Purdy, R. H., Biggio, G. & Concas, A. (2003). Nicotine-induced changes in cerebrocortical neuroactive steroids and plasma corticosterone concentrations in the rat. *Pharmacology Biochemistry and Behavior, 74(3),* 683-690.

Poreisz, C., Boros, K., Antal, A. & Paulus, W. (2007). Safety aspects of transcranial direct current stimulation concerning healthy subjects and patients. *Brain Research Bulletin, 72(4),* 208-214.

Priori, A., Berardelli, A., Rona, S., Accornero, N. & Manfredi, M. (1998). Polarization of the human motor cortex through the scalp. *Neuroreport, 9(10),* 2257-2260.

Priori, A., Hallett, M. & Rothwell, J. C. (2009). Repetitive transcranial magnetic stimulation or transcranial direct current stimulation?. *Brain Stimulation, 2(4),* 241-245.

Provencher, S. W. (1993). Estimation of metabolite concentrations from localized in vivo proton NMR spectra. *Magnetic Resonance in Medicine, 30(6),* 672-679.

Purcell, E. M., Torrey, H. C. & Pound, R. V. (1946). Resonance absorption by nuclear magnetic moments in a solid. *Physical Review, 69(1-2),* 37.

Puri, R., Hinder, M. R., Fujiyama, H., Gomez, R., Carson, R. G. & Summers, J. J. (2015). Duration-dependent effects of the BDNF Val66Met polymorphism on anodal tDCS induced motor cortex plasticity in older adults: a group and individual perspective. *Frontiers in Aging Neuroscience, 7.*

Purpura, D. P. & McMurtry, J. G. (1965). Intracellular activities and evoked potential changes during polarization of motor cortex. *Journal of Neurophysiology, 28(1),* 166-185.

Purves, D., Cabeza, R., Huettel, S. A., LaBar, K., Platt, M. & Woldorff, M. (2013). *Principles of Cognitive Neuroscience.* Sunderland, MA: Sinauer Associates.

Puts, N. A. & Edden, R. A. (2012). In vivo magnetic resonance spectroscopy of GABA: a methodological review. *Progress in Nuclear Magnetic Resonance Spectroscopy, 60,* 29-41.

Puts, N. A., Edden, R. A., Evans, C. J., McGlone, F. & McGonigle, D. J. (2011). Regionally specific human GABA concentration correlates with tactile discrimination thresholds. *The Journal of Neuroscience, 31(46),* 16556-16560.

Puts, N. A., Edden, R. A., Wodka, E. L., Mostofsky, S. H. & Tommerdahl, M. (2013). A vibrotactile behavioral battery for investigating somatosensory processing in children and adults. *Journal of Neuroscience Methods, 218(1),* 39-47.

Quartarone, A., Morgante, F., Bagnato, S., Rizzo, V., Sant'Angelo, A., Aiello, E... & Girlanda, P. (2004). Long lasting effects of transcranial direct current stimulation on motor imagery. *Neuroreport, 15(8),* 1287-1291.

Radman, T., Ramos, R. L., Brumberg, J. C. & Bikson, M. (2009). Role of cortical cell type and morphology in subthreshold and suprathreshold uniform electric field stimulation in vitro. *Brain Stimulation, 2(4),* 215-228.

Ragert, P., Nierhaus, T., Cohen, L. G. & Villringer, A. (2011). Interhemispheric interactions between the human primary somatosensory cortices. *PloS One, 6(2),* e16150.

Ragert, P., Vandermeeren, Y., Camus, M. & Cohen, L. G. (2008). Improvement of spatial tactile acuity by transcranial direct current stimulation. *Clinical Neurophysiology, 119(4),* 805-811.

Rahman, A., Reato, D., Arlotti, M., Gasca, F., Datta, A., Parra, L. C. & Bikson, M. (2013). Cellular effects of acute direct current stimulation: somatic and synaptic terminal effects. *The Journal of Physiology, 591(10),* 2563-2578.

Rampersad, S. M., Janssen, A. M., Lucka, F., Aydin, U., Lanfer, B., Lew, S... & Oostendorp, T. F. (2014). Simulating transcranial direct current stimulation with a detailed anisotropic human head model. *IEEE Transactions on Neural Systems and Rehabilitation Engineering, 22(3),* 441-452.

Rango, M., Cogiamanian, F., Marceglia, S., Barberis, B., Arighi, A., Biondetti, P. & Priori, A. (2008). Myoinositol content in the human brain is modified by transcranial direct current stimulation in a matter of minutes: A 1H-MRS study. *Magnetic Resonance in Medicine, 60(4),* 782-789.

Ray, S. & Maunsell, J. H. (2010). Differences in gamma frequencies across visual cortex restrict their possible use in computation. *Neuron, 67(5),* 885-896.

Raz, N., Lindenberger, U., Rodrigue, K. M., Kennedy, K. M., Head, D., Williamson, A... & Acker, J. D. (2005). Regional brain changes in aging healthy adults: general trends, individual differences and modifiers. *Cerebral Cortex, 15(11),* 1676-1689.

Reato, D., Bikson, M. & Parra, L. C. (2015). Lasting modulation of in-vitro oscillatory activity with weak direct current stimulation. *Journal of Neurophysiology, 113(5),* 1334-1341.

Reato, D., Rahman, A., Bikson, M. & Parra, L. C. (2010). Low-intensity electrical stimulation affects network dynamics by modulating population rate and spike timing. *The Journal of Neuroscience, 30(45),* 15067-15079.

Ridding, M. C. & Ziemann, U. (2010). Determinants of the induction of cortical plasticity by non-invasive brain stimulation in healthy subjects. *The Journal of Physiology, 588(13),* 2291-2304.

Rizzolatti, G. & Luppino, G. (2001). The cortical motor system. *Neuron, 31(6),* 889-901.

Roberto, M., Madamba, S. G., Moore, S. D., Tallent, M. K. & Siggins, G. R. (2003). Ethanol increases GABAergic transmission at both pre-and postsynaptic sites in rat central amygdala neurons. *Proceedings of the National Academy of Sciences, 100(4),* 2053-2058.

Robinson, S. E. & Vrba, J. (1999). Recent advances in biomagnetism. In *Functional neuroimaging by synthetic aperture magnetometry (SAM),* (pp. 302-305). Tohoku University Press Sendai, Japan.

Rodman, H. R. & Albright, T. D. (1987). Coding of visual stimulus velocity in area MT of the macaque. *Vision Research, 27(12),* 2035-2048.

Rogalewski, A., Breitenstein, C., Nitsche, M. A., Paulus, W. & Knecht, S. (2004). Transcranial direct current stimulation disrupts tactile perception. *European Journal of Neuroscience, 20(1),* 313-316.

Rönnqvist, K. C., McAllister, C. J., Woodhall, G. L., Stanford, I. M. & Hall, S. D. (2013). A multimodal perspective on the composition of cortical oscillations. *Frontiers in Human Neuroscience, 7.*

Rosenzweig, M. R., Breedlove, S. M. & Watson, N. V. (2005). *Biological psychology: An introduction to behavioral, cognitive, and clinical neuroscience*. Sunderland, MA: Sinauer Associates.

Rothman, D. L., Arias-Mendoza, F., Shulman, G. I. & Shulman, R. G. (1984). A pulse sequence for simplifying hydrogen NMR spectra of biological tissues. *Journal of Magnetic Resonance, 60(3),* 430-436.

Rothman, D. L., Petroff, O. A., Behar, K. L. & Mattson, R. H. (1993). Localized 1H NMR measurements of gamma-aminobutyric acid in human brain in vivo. *Proceedings of the National Academy of Sciences, 90(12),* 5662-5666.

Rowland, L. M., Krause, B. W., Wijtenburg, S. A., McMahon, R. P., Chiappelli, J., Nugent, K. L... & Hong, L. E. (2015). Medial frontal GABA is lower in older schizophrenia: a MEGA-PRESS with macromolecule suppression study. *Molecular Psychiatry.*

Roy, A., Baxter, B. & He, B. (2014). High definition transcranial direct current stimulation induces both acute and persistent changes in broadband cortical synchronization: a simultaneous tDCS-EEG study. *IEEE Transactions on Biomedical Engineering, 61(7),* 1967-1978.

Ruben, J., Schwiemann, J., Deuchert, M., Meyer, R., Krause, T., Curio, G... & Villringer, A. (2001). Somatotopic organization of human secondary somatosensory cortex. *Cerebral Cortex, 11(5),* 463-473.

Ruff, C. C., Blankenburg, F., Bjoertomt, O., Bestmann, S., Freeman, E., Haynes, J. D... & Driver, J. (2006). Concurrent TMS-fMRI and psychophysics reveal frontal influences on human retinotopic visual cortex. *Current Biology, 16(15),* 1479-1488.

Russell, M. J., Goodman, T., Pierson, R., Shepherd, S., Wang, Q., Groshong, B. & Wiley, D. F. (2013). Individual differences in transcranial electrical stimulation current density. *Journal of Biomedical Research, 27(6),* 495-508.

Sale, M. V., Ridding, M. C. & Nordstrom, M. A. (2007). Factors influencing the magnitude and reproducibility of corticomotor excitability changes induced by paired associative stimulation. *Experimental Brain Research, 181,* 615–624.

Salmelin, R. H. & Hämäläinen, M. S. (1995). Dipole modelling of MEG rhythms in time and frequency domains. *Brain Topography, 7(3),* 251-257.

Salmelin, R. & Hari, R. (1994). Spatiotemporal characteristics of sensorimotor neuromagnetic rhythms related to thumb movement. *Neuroscience, 60(2),* 537-550.

Sampaio-Baptista, C., Filippini, N., Stagg, C. J., Near, J., Scholz, J. & Johansen-Berg, H. (2015). Changes in functional connectivity and GABA levels with long-term motor learning. *Neuroimage, 106,* 15-20.

Sanchez-Panchuelo, R. M., Besle, J., Beckett, A., Bowtell, R., Schluppeck, D. & Francis, S. (2012). Within-digit functional parcellation of brodmann areas of the human primary somatosensory cortex using functional magnetic resonance imaging at 7 tesla. *The Journal of Neuroscience, 32(45),* 15815-15822.

Sanchez-Panchuelo, R. M., Francis, S., Bowtell, R. & Schluppeck, D. (2010). Mapping human somatosensory cortex in individual subjects with 7T functional MRI. *Journal of Neurophysiology, 103(5),* 2544-2556.

Sarvas, J. (1987). Basic mathematical and electromagnetic concepts of the biomagnetic inverse problem. *Physics in Medicine and Biology, 32,* 11–22.

Schambra, H. M., Abe, M., Luckenbaugh, D. A., Reis, J., Krakauer, J. W. & Cohen, L. G. (2011). Probing for hemispheric specialization for motor skill learning: a transcranial direct current stimulation study. *Journal of Neurophysiology, 106(2),* 652-661.

Schoffelen, J. M., Oostenveld, R. & Fries, P. (2005). Neuronal coherence as a mechanism of effective corticospinal interaction. *Science, 308(5718),* 111-113.

Schutter, D. J. & Hortensius, R. (2011). Brain oscillations and frequency-dependent modulation of cortical excitability. *Brain Stimulation, 4(2),* 97-103.

Seeger, U., Mader, I., Nägele, T., Grodd, W., Lutz, O. & Klose, U. (2001). Reliable detection of macromolecules in single-volume 1H NMR spectra of the human brain. *Magnetic Resonance in Medicine, 45(6),* 948-954.

Sehm, B., Hoff, M., Gundlach, C., Taubert, M., Conde, V., Villringer, A. & Ragert, P. (2013a). A novel ring electrode setup for the recording of somatosensory evoked potentials during transcranial direct current stimulation (tDCS). *Journal of Neuroscience Methods, 212(2),* 234-236.

Sehm, B., Kipping, J., Schäfer, A., Villringer, A. & Ragert, P. (2013b). A comparison between uni- and bilateral tDCS effects on functional connectivity of the human motor cortex. *Frontiers in Human Neuroscience, 7.*

Sehm, B., Schäfer, A., Kipping, J., Margulies, D., Conde, V., Taubert, M... & Ragert, P. (2012). Dynamic modulation of intrinsic functional connectivity by transcranial direct current stimulation. *Journal of Neurophysiology, 108(12),* 3253-3263.

Sekihara, K., Nagarajan, S. S., Poeppel, D. & Marantz, A. (2004). Asymptotic SNR of scalar and vector minimum-variance beamformers for neuromagnetic source reconstruction. *Biomedical Engineering, IEEE Transactions on, 51(10),* 1726-1734.

Shibasaki, H. & Hallett, M. (2006). What is the Bereitschaftspotential?. *Clinical Neurophysiology, 117(11),* 2341-2356.

Silén, T., Forss, N., Jensen, O. & Hari, R. (2000). Abnormal reactivity of the ~20-Hz motor cortex rhythm in Unverricht Lundborg type progressive myoclonus epilepsy. *Neuroimage, 12(6),* 707-712.

Silvanto, J., Muggleton, N. & Walsh, V. (2008). State-dependency in brain stimulation studies of perception and cognition. *Trends in Cognitive Sciences, 12(12),* 447-454.

Simons, S. B., Chiu, J., Favorov, O. V., Whitsel, B. L. & Tommerdahl, M. (2007). Duration-dependent response of SI to vibrotactile stimulation in squirrel monkey. *Journal of Neurophysiology, 97,* 2121–2129.

Simons, S. B., Tannan, V., Chiu, J., Favorov, O. V., Whitsel, B. L. & Tommerdahl, M. (2005). Amplitude-dependency of response of SI cortex to flutter stimulation. *BMC Neuroscience, 6:*43.

Sinclair, R. J. & Burton, H. (1993). Neuronal activity in the second somatosensory cortex of monkeys (Macaca mulatta) during active touch of gratings. *Journal of Neurophysiology, 70,* 331-331.

Singer, W. & Gray, C. M. (1995). Visual feature integration and the temporal correlation hypothesis. *Annual Review of Neuroscience, 18(1),* 555-586.

Singh, K. D., Barnes, G. R. & Hillebrand, A. (2003). Group imaging of task-related changes in cortical synchronisation using nonparametric permutation testing. *Neuroimage, 19(4),* 1589-1601.

Smith, M. J., Adams, L. F., Schmidt, P. J., Rubinow, D. R. & Wassermann, E. M. (2002). Effects of ovarian hormones on human cortical excitability. *Annals of Neurology, 51(5),* 599-603.

Smith, S. M. (2002). Fast robust automated brain extraction. *Human Brain Mapping, 17(3),* 143-155.

Smith, S. S., Gong, Q. H., Hsu, F. C., Markowitz, R. S., Ffrench-Mullen, J. M. H. & Li, X. (1998). GABAA receptor α4 subunit suppression prevents withdrawal properties of an endogenous steroid. *Nature, 392(6679),* 926-929.

Snowden, R., Thompson, P. & Troscianko, T. (2012). *Basic Vision: an introduction to visual perception.* Oxford University Press.

Soekadar, S. R., Witkowski, M., Cossio, E. G., Birbaumer, N., Robinson, S. E. & Cohen, L. G. (2013). In vivo assessment of human brain oscillations during application of transcranial electric currents. *Nature Communications, 4.*

Song, M., Shin, Y. & Yun, K. (2014). Beta-frequency EEG activity increased during transcranial direct current stimulation. *Neuroreport, 25(18),* 1433-1436.

Spiegel, D. P., Hansen, B. C., Byblow, W. D. & Thompson, B. (2012). Anodal transcranial direct current stimulation reduces psychophysically measured surround suppression in the human visual cortex. *PloS One, 7(5),* e36220.

Spitoni, G. F., Cimmino, R. L., Bozzacchi, C., Pizzamiglio, L. & Di Russo, F. (2013). Modulation of spontaneous alpha brain rhythms using low-intensity transcranial direct-current stimulation. *Frontiers in Human Neuroscience, 7.*

Stagg, C. J. (2014). Magnetic Resonance Spectroscopy as a tool to study the role of GABA in motor-cortical plasticity. *Neuroimage, 86,* 19-27.

Stagg, C. J., Bachtiar, V., Amadi, U., Gudberg, C. A., Ilie, A. S., Sampaio-Baptista, C... & Johansen-Berg, H. (2014). Local GABA concentration is related to network-level resting functional connectivity. *Elife, 3,* e01465.

Stagg, C. J., Bachtiar, V. & Johansen-Berg, H. (2011b). The role of GABA in human motor learning. *Current Biology, 21(6),* 480-484.

Stagg, C. J., Bachtiar, V. & Johansen-Berg, H. (2011a). What are we measuring with GABA magnetic resonance spectroscopy? *Communicative & Integrative Biology, 4(5),* 573-575.

Stagg, C. J., Best, J. G., Stephenson, M. C., O'Shea, J., Wylezinska, M., Kincses, Z. T... & Johansen-Berg, H. (2009). Polarity-sensitive modulation of cortical neurotransmitters by transcranial stimulation. *The Journal of Neuroscience.* 29*(16),* 5202-5206.

Stagg, C. J., Bestmann, S., Constantinescu, A. O., Moreno, L. M., Allman, C., Mekle, R... & Rothwell, J. C. (2011c). Relationship between physiological measures of excitability and levels of glutamate and GABA in the human motor cortex. *The Journal of Physiology, 589(23),* 5845-5855.

Stagg, C. J., Jayaram, G., Pastor, D., Kincses, Z. T., Matthews, P. M. & Johansen-Berg, H. (2011d). Polarity and timing-dependent effects of transcranial direct current stimulation in explicit motor learning. *Neuropsychologia, 49(5),* 800-804.

Stagg, C. J. & Johansen-Berg, H. (2013). Studying the effects of transcranial direct-current stimulation in stroke recovery using magnetic resonance imaging. *Frontiers in Human Neuroscience, 7.*

Stagg, C. J. & Nitsche, M. A. (2011). Physiological basis of transcranial direct current stimulation. *The Neuroscientist, 17(1),* 37-53.

Stefan, K., Kunesch, E., Cohen, L. G., Benecke, R. & Classen, J. (2000). Induction of plasticity in the human motor cortex by paired associative stimulation. *Brain, 123(3),* 572-584.

Stokes, M. G., Chambers, C. D., Gould, I. C., Henderson, T. R., Janko, N. E., Allen, N. B. & Mattingley, J. B. (2005). Simple metric for scaling motor threshold based on scalp-cortex distance: application to studies using transcranial magnetic stimulation. *Journal of Neurophysiology, 94(6),* 4520-4527.

Sumner, P., Edden, R. A., Bompas, A., Evans, C. J. & Singh, K. D. (2010). More GABA, less distraction: a neurochemical predictor of motor decision speed. *Nature Neuroscience*, *13(7),* 825-827.

Suntrup, S., Teismann, I., Wollbrink, A., Winkels, M., Warnecke, T., Flöel, A... & Dziewas, R. (2013). Magnetoencephalographic evidence for the modulation of cortical swallowing processing by transcranial direct current stimulation. *Neuroimage*, *83*, 346-354.

Supek, S. & Aine, C. J. (1993). Simulation studies of multiple dipole neuromagnetic source localization: model order and limits of source resolution. *Biomedical Engineering, IEEE Transactions on, 40(6),* 529-540.

Supek, S. & Aine, C. (2014). *Magnetoencephalography: From Signals to Dynamic Cortical Networks.* Springer: Heidelberg, Germany.

Sutherling, W. W., Levesque, M. F. & Baumgartner, C. (1992). Cortical sensory representation of the human hand Size of finger regions and nonoverlapping digit somatotopy. *Neurology*, *42(5),* 1020-1028.

Swettenham, J. B., Muthukumaraswamy, S. D. & Singh, K. D. (2009). Spectral properties of induced and evoked gamma oscillations in human early visual cortex to moving and stationary stimuli. *Journal of Neurophysiology*, *102(2),* 1241-1253.

Takakusaki, K., Saitoh, K., Harada, H. & Kashiwayanagi, M. (2004). Role of basal ganglia–brainstem pathways in the control of motor behaviors. *Neuroscience Research*, *50(2),* 137-151.

Tallon-Baudry, C. & Bertrand, O. (1999). Oscillatory gamma activity in humans and its role in object representation. *Trends in Cognitive Sciences*, *3(4),* 151-162.

Tang, M. F. & Hammond, G. R. (2013). Anodal transcranial direct current stimulation over auditory cortex degrades frequency discrimination by affecting temporal, but not place, coding. *European Journal of Neuroscience*, *38(5),* 2802-2811.

Tannan, V., Holden, J. K., Zhang, Z., Baranek, G. T. & Tommerdahl, M. (2008). Perceptual metrics of individuals with autism provide evidence for disinhibition. *Autism Research, 1(4),* 223-230.

Tannan, V., Simons, S., Dennis, R. G. & Tommerdahl, M. (2007). Effects of adaptation on the capacity to differentiate simultaneously delivered dual-site vibrotactile stimuli. *Brain Research, 1186,* 164-170.

Taulu, S. & Simola, J. (2006). Spatiotemporal signal space separation method for rejecting nearby interference in MEG measurements. *Physics in Medicine & Biology, 51,* 1759–1768.

Taylor, M. & Creelman, C. D. (1967). PEST: Efficient estimates on probability functions. *The Journal of the Acoustical Society of America*, *41*, 782-787.

Teplan, M. (2002). Fundamentals of EEG measurement. *Measurement Science Review, 2(2),* 1-11.

Terpstra, M., Ugurbil, K. & Gruetter, R. (2002). Direct in vivo measurement of human cerebral GABA concentration using MEGA-editing at 7 Tesla. *Magnetic Resonance in Medicine, 47(5),* 1009-1012.

Terzuolo, C. A. & Bullock, T. H. (1956). Measurement of imposed voltage gradient adequate to modulate neuronal firing. *Proceedings of the National Academy of Sciences of the United States of America, 42(9),* 687.

Thirugnanasambandam, N., Grundey, J., Adam, K., Drees, A., Skwirba, A. C., Lang, N... & Nitsche, M. A. (2011). Nicotinergic impact on focal and non-focal neuroplasticity induced by non-invasive brain stimulation in non-smoking humans. *Neuropsychopharmacology, 36(4),* 879-886.

Thut, G., Miniussi, C. & Gross, J. (2012). The functional importance of rhythmic activity in the brain. *Current Biology, 22(16),* 658-663.

Tiesinga, P. H., Fellous, J. M., Salinas, E., Jose, J. V. & Sejnowski, T. J. (2004). Inhibitory synchrony as a mechanism for attentional gain modulation. *The Journal of Physiology, 98(4),* 296-314.

Tiihonen, J., Kajola, M. & Hari, R. (1989). Magnetic mu rhythm in man. *Neuroscience, 32(3),* 793-800.

Tommerdahl, M., Favorov, O. & Whitsel, B. L. (2002). Optical imaging of intrinsic signals in somatosensory cortex. *Behavioural Brain Research, 135,* 83–91.

Tommerdahl, M., Favorov, O. V. & Whitsel, B. L. (2010). Dynamic representations of the somatosensory cortex. *Neuroscience & Biobehavioral Reviews, 34(2),* 160-170.

Tommerdahl, M., Tannan, V., Cascio, C. J., Baranek, G. T. & Whitsel, B. L. (2007). Vibrotactile adaptation fails to enhance spatial localization in adults with autism. *Brain Research, 1154,* 116-123.

Tommerdahl, M., Tannan, V., Holden, J. K. & Baranek, G. T. (2008). Absence of stimulus-driven synchronization effects on sensory perception in autism: Evidence for local underconnectivity. *Behavioral and Brain Functions, 4*:19.

Tootell, R. B., Hadjikhani, N. K., Vanduffel, W., Liu, A. K., Mendola, J. D., Sereno, M. I. & Dale, A. M. (1998). Functional analysis of primary visual cortex (V1) in humans. *Proceedings of the National Academy of Sciences, 95(3),* 811-817.

Tremblay, S., Beaulé, V., Proulx, S., Lafleur, L. P., Doyon, J., Marjańska, M. & Théoret, H. (2014). The use of magnetic resonance spectroscopy as a tool for the measurement of bihemispheric transcranial electric stimulation effects on primary motor cortex metabolism. *Journal of Visualized Experiments,* 93, e51631.

Tremblay, S., Beaulé, V., Lepage, J. F. & Théoret, H. (2013). Anodal transcranial direct current stimulation modulates GABAB-related intracortical inhibition in the M1 of healthy individuals. *Neuroreport, 24(1),* 46-50.

Trepel, C. & Racine, R. J. (2000). GABAergic modulation of neocortical long-term potentiation in the freely moving rat. *Synapse, 35(2),* 120-128.

Treutwein, B. (1995). Adaptive psychophysical procedures. *Vision Research, 35(17),* 2503-2522.

Troebinger, L., López, J. D., Lutti, A., Bestmann, S. & Barnes, G. (2014). Discrimination of cortical laminae using MEG. *Neuroimage, 102,* 885-893.

Truong, D. Q., Magerowski, G., Blackburn, G. L., Bikson, M. & Alonso-Alonso, M. (2013). Computational modeling of transcranial direct current stimulation (tDCS) in obesity: impact of head fat and dose guidelines. *Neuroimage: Clinical, 2,* 759-766.

Uğurbil, K., Adriany, G., Andersen, P., Chen, W., Garwood, M., Gruetter, R... & Zhu, X. H. (2003). Ultrahigh field magnetic resonance imaging and spectroscopy. *Magnetic Resonance Imaging, 21(10),* 1263-1281.

Uhlhaas, P. J. & Singer, W. (2006). Neural synchrony in brain disorders: relevance for cognitive dysfunctions and pathophysiology. *Neuron, 52(1),* 155-168.

Uhlhaas, P. J. & Singer, W. (2012). Neuronal dynamics and neuropsychiatric disorders: Towards a translational paradigm for dysfunctional large-scale networks. *Neuron, 75(6),* 963-980.

Upadhyay, J., Ducros, M., Knaus, T. A., Lindgren, K. A., Silver, A., Tager-Flusberg, H. & Kim, D. S. (2007). Function and connectivity in human primary auditory cortex: a combined fMRI and DTI study at 3 Tesla. *Cerebral Cortex, 17(10),* 2420-2432.

Utz, K. S., Dimova, V., Oppenländer, K. & Kerkhoff, G. (2010). Electrified minds: Transcranial direct current stimulation (tDCS) and Galvanic Vestibular Stimulation (GVS) as methods of non-invasive brain stimulation in neuropsychology—A review of current data and future implications. *Neuropsychologia, 48(10),* 2789-2810.

van Doren, J., Langguth, B. & Schecklmann, M. (2014). Electroencephalographic effects of transcranial random noise stimulation in the auditory cortex. *Brain Stimulation, 7(6),* 807-812.

van Elk, M., van Schie, H.T., van den Heuvel, R. & Bekkering, H. (2010). Semantics in the motor system: motor-cortical Beta oscillations reflect semantic knowledge of end-postures for object use. *Frontiers in Human Neuroscience, 4.*

van Veen, B. D., van Drongelen, W., Yuchtman, M. & Suzuki, A. (1997). Localization of brain electrical activity via linearly constrained minimum variance spatial filtering. *Biomedical Engineering, IEEE Transactions on, 44(9),* 867-880.

van Wijk, B.C.M., Daffertshofer, A., Roach, N. & Praamstra, P. (2009). A role of beta oscillatory synchrony in biasing response competition. *Cerebral Cortex, 19,* 1294–1302.

Vargas-Irwin, C. E., Shakhnarovich, G., Yadollahpour, P., Mislow, J. M., Black, M. J. & Donoghue, J. P. (2010). Decoding complete reach and grasp actions from local primary motor cortex populations. *The Journal of Neuroscience, 30(29),* 9659-9669.

Venkatakrishnan, A., Contreras-Vidal, J. L., Sandrini, M. & Cohen, L. G. (2011). Independent component analysis of resting brain activity reveals transient modulation of local cortical processing by transcranial direct current stimulation. *Engineering in Medicine and Biology Society, EMBC, 2011 Annual International Conference of the IEEE,* 8102-8105.

Venkatakrishnan, A. & Sandrini, M. (2012). Combining transcranial direct current stimulation and neuroimaging: novel insights in understanding neuroplasticity. *Journal of Neurophysiology, 107(1),* 1-4.

Verbruggen, F., Adams, R. C., van't Wout, F., Stevens, T., McLaren, I. P. & Chambers, C. D. (2013). Are the effects of response inhibition on gambling long-lasting? *PloS One, 8*(7), e70155.

Verrillo, R. T. (1979). Comparison of vibrotactile threshold and suprathreshold responses in men and women. *Perception & Psychophysics, 26(1),* 20-24.

Verrillo, R. T., Fraioli, A. J. & Smith, R. L. (1969). Sensation magnitude of vibrotactile stimuli. *Perception & Psychophysics, 6(6),* 366-372.

Viera, A. J. & Garrett, J. M. (2005). Understanding interobserver agreement: the kappa statistic. *Family Medicine, 37(5),* 360-363.

Villamar, M. F., Wivatvongvana, P., Patumanond, J., Bikson, M., Truong, D. Q., Datta, A. & Fregni, F. (2013). Focal modulation of the primary motor cortex in fibromyalgia using 4× 1-ring high-definition transcranial direct current stimulation (HD-tDCS): immediate and delayed analgesic effects of cathodal and anodal stimulation. *The Journal of Pain, 14(4),* 371-383.

Vines, B., Cerruti, C. & Schlaug, G. (2008). Dual-hemisphere tDCS facilitates greater improvements for healthy subjects' non-dominant hand compared to uni-hemisphere stimulation. *BMC Neuroscience, 9(1),* 103-109.

Vrba, J., Cheung, T., Cheyne, D., Robinson, S. E. & Starr, A. (1999). Errors in ECD localization with partial sensor coverage. In Yoshimoto, T., Kotani, M., Kuriki, S., Karibe, H., Nakasato, N. (eds.) *Recent advances in biomagnetism.* Sendai, Japan.

Vrba, J. & Robinson, S. E. (2001). Signal processing in magnetoencephalography. *Methods, 25(2),* 249-271.

Wagenmakers, E. J. (2007). A practical solution to the pervasive problems of p values. *Psychonomic Bulletin & Review, 14(5),* 779-804.

Wandell, B. A., Dumoulin, S. O. & Brewer, A. A. (2007). Visual field maps in human cortex. *Neuron, 56(2),* 366-383.

Wassermann, E. M. & Grafman, J. (2005). Recharging cognition with DC brain polarization. *Trends in Cognitive Sciences, 9(11),* 503-505.

Weber, E. H. (1834). *De pulsu, resorptione, auditu et tactu. Annotationes anatomicae et physiologicae.* Leipzig: Koehler.

Westphalen, R. I. & Hemmings, H. C. (2006). Volatile anesthetic effects on glutamate versus GABA release from isolated rat cortical nerve terminals: basal release. *Journal of Pharmacology and Experimental Therapeutics, 316(1),* 208-215.

Wheaton, L., Carpenter, M., Mizelle, J.C. & Forrester, L. (2008). Preparatory band specific premotor cortical activity differentiates upper and lower extremity movement. *Experimental Brain Research, 184,* 121–126.

Whitham, E. M., Pope, K. J., Fitzgibbon, S. P., Lewis, T., Clark, C. R., Loveless, S... & Willoughby, J. O. (2007). Scalp electrical recording during paralysis: quantitative evidence that EEG frequencies above 20Hz are contaminated by EMG. *Clinical Neurophysiology, 118(8),* 1877-1888.

Whitsel, B. L., Kelly, E. F., Delemos, K. A. & Quibrera, P. M. (2000). Stability of rapidly adapting afferent entrainment vs responsivity. *Somatosensory & Motor Research, 17(1),* 13-31.

Whitsel, B. L., Kelly, E. F., Quibrera, M., Tommerdahl, M., Li, Y., Favorov, O. V... & Metz, C. B. (2003). Time-dependence of SI RA neuron response to cutaneous flutter stimulation. *Somatosensory & Motor Research, 20(1),* 45-69.

Wichmann, F. A. & Hill, N. J. (2001). The psychometric function: I. Fitting, sampling, and goodness of fit. *Perception & Psychophysics, 63(8),* 1293-1313.

Wiethoff, S., Hamada, M. & Rothwell, J. C. (2014). Variability in response to transcranial direct current stimulation of the motor cortex. *Brain Stimulation, 7(3),* 468-475.

Wigstrom, H., Gustafsson, B., Huang, Y. Y. & Abraham, W. C. (1986). Hippocampal long-term potentiation is induced by pairing single afferent volleys with intracellularly injected depolarizing current pulses. *Acta Physiological Scandinavica, 126,* 317-319.

Wijtenburg, S. A., Rowland, L. M., Edden, R. A. & Barker, P. B. (2013). Reproducibility of brain spectroscopy at 7T using conventional localization and spectral editing techniques. *Journal of Magnetic Resonance Imaging, 38(2),* 460-467.

Wilson, M., Reynolds, G., Kauppinen, R. A., Arvanitis, T. N. & Peet, A. C. (2011). A constrained least-squares approach to the automated quantitation of in vivo 1H magnetic resonance spectroscopy data. *Magnetic Resonance in Medicine, 65(1),* 1-12.

Winkler, A. M., Ridgway, G. R., Webster, M. A., Smith, S. M. & Nichols, T. E. (2014). Permutation inference for the general linear model. *Neuroimage, 92,* 381-397.

Wirth, M., Rahman, R. A., Kuenecke, J., Koenig, T., Horn, H., Sommer, W. & Dierks, T. (2011). Effects of transcranial direct current stimulation (tDCS) on behaviour and electrophysiology of language production. *Neuropsychologia, 49(14),* 3989-3998.

Xia, M., Wang, J. & He, Y. (2013). BrainNet Viewer: a network visualization tool for human brain connectomics. *PloS One, 8(7).*

Xue, J. G., Masuoka, T., Gong, X. D., Chen, K. S., Yanagawa, Y., Law, S. A. & Konishi, S. (2011). NMDA receptor activation enhances inhibitory GABAergic transmission onto hippocampal pyramidal neurons via presynaptic and postsynaptic mechanisms. *Journal of Neurophysiology,105(6),* 2897-2906.

Yamawaki, N., Stanford, I. M., Hall, S. D. & Woodhall, G. L. (2008). Pharmacologically induced and stimulus evoked rhythmic neuronal oscillatory activity in the primary motor cortex in vitro. *Neuroscience, 151(2),* 386-395.

Yau, J. M., Celnik, P., Hsiao, S. S. & Desmond, J. E. (2014). Feeling Better Separate Pathways for Targeted Enhancement of Spatial and Temporal Touch. *Psychological Science*.

Ye, Y. & Griffin, M. J. (2011). Reductions in finger blood flow in men and women induced by 125-Hz vibration: association with vibration perception thresholds. *Journal of Applied Physiology, 111(6),* 1606-1613.

Yousry, T. A., Schmid, U. D., Alkadhi, H., Schmidt, D., Peraud, A., Buettner, A. & Winkler, P. (1997). Localization of the motor hand area to a knob on the precentral gyrus. *Brain, 120,* 141-157.

Zaehle, T., Rach, S. & Herrmann, C. S. (2010). Transcranial alternating current stimulation enhances individual alpha activity in human EEG. *PloS One, 5(11).*

Zaehle, T., Sandmann, P., Thorne, J. D., Jäncke, L. & Herrmann, C. S. (2011). Transcranial direct current stimulation of the prefrontal cortex modulates working memory performance: combined behavioural and electrophysiological evidence. *BMC Neuroscience, 12:*2.

Zeki, S. M. (1973). Colour coding in rhesus monkey prestriate cortex. *Brain Research, 53(2),* 422-427.

Zeki, S., Watson, J. D., Lueck, C. J., Friston, K. J., Kennard, C. & Frackowiak, R. S. (1991). A direct demonstration of functional specialization in human visual cortex. *The Journal of Neuroscience, 11(3),* 641-649.

Zhang, H., Wang, W., Gao, W., Ge, Y., Zhang, J., Wu, S. & Xu, L. (2009). Effect of propofol on the levels of neurotransmitters in normal human brain: a magnetic resonance spectroscopy study. *Neuroscience Letters, 467(3),* 247-251.

Zhang, Y., Brady, M. & Smith, S. (2001). Segmentation of brain MR images through a hidden Markov random field model and the expectation-maximization algorithm. *Medical Imaging, IEEE Transactions on, 20(1),* 45-57.

Zhang, Z., Francisco, E. M., Holden, J. K., Dennis, R. G. & Tommerdahl, M. (2009). The impact of non-noxious heat on tactile information processing. *Brain Research, 1302,* 97-105.

Zhang, Z., Francisco, E. M., Holden, J. K., Dennis, R. G. & Tommerdahl, M. (2011a). Somatosensory information processing in the aging population. *Frontiers in Aging Neuroscience, 3.*

Zhang, Z., Zolnoun, D. A., Francisco, E. M., Holden, J. K., Dennis, R. G. & Tommerdahl, M. (2011b). Altered central sensitization in subgroups of women with vulvodynia. *The Clinical Journal of Pain, 27(9),* 755-763.

Ziemann, U. (2004). TMS and drugs. *Clinical Neurophysiology, 115(8),* 1717-1729.

Ziemann, U. & Siebner, H. R. (2008). Modifying motor learning through gating and homeostatic metaplasticity. *Brain Stimulation, 1(1),* 60-66.

10. Appendices

Appendix 1 – Edinburgh Handedness Inventory

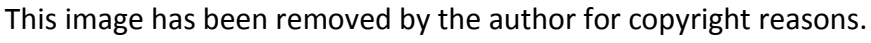

Appendix 2 – tDCS Screening Form

tDCS Safety Screening Questionnaire

Please read the following questions carefully and provide answers. You have the right to withdraw from the screening and subsequent testing if you find the questions unacceptably intrusive. The information you provide will be treated as strictly confidential and will be held in secure conditions. If you are unsure of the answer to any of the questions, please ask the person who gave you this form or the person who will be performing the study.

Volunteer name: _____ Date of birth: _____ Sex: M / F

Have you ever suffered from any neurological or psychiatric conditions? (e.g. stroke, depression, etc)	***YES***	***NO***
Have you ever suffered from epilepsy, febrile convulsions in infancy or had recurrent fainting spells?	***YES***	***NO***
Does anyone in your immediate or distant family suffer from epilepsy? If YES please state your relationship to the affected family member.	***YES***	***NO***
Have you ever undergone a neurosurgical procedure (including eye surgery)? If YES please give details	***YES***	***NO***
Do you currently have any of the following fitted to your body? (please circle) Heart pacemaker Cochlear implant Medication pump Surgical clips	***YES***	***NO***
Are you currently taking any unprescribed or prescribed medication? If YES please give details.	***YES***	***NO***
Are you currently undergoing anti - malarial treatment, or have been in the last 3 days?	***YES***	***NO***
Or drunk more than 3 units of alcohol in the last 24 hours?	***YES***	***NO***
Have you drunk alcohol already today?	***YES***	***NO***
Have you had more than one cup of coffee, or other sources of caffeine in the last hour?	***YES***	***NO***
Have you used recreational drugs in the last 24 hours?	***YES***	***NO***
Did you have very little sleep last night?	***YES***	***NO***
Is there any chance you might be pregnant?	***YES***	***NO***
Have you already participated in a tDCS/ TMS experiment in the last week?	***YES***	***NO***
Do you hold a heavy goods vehicle (HGV) driving license or bus license?	***YES***	***NO***
Have you ever suffered from migraines?	***YES***	***NO***

I have read and understood the questions above and have answered them correctly.

SIGNED…… DATE……..

In the presence of …….. (Name) ……..

Appendix 3 – The 10-10 Electrode Placement System

This image has been removed by the author for copyright reasons.

(Image from http://imgbuddy.com/eeg-electrodes-10-20-system.asp).

Appendix 4 – Adverse Effects Questionnaire

tDCS Questionnaire: Follow-up

1. Sex: □ male
□ female

2. Age:____

3. In how many studies did you participate? □ 1 study
□ 2-3 studies
□ 4-6 studies
□ more

Approximately how many?_____

4. Where on the head were you stimulated (more than one possible if you participated in several studies)?

□ over the motor cortex (one electrode on the left side of the scalp and the other electrode over the right eye brow or vice versa)

□ over the visual cortex (one electrode on the back of the head and the other electrode over the centre of the head)

□ over the parietal cortex (one electrode behind the ear and the other electrode over the centre of the head)

□ over the frontal cortex (one electrode on the left forehead and the other electrode over the right eyebrow or vise versa)

5. Did you notice a flash either at the beginning or at the end of the experiment?

□beginning □end □neither

During stimulation

6. Did you experience any pain under the electrodes during stimulation

□ yes □ no

If yes – how strong was the pain?

1-marginal 2-moderate 3-middle-rate 4-strong 5-not tolerable

7. Was your scalp under the electrodes tingling during stimulation?

□ yes □no

If yes, how strong?

1-marginal 2-moderate 3-middle-rate 4-strong 5-not tolerable

8. Was your scalp itching underneath the electrodes during stimulation?

□ yes □no

If yes, how strong?

1-marginal 2-moderate 3-middle-rate 4-strong 5-not tolerable

9. Was your scalp burning underneath the electrodes during stimulation?

□ yes □no

If yes, how strong?

1-marginal 2-moderate 3-middle-rate 4-strong 5-not tolerable

10. Were you tired during stimulation?

□ yes □no

If yes, how tired were you?

1-slightly 2-moderately 3-middle-rate 4-heavily 5-extremely

11. Were you nervous during stimulation?

□ yes □no

If yes, how nervous were you?

1-slightly 2-moderately 3-middle-rate 4-heavily 5-extremely

12. Did you experience problems with concentration during stimulation?

□ yes □no

If yes, how strong were the concentration problems that you noticed?

1-marginal 2-moderate 3-middle-rate 4-strong 5-extreme

13. Did you experience problems of vision during the stimulation?

□ yes □no

If yes, how severe were the visual problems that you experienced?

1-marginal 2-moderate 3-middle-rate 4-strong 5-extreme

14. Did you suffer from a headache during the stimulation?

□ yes □no

15. Did you feel something unusual during the stimulation?

□ yes □no

If yes, please give a short description:

_____

_____

16. Did you feel anything else during stimulation?

□ yes □no

If yes, please give a short description:

_____

_____

17. Did you experience the stimulation as unpleasant?

□ yes □ no

If yes, how unpleasant?

1-slightly 2-moderately 3-middle-rate 4-heavily 5-extremely

After stimulation

18. Did you experience any pain underneath the electrodes after stimulation?

□ yes □ no

If yes, how strong was the pain?

1-marginal 2-moderate 3-middle-rate 4-strong 5-not tolerable

19. Was your scalp underneath the electrodes tingling after stimulation?

□ yes □no

If yes, how strong was the tingling?

1-marginal 2-moderate 3-middle-rate 4-strong 5-not tolerable

20. Was your scalp itching underneath the electrodes after stimulation?

□ yes □no

If yes, how strong was the itching?

1-marginal 2-moderate 3-middle-rate 4-strong 5-not tolerable

21. Was your scalp burning under the electrodes after stimulation?

□ yes □no

If yes, how strong was the burning?

1-marginal 2-moderate 3-middle-rate 4-strong 5-not tolerable

22. Were you tired after stimulation?

□ yes □no

If yes, how tired were you?

1-slightly 2-moderately 3-middle-rate 4-heavily 5-extremely

23.Were you nervous after stimulation?

□ yes □no

If yes, how nervous were you?

1-slightly 2-moderately 3-middle-rate 4-heavily 5-extremely

24. Did you experience problems with concentration after stimulation?

□ yes □no

If yes, how strong were the concentration problems?

1-marginal 2-moderate 3-middle-rate 4-strong 5-extreme

25. Did you experience any problems with vision after stimulation?

□ yes □no

If yes, how strong were the visual problems?

1-marginal 2-moderate 3-middle-rate 4-strong 5-extreme

26. Did you get a headache after stimulation?

□ yes □no

27. Did you feel sick after stimulation?

□ yes □no

If yes, how long did you feel sick (in hours)?

_____

28. Did you vomit after stimulation?

□ yes □no

If yes, how often?_____

29.Did you experience any sleeping problems after stimulation?

□ yes □no

If yes, for how many days?_____

30. Did you experience any mood changes after stimulation?

□ yes □no

If yes, for how long (in hours)?_____

31. Did you feel cold after stimulation?

□ yes □no

If yes, for how long (in hours)?_____

32. Did you feel warm after stimulation?

□ yes □no

If yes, for how long (in hours)?_____

33. Did you experience anything unusual after stimulation?

□ yes □no

If yes, please give a short description:

_____

_____

34. Did you feel anything else after stimulation?

□ yes □no

If yes, please give a short description:

_____

_____

35. Did you realise any difference between different stimulation sites?

□ yes □no

If yes, please give a short description:

_____

_____

36. Were you anxious about the stimulation?

□ yes □no

37. Would you wish to participate again in a tDCS study?

□ yes □no

Please check that you have answered all the questions.

Thank you very much!

*Appendix 5 – G*Power Sample Size Output (tDCS-MRS)*

Given the expected effect size, the graph shows the number of subjects needed in order to produce power at 0.95.

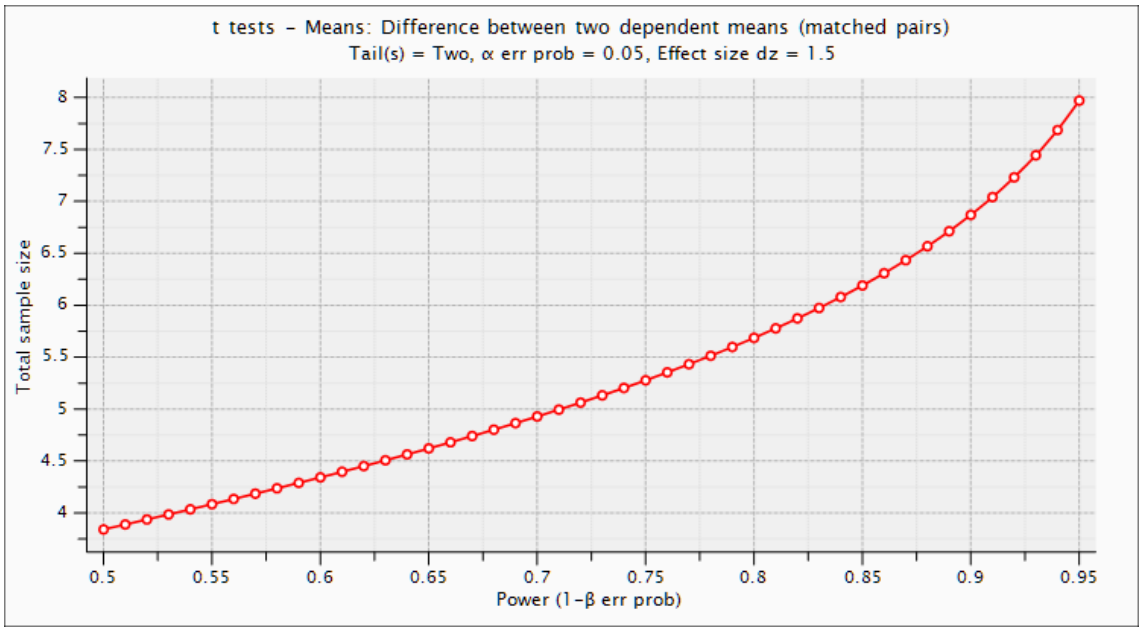

Appendix 6 – Consent Form (tDCS-MRS)

CUBRIC, SCHOOL OF PSYCHOLOGY, CARDIFF UNIVERSITY – MRI UNIT CONSENT FORM
Determining the Neurobiological Mechanisms of transcranial Direct Current Stimulation via Magnetic Resonance Spectroscopy

NAME OF PARTICIPANT …… Sex: M / F Date of Birth:……

Please read the Volunteer Information Sheet and then read the following statements carefully and then add your signature. If you have any questions, please ask the person who gave you this form. You are under no pressure to give your consent and you are free to withdraw from the MRI examination at any time. By signing the form you are agreeing to the following:

I understand that I am to take part in a tDCS-MRS experiment in which I will be placed in the scanner for up to 90 minutes, while my brain activity is measured by the machine, before/after up to 30 minutes of tDCS.

I confirm that I have read and understand the tDCS and MRI Volunteer Information Sheets and have had the opportunity to ask questions about them.

I understand that upon completion of the study, I will receive £20 per session (120 minutes). However, I understand that if I choose to stop at any time during the study, I will receive payment for my participation up to the point of withdrawal from the study.

I understand that participation in this study is entirely voluntary and that I can withdraw from the study at any time without giving a reason and without loss of payment.

I understand that I am free to ask any questions at any time and that I am free to withdraw or discuss my concerns with the lead researcher (Dr. David McGonigle).

I also understand that at the end of the study I will be provided with additional information and feedback about the purpose of the study.

I understand that I can talk to the operators via an intercom and that I will be given an alarm "squeeze ball" that I can squeeze at any time to end the scan and signal to the operator.

I understand that I can require, for any reason and at any time, that I be immediately removed from the MRI machine.

I understand and agree that the MRI scan is not a medical screening procedure and that the researchers are not qualified to provide a clinical diagnosis or identify potential abnormalities. However, if the researchers are concerned that there may be a potential abnormality on the scan, I consent to them disclosing the scan to a specialist neuroradiologist to provide a radiological report on the scan. I further consent to the results of this report being disclosed to my General Practitioner, if appropriate.

I have completed the initial screening form and have been told that it is safe for me to be scanned.

I understand that the information provided by me will be held confidentially, such that only the researchers can trace this information back to me individually. The information will be retained for up to 10 years when it will be deleted/destroyed. I understand that I can ask for the information I provide to be deleted/destroyed at any time.

I, _____(NAME) consent to participate in the study conducted by School of Psychology, Cardiff University.

Signed:

Date:

*Do not write beneath this line, For Staff Use Only*_____

CUBRIC UNIQUE IDENTIFIER:……

Statement by the Researcher carrying out the scan: I certify that the above participant signed this form in my presence. I am satisfied that the participant fully understands the statement made and I certify that he/she had adequate opportunity to ask questions about the procedure before signing.

Signature…… Name…… Date ……

Appendix 7 – Fit Error (tDCS-MRS)

Mean ± standard deviation values for fit error across Time and tDCS conditions. A) Ratios to N-acetyl-aspartate (NAA). B) Ratios to Creatine (Cr). Values are given as percentages (%).

A) **GABA'+MM:NAA**

Pre Anodal	Post Anodal	Pre Sham	Post Sham
5.122 ± 1.012	4.980 ± .953	5.622 ± 1.513	6.129 ± 1.582

GABA':NAA

Pre Anodal	Post Anodal	Pre Sham	Post Sham
10.080 ± 2.538	12.671 ± 3.194	10.968 ± 2.656	11.287 ± 3.291

Glx:NAA

Pre Anodal	Post Anodal	Pre Sham	Post Sham
5.377 ± 1.762	5.068 ± 1.375	5.526 ± 1.399	5.372 ± 1.776

B) **GABA'+MM:Cr**

Pre Anodal	Post Anodal	Pre Sham	Post Sham
8.154 ± 1.515	8.017 ± 1.091	8.311 ± 1.315	9.001 ± 1.303

GABA':Cr

Pre Anodal	Post Anodal	Pre Sham	Post Sham
11.119 ± 2.504	12.861 ± 3.275	11.024 ± 2.447	12.000 ± 3.035

Glx:Cr

Pre Anodal	Post Anodal	Pre Sham	Post Sham
8.525 ± 1.594	8.139 ± 1.098	8.665 ± 1.897	8.721 ± 1.543

Appendix 8 – NAA/Cr Correlations (tDCS-MRS)

GABA'+MM	Pre-tDCS (r(15)=.834, p=.000, CI=.406 .950)
	Post-tDCS (r(15)=.796, p=.000, CI=.649 .900)
GABA'	Pre-tDCS (r(15)=.918, p=.000, CI=.808 .976)
	Post-tDCS (r(15)=.837, p=.000, CI=.645 .952)
Glx	Pre-tDCS (r(12)=.826, p=.001, CI=.552 .936)
	Post-tDCS (r(12)=.914, p=.000, CI=.761 .974)

Appendix 9 – Creatine Statistics (*tDCS-MRS)*

2 x 2 ANOVA Analysis

GABA'+MM	Time (F(1,14)=.302, p=.591)
	tDCS (F(1,14)=.018, p=.894)
	Interaction (F(1,14)=2.573, p=.131)
GABA'	Time (F(1,14)=10.648, p=.006)
	tDCS (F(1,14)=1.112, p=.310)
	Interaction (F(1,14)=1.239, p=.284)
Glx	Time (F(1,11)=1.184, p=.300)
	tDCS (F(1,11)=1.401, p=.261)
	Interaction (F(1,11)=.148, p=.708)

Correlation Analysis (Baseline GABA concentration, % change in GABA concentration)

GABA'+MM	Anodal (r(15)=-.629, p=.012, CI=-.848 -.302)
	Sham (r(15)=-.668, p=.006, CI=-.860 -.509)
GABA'	Anodal (r(15)=-.763, p=.001, CI=-.925 -.423)
	Sham (r(15)=-.692, p=.004, CI=-.918 -.399)

Appendix 10 – Consent Form (tDCS-MEG)

CUBRIC, SCHOOL OF PSYCHOLOGY, CARDIFF UNIVERSITY - MEG UNIT CONSENT FORM
Determining the Neurobiological Mechanisms of tDCS via MEG

NAME OF PARTICIPANT …… Sex: M / F Date of Birth:……

Please read the Volunteer Information Sheet and then read the following statements carefully and then add your signature. If you have any questions, please ask the person who gave you this form. You are under no pressure to give your consent and you are free to withdraw from the MEG examination at any time. By signing the form you are agreeing to the following:

I understand that I am to take part in an MEG experiment in which I will be placed in the scanning machine for up to an hour, while my brain activity will be measured by the machine. During this time I will undergo tDCS for a period of 10 minutes. I will be shown visual stimuli and will respond using simple finger movements.

I confirm that I have read and understand the tDCS and MEG Volunteer Information Sheets and have had the opportunity to ask questions about them.

I understand that participation in this study is entirely voluntary and that I can withdraw from the study at any time without giving a reason.

I understand that I am free to ask any questions at any time and that I am free to withdraw or discuss my concerns with the lead researcher (Dr David McGonigle).

I also understand that at the end of the study I will be provided with additional information and feedback about the purpose of the study.

I understand that I can talk to the operators via an intercom, that I will always be monitored by camera and can ask to end the scan at any time.

I understand that I can require, for any reason and at any time, that I be immediately removed from the MEG machine.

I understand and agree that the MEG scan is not a medical screening procedure and that the researchers are not qualified to provide a clinical diagnosis or identify potential abnormalities. However, if the researchers are concerned that there may be a potential abnormality on the scan, I consent to them disclosing the scan to a specialist neurological consultant to provide a report on the scan. I further consent to the results of this report being disclosed to my General Practitioner, if appropriate.

I have completed the tDCS and MEG screening forms and have been told that it is safe to be scanned.

I understand that the information provided by me will be held confidentially, such that only the researchers can trace this information back to me individually. The information will be retained for up to 10 years when it will be deleted/destroyed. I understand that I can ask for the information I provide to be deleted/destroyed at any time and, in accordance with the Data Protection Act, I can have access to the information at any time.

I, _____(NAME) consent to participate in the study conducted by School of Psychology, Cardiff University.

Signed: Date:

Do not write beneath this line, For Staff Use Only

CUBRIC UNIQUE IDENTIFIER:……

Statement by the Researcher carrying out the scan: I certify that the above participant signed this form in my presence. I am satisfied that the participant fully understands the statement made and I certify that he/she had adequate opportunity to ask questions about the procedure before signing.

Signature…… Name…… Date ……...

Appendix 11 –Head Movement (tDCS-MEG)

Values correspond to the time point of acquisition, montage used and the administered stimulation polarity. Values are reported in mm.

	Visual Anodal	**Visual Sham**	**Motor Anodal**	**Motor Sham**
Pre	5.75 ± 3.79	4.95 ± 4.22	3.92 ± 3.15	4.46 ± 3.06
During	5.32 ± 3.30	5.91 ± 5.19	7.41 ± 6.86	7.92 ± 6.78
Post	5.54 ± 4.04	5.18 ± 4.00	4.04 ± 2.48	4.46 ± 4.08

Appendix 12 – Average Power Values (tDCS-MEG)

Calculated across the corresponding frequency band (beta: 15-30 Hz, gamma: 30-80 Hz) and reported as percentage (%) change from baseline, pre-stimulus values.

ERD	**Visual Anodal**	**Visual Sham**	**Motor Anodal**	**Motor Sham**
Pre	-15.09 ± 6.70	-15.94 ± 6.19	-13.95 ± 5.29	-15.61 ± 6.80
During	-14.00 ± 6.56	-13.46 ± 6.23	-14.05 ± 5.01	-14.21 ± 6.15
Post	-14.06 ± 5.15	-12.89 ± 5.17	-11.90 ± 4.55	-13.84 ± 5.01

PMBR	**Visual Anodal**	**Visual Sham**	**Motor Anodal**	**Motor Sham**
Pre	26.45 ± 15.30	26.06 ± 17.19	24.10 ± 10.70	30.19 ± 20.45
During	24.41 ± 16.09	25.40 ± 16.68	27.00 ± 10.12	28.83 ± 16.45
Post	21.59 ± 10.58	22.36 ± 13.37	26.88 ± 13.43	30.42 ± 15.98

Visual Gamma	**Visual Anodal**	**Visual Sham**	**Motor Anodal**	**Motor Sham**
Pre	27.51 ± 12.28	28.33 ± 12.15	31.96 ± 13.34	36.71 ± 18.96
During	25.44 ± 11.25	28.25 ± 12.41	32.87 ± 14.34	36.98 ± 18.93
Post	27.34 ± 13.86	30.16 ± 11.71	35.58 ± 18.59	36.93 ± 21.89

Appendix 13 – Group SAM Pairwise Comparisons (tDCS-MEG)

Significant differences between stimulation conditions established within task-related regions of interest (restricted to visual/motor cortices; Talairach coordinates). t values were thresholded at the critical value of 2.13 ($p<.05$, uncorrected). Contrast: A=Anodal, S=Sham. Region: L=Left hemisphere, R=Right hemisphere.

Analysis	Time	Contrast	Region	Co-ordinates	t	p
Visual	Pre	A > S	Middle Occipital Gyrus (L)	-31.1 -95.4 7	2.179	.046
		S > A	Middle Occipital Gyrus (L)	-55.2 -65.3 -13	-2.579	.021
			Pre Central Gyrus (L)	-43.2 -5 41	-2.951	.010
			Post Central Gyrus (L)	-37.1 -23.1 45	-2.588	.021
	tDCS	A > S	Pre Central Gyrus (L)	-11 -35.1 75	2.867	.012
			Pre Central Gyrus (R)	63.2 3 33	2.224	.042
	Post	S > A	Middle Occipital Gyrus (R)	17.1 -101.4 13	-2.209	.043
ERD	Pre	A > S	Post Central Gyrus (R)	9 -43.2 65	3.032	.008
	tDCS		Post Central Gyrus (L)	-39.2 -39.2 61	2.478	.026
			Pre Central Gyrus (R)	37.1 -25.1 71	2.183	.045
		S > A	Pre Central Gyrus (L)	-37.1 -17.1 45	-2.18	.046
	Post	A > S	Pre Central Gyrus (R)	41.2 15.1 37	3.058	.008
			Pre Central Gyrus (L)	-9 -19.1 71	3.139	.007
PMBR	Pre	A > S	Middle Occipital Gyrus (L)	-29.1 -97.4 7	2.513	.024
	tDCS	S > A	Middle Occipital Gyrus (R)	25.1 -85.3 1	-2.184	.045
	Post		Pre Central Gyrus (L)	-39.2 -25.1 69	-3.122	.007

Appendix 14 – Peak Sustained & Transient Gamma Values (tDCS-MEG)

Gamma frequency and amplitude values: Transient responses correspond to those 0-0.3 s from stimulus onset, sustained responses correspond to those 0.3-0.8 s from stimulus onset. Reported as percentage (%) change from baseline.

Sustained Frequency	**Visual Anodal**	**Visual Sham**	**Motor Anodal**	**Motor Sham**
Pre	53.66 ± 7.80	52.69 ± 6.09	55.22 ± 4.71	54.31 ± 4.92
During	56.03 ± 5.00	54.75 ± 5.62	56.16 ± 6.22	54.84 ± 5.34
Post	53.63 ± 5.88	54.06 ± 5.25	53.47 ± 6.46	55.31 ± 5.36

Sustained Amplitude	**Visual Anodal**	**Visual Sham**	**Motor Anodal**	**Motor Sham**
Pre	62.30 ± 29.58	65.02 ± 31.95	71.70 ± 35.24	79.30 ± 36.62
During	58.71 ± 35.17	61.30 ± 32.07	72.60 ± 37.13	80.43 ± 40.69
Post	62.99 ± 37.79	65.30 ± 29.43	76.94 ± 36.65	82.16 ± 52.81

Transient Frequency	**Visual Anodal**	**Visual Sham**	**Motor Anodal**	**Motor Sham**
Pre	57.97 ± 8.47	55.66 ± 4.54	57.16 ± 8.37	54.91 ± 6.10
During	58.31 ± 7.31	57.03 ± 7.96	58.25 ± 5.85	57.22 ± 8.24
Post	57.44 ± 4.88	54.56 ± 6.17	56.53 ± 6.11	56.25 ± 4.99

Transient Amplitude	**Visual Anodal**	**Visual Sham**	**Motor Anodal**	**Motor Sham**
Pre	62.19 ± 24.87	61.24 ± 26.26	70.77 ± 26.43	80.31 ± 39.51
During	60.79 ± 27.08	65.39 ± 28.86	75.97 ± 35.03	79.42 ± 40.31
Post	64.83 ± 35.41	68.60 ± 27.23	84.27 ± 45.74	82.43 ± 45.32

Appendix 15 – Sustained Gamma Frequency Order Effect (tDCS-MEG)

Comparison (ASAS/SASA)	**t**	**p**
Post Motor Anodal	2.584	.042

Comparison (ASAS/AASS)	**t**	**p**
Pre Motor Sham	2.494	.047
tDCS Motor Anodal	2.734	.034
tDCS Motor Sham	3.843	.009
Post Motor Anodal	2.522	.045
Post Motor Sham	2.456	.049

Comparison (ASAS/SSAA)	**t**	**p**
tDCS Motor Sham	4.525	.014
Post Motor Anodal	3.857	.008
Post Motor Sham	2.778	.032

Appendix 16 – Transient Gamma Amplitude Order Effect (tDCS-MEG)

Comparison (ASAS/SSAA)	**t**	**p**
Pre Visual Anodal	-2.652	.038
Pre Visual Sham	-2.844	.029

Comparison (SASA/SSAA)	**t**	**p**
Pre Visual Anodal	-2.451	.050
Pre Visual Sham	-2.887	.028
Pre Motor Sham	-2.738	.034
tDCS Visual Anodal	-2.610	.040
tDCS Visual Sham	-2.796	.031
Post Visual Anodal	-2.564	.043
Post Visual Sham	-4.057	.007
Post Motor Sham	-2.841	.030

Comparison (AASS/SSAA)	**t**	**p**
Pre Visual Anodal	-2.646	.038
Pre Visual Sham	-2.534	.044
Pre Motor Sham	-3.822	.009
Post Visual Sham	-2.613	.040

Appendix 17 – Evoked Response Latency & Magnitude Values (tDCS-MEG)

Peaks were derived for each subject as the maximum or minimum value within the specified time window. Peaks from motor-based waves are reported for ERD and PMBR data. Each value represents the Mean ± SD. Latency is given in seconds (s). Magnitude is given as percentage (%) change from baseline values.

Latency

	ERD		PMBR	
MF	**Motor Anodal**	**Motor Sham**	**Motor Anodal**	**Motor Sham**
Pre	0.018 ± 0.079	0.018 ± 0.074	0.047 ± 0.050	0.031 ± 0.051
During	0.009 ± 0.082	-0.002 ± 0.087	0.030 ± 0.059	0.027 ± 0.081
Post	0.003 ± 0.089	0.008 ± 0.071	0.056 ± 0.077	0.035 ± 0.070

	ERD		PMBR	
MEF1	**Motor Anodal**	**Motor Sham**	**Motor Anodal**	**Motor Sham**
Pre	0.182 ± 0.103	0.165 ± 0.086	0.182 ± 0.079	0.203 ± 0.119
During	0.165 ± 0.090	0.150 ± 0.079	0.200 ± 0.080	0.190 ± 0.113
Post	0.186 ± 0.105	0.160 ± 0.084	0.203 ± 0.079	0.209 ± 0.110

M100	**Visual Anodal**	**Visual Sham**
Pre	0.096 ± 0.017	0.093 ± 0.010
During	0.098 ± 0.016	0.095 ± 0.011
Post	0.098 ± 0.012	0.093 ± 0.011

Magnitude

	ERD		PMBR	
MF	**Motor Anodal**	**Motor Sham**	**Motor Anodal**	**Motor Sham**
Pre	4.911 ± 5.041	4.611 ± 3.868	3.480 ± 2.947	3.998 ± 2.010
During	15.172 ± 16.070	4.842 ± 4.742	12.924 ± 18.924	4.750 ± 5.004
Post	4.712 ± 3.952	3.668 ± 2.685	4.563 ± 3.929	4.833 ± 3.826

	ERD		PMBR	
MEF1	**Motor Anodal**	**Motor Sham**	**Motor Anodal**	**Motor Sham**
Pre	-4.271 ± 3.197	-4.687 ± 4.048	-4.051 ± 3.182	-5.546 ± 4.403
During	-36.395 ± 41.026	-10.399 ± 12.693	-26.886 ± 45.083	-6.941 ± 4.789
Post	-5.234 ± 2.470	-4.747 ± 3.585	-4.358 ± 3.460	-5.432 ± 5.072

M100	**Visual Anodal**	**Visual Sham**
Pre	7.944 ± 3.520	9.376 ± 5.786
During	7.975 ± 4.067	9.739 ± 4.844
Post	8.221 ± 4.208	7.573 ± 4.090

*Appendix 18 – G*Power Sample Size Output (SSA)*

Given the expected effect size, the graph shows the number of subjects needed in order to produce power at 0.95.

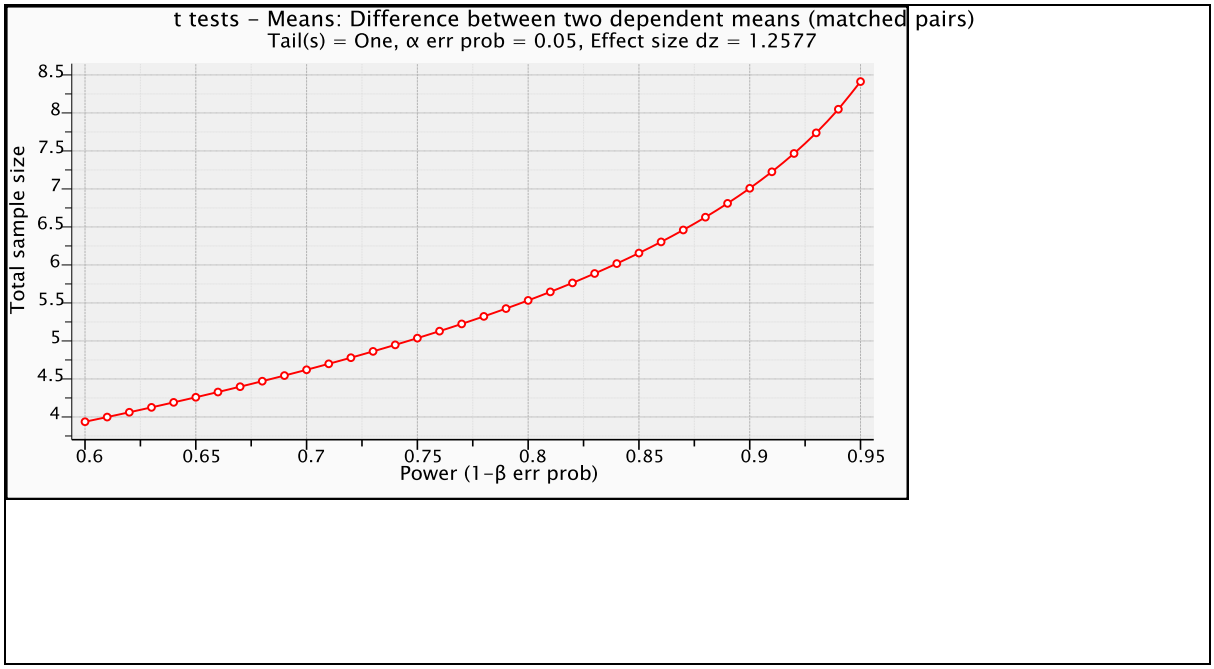

Appendix 19 – Counterbalancing (SSA)

Subject	**Anodal → Sham**	Subject	**Sham → Anodal**
1	SIM → SEQ → SSA	7	SIM → SEQ → SSA
2	SIM → SSA → SEQ	8	SIM → SSA → SEQ
3	SEQ → SIM → SSA	9	SEQ → SIM → SSA
4	SEQ → SSA → SIM	10	SEQ → SSA → SIM
5	SSA → SIM → SEQ	11	SSA → SIM → SEQ
6	SSA → SEQ → SIM	12	SSA → SEQ → SIM

Appendix 20 – Lack of Distinction between Anodal and Sham tDCS (SSA)

Paired t-test results supporting the lack of significant difference between stimulation modes, with respect to each of the task conditions.

Comparison	Sig
SIM_A_Pre - SIM_S_Pre	.286
SIM_A_Post1 - SIM_S_Post1	.160
SIM_A_Post2 - SIM_S_Post2	.232

Comparison	Sig
SEQ_A_Pre - SEQ_S_Pre	.474
SEQ_A_Post1 - SEQ_S_Post1	.466
SEQ_A_Post2 - SEQ_S_Post2	.059

Comparison	Sig
SSA_A_Pre - SSA_S_Pre	.154
SSA_A_Post1 - SSA_S_Post1	.261
SSA_A_Post2 - SSA_S_Post2	.585

Appendix 21 – Distinctions in Amplitude Discrimination Performance (SSA)

Post-tDCS, paired t-test results defining the main effect of Condition.

Comparison	Sig
SIM_A_Pre - SEQ_A_Pre	.446
SIM_A_Pre - SSA_A_Pre	.001
SEQ_A_Pre - SSA_A_Pre	.000
SIM_S_Pre - SEQ_S_Pre	.013
SIM_S_Pre - SSA_S_Pre	.001
SEQ_S_Pre - SSA_S_Pre	.001

Comparison	Sig
SIM_A_Post1 - SEQ_A_Post1	.009
SIM_A_Post1 - SSA_A_Post1	.005
SEQ_A_Post1 - SSA_A_Post1	.000
SIM_S_Post1 - SEQ_S_Post1	.004
SIM_S_Post1 - SSA_S_Post1	.003
SEQ_S_Post1 - SSA_S_Post1	.000

Comparison	Sig
SIM_A_Post2 - SEQ_A_Post2	.017
SIM_A_Post2 - SSA_A_Post2	.005
SEQ_A_Post2 - SSA_A_Post2	.000
SIM_S_Post2 - SEQ_S_Post2	.029
SIM_S_Post2 - SSA_S_Post2	.001
SEQ_S_Post2 - SSA_S_Post2	.000

Appendix 22 – tDCS Order Effect (SSA)

A) Vibrotactile-tDCS mean scores by tDCS order. B) Independent t-test results defining the Condition*tDCS Order interaction (t=5, N=6).

A)

Condition	Order	Mean
SIM_A_Pre	A/S	37.50
	S/A	52.83
SIM_A_Post1	A/S	59.67
	S/A	35.67
SIM_A_Post2	A/S	48.00
	S/A	54.50
SIM_S_Pre	A/S	37.67
	S/A	75.67
SIM_S_Post1	A/S	63.50
	S/A	61.00
SIM_S_Post2	A/S	52.17
	S/A	75.33

Condition	Order	Mean
SEQ_A_Pre	A/S	45.67
	S/A	23.33
SEQ_A_Post1	A/S	35.17
	S/A	29.33
SEQ_A_Post2	A/S	29.17
	S/A	19.33
SEQ_S_Pre	A/S	30.33
	S/A	27.33
SEQ_S_Post1	A/S	29.00
	S/A	28.00
SEQ_S_Post2	A/S	36.33
	S/A	43.17

Condition	Order	Mean
SSA_A_Pre	A/S	90.67
	S/A	137.33
SSA_A_Post1	A/S	74.83
	S/A	148.00
SSA_A_Post2	A/S	106.00
	S/A	154.67
SSA_S_Pre	A/S	112.67
	S/A	188.67
SSA_S_Post1	A/S	98.67
	S/A	162.00
SSA_S_Post2	A/S	80.67
	S/A	156.00

B)

Condition	Sig
SIM_A_Pre	.346
SIM_A_Post1	.121
SIM_A_Post2	.668
SIM_S_Pre	.010
SIM_S_Post1	.875
SIM_S_Post2	.262

Condition	Sig
SEQ_A_Pre	.132
SEQ_A_Post1	.592
SEQ_A_Post2	.238
SEQ_S_Pre	.725
SEQ_S_Post1	.876
SEQ_S_Post2	.559

Condition	Sig
SSA_A_Pre	.098
SSA_A_Post1	.005
SSA_A_Post2	.255
SSA_S_Pre	.132
SSA_S_Post1	.088
SSA_S_Post2	.001

Appendix 23 – Counterbalancing (DSA)

Task order

A	BASELINE	BASELINE	ADAPT	ADAPT
B	BASELINE	ADAPT	BASELINE	ADAPT
C	BASELINE	ADAPT	ADAPT	BASELINE
D	ADAPT	ADAPT	BASELINE	BASELINE
E	ADAPT	BASELINE	ADAPT	BASELINE
F	ADAPT	BASELINE	BASELINE	ADAPT

tDCS order

1	ANODAL	CATHODAL	SHAM
2	ANODAL	SHAM	CATHODAL
3	CATHODAL	ANODAL	SHAM
4	CATHODAL	SHAM	ANODAL
5	SHAM	ANODAL	CATHODAL
6	SHAM	CATHODAL	ANODAL

Integrated Task/tDCS order (orders selected are given in red)

A1	A2	**A3**	A4	**A5**	A6
B1	B2	**B3**	B4	**B5**	B6
C1	C2	**C3**	C4	**C5**	C6
D1	**D2**	D3	**D4**	D5	**D6**
E1	**E2**	E3	**E4**	E5	**E6**
F1	**F2**	F3	**F4**	F5	**F6**